

Human – Robot Collaboration

Methods for Target Recognition in

Unstructured Environments

Thesis submitted in partial fulfillment
of the requirements for the degree of
“DOCTOR OF PHILOSOPHY”

by
Avital Bechar

Submitted to the Senate of Ben-Gurion University
of the Negev

2006

BEER-SHEVA

Human – Robot Collaboration

Methods for Target Recognition in

Unstructured Environments

Thesis submitted in partial fulfillment
of the requirements for the degree of
“DOCTOR OF PHILOSOPHY”

by
Avital Bechar

Submitted to the Senate of Ben-Gurion University
of the Negev

Approved by the advisor	Prof Yael Edan	_____
Approved by the advisor	Prof Joachim Meyer	_____
Approved by the Dean of the Kreitman School of Advanced Graduate Studies		_____

2006

Beer-Sheva

This work was carried out under the supervision of
Prof Yael Edan and Prof Joachim Meyer

In the Department of Industrial Engineering and Management

Faculty of Engineering Sciences

Acknowledgments

My gratitude is extended to my advisors, **Prof. Yael Edan**, for her guidance, her constant assistant, her immense knowledge and for providing me with the opportunity to conduct this research. **Prof. Joachim Meyer**, for his valuable remarks and priceless input that were essential in this thesis and for enriching this work with his unique view.

I would like to thank **Prof. Lea Friedman** for her consultations in planning the preliminary experiment structure and **Dr. Masha Maltz** for her help in developing the preliminary experiment procedure.

I would like to extend thanks to **Nissim Abuhazira**, **Ariel Plotkin** and **Yossi Zahavi** for their administrative help and cooperation.

I wish to express my gratitude to the members of my Ph.D. committee: **Prof. David Shinar**, **Prof. Itzhak Shmulevich** and **Prof. Avraham Shtub** for their comments, which helped improve my research.

I would like to thank my colleagues and classmates, **Shahar Laykin**, **Ami Eliav**, **Uri Kartoun**, **Juan Wachs** and **Yoash Hasidim** who have been a good company in the long hours during these years.

Avital Bechar.

Table of Contents

List of Figures	II
List of Tables	IV
List of Appendixes	V
List of Symbols	VI
Abstract	VIII
1 INTRODUCTION	1
1.1 Problem description	1
1.2 Research objectives	3
1.3 Research significance	3
1.4 Research contributions and innovations	4
1.5 Thesis structure	5
2 SCIENTIFIC BACKGROUND	7
2.1 Autonomous Robots	7
2.2 Agricultural robots	9
2.3 Human-Robot Collaboration	11
3 METHODOLOGY	15
3.1 Problem objective	15
3.2 Outline	15
3.3 Definitions	15
3.4 Assumptions	16
3.5 Collaboration levels	16
3.6 System objective function	16
3.7 Numerical computation	17
3.8 Experiment	17
3.9 Performance measures	18
4 FORMULATION OF AN OBJECTIVE FUNCTION	19
4.1 General	19
4.2 Objective function	19
4.3 Signal Detection Theory	23
5 NUMERICAL COMPUTATIONS	32
5.1 Numerical computation of objective function with optimal cutoff points	32
5.2 Sensitivity analysis	44
5.3 Summary and conclusions	50
6 MELON DETECTION EXPERIMENT	53
6.1 General	53
6.2 Apparatus and design	53
6.3 Procedure	57
6.4 Results	59
7 DISCUSSION	93
8 CONCLUSIONS and FUTURE WORK	98
8.1 Conclusions	98
8.2 Future research	101
9 REFERENCES	103
10 APPENDIXES	113

List of Figures

Figure 1: An example for a signal-noise (S-N) probability graph.	26
Figure 2: An example for a ROC curve.	27
Figure 3: Flowchart of the target recognition process in an integrated human-robot system. ...	28
Figure 4: System objective function optimal score for different human and robot sensitivities and different target probabilities of the four collaboration levels: a) H, b) R, c) HR, and d) HOR. Each of the subfigures contain a family of isobar curves of the objective function score. Each family corresponds to a different collaboration level.	36
Figure 5: Objective function score for different human and robot sensitivities of the four collaboration levels. H – blue, HR – cyan, HOR yellow and R – red.	37
Figure 6: Maximum objective function score for different human and robot sensitivities and for all four collaboration levels combined.	37
Figure 7: Best collaboration level map for different human and robot sensitivities. The colors represent different collaboration levels: HR – cyan, HOR - yellow and R – red.	38
Figure 8: Best collaboration level map for different P_s , $d'r$ and $d'h$ values. Each subfigure presents a map for different target probability. The colors represent different collaboration levels: HR –cyan, HOR yellow and R – red.	39
Figure 9: System objective function score of the best collaboration level for different P_s , $d'r$ and $d'h$ values. Each subfigure presents a map for different target probability. The contour lines represent equal score areas.	40
Figure 10: System sensitivity of the best collaboration levels for different human and robot sensitivities and different target probabilities and for objective function including (left) and excluding (right) the operational cost. The contour lines represent equal system sensitivity areas.	43
Figure 11: The system likelihood ratio of the best collaboration levels for different human and robot sensitivities and different target probabilities and for objective function including (left) and excluding (right) the operational cost. The contour lines represent equal system likelihood ratio areas.	43
Figure 12: An example for the influence of small deviations from the optimal values of (a) β_{rh} , (b) β_h and (c) β_r when R is the best collaboration level on the objective function score and $P_s=0.5$, $d'r=2$ and $d'h=1$. the colors represents the different collaboration levels: H – blue, HR – cyan, HOR yellow and R – red.	45
Figure 13: An example for the influence of small deflections in the optimal values of (a) β_{rh} , (b) β_h and (c) β_r when HR is the best collaboration level and it objective function score and $P_s=0.2$, $d'r=1$ and $d'h=2$. The colors represent the different collaboration levels: H – blue, HR – cyan, HOR yellow and R – red.	46
Figure 14: An example for the influence of small deflections in the optimal values of (a) β_{rh} , (b) β_h and (c) β_r when HOR is the best collaboration level and it objective function score and $P_s=0.5$, $d'r=2$ and $d'h=2$. The colors represent the different collaboration levels: H – blue, HR – cyan, HOR yellow and R – red.	47
Figure 15: Robotic melon harvester (Edan, 1995).	54
Figure 16: An example for the display during the experiment.	58
Figure 17: Information windows between images.	59
Figure 18: Probability of Hit for the blocks as a function of the stimulus complexity.	62
Figure 19: Probability of a Hit for the five experimental groups as a function of the stimulus complexity.	63
Figure 20: Probability of a hit for the two robot quality levels as a function of the stimulus complexity.	65

Figure 21: Probability of a hit for the two automation levels as a function of the stimulus complexity and block number.	65
Figure 22: Normalized false alarm rate for the three blocks as a function of the stimulus complexity.	67
Figure 23: Image mean time for the five experimental groups as a function of the blocks.	70
Figure 24: Image mean time for the three blocks as a function of the stimulus complexity. ..	70
Figure 26: Block score for the three blocks as a function of the reward system.	73
Figure 27: Block score for the five experimental groups.	73
Figure 28: Probability of a human hit of targets marked by the robot as a function of the automation level.	76
Figure 29: Probability of a human hit of targets marked by the robot as a function of the reward system.	76
Figure 30: Human hit probability of unmarked targets for the experimental groups.	77
Figure 31: Human hit probability of unmarked targets for the different automation levels. ...	78
Figure 32: Human hit probability of unmarked targets for the experimental groups.	79
Figure 33: Human hit probability as a function of the image complexity.	80
Figure 34: The probability of FA of objects already marked by the robot as a function of the automation level.	81
Figure 35: The probability of FA of objects already marked by the robot as a function of the robot quality.	82
Figure 36: Human normalized false alarm as a function of the experimental group.	83
Figure 37: Human normalized false alarm as a function of the block number.	84
Figure 38: Human normalized false alarm as a function of image complexity.	84
Figure 39: Normalized human FA as a function of the robot quality.	86
Figure 40: Human normalized FA for the two robot qualities as a function of the image complexity.	86
Figure 41: The human sensitivity for objects marked by the robot as a function of the automation level.	88
Figure 42: The human sensitivity for objects marked by the robot as a function of the reward system.	88
Figure 43: The human sensitivity for objects marked by the robot as a function of robot quality.	89
Figure 44: The human sensitivity for objects marked by the robot as a function of the automation level and reward system.	90
Figure 45: The human sensitivity for objects marked by the robot as a function of the automation level and robot quality.	91
Figure 46: The human sensitivity for objects marked by the robot as a function of the reward system and robot quality.	91

List of Tables

Table 1: Sheridan's levels of automation of decision and action selection	14
Table 2: The defined independent parameters	34
Table 3: The experimental groups.....	55
Table 4: The repeated measures analysis of variance results.....	60
Table 5: Post-hoc comparisons between the five Newgroups.....	61
Table 6: Post-hoc comparisons between the Block*Complexity combinations.	62
Table 7: The repeated measures analysis of variance results.....	64
Table 8: post-hoc comparisons between the Complexity*Robot-quality combinations.....	65
Table 9: The repeated measures analysis of variance results.....	66
Table 10: The repeated measures analysis of variance results.....	68
Table 11: The repeated measures analysis of variance results.....	69
Table 12: The repeated measures analysis of variance results.....	71
Table 13: Post-hoc comparisons between the Complexity*Automation-level combinations..	72
Table 14: The repeated measures analysis of variance results.....	72
Table 15: The repeated measures analysis of variance results.....	74
Table 16: The repeated measures analysis of variance results.....	75
Table 17: The repeated measures analysis of variance results.....	77
Table 18: The repeated measures analysis of variance results.....	78
Table 19: The repeated measures analysis of variance results.....	79
Table 20: The repeated measures analysis of variance results.....	80
Table 21: The repeated measures analysis of variance results.....	82
Table 22: The repeated measures analysis of variance results.....	85
Table 23: The univariate tests of significance results.	87
Table 24: Post-hoc comparisons between the automation level*rewards combinations.	89
Table 25: Post-hoc comparisons between the automation level*robot quality combinations.	90

List of Appendixes

Appendix I:	Transformation of the probability function from X to Z	114
Appendix II:	Expression of Z as a function of β and d'	114
Appendix III:	Development of optimal β_s for human-robot systems without operational costs	115
Appendix IV:	Human optimal hit and false alarm in human-robot systems	117
Appendix V:	Paper: Human-robot collaboration for improved target recognition of agricultural robots	119
Appendix VI:	Analysis of Non optimal cases.....	126
Appendix VII:	The experimental simulator program.....	180
Appendix VIII:	Example for subjects' raw data	210
Appendix IX:	Algorithm for extracting the subjects' performance measures from the raw data recorded in the experiment.....	249
Appendix X:	Statistica data sheets	254
Appendix XI:	Numerical analysis programs.....	257
Appendix XII:	Sensitivity analysis programs	264
Appendix XIII:	Analysis of β_{rh}	270

List of Symbols

β	likelihood ratio, cutoff ratio
μ	mean
σ	standard deviation
CR index	correct rejection
d'	sensitivity
F	density function
FA index	false alarm
F_{CRs}	the correct rejection density function for the system
F_{FAs}	the number of system false alarm objects
H	manual collaboration level
H index	hit
h index	human
HOR	collaboration level where the human supervise the robot
HR	collaboration level where the robot recommends the human
N	the number of objects
N index	noise
p_{FAh}	the human false alarm probability
p_{FAr}	the robot false alarm probability
p_{FArh}	the human probability of not correcting the robot false alarm
p_{Hh}	the human probability of detecting a target which the robot did not detect
p_{Hr}	the robot probability of a hit
p_{Hrh}	the human probability of confirming a robot hit
p_{Hs}	the system probability for a hit
p_{Ms}	the probability of a system miss
P_s	target probability
R	fully autonomous collaboration level
r index	robot
rh index	human operation on robot operations
ROC	receiver operating characteristic
S index	signal
SDT	signal detection theory
t_{CRh}	the HO correct rejection time

t_{CRrh}	the human time to correctly reject a robot false alarm
t_D	decision time
t_{FAh}	the human false alarm time
t_{FArh}	the human time needed to correct a robot false alarm
t_{Hh}	the human time required to hit a target which the robot did not hit
t_{Hrh}	the human time required to confirm a robot hit
t_M	motoric time
t_{Mh}	the human time invested when missing a target which the robot did not hit
t_{Mrh}	the human time lost when a robot hit is missed
t_r	the robot time
t_s	the system time that is required to perform the task
V_{AR}	payoff ratio $V_{AR} = -\frac{V_{FA}}{V_H}$
V_C	the cost of one object recognition operation
V_{CR}	the gain from a single correct rejection
V_{CRs}	the system gain for correct rejection
V_{FA}	the damage from a single false alarm
V_{FAs}	the system penalty for false alarms
V_H	the gain from a single hit
V_{Hs}	the system gain for target detection (hit)
V_{Is}	the system objective function
V_M	the penalty of a single miss
V_{Ms}	the system penalty for missing the target (miss)
V_t	the cost of one time unit
V_{Ts}	the system operation cost.
X	The measurement unit X of object features
x	a position along coordinate X , represents the cutoff point
Z	the distance in standard deviation units
$*$	indicates optimal value

Abstract

Autonomous robots are systems that can perform tasks, make decisions, and act in real-time without human intervention. They are best fit for applications that require repeatable accuracies and high yield under stable conditions. However, they lack the capability to respond to ill-defined, unknown, changing, and unpredicted events such as exist in unstructured environments, and the current status of autonomous robots still falls short of implementing solutions to most real-world applications. Furthermore, the problems are enhanced in applications dealing with natural objects since the objects also have high degrees of variability, and their positions and orientations are not known and cannot be determined *a priori*. This complicates the robotic system and results in a system that is difficult and expensive to develop. Integrating a human operator into a robotic system can help increase target recognition rate and reliability, reduce the complexity of the robotic system, and handle unknown and unpredictable events that autonomous systems are incompetent to deal with.

This work focuses on aspects of collaboration levels of an integrated human-robot system for target recognition tasks in unstructured environments. We present a methodology to determine the best collaboration level based on the system, the environment, and the task parameters, and the evaluation and prediction of its performance.

Four human-robot collaboration levels for target recognition tasks were defined, tested, and evaluated. The collaboration levels were designed specifically for target recognition tasks and adjusted to an extensive range of automation, from manual to fully autonomous. The collaboration level can be custom fitted to the human or the robot to increase system performance.

An objective function for target recognition in human-robot systems was developed to allow computation of the expected value of system performance given the human, robot, environmental and task parameters. The objective function includes operational and time costs, both of which are important in the evaluation and optimization of system performance. The objective function quantifies the multitude of influencing parameters through a weighted sum of performance measures, and enables the prediction of system performance and the desirable level of collaboration. It can also be applied to help design optimal systems for specific tasks.

A methodology for determining the best collaboration level based on the human, robot, task, and environmental variables was developed. Numerical computations of the developed objective function combined with signal detection theory were applied for the defined

collaboration levels, and a sensitivity analysis of the influencing variables was performed on the optimum values. These developments provide the basis for adjusting the combined human-robot system to each task and environment and aid in effective system design.

This research provides tools to develop an integrated human-robot system for target recognition in unstructured environments. This will help simplify the robotic system, reduce its costs and improve its performance and robustness. System designers can use the objective function to predict the performance of a developed system and to determine the best-fit collaboration levels *a priori*. The system can be designed to fit a specific task and environment.

Methodology

Research developments

The research consists of three interrelated and independent developments related to human-robot cooperation in target recognition tasks: definition of human-robot collaboration levels; development of an objective function to evaluate performance; and, a methodology to determine the best collaboration level.

The first development includes the definition of four human-robot collaboration levels fitted for target recognition tasks in unstructured environments. The collaboration levels are based on the four degrees of autonomy from Sheridan's scale of "action selection and automation of decision." They are compatible with an extensive range of automation, they are denoted as H, HR, HOR and R from manual to fully autonomous, respectively. The recognition process is performed in two sequential steps; first the robot detects the targets, then the human acts on these detections.

The system objective function is designed to enable determination of the expected value of task performance, given the parameters of the system, the task, and the environment. The objective function parameters can be divided into four major categories - human, robot, environment, and task parameters. The objective function includes five parts: correct detection (hit); false alarm (FA); miss; correct rejection, and operational cost. The operational cost variable includes costs related to operational time and costs of actions that should be performed on the detected objects, either hit or false alarm (*e.g.*, picking detected melons, landmine neutralization).

A methodology was developed to determine the best collaboration level for the design of a specific system and to use in modeling and simulating the system's performance. To describe the relations between the objective function parameters, we utilized a modified version of signal detection theory (SDT). This reduced the number of independent variables

by relating human and robot performance measures (*e.g.*, hit and false alarm probabilities) to their basic characteristics (*e.g.*, sensitivity and cutoff point decisions).

Numerical computations

Numerical computations were implemented on a personal computer with Matlab 7™ software. The numerical analysis examines the influence of the human and robot characteristics (*e.g.*, sensitivity) and the effect of different human-robot collaboration levels on the system objective function. It determines the optimal human and robot characteristics for different task characteristics, and the best collaboration level for different human, robot, and task characteristics. In addition, a sensitivity analysis was performed on the optimal characteristics and their influences on the best collaboration level and the system objective function value.

Experiment

An experimental system was designed to test and examine the influence of different human-robot collaboration levels in a specific target recognition task. The experimental system consisted of a simulator using images taken from a melon field by a video camera mounted on a robotic melon harvester moving along a melon row, and the participants were asked to identify melons in the images. 120 undergraduate students participated in the experiment. The participants were divided randomly into 10 groups, 12 students per group, each of which was assigned one of two objective function weights (parameters), one of two different robot qualities (high and low), and one of three possible collaboration levels. The images were viewed by a panel of experts and classified according to three levels of complexity and arranged in three statistical blocks. During the experiment the human operator's activities, the objects marked, and the time signature of each action were recorded. Performance measures were calculated from the recorded raw data.

A statistical analysis was performed on the data. Analyses examined the influence of the block, the image complexity, the reward, the level of cooperation, and the robot quality on both system and human performances. Statistical analyses, including repeated measures analysis of variance, a Fisher LSD post-hoc comparison, and a general linear model of univariate tests of significance, were all performed with Statistica™ 7 on a personal computer.

Results

Numerical analysis

The numerical analysis was executed for several target probability conditions, P_s , human and robot sensitivities, d'_h and d'_r , and payoff value ratios, V_{AR} . The optimal likelihood ratios, β_r , β_h and β_{rh} were determined. The system objective function was analyzed for cases including and excluding the operational cost variable. The objective function excluding the operational cost serves as the upper boundary of system performance and demonstrates the effectiveness of the best collaboration level.

In the analysis each collaboration level is represented as a plane in the parameter's space, where the Z-axis is the objective function value. The intersection of all collaboration level planes creates a plane of the highest objective function value for each parameter combination. The collaboration level that achieved the highest score in each parameter combination is defined as the best collaboration for those combinations and can be presented in a domination map.

Sensitivity analysis was performed for the human, robot, and environmental independent parameters since these can vary during task performance and their precise values are unknown. The influence of the changes in the optimal values of the parameters on the objective function score and the best collaboration level were analyzed to reflect cases in which the human and robot performances were in optimum proximity or in which the environment parameters diverged slightly from their expected or calculated values. The parameters analyzed were the human likelihood ratio, β_{rh} and β_h , human sensitivity, d'_h , the robot likelihood ratio, β_r , robot sensitivity, d'_r , and the target probability, P_s . The payoff ratio, V_{AR} , the time cost, the operational cost, and the hit rewards were not sensitivity analyzed since the parameters are fixed during the entire task.

The numerical analysis indicates that when target probability increases the system is less influenced by false alarms, and therefore, the probabilities of hits and false alarms increased, the likelihood ratios β_r , β_h , and β_{rh} decreased, the operational cost increased, and the objective function score increased. For all collaboration levels the highest objective function score increases with the increase in human and robot sensitivities. A comparison between the HR and the HOR collaboration levels showed that the HR collaboration level performs better when the target probability is low and the robot sensitivity is low for the objective function that includes operational cost. The H collaboration level is never the best collaboration level probably due to its high operational cost and low hit rate relative to the other collaboration levels. Thus, collaboration of human and robot in target recognition tasks will always improve the optimal performance of a single human detector. This finding indicates that when robot

sensitivities are higher than human sensitivities the best collaboration level is R. Analysis of the overall system sensitivity showed that when working in the best collaboration level, the system likelihood ratio and the system sensitivity both decrease with the increase in the target probability. Moreover, the system sensitivity never decreases beneath the robot sensitivity.

Elimination of the operational cost from the objective function unites HR and HOR into one collaboration level, since the only difference between the HR and the HOR collaboration levels, as expressed in the system objective function, is in the time parameters. When omitting the operational cost variable from the objective function equation, there is no difference between these two collaboration levels. The objective function score increased. The best collaboration level for the objective function excluding the operational cost part will be the HOR collaboration level for the entire sensitivity space and for all target probabilities. The combination of both human and robot in the HOR collaboration level increases the sensitivity in most cases and increases the probability of a hit while reducing the probability of false alarms.

A sensitivity analysis of the optimal values of the robot and human likelihood ratios, β_r , β_h , and β_{rh} , of the best collaboration levels showed that any change in both directions from the optimal values will decrease the objective function score of the best collaboration level. A sensitivity analysis of d'_r , d'_h , and target probability showed that small, positive deviations from the optimal values will increase the objective function score of the best collaboration level. Deviations in the optimal value of d'_h have no influence on the objective function when the best collaboration level is R.

The sensitivity analysis showed that small deviations in the optimal values of the analyzed parameters may shift the best collaboration level from one to another. For each parameter the behavior of the shift is different. But for deviations in the optimal value of β_r , β_h , β_{rh} , d'_r , and d'_h , the best collaboration level will never be H and will never shift to H.

Experiment

The experiment results were correspondence with the numerical analyses. Experimental results indicate that the reward system has a significant effect on the system hit rate, false alarms, and the system objective function score. The system hit rate of participants who were rewarded for maximum hits was higher than for the others; likewise, the system false alarms of participants who were rewarded for minimum FA was lower than for the others. The reward has no influence on the system time.

It was found that the robot quality has a significant influence on the system hit rate, and the system objective function score: an increase in the robot quality led to increases in the

system objective function score of the experiment. Although the increase in robot quality reduces the number of system false alarms, this finding was insignificant. However, a higher level of automation (HOR) combined with a 'low quality' robot, significantly increases the number of false alarms when compared to no automation (HO). For the 'low quality' robot, the increase in the automation level increases detection time, but for the 'high quality' robot, increases in the automation level reduce the detection time. This effect was partially significant. A 'low quality' robot impairs the system hit rate and overall score. As image complexity increases, the system hit rate decreases, the system false alarms number increases, and the system time increases – all at significant levels.

Statistical analysis indicates that the reward system has a marginally significant effect on human hits of robot marks (P_{Hrh}), a significant affect on human hits of the objects the robot did not mark (P_{Hh}), and the human sensitivity (d'_h). The human hit rates, P_{Hrh} and P_{Hh} , of participants were rewarded for maximum hits, were higher than for the participants who were rewarded for minimum FA; likewise, the human sensitivity of participants who were rewarded for maximum hits was higher than for those who were rewarded for FA. It appears that the participants internalize the reward structure, whether it was to minimize the number of false alarms or to maximize the number of hits, and as such they focus their attention on the reward.

Robot quality has a significant influence on human hits of the robot marks (P_{Hrh}), the human false alarms of the robot marks (P_{FArh}), the human false alarms of the objects the robot did not mark (P_{FAh}), and the human sensitivity. Increases in robot quality increased the system objective function score of the experiment. The increase in robot quality increases the values of P_{Hrh} , P_{FArh} , P_{FAh} , and the human sensitivity. It seems that during the experiment the participants perceived the robot quality and relied on the robot decisions when its quality was high.

The image complexity significantly influenced the number of human hits and the false alarms of objects the robot did not mark (P_{Hh} and P_{FAh}). An increase in the image complexity decreases P_{Hh} and increases P_{FAh} .

The collaboration level significantly affects human hits and false alarms of objects the robot did mark (P_{Hrh} and P_{FArh}). Increase in the automation level increases P_{Hrh} and P_{FArh} . It seems that for high automation levels the participant tends to accept the robot decisions. Furthermore, the human sensitivity of the participants who had a 'high quality' robot, decreased with increase in the automation level. This finding indicates that the increase in robot quality reduces both human control and sensitivity.

The block number significantly affected the system false alarm (decreases), the system time (decreases), the experiment score (increases), and the human false alarms of the objects the robot did not mark (P_{FAh}). The values and the confidence intervals of P_{FAh} decreased with the increase in the block number. This hints at a learning effect during the experiment.

Conclusions

This thesis includes a comprehensive development to evaluate the influence of different collaboration levels on the performance of an integrated human-robot system for target recognition tasks in different cases. It includes the development of collaboration levels, an objective function to measure system performance, and a methodology to determine the best collaboration level. The objective function was evaluated using numerical and experimental analyses.

Numerical analysis results indicate that the best system performance, the optimal performance measures values, and the best collaboration level depend on task, environment, human, and robot parameters as well as the system characteristics. Since the number of independent parameters is vast and, in addition, there are interactions between the parameters, a prediction of system performance and the optimal solution is comprehensive and not obvious. However, it can be determined by investigating the objective function.

The sensitivity analysis finding can be exploited for the design and operation of an integrated human-robot system under dynamic and realistic conditions where the true value of the parameters is unknown and the resolution and accuracy are low, or in cases where the parameters are dynamic and drifting around their expected values.

Throughout the development, great care was taken to quantify the independent parameters and the results and to validate the theoretical findings with the experiment. The objective function was developed in a way to facilitate a comparison of different systems, environments, and tasks.

The advantage of this method is that it can be conducted off-line and even in the absence of an actual system, and it allows the comprehensive survey of the influence of various parameters on the system performance. System designers can use these methodologies to develop an adjusted, integrated human-robot system for target recognition tasks in unstructured environments. Furthermore, this methodology can be used to analyze system performance during the task performance and to recommend the best collaboration and the human performance on-line.

Contributions

The main contributions of this research are:

- The definition and evaluation of human-robot collaboration levels for target recognition tasks. The collaboration levels were based on Sheridan's ten levels of automation and were designed specifically for target recognition tasks. The collaboration level can be fitted to the human or robot to increase system performance. The collaboration levels were mathematically modeled to quantify its influence on system performance.
- The development of an objective system function for target recognition in human-robot systems to allow computation of the expected value of system performance given the human, robot, environmental, and task parameters. The objective function can be fitted to different tasks and environments, to predict system performance and desirable level of collaborations, and to help design optimal systems for specific tasks. The objective function includes operational and time costs that are important both in evaluation and optimization of system performance.
- A methodology for determining the best collaboration level based on the human, robot, task, and environment parameters. The methodology consists of a numerical analysis of the developed objective function combined with signal detection theory. The methodology makes it possible to improve system performance and to fit the best collaboration level for each case.

Keywords: collaboration levels, human robot interaction, target recognition, unstructured environments, objective function

This thesis is in part based on the following publications:

Journal papers

1. Bechar, A. and Edan Y. 2003. Human-robot collaboration for improved target recognition of agricultural robots. *Industrial Robot* 30 (5): 432-436. (*Invited paper*).

Reviewed conference papers

1. Edan Y and Bechar A. 1998. Multi-purpose agricultural robot. Proceedings of the Sixth IASTED International Conference, Robotics And Manufacturing, Banff, Canada. 205-212.
2. Bechar A., Edan Y. and Meyer J. 2004. An objective function for performance measurement of human-robot target recognition systems in unstructured environments. IEEE SMC Paper No. 520. International Conference on Systems, Man and Cybernetics, The Hague, The Netherlands.
3. Bechar A., Edan Y. and Meyer J. 2006. Optimal Collaboration in Human-Robot Target Recognition Systems. IEEE SMC Paper No. 01113. International Conference on Systems, Man and Cybernetics, Taipei, Taiwan.

Conference papers

1. Bechar A., Edan Y., Meyer J., Rotman M. and Friedman L. 2000. Human-machine collaboration for melons detection. ASAE Paper No. 003143. ASAE Annual International Meeting, Milwaukee, Wisconsin.
2. Bechar A. and Edan Y. 2000. Human-robot collaboration for agricultural robot guidance. ASAE Paper No. 003135. ASAE Annual International Meeting, Milwaukee, Wisconsin.
3. Bechar A. and Edan Y. 2002. Human-robot collaboration in agricultural tasks. 12th Industrial Engineering and Management Conference, IE & M 2002. Tel-Aviv, Israel.
4. Bechar A., Edan Y. and Meyer J. 2003. Performance Measurement of collaborative human-robot target recognition systems in unstructured environments. ICPR Paper No. 0321. 17th International Conference on Production Research, Blacksburg, Virginia.
5. Bechar A., Edan Y. and Meyer J. 2004. Optimal levels of human-robot collaboration for target recognition in unstructured environments. (*Abstract*). The Annual Meeting of the Operations Research Society of Israel, Ashkelon, Israel.
6. Bechar A., Edan Y. and Meyer J. 2005. Influence of operational costs on human-robotic performance in target recognition tasks. 18th International Conference on Production Research, Salerno, Italy.
7. Bechar, A., Y. Edan and J. Meyer. 2006. Human-robot collaboration methods for target recognition tasks in unstructured environments. (*Abstract*). The Israel Conference on Robotics – ICR 2006. Tel-Aviv, Israel.

1 INTRODUCTION

1.1 Problem description

Robots and autonomous systems perform well in industrial environments where working conditions are constant, structured and predictable (Lopez-Juarez and Howarth, 2002; Gonzalez-Galvan et al., 2003). Unstructured environments such as agriculture, military, underwater and space are characterized by rapid changes in time and space (Bechar et al., 2003). The terrain, vegetation landscape, visibility, illumination, and other atmospheric conditions are not well defined, continuously vary, have inherent uncertainty, and generate unpredictable and dynamic situations. In some environments the objects or the targets are also unstructured and differ in size, hue, orientation, reflection and shape, in contrary to structured object like cube, pyramid or bolt where the object definitions are fixed and rigid. This results in a lack of information, due both to inadequate sensor performance as well as the limited ability of computers to reason and plan in such environments (Everett and Dubey, 1998). Hence, in unstructured environments operation of an autonomous robot is difficult (Al-Jumaily and Amin, 2000; Fletcher et al., 2005), and not advisable (Penin et al., 1998). Moreover, "the current status still falls short of implementing solutions to most real-world applications" (Kim and Shim, 2003). Furthermore, in such environments there are many situations in which autonomous robots fail due to the many unexpected events (Steinfeld, 2004). The problems are enhanced in applications dealing with natural objects (*e.g.*, medical, agriculture environments) since the objects also have high degrees of variability (in shape, texture, color, and size) and their positions and orientations are not known and cannot be determined *a-priori*. This further complicates the robotic system and results in a system which is difficult and expensive to develop.

Target recognition is a common task and usually an essential part of a robotic system (Bicho et al., 2000; Ye and Tsotsos, 1999). However, automatic target recognition in unstructured environments is characterized by poor performances (Edan, 1999; Ponweizer et al., 2005) due to the high degree of objective variability and changing and unknown environmental conditions (Bhanu et al., 2000; Venkataramani et al., 2005).

Humans have superior recognition capabilities (Matthews et al., 1996; Hill et al., 1997; Ayrulu and Barshan, 2001) and can easily adapt to changing environmental and objective conditions (Rodriguez and Weisbin, 2003). Peoples' acute perceptive capabilities enable humans to deal with a flexible, vague, changing, and wide scope of definitions (Chang, 1998). However, a human operator is inconsistent, tends to fatigue and suffer from distractions (Van

Erp et al., 2004), and ultimately might reduce the system's production rate relative to that of a fully autonomous system in a fixed environment. Human operators, then, can impair smooth system operation (Parasuraman et al., 2000) and increase errors.

Autonomous systems are most suitable for cases that require repeatable accuracies and high yields in stable conditions (Holland and Nof, 1999). However, they lack the capability to respond to ill-defined, unknown, changing, and unpredictable events.

The assumption of this research is that integrating a human operator into a robotic system can help increase target identification rate and reliability, reduce the complexity of the robotic system (Kirlik et al., 1993; Sidenbladh et al., 1999; Itoh et al., 2000; Parasuraman et al., 2000), and handle unknown and unpredictable events that the autonomous systems are incompetent to deal with (Pook and Ballard, 1996).

Human-robot collaboration research addresses the issue of how the human-robot association affects automation in aspects of data acquisition, data and information analysis, decision making, action selection, and action implementation (Parasuraman et al., 2000), in accordance with specific task or sub-task goals and parameters (Bechar et al., 2004). Types and levels of automation are evaluated by examining their associated human performance consequences such as mental workload, situation awareness, complacency, and skill degradation (Guida and Lamperti, 2000; Steinfeld et al., 2006). Parasuraman et al. (2000) developed a model for types and levels of automation that provides a framework and supplies an objective basis for determining the degree of automation for each system. Sheridan (1978) divides automation into ten levels, from fully autonomous, with no human intervention to fully manual. Xu et al. (2002) modeled the human-computer strategies through cascade neural networks for a driving task. Fletcher et al. (2005) developed an on-line driver assistance system that supports the driver and provides immediate feedback.

Rodriguez and Weisbin (2003) indicate that human capabilities of perception, thinking, and action are still unmatched in environments with anomalies and unforeseen events, and that human and robot skills are complementary. By taking advantage of human perceptive faculties and the autonomous systems' accuracy and consistency, the combined human-robotic system can be simplified, resulting in improved performance (Parasuraman et al., 2000).

In target recognition tasks there are several performance measures to evaluate quality of recognition (Maltz, 2000; Swets et al., 2000; Filippidis et al., 2000; Sun et al. 2004; Pei and Lai, 2001; Gao and Hinders, 2005) including probability of target detection (hit), probability of non-target detection (false alarm; Liu and Haralick, 2002), and detection time (Steinfeld et al., 2006). However, the quality and value of performance measures are task dependent. For

example, in medical applications, the hit and false alarm probabilities are more important than the detection time, and therefore maximum hit probability with minimum false alarm probability is necessary. On the other hand, in real-time systems detection time is critical and should be minimized. In detecting landmines, however, the goal is a high hit rate while the false alarm rate and detection times are usually less important. Hence, it is essential to combine the different performance measures (Rodriguez and Weisbin, 2003) and consider the task goal when evaluating system performance. The given examples were presented as extreme cases to indicate the importance of the different weights; they do not necessarily present different industries.

System performance also depends on environmental conditions (*e.g.*, illumination, visibility, terrain type), human conditions (fatigue, stress, workload), and system parameters (error, accuracy, reliability). Hence, these must also be considered when evaluating system performance. For example, environmental conditions such as highly occluded objects, shading, and changing illumination conditions strongly influence target recognition performance of both human and automatic systems. Maltz and Shinar (2003) found that system cueing helps in complex tasks but lowers the performance in simple tasks. A methodology to determine the appropriate alerting thresholds and quantify the possible potential benefits through changes in the design of the system shown by Kuchar (1996) reduced the frequency of false alarms in traffic alert and collision avoidance system. Meyer and Kuchar (2006) analyzed the effect of an alerting system on signal detection performance and found that the introduction of an alerting system may actually lower performance if the operator uses non-optimal weights for the warning information.

1.2 Research objectives

The research objectives include developing:

- Human-robot collaboration levels suitable for target recognition tasks in unstructured environments.
- An objective function to evaluate performance of an integrated human-robot system for target recognition tasks, and to compare the performance of different target recognition systems and cases.
- A tool to determine the best collaboration level based on the system, task, and environmental parameters.

1.3 Research significance

Target recognition is an important and essential task in most robotic systems. The development of an autonomous system operating in an unstructured environment is

problematic, complex, and expensive. This research provides tools to develop an integrated human-robot system for target recognition in unstructured environments. This will help simplify the robotic system, reduce its costs and improve its performance and robustness.

Human-robot collaboration levels were developed for target recognition in unstructured environments. The four collaboration levels defined fit an extensive range of automation, from manual to fully autonomous. The advent in using four levels of collaboration, of which only three include a human operator, simplifies the integrated human-robot system, thus enabling the human to better control each collaboration level, remember the characteristics of each collaboration level, and increase his awareness when shifting from one collaboration level to another.

An objective function was developed to evaluate performance of an integrated human-robot system for target recognition tasks. The objective function is task dependent and consists of a multitude of performance measures. It includes operational costs and time costs, which consider the system characteristics involved in the performance evaluation and not merely the detection quality parameters. It makes it possible to rank and compare different systems and to analyze the influence of different human, robot, task, and environment parameters on the system performance.

Additionally, a methodology to determine the best collaboration level based on the objective function was developed. The methodology can improve system performance when environmental conditions are known *a-priori*. Such developments form the basis for effective system design and enable the easy adaptation of the combined human-robot system to each new task and environment.

1.4 Research contributions and innovations

Integrating humans into robotic systems can help simplify the systems and improve their performances. By taking advantage of human capabilities, a more flexible and simpler system that can deal with more dynamic and complex conditions can be designed.

Human-robot collaboration levels for target recognition tasks were defined, tested, and evaluated. The collaboration levels were based on Sheridan's (1978) ten levels of automation and were designed specifically for target recognition tasks. The collaboration level can be fitted to the human or robot to increase system performance.

A system objective function for target recognition in human-robot systems was developed to allow computation of the expected value of system performance given the human, robot, environmental, and task parameters. The objective function quantifies the multitude of parameters influencing the system through a weighted sum of performance measures. The weights enable one to adapt the system's objective function to different tasks and

environments, to predict system performance and desirable level of collaboration, and to help design optimal systems for specific tasks. In addition, the objective function developed in this thesis includes operational and time costs that are important in both evaluation and optimization of system performance.

A methodology was developed for determining the best collaboration level based on human, robot, task, and environment variables. Numerical analysis of the objective function combined with signal detection theory was applied for the defined collaboration levels, and sensitivity analysis of the influencing variables was performed on the optimum values. The methodology makes it possible to improve system performance and to fit the best collaboration level for each case.

System designers can use the objective function to predict the performance of a developed system and to determine the best-fit collaboration levels *a-priori*. The system can be designed to fit a specific task and environment.

1.5 Thesis structure

The dissertation is organized as follows: chapter 2 presents a literature review on autonomous robots, agricultural robots and human-robot collaboration. The methodology chapter starts with the description of the problem objective of an integrated human-robot system for target recognition tasks in unstructured environments, continues with the outline of the research, definitions of major terms, the research assumptions, the collaboration levels used in this work and a brief presentation of the system objective function, the numerical computations conducted on the system objective function and the experiment conducted. The chapter ends with a description of the performance measures. Chapter 4 deals with formulation of the system objective function. The theoretical equation is developed and a signal detection theory (SDT) model is modified to fit the case of a human-robot system in a target recognition task. The SDT equations are included in the system objective function in order to simplify it. Chapter 5 begins with numerical computations of the optimal cutoff ratios (β_s) based on the system objective function to determine the optimal human and robot parameters for different task parameters and to determine the best collaboration level for different human, robot, and task parameters (section 5.1). It continues with sensitivity analyses of the human, the robot, and the independent environmental parameters and the influence of changes in the optimal values of the parameters on the objective function score and the best collaboration level to reflect cases in which the human and robot performances were in the proximity of optimum values or when the environmental parameters diverged only slightly from their expected or calculated values (section 5.2). Findings are summarized with conclusions at the end of the chapter (section 5.3). Chapter 6 describes the apparatus and

design of the melon detection experiment conducted on a simulated human-robot system, the experimental procedure and results.

A discussion of the results comparing the experiment to the numerical calculations is presented in chapter 7. The thesis concludes in chapter 8, including conclusion and discussion of future research.

2 SCIENTIFIC BACKGROUND

The scientific background includes a review of autonomous robots and their limitations, and the current status of agricultural robots. Human-robot collaboration methods that served as the basis for the development of the thesis methodologies are also reviewed.

2.1 *Autonomous Robots*

Autonomous robots are systems that can perform tasks, make decisions, and act in real-time without human intervention. They are required in fields, which normally demand reductions in manpower and workload, and are best-suited for applications that require repeatable accuracies and high yield under stable conditions (Holland and Nof, 1999). However, they lack the capability to respond to ill-defined, unknown, changing, and unpredicted events.

Sensing and reasoning are the basic requirements for attaining a reasonable degree of autonomy (Oriolo et al., 1998). According to Rucci et al. (1999), autonomous robotic systems must possess a high degree of flexibility to adapt to the continuously changing conditions of the environment as well as to the information from their own sensors and motors.

In designing autonomous robotic systems, two important challenges are frequently encountered. The first deals with the nonlinear, real-time response requirements underlying the sensor-motor control formulation. The second deals with how to model and use the approach with which a human will address such a problem (Ng and Trivedi, 1998).

In recent years, an increasing amount of robotics research has focused on autonomous mobile robots in unstructured environments (indoors and outdoors). Comprehensive research investigated many aspects of this area. The research can be divided into two categories. The first category deals with the basic elements necessary for autonomous robots, such as obstacle avoidance (Chakravarthy and Ghose, 1998; Ku and Tsai, 1999; Carelli and Freire, 2003; Belkhouche and Belkhouche, 2005), self-localization and map building (Neira et al., 1999; Mouaddib and Marhic, 2000; Olson, 2000; Ip and Rad, 2004; Se et al., 2005), and navigation and path planning (Araújo and de Almeida, 1999; Oriolo et al., 1998; Cherif, 1999; Millan and Floreano, 1999; Tsourveloudis et al., 2001; Garcia and De Santos, 2004; Roy, 2005). The second category deals with applications such as vehicle dispatching for transportation (Benyahia and Potvin, 1998; Yamashita, 2001; Lacomme et al., 2005), security, reconnaissance and exploration (Dollarhide and Agah, 2003; Birk and Kenn, 2002; Flann et al., 2002; Matthies et al., 2002; Thrun et al., 2004), industry (Klas and Rolf, 1999; Peungsungwal et al., 2001), agriculture (Torri, 2000; Van Henten et al., 2003), underwater missions (Kondo and Ura, 2004; Rosenblatt et al., 2002), maintenance and service (Luk et al.,

2005; Balakirsky et al., 2004; Aracil et al., 2003), and space missions (Arena et al., 2004; Chirikjian et al., 2002).

Target recognition is a critical element in most robotic systems (Bicho et al., 2000; Ye and Tsotsos, 1999; Bechar and Edan, 2003; Tan et al., 2005); for example, the detection of parts in assembly lines, the detection of landmarks in autonomous navigation, the detection of hand gestures for robot control, or the detection of fruits for robotic harvesters. Target recognition is a common and important topic in many other research areas such as medical and brain research (Potts and Tucker, 2001; Bhanu and Fonder, 2004), quality assurance (Schmitter, 1995), human factors (Aviram and Rotman, 2000; Maltz and Meyer, 2001), agriculture (Sevila & Baylou, 1991; Dobrusin et al., 1992; Plebe and Grasso, 2001; Bulanon et al., 2001; Hannan and Burks, 2004; Alchanatis et al., 2005), and remote sensing using infra-red (Jean et al., 2000; Nelson, 2001), radar (Liang and Palakal, 2002; Banerjee et al., 1999), visual images (Patnaik and Rajan, 2000), and hyperspectral imagery (Du and Ren, 2002).

Target recognition systems have undergone a variety of changes due to intensive technological developments. Initial systems exploited signal-processing techniques to detect ground-based targets based on one-dimensional signals (Gilmore, 1991). Limitations of these systems eventually led to the development of automated target recognizers that processed two-dimensional digital images to detect, classify, and identify targets (Gilmore, 1991). Target recognition can be described as a multilevel process requiring a sequence of algorithms at low, intermediate, and high levels (Bhanu et al., 2000). Generally, such systems are open loop with no feedback between levels, and assuring their performance at the given probability of correct identification and probability of false alarm is a key challenge (Bhanu et al., 2000). The main limiting parameters in target recognition are the characteristics of unstructured environments (Venkataramani et al., 2005); thereby restricting the system's ability to determine if an object can be classified as a target. The attributes of unstructured environments also impede the quantification or numericalization of target description criteria, which are determined by human operators and are implemented by autonomous detection algorithms.

Automatic target recognition is characterized by poor performances (Edan, 1999; Ponweizer et al., 2005), and detection is restricted to a certain group of objects with similar physical characteristics for which the autonomous detection algorithms were developed. Maltz and Shinar (2003) found that system cueing helps in complex tasks but lowers the performance in simple tasks. A methodology to determine the appropriate alerting thresholds and quantify the possible potential benefits through changes in the design of the system

shown by Kuchar (1996) reduced the false alarms in traffic alert and collision avoidance system. Meyer and Kuchar (2006) analyzed the effects of an alerting system on signal detection performance and found that the introduction of an alerting system may actually lower performance if the operator uses non-optimal weights for the warning information.

Different optimization methods have been developed and implemented for parallel detection systems, *e.g.*, least squares, weighted least squares, mean square error; Bayesian weighted least squares, and maximum likelihood estimate (Hall, 1992). On the other hand, humans have superior recognition capabilities (Matthews et al., 1996, Hill et al., 1997; Ayrulu and Barshan, 2001) and can easily adapt to changing environmental and objective conditions (Rodriguez and Weisbin, 2003). Their acute perception capabilities enable humans to deal with a flexible, vague, changing, and wide scope of definitions (Chang et al., 1998). However, a human operator is not consistent, tends to fatigue, and suffers from distraction (Van Erp et al., 2004).

2.2 *Agricultural robots*

Agricultural tasks have been an important area of application for different kinds of technologies to improve crop production and other farming related operations. In the 20th century, technological progress has reduced the need for the manpower traditionally devoted to these activities in the developed countries by a ratio of 1/80 (Cereset al., 1998; Pons et al., 1996). Robots are perceptive machines that can be programmed to perform a variety of agricultural tasks such as cultivating, transplanting, spraying, and selective harvesting (Edan, 1999). Agricultural robots have the potential to raise the quality of the fresh produce, lower production costs, and reduce the drudgery of manual labor (Edan, 1995).

Activating a continuously moving robot in the agricultural environment is a difficult task, as a result of the unpredictable locations of targets that are difficult to locate (due to the natural variability in size, shape, color, and texture) and since the terrain, the landscape, the atmospheric conditions, and other environment parameters are unstructured, uneven, and continuously change. The development of systems that can cope with the variety of agricultural situations and unknown disturbances encountered is difficult and complicated.

Extensive research has been conducted in applying robots to a variety of agricultural tasks, and their technical feasibility has been widely demonstrated: picking citrus (Harrell and Levi, 1988; Harrell et al., 1990; Kawamura et al., 1985; Kawamura et al., 1987; Edan et al., 1990; Edan et al., 1991; Jiminez et al. 2000; Plebe and Grasso, 2001; Brown, 2002; Hannan and Burks, 2004; Muscato et al., 2005), picking apples (Grand d'Esnon et al., 1987; Bulanon et al., 2001), picking tomatoes (Kondo et al., 1996), picking asparagus, cucumbers, and

harvesting melons (Edan and Miles, 1993; Benady et al., 1992), harvesting alfalfa (Hoffman et al., 1996), transplanting (Beam et al., 1991, Ling et al., 1990, Bar et al., 1996), conveying, and transportation (Gerrish et al., 1986, Kazaz and Gan-Mor, 1993; Edan and Bechar, 1998; Billingsley, 2000; Thuilot et al., 2002; Wei et al., 2005). The main problem in fruit recognition is due to shading, occlusion, variations in fruit properties, and changing illumination properties. Several technologies for fruit detection have been explored, including vision (Sevila & Baylou, 1991), infra-red (Dobrusin et al., 1992), and structured light (Benady et al., 1992; Yamashita & Kondo, 1992), but with each of these techniques only 85% of the fruits were identified (Edan, 1999).

Despite the tremendous amount of research in the last decade, the commercial application of robots in complex agriculture applications is still unavailable. The main limiting factors are production inefficiencies and a lack of economic justification (Edan, 1999). Production inefficiency is caused by problems in fruit identification (75-85%), low cycle times of 3-4 seconds per fruit, and the inability to autonomously deal with obstacles.

Introducing a human operator into the operation cycle to interact with the system not just as a supervisor is a new trend in agricultural research and can help improve performance and reduce system complexity (Bechar and Edan, 2003). The uncertainties in the fruit locations, size, shape, and maturity necessitate a sophisticated sensory system combined with a human operator to raise fruit identification to 95%, and to ensure rapid picking. Also, navigation and transportation on agricultural terrain must be reinforced by a human operator to solve the problem of navigating and driving the robot through the field. According to Ceres et al. (1998) cooperation of an agricultural robot with a human operator will help solve three difficult problems: (a) driving the robot through the field, from tree to tree and from row to row; (b) detection and localization of fruits; and (c) grasping and detaching of selected targets.

Khadraoui et al. (1998) developed and tested a neural network-learning model of vision-based control in driving assistance of agricultural vehicles, in which the model considers the vehicle properties and kinematics. A multilayer neural network receives information from the camera and a human driver makes corrections to the course. Ceres et al. (1998) developed "AGRIBOT", a system that combines human and machine functions harmoniously by assigning different, non-overlapping, non-redundant tasks to the human operator and to the robot. The human tasks are the more complex and intellectual parts of the operation, which do not require physical effort, *i.e.*, detecting the fruits and marking them with a laser beam, and driving the vehicle. The robot fulfills the physically demanding and more precise tasks, mainly the localization and harvesting with the manipulator and gripper system. Fruit detection, the most complicated task, is done solely by the human operator. Agribot detected

70% of the visible fruits, with 70 – 90% of the detected fruits successfully picked in cycles of around 4 - 10 seconds (Pons, 1996).

2.3 *Human-Robot Collaboration*

Unstructured environments are very complex and variable, requiring an adjustable, adaptable system. The use of an autonomous robotic device, therefore, is not advisable (Penin et al., 1998). The operation of autonomous robots is difficult (Al-Jumaily and Amin, 2000; Fletcher et al., 2005), and the promise of automatic and efficient remote operations has fallen short of expectations (Kim and Shim, 2003; Steinfeld, 2004) due to inadequate sensor accuracy and the limited ability of computers to reason and plan in such environments (Everett and Dubey, 1998). Rodriguez and Weisbin (2003) indicate that human capabilities of perception, thinking, and action are still unmatched in environments with anomalies and unforeseen events, and that human and robot skills are complementary. By taking advantage of the human perception skills and the autonomous systems' accuracy and consistency the combined human-robotic system can be simplified, resulting in improved performance (Parasuraman et al., 2000).

Human–Robot Interaction (HRI) is a highly interdisciplinary field where behavioral and psychological approaches towards understanding the nature of human–robot interaction complement robotics and engineering oriented work (Salter et al., 2006)

There is a large and rapidly developing class of technical systems that are dependent on human contribution for their operation (Ivanisevic and Lumelsky, 1997). This class is known as telecollaboration, and in robotics terminology, telerobotics, telemanipulation, or teleoperation. Since their first appearance in the 40's, many teleoperated systems have been developed and employed for dealing with unstructured environments and in applications where there is clear and unavoidable danger for the human operator (Sheridan, 1992).

Penin et al., (1998) state five reasons for using telerobotics: i) ability to do and improve outage-free maintenance in countries with strict regulations regarding the interaction of humans with energized components; ii) increase the safety and comfort of the workers; iii) decrease the cost by eliminating the need for the operator to work in a hazardous environment; iv) ability to work under moderate bad weather conditions; and v) decrease in labor requirements.

A telemanipulation system consists of a master manipulator, which is operated by a human operator, and a slave manipulator, which is used for real tasks in a remote site. The operational force and the environmental force are assigned to each manipulator during a task (Itoh et al., 2000). Hiragana et al. (1997) classified teleoperation systems into two categories: 1) manipulating objects at a remote site through communication channels, and 2) planning the

motions of objects in off-line mode on a real world simulator, and then sending the planned motions to a remote site. According to Sheridan (1989), a telerobotics manipulator is a more advanced form of teleoperation in which a human operator supervises through a computer intermediary.

Considerable research has been conducted on master-slave manipulator telerobotics and guidance/navigation control methods (Kosuge, 1990; Yokokoji et al., 1994; Ogasawara et al., 1998; Wilson and Neal, 2001; Ethier et al., 2002; Stanczyk and Buss, 2004; Hasegawa et al., 2004; Al-Mouhamed et al., 2005; Xiao-Gang et al., 2003; Wang and Liu, 2005), system stability (Raju et al., 1989; Kim et al., 1992; Lam and Leung, 2004; Jee-Hwan et al., 2004; Hannaford and Jee-Hwan, 2002; Jing, 2005), interfaces and displays (synergy, 2001; Iwahashi, 2003; Salter et al., 2006; Kofman et al., 2005; Scholtz et al., 2005), communication and data translation (Oboe and Fiorini, 1998; Sano et al., 1998; Michaud et al., 2001;), and architectures (Banerjee et al., 2000; Peshkin et al., 2001; Farahvash and Boucher, 2004; Speich and Goldfarb, 2005; Gowadia et al., 2005).

Teleoperated systems do not give the human operator the true sensation that he would have if he were on location with the system, since the information does not reach the operator's cognitive system directly, but through sensors with limited resolution, angle of vision, depth, *etc.* (Synergy, 2001). Interaction between the user and the teleoperated system is accomplished by means of an interface (Ivanisevic and Lumelsky, 1997). In the user's mind, however, there is often no difference between the system and the interface. Guida and Lamperti (2000) state that human-computer interaction is about designing computer systems that support people, so they can carry out their activities productively and safely. According to Synergy (2001), the goal of planning an interface for a telerobotic system is to achieve a state of human operator control that mimics as closely as possible the situation where the human operator is inside the system and activating it by directly using his senses.

Human-computer interaction depends on user factors, organizational factors, environmental factors (noise, heating, lighting, *etc.*), health and safety factors, comfort factors, task factors, constraints, and productivity factors (Guida and Lamperti, 2000). The system requirements can be classified into functional requirements, data requirements, and usability requirements (Guida and Lamperti, 2000) that can be operationally formalized to learn ability, throughput, flexibility, and attitude. Types and levels of automation are evaluated by examining their associated human performance consequences such as mental workload, situation awareness, complacency, and skill degradation.

Human-Computer/robot interfaces draw from the knowledge and methods of several different disciplines, including computer science, artificial intelligence, knowledge

engineering, cognitive psychology, social and organizational psychology, ergonomics, sociology, and anthropology (Guida and Lamperti, 2000). Extensive research has been conducted in these fields (Ivanisevic and Lumelsky, 1997; Radix et al., 1999; St-Amant, 1999; Raghavan et al., 1999; Perzanowski et al., 2001; Iwahashi, 2003; Kofman et al., 2005).

Over the past two decades, researchers have examined a number of different aspects of human interaction with automated systems. Types and levels of automation are evaluated by examining their associated human performance consequences, such as mental workload, situation awareness, complacency, and skill degradation (Guida and Lamperti, 2000; Steinfeld et al., 2006). Parasuraman et al. (2000) developed a model for types and levels of automation that provides a framework and supplies an objective basis for determining the degree of automation for each system. They suggest that automation can be applied to four broad classes of functions: 1) information acquisition; 2) information analysis; 3) decision and action selection; and 4) action implementation. Sheridan (1978) divides automation into ten levels, from fully autonomous, with no human intervention, to fully manual (Table 1). Xu et al. (2002) modeled human-computer strategies through cascade neural networks for a driving task, defined performance measures for evaluating the strategy models, and proposed an iterative optimization algorithm for improving the performance of learned models of human-computer strategies. Banerjee et al. (2000) described a combination of 3- D graphics systems and the gradual availability of high bandwidth networks that has made collaborative virtual reality feasible. Parasuraman et al. (2000) found that automation can have both beneficial and negative effects on human performance. They showed that automation does not simply supplant human activity, but rather changes it and poses new coordination demands on the human operator. They also indicate that high levels of automation may be associated with potential costs of reduced situation awareness, complacency, and skill degradation. Fletcher et al. (2005) developed an on-line driver assistance system that supports the driver and provides immediate feedback. Kidono et al. (2002) developed a human-robot guidance method for mobile robot navigation. Tsuji and Tanaka (2005) investigated a system for a tracking task where the human and the machine act simultaneously. Bruemmer et al. (2005) and Hughes and Lewis (2005) developed several automation levels for a human-robot vehicle in an indoor exploration task. Graves and Czarnecki (2000) describe a scale of five human-robot interaction levels for a telerobotic system.

Table 1: Sheridan's levels of automation of decision and action selection.

HIGH 10. the computer decides everything, acts autonomously, ignoring the human

9. informs the human only if it, the computer, decides to

8. informs the human only if asked to, or

7. executes automatically, then necessarily informs the human, and

6. allows the human a restricted time to veto before automatic execution, or

5. executes that suggestion if the human approves, or

4. suggest one alternative

3. narrows the selection down to a few, or

2. the computer offers a complete set of decision/action alternatives, or

LOW 1. the computer offers no assistance; human must make all decisions and actions

3 METHODOLOGY

3.1 Problem objective

The study aims to evaluate the performance of an integrated human-robot system for target recognition tasks in unstructured environments and to determine the collaboration level that will result in the best performance.

3.2 Outline

The research consists of three interrelated and independent parts that address human robot cooperation in target recognition tasks:

1. Definition of human robot collaboration levels fitted for target recognition tasks in unstructured environments. The collaboration levels are compatible with an extensive range of automation, from manual to fully autonomous (Sheridan, 1978).
2. Development of an objective function to measure the performances of integrated human-robot systems in target recognition tasks. The objective function considers operational costs and parameters related to the human, robot, targets, tasks, and environments. The objective function was evaluated in numerical analyses and in an indoor experiment.
3. Development of a methodology to determine the best collaboration level for the design of a specific system and to model and simulate its performance. Signal detection theory was adapted to evaluate the relations between the parameters.

3.3 Definitions

In this research we investigated an integrated human-robot system for target recognition tasks. Although 'system' and 'robot' are usually denoted similar connotations, in this work they do not represent the same concept. The term 'system' includes both the 'human' and 'robot' subsystems and indicates their overall combined performances and parameters. The 'human' subsystem is the human operator and is defined by manual operations; the 'robot' subsystem comprises the autonomous operations defined by automatic programs residing in the robot computer. The phrases 'human' and 'robot' refer to the subsystems and to their specific performances and parameters. The phrase 'environment' refers to the surrounding conditions the 'system' operates in. It includes parameters such as target probability, number of objects, and other parameters that are not related to the 'system' or the 'task'.

3.4 Assumptions

- Human performance has no influence on robot performance.
- The human, robot, and system performances do not influence the appearance of target and non-target objects.
- The human, robot, task, and environmental parameters are stable in time.

3.5 Collaboration levels

Four basic levels for human-robot collaboration were defined, tested, and evaluated. The collaboration levels were based on four degrees of autonomy from Sheridan's (1978) scale of "action selection and automation of decision" as follows: i) H: The H detects and marks the desired target solely; ii) HR: The H marks targets, aided by recommendations from an automatic detection algorithm, *i.e.*, the targets are automatically marked by a robot detection algorithm, the human acknowledges the robot's correct detections, ignores false detections and marks targets missed by the robot; iii) HOR: targets are identified automatically by the robot's detection algorithm; the human's assignment is to unmark false detections and to mark the targets missed by the robot system; and iv) R: the targets are marked automatically by the system.

In both the HR and HOR collaboration levels the human has the final decision on each detection. The difference between the two is that in the HOR collaboration level the human has to unmark objects he or she thinks are non-targets and were marked by the robot, and in the HR collaboration level, the human has to remark (approve) objects already marked by the robot that he or she also considers to be targets (and to ignore non-target objects marked by the robot).

3.6 System objective function

The system objective function is designed to enable determination of the expected value of task performance, given the parameters of the system, the task, and the environment. The objective function parameters can be divided into four major categories - human, robot, environmental, and task parameters.

The objective function includes five parts: correct detection (hit), false alarm, miss, correct rejection, and operational cost. The operational cost part includes the costs related to operational time and the costs of actions that should be performed on the detected objects, whether they are hits or false alarms (*e.g.*, picking detected melons, landmine neutralization).

To describe the relations between the objective function parameters in a target recognition task of a human-robot collaborative system, we applied a modified version of signal detection theory (SDT). This reduces the number of independent variables by relating human and robot

performance measures (*e.g.*, hit and false alarm probabilities) to their basic characteristics (*e.g.*, sensitivity and cutoff point decisions). The weakness in the use of SDT is that simple signal and noise distributions are assumed in order to cope with it mathematically. Hits and false alarms are computed from the sensitivity and cutoff points. Changes in the hit and false alarm values are limited and constrained by the changes of the characteristics. It is difficult to obtain the values of all human and robot performance measures in real world cases. Furthermore, in a regular analysis of the system objective function, the human and robot performance measures are defined and the system objective function is calculated according to them. However, when applying SDT, the human and robot characteristics such as sensitivity or decision cutoff are defined, the performance measures are then evaluated according to them, and the objective function is calculated accordingly.

For each signal probability and payoff values ratio combination there is a single optimal cutoff ratio, β^* in the case of a single detector (Swets et al., 2000). This ratio is independent of detector sensitivity, d' . For a two detector case, as in human-robot systems, there is a set of three β 's and two sensitivities, one for each detector (Robinson and Sorkin, 1985). The performance of the first detector (robot) is determined by its sensitivity (d'_r) and its cutoff ratio (β_r). The second detector (human) uses his/her sensitivity (d'_h) and two cutoff ratios, one for objects already marked by the robot, β_{rh} , and one for the other objects unmarked by the robot, β_h . Robot and human performance measures and overall system performance were described using signal detection theory parameters.

3.7 Numerical computation

A numerical computation was implemented on a personal computer with Matlab 7TM software to: i) examine the influence of the human and robot characteristics (*e.g.*, sensitivity) and the effects of different human-robot collaboration levels on the system objective function; ii) determine the optimal human and robot characteristics for different task characteristics; iii) determine the best collaboration level for different human, robot, and task characteristics; and, iv) perform a sensitivity analysis on the optimal characteristics and their influence on the best collaboration level and the system objective function value.

3.8 Experiment

An experimental system was developed with Matlab 7TM to test and examine the influence of different human-robot collaboration levels in a specific target recognition task.

The experimental system consisted of a simulator, using images taken from a melon field by a video camera mounted on a robotic melon harvester moving along a melon row. The location of true targets in each image was identified and saved by a panel of experts. The

images were manually classified into three complexity levels. During the experiment the experimental system recorded the human operator operations, the objects marked, and the time signature of each action. Performance measures were calculated from the recorded raw data.

Statistical analyses of the experiment results included descriptive statistics for the human performance measures, the system performance measures, and significance tests. The level of significance was set to $\alpha=0.05$.

A comparison of human sensitivity, the human likelihood ratio of the cutoff points, and the best collaboration level based on both the experimental results and the numerical analysis was conducted. Notwithstanding, the experiment did not deal with optimal system performance since the participants could not determine their required optimal variables during the experiment process.

3.9 Performance measures

Nine performance measures were grouped into two classes: target identification and time. The first class consists of eight performance measures representing the robot and human hit and false alarm parameters. The second class includes the time required for the human-robot integrated system to fulfill the task. The system objective function combines all mentioned performance measures into a single parameter.

4 FORMULATION OF AN OBJECTIVE FUNCTION

This chapter deals with the formulation of the system objective function. The theoretical equation is developed and a signal detection theory (SDT) model is modified to fit the case of a human-robot system in a target recognition task. The SDT equations are included in the system objective function in order to simplify it.

4.1 General

Evaluation of a multi-objective decision problem can be performed in several methods; two common methods are Pareto optimal sets (Deb et al., 2002) and value function (objective function). Pareto sets are used when the solution consists of different objective values that cannot be compared and calculates their optimal weights. In target recognition tasks, each of the variables has a predefined weight according to the task and system characteristics and therefore can be compared or superimposed with other variables to a single objective function. System performance is evaluated by the variables and their predefined weights. Although target recognition is a multi objective decision problem, the different objectives can be compared on a single scale and the objectives' weights are predetermined, and therefore the strength of Pareto set does not manifest itself in this case.

An objective function to evaluate system performance in integrated human-robot systems was developed for target recognition tasks. The objective function includes task, robot, human, and environmental parameters and considers operational costs to evaluate the expected overall system performance. To simplify the analysis of the system objective function the number of parameters was reduced using signal detection theory.

4.2 Objective function

The objective function describes the expected value of system performance, given the properties of the system, and the task is defined as the combined function of the multitude of performance measures. It considers several human and robot parameters that contribute to the overall value. The goal is to maximize the objective function. The value of the objective function can be translated to a monetary value. The system objective function in a target detection task (V_{Is}) is composed of the four responses of the detection process and the system operational costs and can be defined as:

$$V_{Is} = V_{Hs} + V_{Ms} + V_{FAs} + V_{CRs} + V_{Ts} \quad (1)$$

where V_{Hs} (equation 2) is the system gain for target detection (hit), V_{FAs} (equation 4) is the system penalty for false alarms (FA), V_{Ms} (equation 3) is the system penalty for missing the target (miss), V_{CRs} (equation 5) is the system gain for correct rejection, and V_{Ts} (equation 6) is

the system operation cost. All gain, penalty and cost values mentioned above have the same units (*i.e.*, a common monetary value such as US dollar) which enables us to add them together to a single objective function. The gain function for detecting the targets is:

$$V_{H_s} = N \cdot P_s \cdot p_{H_s} \cdot V_H \quad (2)$$

where,

- (a) N is the number of objects,
- (b) P_s is the probability of an object becoming a target,
- (c) V_H is the gain from a single hit, where the units of V_H are 'monetary value'. The value of V_H is target dependent (*e.g.*, the price of one melon for the farmer).
- (d) p_{H_s} is the system probability for a hit, composed of the human probability to confirm a robot hit and the probability to detect a target that the robot did not detect and that neither marked as a false alarm: $p_{H_s} = p_{H_r} \cdot p_{H_{rh}} + (1 - p_{H_r}) \cdot p_{H_h}$
- (e) p_{H_r} is the robot probability of a hit,
- (f) $p_{H_{rh}}$ is the human probability of confirming a robot hit, and
- (g) p_{H_h} is the human probability of detecting a target which the robot did not detect.

The penalty of missed targets is shown in equation (3):

$$V_{M_s} = N \cdot P_s \cdot p_{M_s} \cdot V_M = N \cdot P_s \cdot (1 - p_{H_s}) \cdot V_M \quad (3)$$

where,

- (a) V_M is the penalty of a single miss where the units of V_M are 'monetary value'. The value of V_M is target dependent (*e.g.*, the damage created from not detecting one landmine can be the destruction of one vehicle).
- (b) p_{M_s} is the probability of a system miss, composed of the human probability to not confirm a robot hit and the probability to miss a target that the robot did not detect and that neither marked as a FA: $p_{M_s} = p_{H_s} \cdot (1 - p_{H_{rh}}) + (1 - p_{H_r}) \cdot (1 - p_{H_h})$

The penalty from false alarms is specified in equation (4):

$$V_{FAs} = F_{FAs} \cdot V_{FA} \quad (4)$$

where

- (a) V_{FA} is the damage from a single false alarm, where the units of V_{FA} are 'monetary value'. The value of V_{FA} is system, environment and non-target object dependant (*e.g.* the damage created by one non-target object to the machine or system, if the system will detect and pick a rock instead of a melon it could damage the robot or system mechanism).

- (b) F_{FAS} is the number of system false alarm objects, composed of the robot's false alarms that the human does not correct and the human false alarm:

$$F_{FAS} = N \cdot (1 - P_S) \cdot [p_{FAr} \cdot p_{FArh} + (1 - p_{FAr}) \cdot p_{FAh}]$$

- (c) p_{FAr} is the robot false alarm probability,
 (d) p_{FArh} is the human probability of not correcting the robot false alarm, and
 (e) p_{FAh} is the human false alarm probability.

The gain from correct rejection is specified in equation (5):

$$V_{CRs} = F_{CRs} \cdot V_{CR} \quad (5)$$

where

- (a) V_{CR} is the gain from a single correct rejection, where the units of V_{CR} are 'monetary value'.
 (b) F_{CRs} is the correct rejection density function for the system, composed of the robot correct rejections that the human does correct and the human correct

rejection marks:

$$F_{CRs} = N \cdot (1 - P_S) \cdot [p_{FAr} \cdot (1 - p_{FArh}) + (1 - p_{FAr}) \cdot (1 - p_{FAh})]$$

The system operational cost includes both costs of time and operation as illustrated in equation (6)

$$V_{Ts} = t_s \cdot V_t + (N \cdot P_S \cdot p_{Hs} + F_{FAS}) \cdot V_C \quad (6)$$

where,

- (a) t_s is the system time that is required to perform the task,
 (b) V_t is the cost of one time unit and its units are 'monetary value/time', and
 (c) V_C is the cost of one object recognition operation (hit or false alarm) and its units are 'monetary/operations'. The cost values can be determined according to the time costs of the workers and the system and system operational costs and maintenance. The value of V_C is equal for hit and FA since it required the same treatment and manipulation for both.

We assume that the picking times are shorter than the sum of detection times and technical times related to the detection process. Therefore, the time terms in the objective function express only the detection times and do not consider the related operational time (picking times).

The system time consists of the time for the human to confirm the robot hits, the time for the human to hit additional targets, the time for the human to correct the robot false alarms, the time for the human to mark false alarms, and the robot time to process the images and to perform hits or false alarms. Also included in t_s is the time it takes the human to decide whether an object has been correctly rejected (CR) or missed (M).

$$\begin{aligned}
t_s = & N \cdot P_S \cdot p_{Hr} \cdot p_{Hrh} \cdot t_{Hrh} + N \cdot P_S \cdot (1 - p_{Hr}) \cdot p_{Hh} \cdot t_{Hh} + \\
& + N \cdot (1 - P_S) \cdot p_{FAr} \cdot p_{FArh} \cdot t_{FArh} + N \cdot (1 - P_S) \cdot (1 - p_{FAr}) \cdot p_{FAh} \cdot t_{FAh} + \\
& + N \cdot P_S \cdot p_{Hr} \cdot (1 - p_{Hrh}) \cdot t_{Mrh} + N \cdot P_S \cdot (1 - p_{Hr}) \cdot (1 - p_{Hh}) \cdot t_{Mh} + \\
& + N \cdot (1 - P_S) \cdot p_{FAr} \cdot (1 - p_{FArh}) \cdot t_{CRrh} + N \cdot (1 - P_S) \cdot (1 - p_{FAr}) \cdot (1 - p_{FAh}) \cdot t_{CRh} + t_r
\end{aligned} \tag{7}$$

where,

- (a) t_{Hrh} is the human time required to confirm a robot hit,
- (b) t_{Hh} is the human time required to hit a target which the robot did not hit,
- (c) t_{FArh} is the human time needed to correct a robot false alarm,
- (d) t_{FAh} is the human false alarm time,
- (e) t_{Mrh} is the human time lost when a robot hit is missed,
- (f) t_{Mh} is the human time invested when missing a target which the robot did not hit,
- (g) t_{CRrh} is the human time to correctly reject a robot false alarm,
- (h) t_{CRh} is the HO correct rejection time, and
- (i) t_r is the robot time.

We assumed that each of the human time variables represents a superposition of a decision time, t_D , and a motoric time, t_M , in accordance with the collaboration level.

Explicit operation of the system objective function, V_{Is} (1), that is suitable for all collaboration levels is described in equation (8):

$$\begin{aligned}
V_{Is} = & N \cdot P_S \cdot [p_{Hr} \cdot p_{Hrh} \cdot (V_H + V_C + t_{Hrh} \cdot V_t) + (1 - p_{Hr}) \cdot p_{Hh} \cdot (V_H + V_C + t_{Hh} \cdot V_t)] + \\
& + N \cdot P_S \cdot [p_{Hr} \cdot (1 - p_{Hrh}) \cdot (V_M + t_{Mrh} \cdot V_t) + (1 - p_{Hr}) \cdot (1 - p_{Hh}) \cdot (V_M + t_{Mh} \cdot V_t)] + \\
& + N \cdot (1 - P_S) \cdot [p_{FAr} \cdot p_{FArh} \cdot (V_{FA} + V_C + t_{FArh} \cdot V_t) + (1 - p_{FAr}) \cdot p_{FAh} \cdot (V_{FA} + V_C + t_{FAh} \cdot V_t)] \\
& + N \cdot (1 - P_S) \cdot [p_{FAr} \cdot (1 - p_{FArh}) \cdot (V_{CR} + t_{CRrh} \cdot V_t) + (1 - p_{FAr}) \cdot (1 - p_{FAh}) \cdot (V_{CR} + t_{CRh} \cdot V_t)] + t_r \cdot V_t
\end{aligned} \tag{8}$$

For the H collaboration level the objective function will be a degenerate form of equation (8), will not include the robot variables and therefore results in:

$$\begin{aligned}
V_{Is} = & N \cdot P_S \cdot [p_{Hh} \cdot (V_H + V_C + t_{Hh} \cdot V_t) + (1 - p_{Hh}) \cdot (V_M + t_{Mh} \cdot V_t)] + \\
& + N \cdot (1 - P_S) \cdot [p_{FAh} \cdot (V_{FA} + V_C + t_{FAh} \cdot V_t) + (1 - p_{FAh}) \cdot (V_{CR} + t_{CRh} \cdot V_t)]
\end{aligned} \tag{9}$$

In the R collaboration level the system objective function, V_{Is} will be a degenerate form of equation (8) will not include the human variables:

(10)

$$V_{Is} = N \cdot P_S \cdot [p_{Hr} \cdot (V_H + V_C) + (1 - p_{Hr}) \cdot V_M] + N \cdot (1 - P_S) \cdot [p_{FAr} \cdot (V_{FA} + V_C) + (1 - p_{FAr}) \cdot V_{CR}] + t_r \cdot V_t$$

The time parameters for the H, HR, and HOR collaborations are shown in equations (11), (12), and (13), respectively.

$$\begin{aligned} t_{Hh} &= t_D + t_M \\ t_{FAh} &= t_D + t_M \\ t_{Mh} &= t_D \\ t_{CRh} &= t_D \end{aligned} \quad (11)$$

$$\begin{aligned} t_{Hh} &= t_D + t_M \\ t_{FAh} &= t_D + t_M \\ t_{Mh} &= t_D \\ t_{CRh} &= t_D \\ t_{Hrh} &= t_D + t_M \\ t_{FArh} &= t_D + t_M \\ t_{Mrh} &= t_D \\ t_{CRrh} &= t_D \end{aligned} \quad (12)$$

$$\begin{aligned} t_{Hh} &= t_D + t_M \\ t_{FAh} &= t_D + t_M \\ t_{Mh} &= t_D \\ t_{CRh} &= t_D \\ t_{Hrh} &= t_D \\ t_{FArh} &= t_D \\ t_{Mrh} &= t_D + t_M \\ t_{CRrh} &= t_D + t_M \end{aligned} \quad (13)$$

4.3 Signal Detection Theory

4.3.1 Background

In the detection process there are four types of responses: 1) hit – when a detector recognizes a target; 2) miss – when a detector does not recognize a target; 3) false alarm (FA) – when a detector recognizes a non-target object as a target; and 4) correct rejection (CR) -

when a detector does not detect a non-target object as a target. The sum of the probabilities of hit and miss equal to 1 and so do the sum of the probabilities of FA and CR (Figure 1).

Signal detection theory (SDT) is a method of assessing the decision making process for binary categorization decisions. Signal detection analyses are based on hit and false alarm rates, where a hit is an event when a person correctly identifies a signal, and a false alarm is the identification of a noise when it is presented.

The theory of signal detection evolved from the development of communications and radar equipment in the early forties (Forero et al., 2004). It migrated to psychology, initially as part of sensation and perception, in the 50's and 60's as an attempt to understand some of the features of human behavior when detecting very faint stimuli that were not being explained by traditional theories of thresholds (Brown and Davis, 2006).

There are several advantages in applying SDT to the system objective function: the number of target identification parameters (*e.g.*, hit probability) are reduced; SDT is related to basic human and robot characteristics such as sensitivity and quality of decision making, attributes from which the target identification parameters are calculated; the optimal analysis of the system objective function is coherent and reasonable when dealing with the basic human and robot characteristics of the SDT rather than directly with the human and robot target identification parameters.

Incorporating SDT into the system objective function requires the following assumptions about the human and robot target identification parameters: the targets and non-target objects are normally distributed and must have identical variance even though they are independent.

The observer's ability to discriminate between noise and a target with noise is limited by the distance between the means of the two distributions (Figure 1), defined as the variable d' , which is also defined as the observer sensitivity. When $d'=0$, the two distributions completely overlap and it is impossible to distinguish between them. As d' increases, it becomes easier to distinguish between them. The location of the threshold is often defined in terms of the cutoff point or the likelihood ratio between the signal-plus-noise and the noise-only probability distributions as measured at the threshold position and is denoted as β (Swets et al., 2000). Shifts of the threshold will result in changes in the tradeoff between hits and false alarms. Shifting the threshold to the left will increase the hit and false alarm probabilities. The observer governs threshold placement. In this work we are using the likelihood ratio β as the human threshold value instead of the cutoff point.

The discrimination ability can be also performed using the Receiver Operating Characteristic (ROC) curve (Figure 2). ROC curves were developed in the 1950's as a by-product of research into making sense of radio signals contaminated by noise (Metz, 1978).

Today ROC curves are applied intensively in the medical area for discriminating diseases cases from normal cases (Metz, 1978; Zweig and Campbell, 1993) and to compare the diagnostic performance of different diagnostic tests (Griner et al., 1981). In a ROC curve each detector or diagnostic is represented by a single curve on the hit-FA space where the sensitivity is influencing the convexity of the curve. The cutoff ratio (β) is represented by a point along the curve, where increasing the value of β will reduce the hit and FA probabilities and the point will move on the curve towards the origin of axes.

A description of all SDT parameters for a single detector is listed below:

X – The measurement unit X is the sum of all object features. In classic uni-dimensional signal detection theory it is easy to define unit X as a single measurement parameter, such as intensity, size, weight, pressure *etc.* In a target recognition task, unit X is the sum of all target features, such as size, shape, color, hue, texture *etc.* In Figure 1, X is just a theoretic illustration of the SDT on target recognition.

x - a position along coordinate X , represents the cutoff point that separates hit from miss and FA from CR, range: $-\infty \rightarrow +\infty$

N – noise index

S – signal index

$\mu_{S,N}$ – signal/noise mean

$\sigma_{S,N}$ – signal/noise standard deviation

Z_S – the distance in standard deviation units between x and μ_S (along coordinate Z). Z_S is positive where x is bigger than μ_S and negative where x is smaller than μ_S . $Z_S = \frac{x - \mu_S}{\sigma_S}$

Z_N – the distance in standard deviation units between x and μ_N (along coordinate Z). Z_N is positive where x is bigger than μ_N and negative where x is smaller than μ_N . $Z_N = \frac{x - \mu_N}{\sigma_N}$

P_S – probability that an object is a signal (target)

$F_S(Z_S)$ – the signal density function value at Z_S . $f_S(Z_S) = \frac{e^{-\frac{Z_S^2}{2}}}{\sqrt{2\pi}}$

$F_N(Z_N)$ – the noise density function value at Z_N . $f_N(Z_N) = \frac{e^{-\frac{Z_N^2}{2}}}{\sqrt{2\pi}}$

d' – the distance between μ_S and μ_N on X coordinate. $d' = \mu_S - \mu_N$

β - the likelihood ratio of the two distributions at the cutoff point x . $\beta = \frac{f_S(Z_S)}{f_N(Z_N)}$

β^* - optimal β for one detector case. $\beta^* = \frac{1-P_S}{P_S} \cdot \frac{V_{CR} - V_{FA}}{V_H - V_M}$ (Swet et al., 2000)

P_M – the probability of a miss. $P_M(Z_S) = \int_{-\infty}^{Z_S} f_S(Z) dZ = \frac{1}{\sqrt{2\pi}} \int_{-\infty}^{Z_S} e^{-\frac{Z^2}{2}} dZ$

P_H – the probability of a hit. $P_H(Z_S) = 1 - \int_{-\infty}^{Z_S} f_S(Z) dZ = 1 - \frac{1}{\sqrt{2\pi}} \int_{-\infty}^{Z_S} e^{-\frac{Z^2}{2}} dZ = 1 - P_M$

P_{CR} – the probability of correct rejection. $P_{CR}(Z_N) = \int_{-\infty}^{Z_N} f_N(Z) dZ = \frac{1}{\sqrt{2\pi}} \int_{-\infty}^{Z_N} e^{-\frac{Z^2}{2}} dZ$

P_{FA} – the probability of a false alarm. $P_{FA}(Z_N) = 1 - \int_{-\infty}^{Z_N} f_N(Z) dZ = 1 - \frac{1}{\sqrt{2\pi}} \int_{-\infty}^{Z_N} e^{-\frac{Z^2}{2}} dZ = 1 - P_{CR}$

V_{CR} – value of each correct rejection, positive values.

V_{FA} – value of each false alarm, negative values.

V_H – value of each hit, positive values.

V_M – value of each miss, negative values.

V_{AR} – payoff ratio. $V_{AR} = -\frac{V_{FA}}{V_H}$

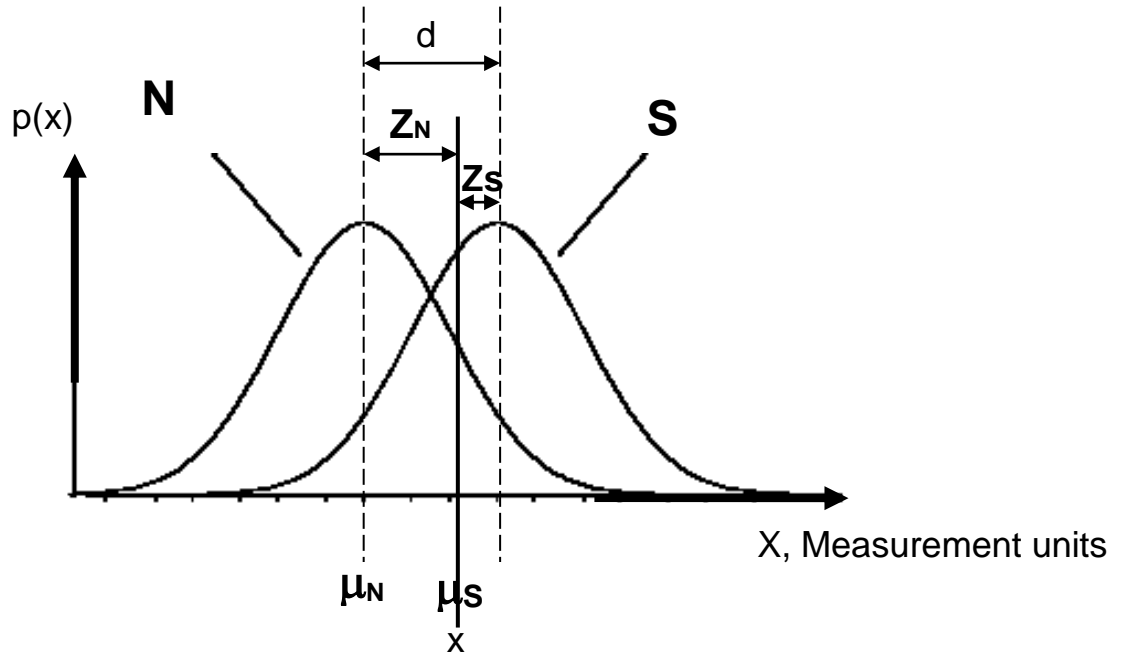


Figure 1: An example for a signal-noise (S-N) probability graph.

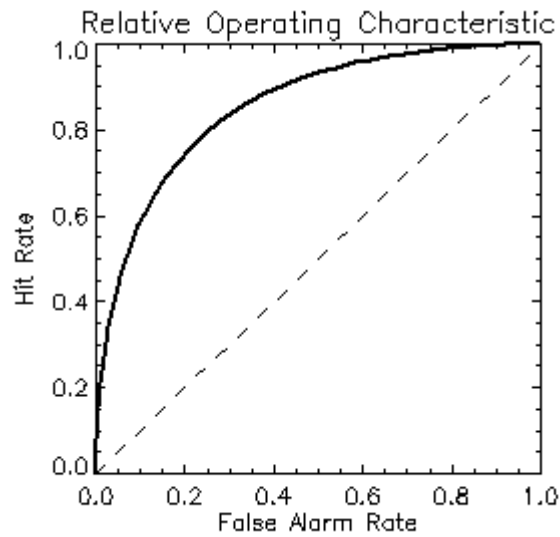


Figure 2: An example for a ROC curve.

SDT for human-robot systems

Signal detection theory for a human-robot system is similar to a two-detector case (Robinson and Sorkin, 1985). In a single detector case there are two distributions, noise and signal, one sensitivity parameter, d' , and one likelihood ratio parameter, β . In a human-robot system, there are two sets of distributions, one for the human and one for the robot. In addition there is a set of three β 's and two sensitivities. The performance of the first detector (robot) is determined by its sensitivity (d'_r) and its cutoff ratio (β_r). The second detector (human) uses its sensitivity (d'_h) and two cutoff ratios, one for objects already marked by the robot, β_{rh} , and one for objects unmarked by the robot, β_h .

A description of all SDT parameters for a single detector is listed below:

$Z_{Sr} - Z_S$ of the robot.

$Z_{Nr} - Z_N$ of the robot.

Z_{Srh}^* - optimal Z_S of human for object marked by the robot.

Z_{Nrh}^* - optimal Z_N of human for object marked by the robot.

Z_{Sh}^* - optimal Z_S of human for object unmarked by the robot.

Z_{Nh}^* - optimal Z_N of human for object unmarked by the robot.

d'_r - sensitivity of the robot.

d'_h - sensitivity of the human.

β_r - the likelihood ratio of the robot (first detector).

β_{rh} - the likelihood ratio of the human for object marked by the robot.

β_h^* - the likelihood ratio of the human for object unmarked by the robot.

P_{Hr} - the robot probability of a hit.

P_{Hrh} - the human probability of a hit of objects marked by the robot.

P_{Hh} - the human probability of a hit of objects unmarked by the robot.

P_{FAr} - the robot probability of a false alarm.

P_{FArh} - the human probability of a false alarm of objects marked by the robot.

P_{FAh} - the robot probability of a false alarm of objects unmarked by the robot.

P_{Mr} - the robot probability of a miss.

P_{Mrh} - the human probability of a miss of objects marked by the robot.

P_{Mh} - the human probability of a miss of objects unmarked by the robot.

P_{CRr} - the robot probability of a correct rejection.

P_{CRrh} - the human probability of a correct rejection of objects marked by the robot.

P_{CRh} - the robot probability of a correct rejection of objects unmarked by the robot.

Figure 3 represents a flowchart diagram of the target recognition process in an integrated human-robot system. The system is serial; each object is at first analyzed by the robot and then by the human operator. However, the robot analysis is exposed to the human operator. In some cases the human response and the system outcome, or the system outcome by itself, can influence the robot threshold. To simplify the development and the mathematical expression we assume that the signal distribution is bigger than the noise distribution, $\mu_S > \mu_N$ and $\sigma_S = \sigma_N = 1$, and define that there is no utility or penalty for correct rejection ($V_{CR} = 0$) and miss ($V_M = 0$).

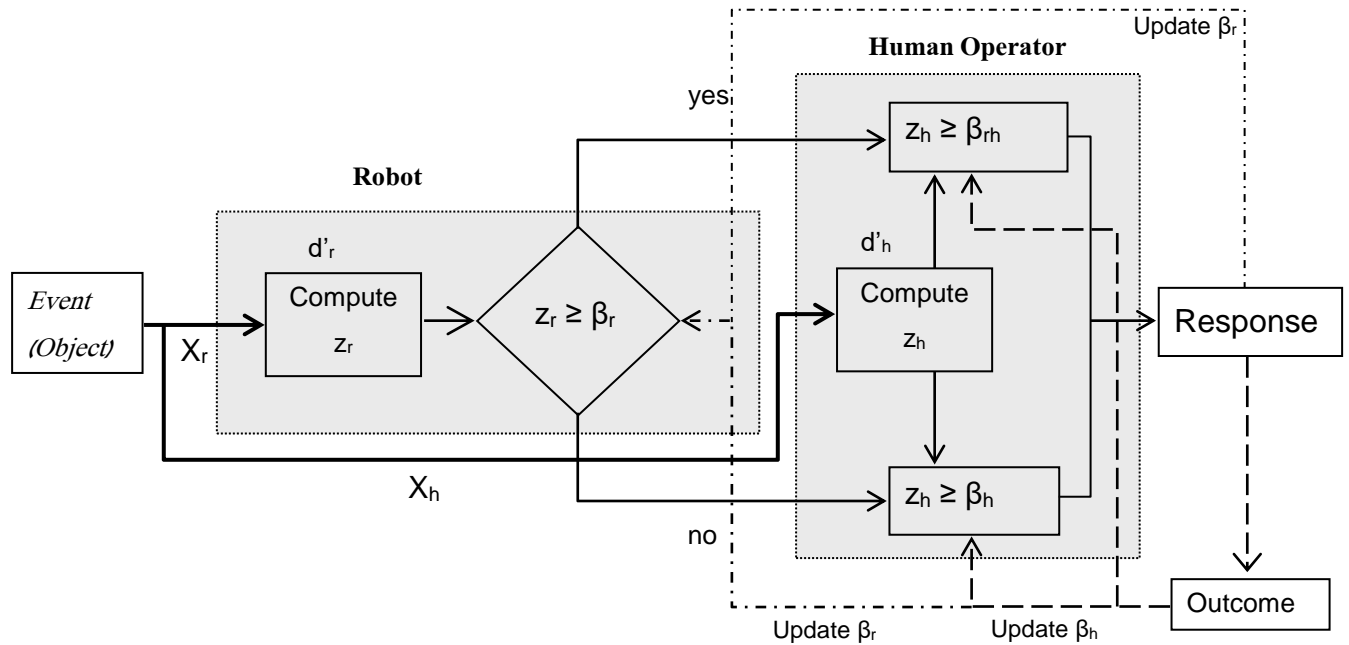


Figure 3: Flowchart of the target recognition process in an integrated human-robot system.

4.3.2 Transformation of the probability function from X to Z

It is important to describe the problem in standard deviation units in order to compare different cases and to attain a general solution that will not suit to the specific case examined. To describe the problem in standard deviation units rather than in actual units, the probability functions are transformed from the actual units, X, to standard deviation units, Z. The entire development is shown in Appendix I.

$$P_M(Z_S) = \frac{1}{\sqrt{2\pi}} \int_{-\infty}^{Z_S} e^{-\frac{(Z_S)^2}{2}} dZ \quad (14)$$

4.3.3 Expression of Z as a function of β and d'

The standard deviation unit, Z, can be expressed for the signal and noise distributions by the likelihood ratio, β , and the distance between the means of the signal and noise distributions, which is the sensitivity parameter, d' . The entire equation's development is detailed in Appendix II.

$$\begin{aligned} Z_N &= \frac{\ln(\beta)}{d'} + \frac{d'}{2} \\ Z_S &= \frac{\ln(\beta)}{d'} - \frac{d'}{2} \end{aligned} \quad (15)$$

4.3.4 Human optimal hit and false alarm probabilities in human-robot systems

The human optimal hit and false alarm probabilities according to the robot and human sensitivities (d'_r and d'_h) and Z_{Sr} , are presented. The entire equation's development is shown in Appendix IV.

The optimal human hit and false alarm equations for an integrated human-robot system are:

$$p_{H_{rh}} = 1 - \frac{1}{\sqrt{2\pi}} \int_{-\infty}^{\frac{\ln\left(\frac{P_{FA_r}}{P_{H_r}}\right)}{d'_h} + C_1} e^{-\frac{Z^2}{2}} dZ \quad (16)$$

$$p_{FA_{rh}} = 1 - \frac{1}{\sqrt{2\pi}} \int_{-\infty}^{\frac{\ln\left(\frac{P_{FA_r}}{P_{H_r}}\right)}{d'_h} + C_2} e^{-\frac{Z^2}{2}} dZ \quad (17)$$

$$p_{H_h} = 1 - \frac{1}{\sqrt{2\pi}} \int_{-\infty}^{\frac{\ln\left(\frac{1-P_{FA_r}}{1-P_{H_r}}\right)}{d'_h} + C_1} e^{-\frac{Z^2}{2}} dZ \quad (18)$$

$$p_{FA_h} = 1 - \frac{1}{\sqrt{2\pi}} \int_{-\infty}^{\frac{\ln\left(\frac{1-p_{FA_r}}{1-p_{H_r}}\right) + C_2}{d'_h}} e^{-\frac{z^2}{2}} dZ \quad (19)$$

Where C_1 and C_2 are auxiliary variables defined as:

$$\begin{aligned} C_1 &= \frac{\ln(\beta^*)}{d'_h} - \frac{d'_h}{2} \\ C_2 &= \frac{\ln(\beta^*)}{d'_h} + \frac{d'_h}{2} \end{aligned} \quad (20)$$

And the robot hit and false alarm variables are:

$$\begin{aligned} p_{H_r} &= 1 - \frac{1}{\sqrt{2\pi}} \int_{-\infty}^{Z_{S_r}} e^{-\frac{z^2}{2}} dZ \\ p_{FA_r} &= 1 - \frac{1}{\sqrt{2\pi}} \int_{-\infty}^{Z_{S_r} + d'_r} e^{-\frac{z^2}{2}} dZ \end{aligned} \quad (21)$$

4.3.5 Development of optimal β_s for human-robot systems without operational costs

In human-robot system there are three β s: one robot β (β_r) and two human β s, the first for the already detected objects by the robot (β_{rh}) and the second for the undetected objects (β_h). The entire development of the equation is shown in Appendix III.

The basic description of the likelihood ratio, β , as a function of the standard deviation unit of the signal distribution (Z_S) and noise distribution (Z_N) is presented in equation (22):

$$\ln(\beta) = -\frac{1}{2}(Z_S^2 - Z_N^2) \quad (22)$$

The optimal β for a single detector is given in equation (23):

$$\beta^* = \frac{1 - P_S}{P_S} \cdot \frac{-V_{FA}}{V_H} \quad (\text{Swets et al., 2000}) \quad (23)$$

Likewise, the optimal human likelihood ratio of objects already marked by the robot, β_{rh}^* is:

$$\beta_{rh}^* = \frac{1 - P_{rh}}{P_{rh}} \cdot \frac{-V_{FA}}{V_H} \quad (24)$$

The human target probability of objects marked by the robot, p_{rh} , is expressed in equation (25):

$$p_{rh} = \frac{P_S \cdot P_{H_r}}{P_S \cdot P_{H_r} + (1 - P_S) \cdot p_{FA_r}} \quad (25)$$

Combining equations (24) and (25) implies that the optimal human likelihood ratio of objects already marked by the robot, β_{rh}^* depends in the optimal likelihood ratio in a single detector system (β^*), which depends on the payoff values and the hit and false alarm probabilities of the robot in a human-robot system case (equation 26).

$$\beta_{rh}^* = \beta^* \cdot \frac{P_{FAr}}{P_{Hr}} \quad (26)$$

In a similar way, the optimal human likelihood ratio of objects unmarked marked by the robot, β_h^* is:

$$\beta_h^* = \frac{1 - P_h}{P_h} \cdot \frac{-V_{FA}}{V_H} \quad (27)$$

Where the human target probability of objects marked by the robot, p_h , is:

$$p_h = \frac{p_s \cdot (1 - p_{Hr})}{p_s \cdot (1 - p_{Hr}) + (1 - p_s) \cdot (1 - p_{FAr})} \quad (28)$$

Combining equations (27) and (28) implies that the optimal human likelihood ratio of objects already marked by the robot, β_h^* depends on the optimal likelihood ratio in a single detector system (β^*), which depends on the payoff values and the hit and false alarm probabilities of the robot in a human-robot system case (equation 29).

$$\beta_h^* = \beta^* \cdot \frac{(1 - p_{FAr})}{(1 - p_{Hr})} \quad (29)$$

The hit and false alarm probabilities of the robot are determined by the β_r and d'_r of the robot itself (expressed in Z of the robot).

5 NUMERICAL COMPUTATIONS

Optimal parameters were determined by numerical computations of the objective function without the miss and correct rejection (CR) parts. The best collaboration level and the objective function score were calculated for each optimal case. Sensitivity analyses of the main influencing parameters were performed to investigate the influence of small deviations from the optimal values on the objective function score and the best collaboration level.

This chapter begins with numerical computations of the optimal cutoff ratios (β s), based on the system objective function, to determine the optimal human and robot parameters for different task parameters and to determine the best collaboration level for different human, robot, and task parameters (section 5.1). It continues with sensitivity analyses of the human, the robot, and the independent environmental parameters and the influence of the changes in the optimal values of the parameters on the objective function score and the best collaboration level to reflect cases in which the human and robot performances were in the proximity of optimum values or when the environmental parameters diverged only slightly from their expected or calculated values (section 5.2). At the end of the chapter, the findings are summarized and conclusions are derived (section 5.3).

5.1 Numerical computation of objective function with optimal cutoff points

Numerical computations were performed to determine the optimal human and robot parameters for different task parameters and to determine the best collaboration level for different human, robot, and task parameters. An in depth analysis of a multitude of human and robot parameter ranges for different task parameters was conducted as well and is illustrated in Appendix VI. The numerical computations were performed on a PC with Matlab 7™. The numerical computations were executed for several target probability conditions, P_s , human and robot sensitivities, d'_h and d'_r , and payoff value ratios, V_{AR} . The optimal likelihood ratios, β_r , β_h , and β_{rh} , were determined in the range between the logarithm of -4 and the logarithm of 4, in order to cover the available hit and false alarm probabilities. The system objective function was analyzed for two cases, one including the operational cost part and one excluding the operational cost part. The objective function that excludes operational cost functions as the upper boundary of system performance, represents systems without any operational cost, and shows its influence on the best collaboration level.

The specific values were extracted from a preliminary experiment (appendix V) and were set close to real values and consequential to the difference between the various collaboration levels.

The difference between the HR and the HOR collaboration levels is in the time parameters and in the operational cost part (as expressed in the system objective function equations). Therefore, in cases where the system objective function did not include the operational cost part, the task time has no influence on either system performance or on the optimal solution. By removing the operational costs from the objective function the difference between these two collaboration levels will be eliminated and we will consider them as one collaboration level. This is denoted as the HOR collaboration level.

Task parameters

The independent parameters were arbitrarily determined. The meanings of the gain-penalty-cost weights are that each hit is rewarded by 50 points. To examine the influence of different false alarm to hit ratios the value of V_{FA} was set to different values (0.1, 1, and 10) and therefore, each false alarm carried a different penalty (5, 50 or 500 points). This influences the task nature by inducing operators to maximize the hits or to reduce the false alarms to minimum. The operational cost and time was arbitrarily predetermined so it will not succeed 12% of the hit value magnitude in order to limit its influence on the system decisions. Hence, each hit or false alarm operation costs 2 points, and, each hour of operation costs 2000 points. According to the time parameters the system can detect between 514 and 720 objects (hits and false alarms). Therefore, the time cost of each detection varied between 2.78 points and 3.9 points in addition to the operational costs. The total gain from a hit is between 44.1 and 45.22 points and the total penalty-cost from a false alarm is between 9.78 and 505.9 points (according to the false alarm penalty). The actual value of the gain-penalty-cost weights was less important in the analysis than the ratio between all weights which determine the task nature (*e.g.*, whether it is more important to detect melons, to reduce the number of FAs or to finish the task in minimum time). The defined independent parameters are listed in Table 2.

5.1.1 Analysis of Ps for objective function with optimal cutoff points

In this analysis the payoff ratio was set at $V_{AR}=-1$ (and therefore $V_{FA}=-50$). The target probability, P_s , represents the fraction of the targets from all objects (targets and non-targets objects), it can vary during the task, and it consider to be one of the parameters that determine the environment type.

Table 2: The defined independent parameters.

Parameter	Value	remarks
N	1000	
V_H	50	
V_{AR}	-0.1, -1, -10	and therefore $V_{FA}=-5, -50$ and -500 respectively
V_{CR}	0	
V_M	0	
P_s	ranged from 0.1 to 0.9	
V_C	-2	$V_C=0$ and $V_t=0$ in analysis of the system objective function where the operational cost part is excluded
V_t	-2000 hr^{-1}	
decision time, t_D	5 s/object	
motoric time, t_M	2 s/(detected object)	
robot time, t_r	0.01 s/object	
Robot sensitivity, d'_r	ranged between 0.5 and 3	
Human sensitivity, d'_h	ranged between 0.5 and 3	

5.1.1.1 System objective function score

Objective function including the operational cost part

For all collaboration levels, the maximum objective function score increases with the increase in the target probability, P_s (Figure 4a and b). At the H and R collaboration levels the maximum objective function score increases with the human and robot sensitivities, respectively (Figure 4a and b). The largest influence of sensitivity on the objective function score appears in the intermediate range of the target probability, though the influence of the target probability on the score is bigger in comparison to the influence of the human or robot sensitivity.

In the HR and the HOR collaboration levels, for all target probabilities the score of the objective function with optimal cutoff points values, increases with the increase in human and robot sensitivities (Figure 4c and d). The maximum score is achieved for a system with high robot and human sensitivities.

Objective function excluding the operational cost part

The system objective function score for all collaboration levels has the same tendency as for the case of the objective function including the operational cost although the probability values are higher for all sensitivities and target probabilities.

The location of the maximum objective function score in the R collaboration level is not influenced by the operational cost.

5.1.1.2 Best Collaboration Level

Description

The best collaboration level is that which achieves the highest objective function score for a specific case and can be defined as:

$$\text{Max}\{V_{\text{IS}}(\text{H}), V_{\text{IS}}(\text{HOR}), V_{\text{IS}}(\text{HR}), V_{\text{IS}}(\text{R})\} \quad (30)$$

The best collaboration domination zone is an area in a chosen parameter's space for which a specific collaboration level achieves the highest objective function score. For example, when the target probability is 0.2 and $V_{\text{AR}}=-1$, each surface represents a different collaboration level (Figure 5). The surface created from the intersection of the surfaces of all four collaboration levels represents the highest objective function score for each human and robot sensitivity combination. Figure 6 shows the objective function score of all four collaboration levels in the sensitivity space (d'_h and d'_r).

The collaboration level that achieved the highest score for each d'_h and d'_r is defined as the best collaboration for those combinations and can be presented in a domination map (Figure 7). A single collaboration level dominates each colored zone. In the present case, each of the three collaboration levels (H, HR and HO-R) achieves its best score in different zones. This example indicates that for the same task the best collaboration could be changed from one collaboration level to another, and that there are tasks for which the manual collaboration level, H, is never the best collaboration level. Different task objectives and different system objective function properties will produce different best collaboration maps.

Objective function including operational costs

Figure 8 shows a best collaboration level map of the optimal objective function score cases for different human and robot sensitivities, d'_h and d'_r and different target probabilities, P_s . A single collaboration level dominates each zone. This figure presents the collaboration level required to achieve the best system performance.

For all target probabilities related to the sensitivities analyzed, the H collaboration level is never the best collaboration level probably due to its high operational cost and relatively low hit rate. Thus, human-robot collaboration for target recognition tasks will always surpass the optimal performance of a single human detector.

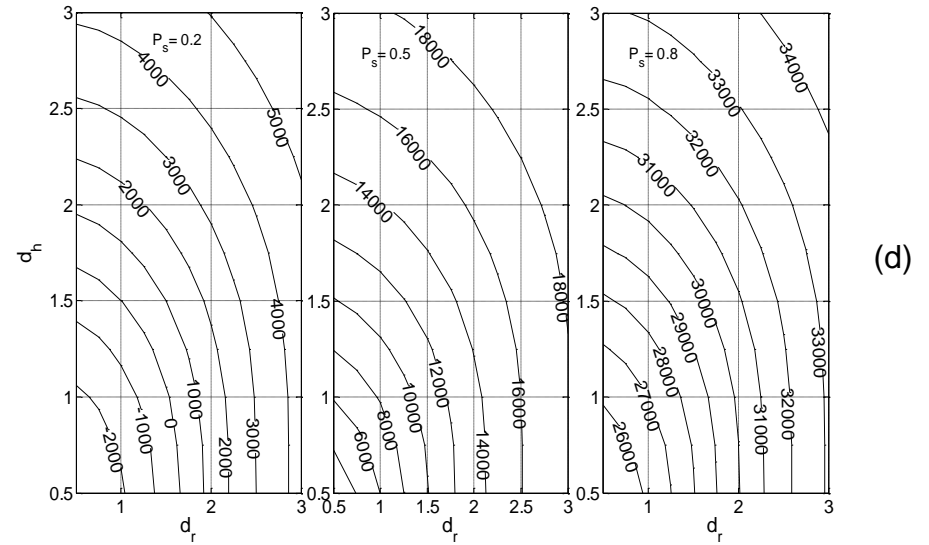
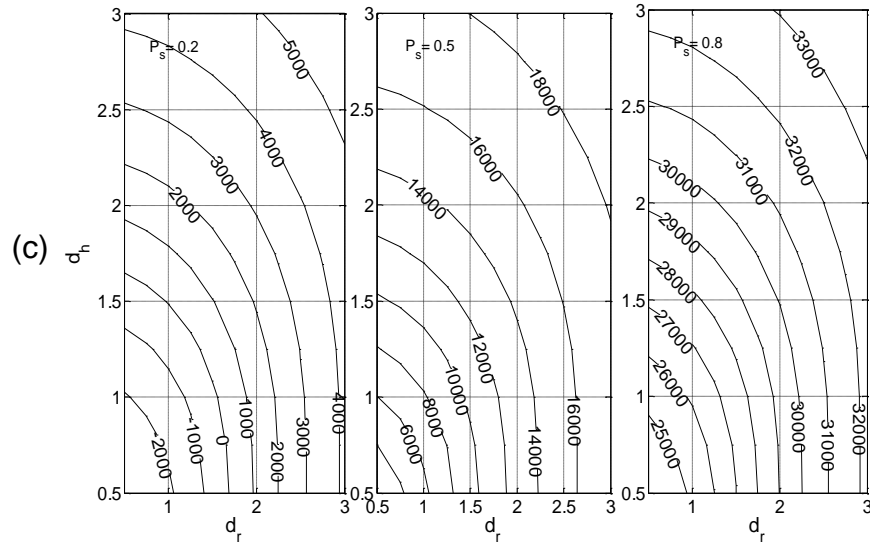
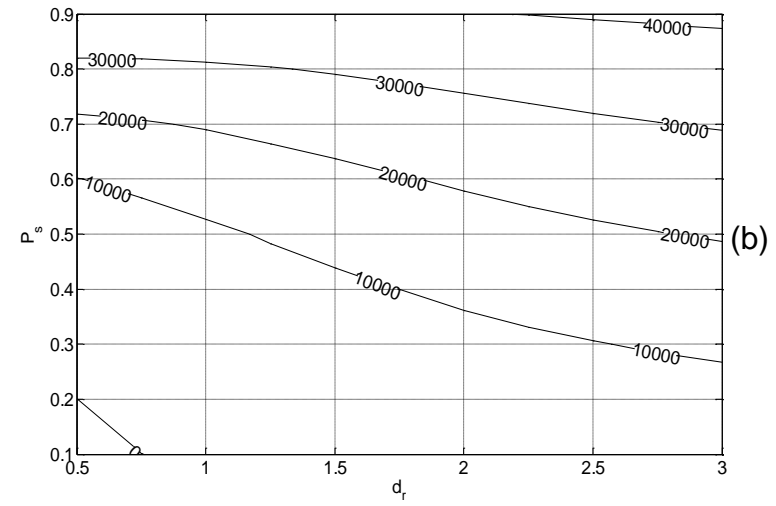
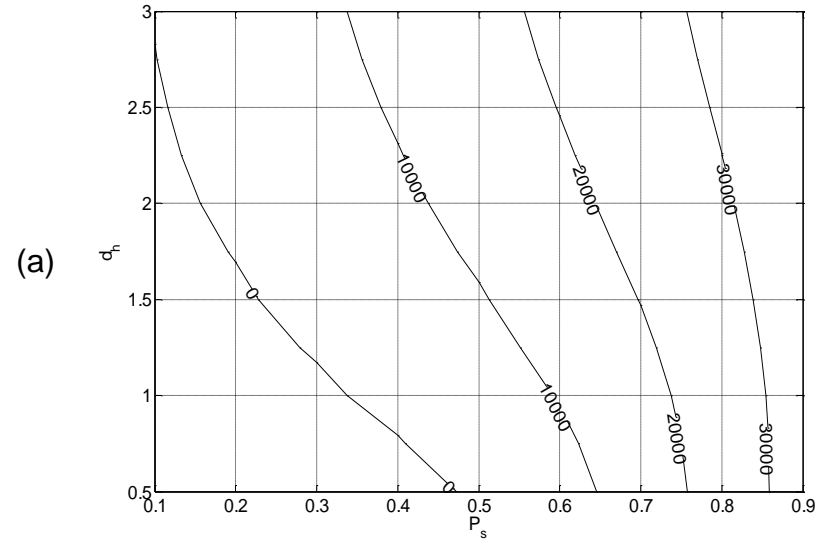


Figure 4: System objective function optimal score for different human and robot sensitivities and different target probabilities of the four collaboration levels: a) H, b) R, c) HR, and d) HOR. Each of the subfigures contain a family of isobar curves of the objective function score. Each family corresponds to a different collaboration level.

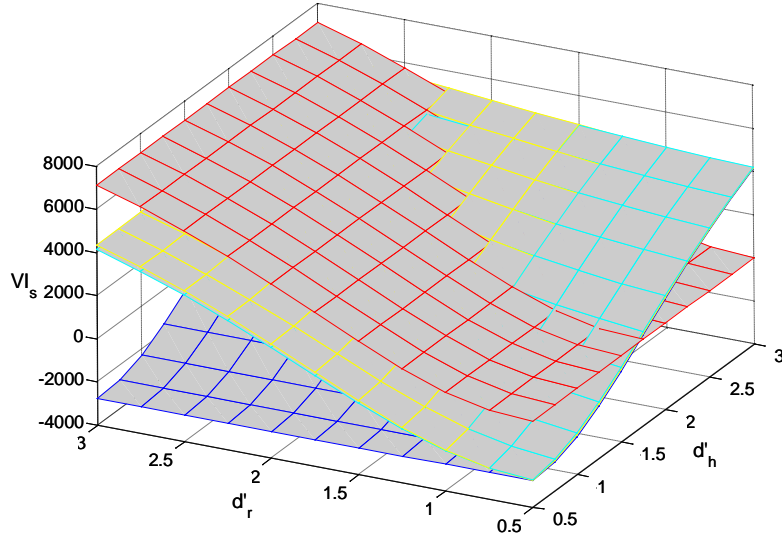


Figure 5: Objective function score for different human and robot sensitivities of the four collaboration levels. H – blue, HR – cyan, HOR yellow and R – red.

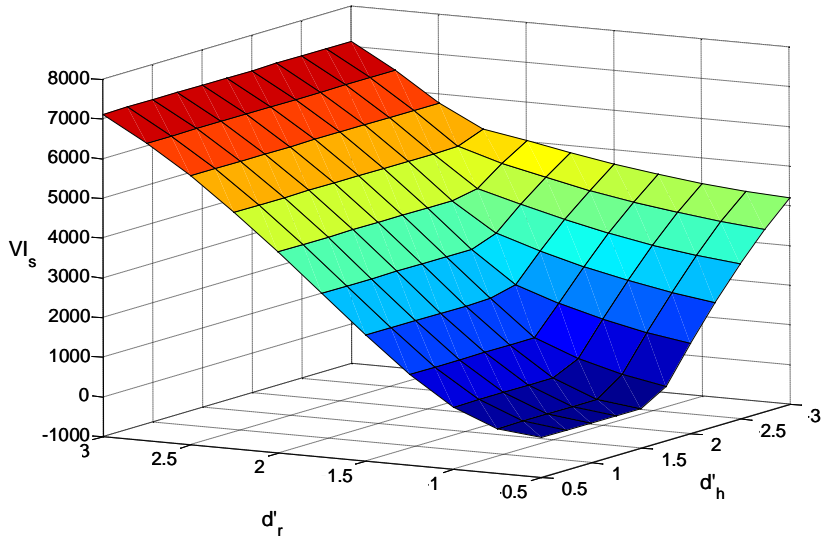


Figure 6: Maximum objective function score for different human and robot sensitivities and for all four collaboration levels combined.

The R collaboration level is the best collaboration level when robot sensitivity is higher than human sensitivity. For instances of extremely high and low target probabilities, R is again the best collaboration level for the entire sensitivity space excluding a small area where human sensitivity is high and robot sensitivity is low. Compared with other collaboration levels, the R collaboration level's operational cost is relatively low since task time is small and constant. When robot sensitivities are high, R achieves higher hit rates and therefore results in higher scores than other collaboration levels. In high target probabilities, the system marks large numbers of objects,

therefore the operational cost in the H, HR and HOR collaboration levels is high indicating that R is the best collaboration level in most of the sensitivity space. Similarly, in low target probabilities the operational cost of H, HR and HOR collaboration levels is high due to the large number of false alarms and the task times. Only when human sensitivity increases, it reduces the operational cost and with the decrease in robot sensitivity the hit rate of the R collaboration level is decreased. This causes the R collaboration level to be inferior to the other collaboration levels.

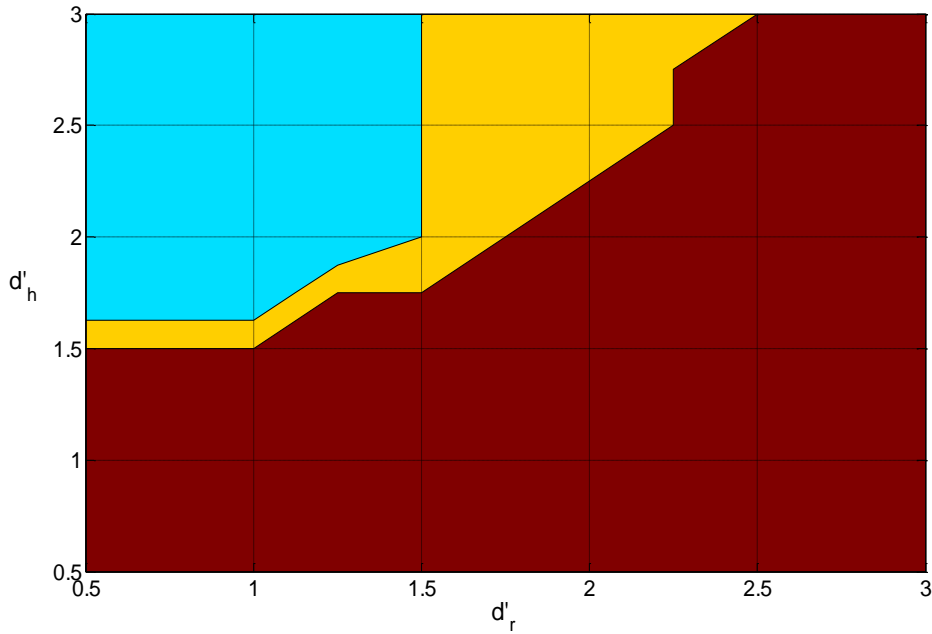


Figure 7: Best collaboration level map for different human and robot sensitivities. The colors represent different collaboration levels: HR – cyan, HOR - yellow and R – red.

The HR is the best collaboration level only when both target probability and robot sensitivity are low and human sensitivity is high, since for low target probabilities the operational cost of the HR is lower than that for the HOR collaboration level.

The HOR is the best collaboration level for the areas not dominated by the R collaboration level where the human sensitivity is high and the robot sensitivity is low.

A comparison between the HR and the HOR collaboration levels indicates that at low target probabilities where robot sensitivity is low and human sensitivity is high, the HR collaboration level performs better. In these cases the robot produced a relatively high number of false alarms that increase the task time needed for the human in time spent unmarking the false alarms in the HOR collaboration level. For high target probabilities, the HOR collaboration level shows better performance since the robot produced a relatively high number of hits thus increasing the task time for remarking them by the human in the HR collaboration level.

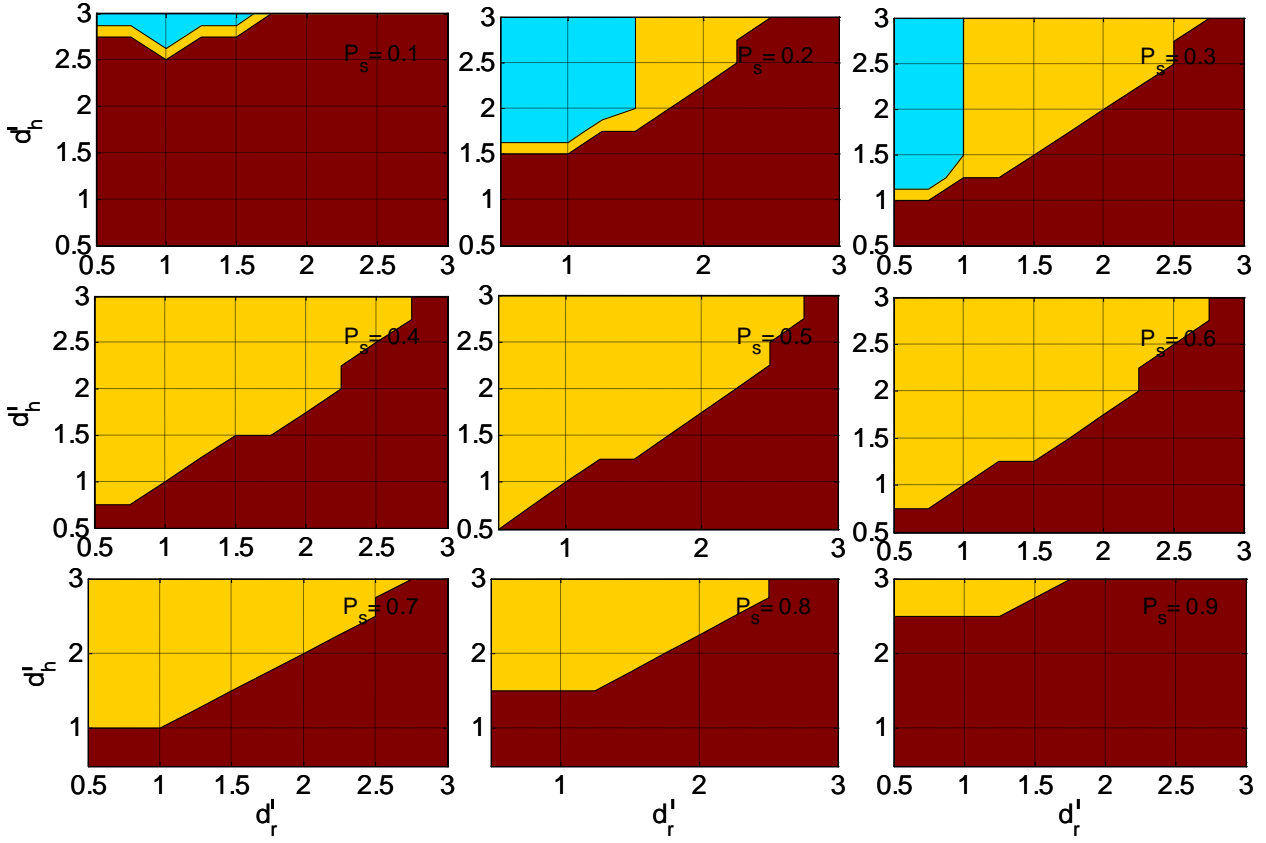


Figure 8: Best collaboration level map for different P_s , d'_r and d'_h values. Each subfigure presents a map for different target probability. The colors represent different collaboration levels: HR –cyan, HOR yellow and R – red.

Figure 9 describes an "envelope performance" of the given system. The "envelope performance" describes the highest achievable objective function score for specific d'_h and d'_r values and a specific target probability value, and acts as an upper boundary for system performance.

The system objective function behaves in each zone for which a collaboration level is optimal as the objective function of the collaboration level in that zone. It increases with the increase in the target probability, P_s , for the entire sensitivity space. For all target probabilities the score increases with the increase in robot sensitivity. Furthermore, the score increases with increases in human sensitivity in the zones where the best collaboration level is HR or HOR. The maximum score is achieved for a system with high robot sensitivity.

The system's overall sensitivity in each zone for which a collaboration level is optimal is the sensitivity of the collaboration level that is the best in that zone (Figure 10a). The overall system sensitivity is equal to the robot sensitivity whereas the best collaboration is the R collaboration level. For areas where the best collaboration level is HR or HOR, system sensitivity decreases with the increase in target probability. However, the overall system sensitivity is always higher than the robot sensitivity. The system sensitivity in the HOR collaboration level is lower than in the HR

collaboration level for the same human and robot sensitivities even for zones where the HOR is the best collaboration level. Nevertheless, for these sensitivities the HOR collaboration level achieves the highest score.

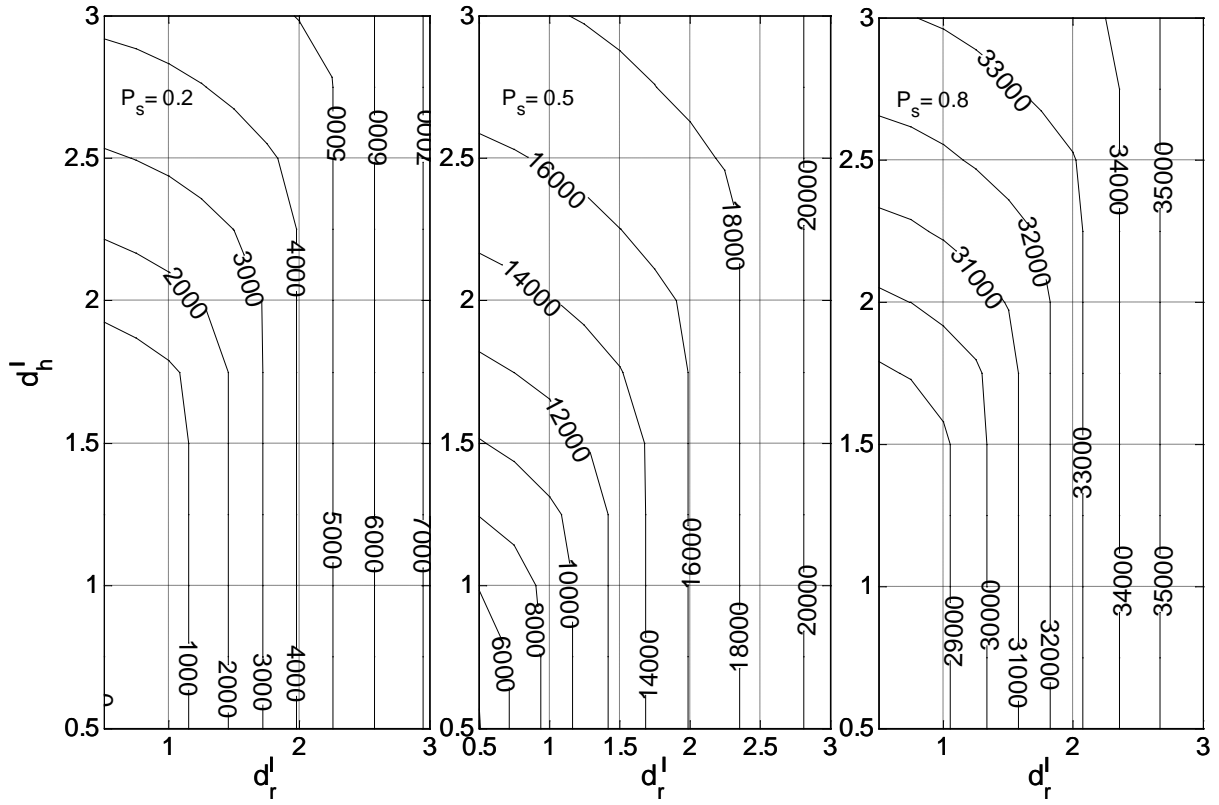


Figure 9: System objective function score of the best collaboration level for different P_s , d_r' and d_h' values. Each subfigure presents a map for different target probability. The contour lines represent equal score areas.

In each zone for which a collaboration level is optimal, the system likelihood ratio, β_s , functions as the overall likelihood ratio of the collaboration level which is the best in that zone (Figure 11a). The system likelihood ratio is equal to the robot likelihood ratio, β_r , whereas the best collaboration level is the R collaboration level. The system likelihood ratio decreases with the increase in target probability. For the area in the sensitivity space dominated by either the HR or HOR collaboration level, the value of the system overall likelihood ratio is always lower than the value of the robot likelihood ratio. β_s in the HOR collaboration level is lower than in the HR collaboration level for the same human and robot sensitivities.

When the best collaboration level is either HR or HOR, the likelihood ratio's value is relatively close to that of the R collaboration level. It seems that in order to obtain optimal performance in a human robot collaboration system, the value of the system likelihood ratio for the HR or HOR collaboration level has to be similar to that of the robot likelihood ratio for the R collaboration level.

Objective function excluding operational costs

For the entire sensitivity space and for all target probabilities the HOR collaboration level is the best collaboration level for the objective function excluding the operational cost variable. The objective function scores of the H and R collaboration levels are equal to each other for matched human to robot sensitivities due to the absence of the operational cost. The HOR collaboration level combines all three collaboration levels. By increasing the value of the likelihood ratio of the robot, β_r , it reduces the robot's involvement in the task, thus making it similar to the H collaboration level. By increasing both values of the human likelihood ratio, β_{rh} and β_h , it reduces human involvement in the task becoming more similar to the R collaboration level. In addition, the combination of both human and robot in the HOR collaboration level increases the sensitivity in most cases while increasing the probability of a hit and reducing the probability of false alarms.

The influence of robot sensitivity (d'_r) on overall system sensitivity is reduced with the increase in the target probability (Figure 10b). Although system sensitivity increases with the increase in robot sensitivity for all target probabilities, at low target probabilities an increase in human sensitivity has a local minimum phenomenon that occurs when robot sensitivity is low. The overall system sensitivity will always be higher than the human sensitivity.

The overall likelihood ratio, β_s , of the system decreases with the increase in the target probability and its values are lower than in the case that includes the operational cost (Figure 11b). Lower values of β_s indicate increases in the hit and false alarm rates. Elimination of the operational cost reduces the overall system cost, which enables the system to mark more false alarms and more hits, thereby resulting in an increase of the system objective function score.

5.1.2 Analysis of payoff ratio for the optimal system objective function

Task parameters

V_{AR} is one of the independent parameters determining the task, different V_{AR} values represent different task types.

5.1.2.1 System objective function score

An increase in the V_{AR} value increases the penalty of each false alarm and reduces the objective function value at all collaboration levels. At the H collaboration level an increase in the V_{AR} reduces the influence of the human sensitivity parameter on the objective function score. At the R collaboration level, with the increase in the V_{AR} the influence of robot sensitivity on the objective function score increases.

5.1.2.2 Best collaboration level

How target probability influences the best collaboration level depends on the payoff ratio value. For low values of V_{AR} , target probability has no influence on the best collaboration level. The best collaboration level for the entire sensitivity space is the R collaboration level for all target probabilities.

For high payoff ratios, the area in the sensitivity space in which the R is the best collaboration level decreases with the increase in target probability. The area in which the HOR or the HR is the best collaboration level increases with the increase in the target probability.

For payoff ratios equal to one, R is always the best collaboration level in the areas where the robot sensitivity is higher than the human sensitivity. At extremely high and low target probabilities, R is the best collaboration level for the entire sensitivity space. The area in which HOR or HR is the best collaboration level is reaching maximum size when the target probability equals 0.5.

5.1.3 Analysis of human and robot sensitivities for the optimal objective function

The human and robot sensitivities, d'_h and d'_r , respectively, indicate the ability to distinguish between true targets (signal) and false targets (noise). An increase in sensitivity will enhance the discrimination between true and false targets. An increase in human and robot sensitivities will increase the system objective function score for all collaboration levels. The best collaboration will shift to R with the increase in the robot sensitivity. The best collaboration will shift to HR or HOR with the increase in human sensitivity. R, at which robot sensitivity is higher than the human sensitivity, will be the best collaboration level.

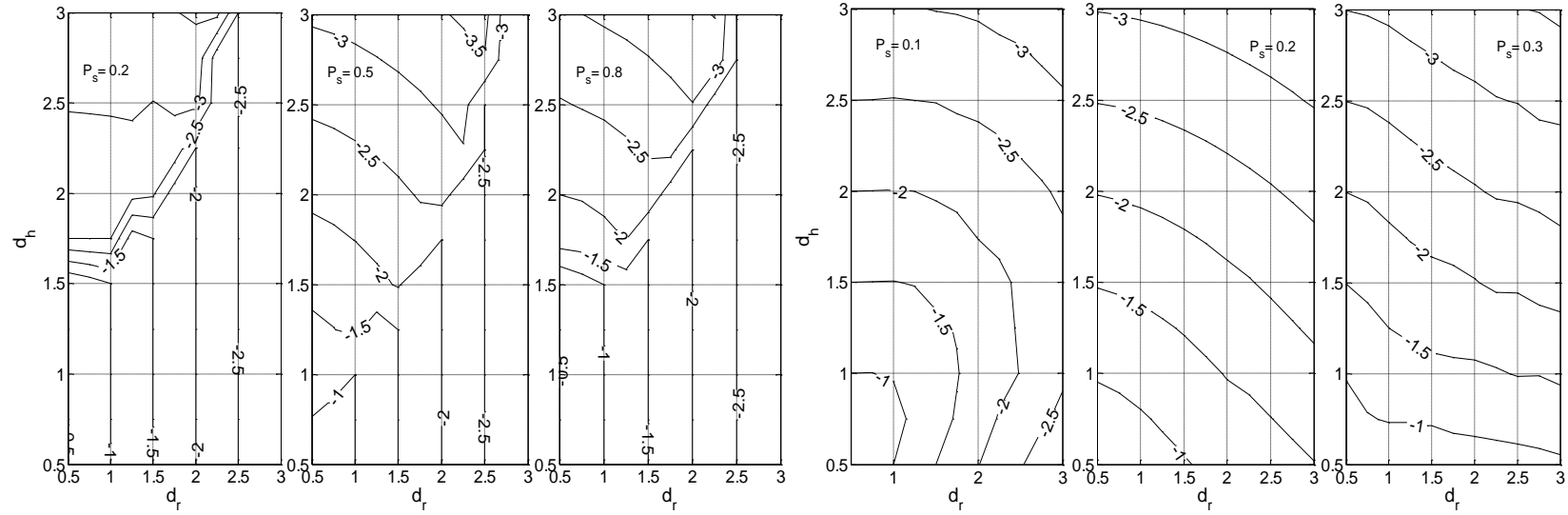
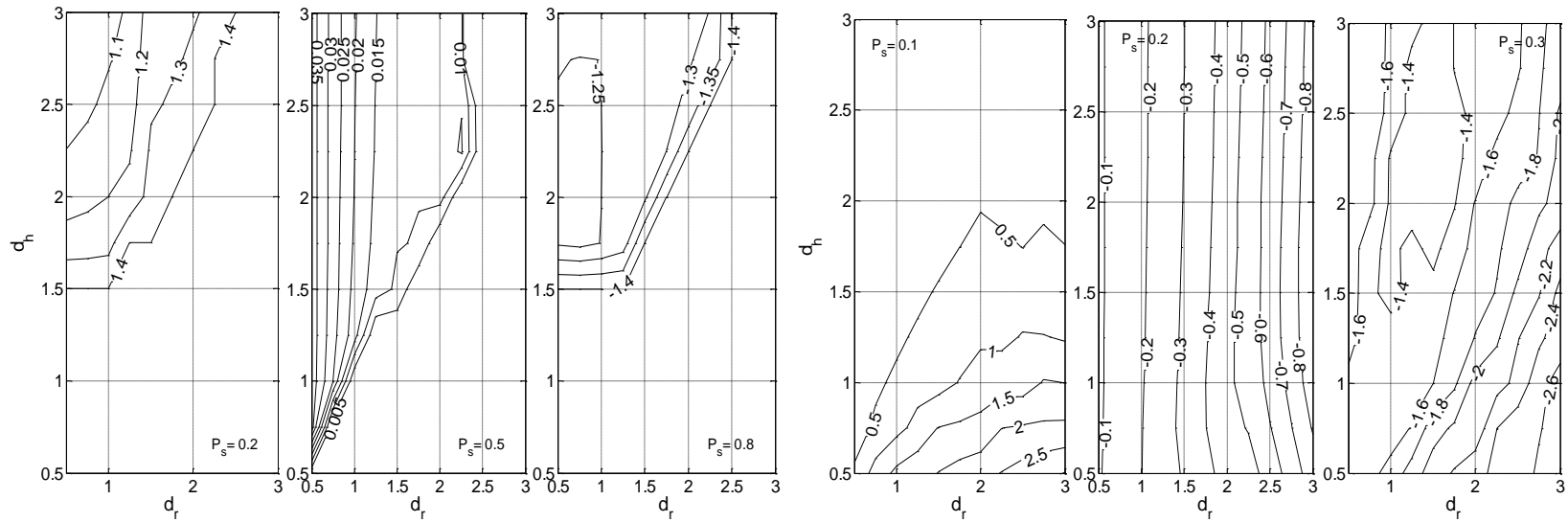


Figure 10: System sensitivity of the best collaboration levels for different human and robot sensitivities and different target probabilities and for objective function including (left) and excluding (right) the operational cost. The contour lines represent equal system sensitivity areas.



5.2 Sensitivity analysis

Sensitivity analyses were performed for the human, the robot, and the independent environmental parameters since the precise values are unknown and they can vary during task performance and. The influence of the changes in the optimal values of the parameters on the objective function score and the best collaboration level were analyzed to reflect cases in which the human and robot performances were in the proximity of optimum values or that the environmental parameters diverged only slightly from their expected or calculated values. The parameters analyzed were the human likelihood ratios, β_{rh} and β_h , human sensitivity, d'_h , the robot likelihood ratio, β_r , the robot sensitivity, d'_r , and the target probability, P_s . The payoff ratio, V_{AR} , the time cost, the operational cost, and the hit rewards were not sensitivity analyzed since the parameters are fixed during the entire task.

5.2.1 Sensitivity analysis of β_r , β_h , and β_{rh}

The value of the logarithm of the different robot and human likelihood ratios, β_r , β_h , and β_{rh} , ranged between -4 and +4. A sensitivity analysis was performed on the optimal values of β_r , β_h , and β_{rh} in terms of the best collaboration level. The sensitivity analysis investigated the influence of deflections of ± 1 in the logarithm of the optimal value of the likelihood ratio (set to b equal to one quarter of the entire range).

For cases in which the best collaboration level was R, the objective function score decreases with changes in the optimal robot likelihood ratio, β_r . The magnitude of the decrease in the score is influenced by target probability; the decrease reaches its maximum when the target probability is equal to 0.5. In addition, the magnitude of the score decrease is reduced with the increase in the robot and human sensitivities. The maximum decrease in the score was achieved when the robot and human sensitivities were equal to 1. The maximum decrease reaches 40% for maximum determined deviation and a target probability of 0.5. In all cases, the score of the R collaboration level was higher than each of the scores of the other collaboration levels.

The values of the human payoff ratios, β_h and β_{rh} , do not influence the objective function score of the R collaboration level. Although they do influence the objective function scores of all other collaboration levels, their score do not exceed the R collaboration score and the best collaboration level does not change. This is true for all human and robot sensitivities; all target probabilities, and all payoff ratios. An example is given in Figure 12.

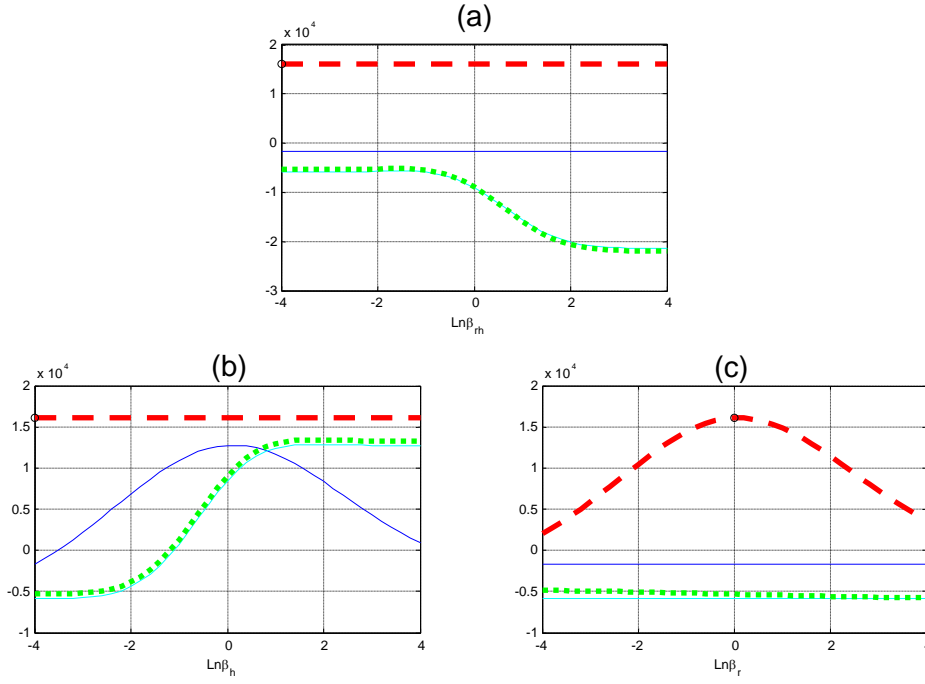


Figure 12: An example for the influence of small deviations from the optimal values of (a) β_{rh} , (b) β_h and (c) β_r when R is the best collaboration level on the objective function score and $P_s=0.5$, $d'_r=2$ and $d'_h=1$. the colors represents the different collaboration levels: H – blue, HR – cyan, HOR yellow and R – red.

When the best collaboration level was HR, deviation from the optimal values of β_r by up to 1 lowers the objective function score by about 30%. The objective function score of the HR collaboration level will never decrease beneath the corresponding score of the H and R collaboration levels for the same likelihood ratio values within the pre-determined deviation boundaries. However, with the increase in the target probability, an increase in the value of β_r will reduce the HR collaboration level score to a value lower than that of the HOR collaboration level, thereby shifting the best collaboration level from HR to HOR (Figure 13).

A deviation in β_{rh} from the optimal value reduces the objective function score by up to 7% within the pre-determined deviation boundaries. The magnitude of the decreased score grows with the increase in target probability and the decrease in human sensitivity. Within the pre-determined deviation boundaries and for the same likelihood ratio values, the score of the HR collaboration level will never decrease to values lower than those of the other collaboration levels.

A deviation in β_h from the optimal value reduces the objective function score by not more than 2% within the pre-determined deviation boundaries. Likewise, when the score of the HR collaboration level is within the pre-determined deviation boundaries it will never decrease to a score that is lower than those of the other collaboration levels for the same likelihood ratio values.

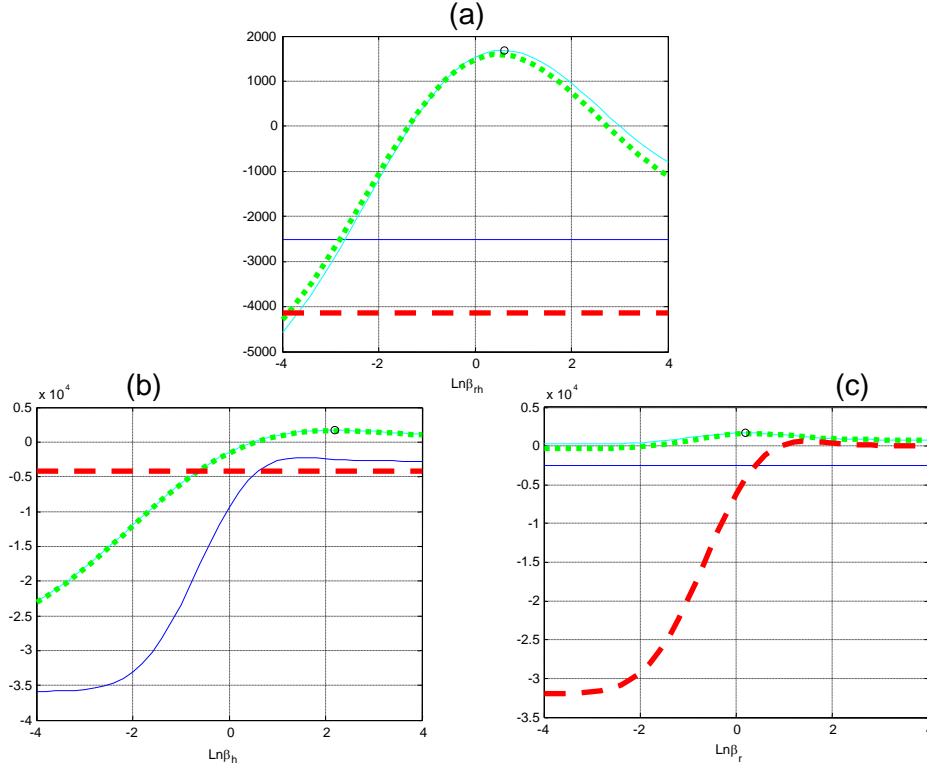


Figure 13: An example for the influence of small deflections in the optimal values of (a) β_{rh} , (b) β_h and (c) β_r when HR is the best collaboration level and its objective function score and $P_s=0.2$, $d'_r=1$ and $d'_h=2$. The colors represent the different collaboration levels: H – blue, HR – cyan, HOR yellow and R – red.

Under conditions in which the best collaboration level is HOR, a deviation from the optimal β_r values by up to 1 decreases the objective function score by up to 37%. The magnitude of this reduction reaches its maximum when the target probability is 0.5, but it will decrease with the increase in robot sensitivity. Within the pre-determined deviation boundaries and for the same likelihood ratio values, the HOR collaboration level's objective function score will never decrease beneath that of either the H or R collaboration levels. However, for target probabilities lower than 0.5, a decrease in the value of β_r will lower the score of HOR to beneath that of the HR collaboration level, thus shifting the best collaboration level from HOR to HR. In some cases this phenomenon occurs within the pre-determined deviation boundaries (Figure 14).

Deviations in β_{rh} from the optimal value will decrease the objective function score by up to 5% within the pre-determined deviation boundaries. The magnitude of the score decreases when target probability, human sensitivity, and robot sensitivity are all increasing. In terms of the pre-determined deviation boundaries, the score of the HOR collaboration level will never decrease beneath those of the H and HR collaboration levels for the same likelihood ratio values. When the value of β_{rh} exceeds the upper deviation boundary, however, the score of

HOR will decrease to values beneath that of HR. When the human and robot sensitivities are equal to 2, a deviation in the optimal value of β_{rh} will reduce the HOR score relative to the score for R and will shift the best collaboration level from HOR to R.

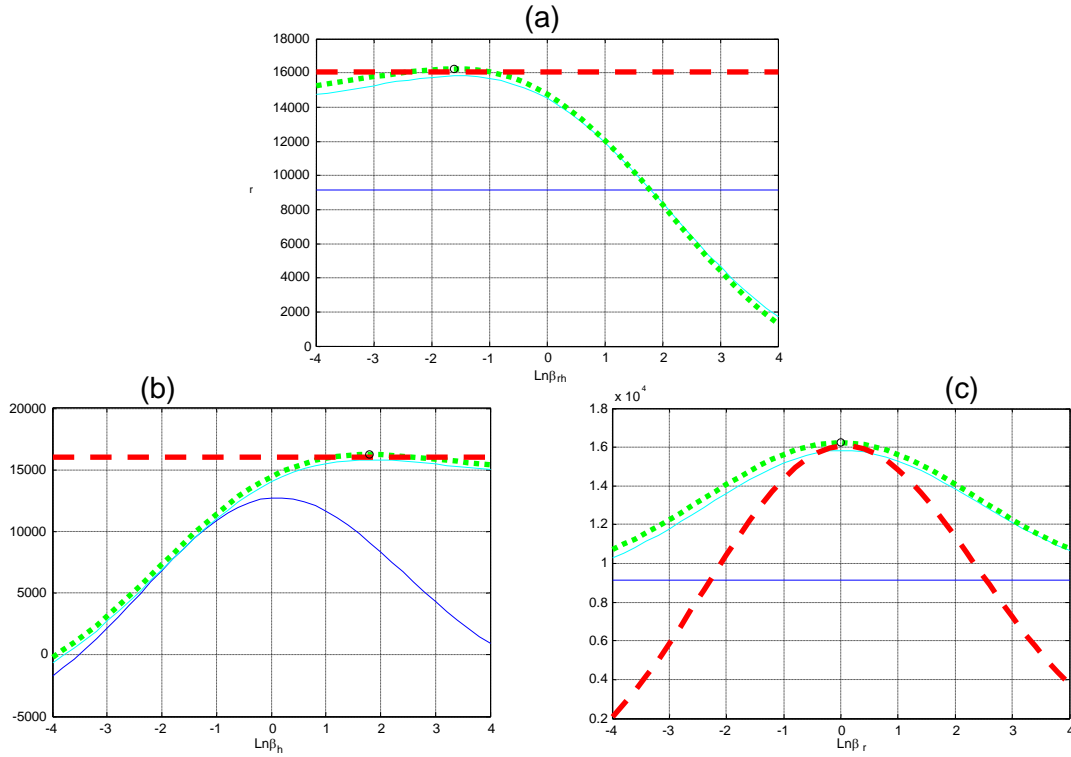


Figure 14: An example for the influence of small deflections in the optimal values of (a) β_{rh} , (b) β_h and (c) β_r when HOR is the best collaboration level and its objective function score and $P_s=0.5$, $d'_r=2$ and $d'_h=2$. The colors represent the different collaboration levels: H – blue, HR – cyan, HOR yellow and R – red.

Deviations in β_h from the optimal value will decrease the objective function score by up to 4% within the pre-determined deviation boundaries. The magnitude of the decreased score grows with increases in the target probability while it shrinks when human and robot sensitivities are increasing. In the pre-determined deviation boundaries, the score of the HOR collaboration level will never decrease beneath the scores of the H and HR collaboration levels for the same likelihood ratio values. When the human and robot sensitivities are equal to 2, a deviation of the optimal value of β_h will decrease the HOR score to beneath the R score and will shift the best collaboration level from HOR to R.

The sensitivity analysis on the optimal likelihood ratios, β_r , β_h , and β_{rh} in terms of the best collaboration level showed, as expected, that deviations in the optimal values can decrease the objective function score of the best collaboration level, and in some cases they can even cause a shift from one collaboration level to another. The shift will be to the adjacent level.

For the cases examined in the sensitivity analysis of d'_r and d'_h , H collaboration level was never the best collaboration level.

5.2.2 Sensitivity analysis of d'_r and d'_h

The robot and human sensitivities, d'_r and d'_h , ranged between 0.5 and 3. Sensitivity analyses were performed on the optimal values of β_r , β_h , and β_{rh} in terms of the best collaboration level. The sensitivity analyses investigated the influence on the objective function score and the best collaboration level of deflections in the sensitivity value of ± 0.25 and ± 1 .

The objective function scores of the R, HR, and HOR collaboration levels increase with the increase in robot sensitivity. The H collaboration level, however, is not influenced by robot sensitivity.

In instances when R is the best collaboration level, the objective function score did not decrease to values lower than the scores of all other collaboration levels for the smallest and the largest robot sensitivity values. For intermediate target probability values and robot sensitivities equal to human sensitivities, the objective function score of the R collaboration level decreases to levels lower than at least one other collaboration level for small decreases in the robot sensitivity. In those cases the HOR collaboration level achieves the highest score. For low robot sensitivity equal to 1, small changes in robot sensitivity will change the objective function score by up to 18%. The highest change in the score occurs for a target probability of 0.5. When robot sensitivity is high, *i.e.*, equal to 3, small changes in robot sensitivity will change the objective function score by up to 26%. The smallest change in the objective function scores, then, is obtained for a target probability of 0.5.

Under conditions when HR is the best collaboration level small changes in robot sensitivity did not reduce the objective function score to values lower than the scores of all other collaboration levels. In some cases, increases in robot sensitivity cause the HOR collaboration level score to exceed that of the HR collaboration level, resulting in a shift of the best collaboration level to HOR. For small changes in the robot sensitivity, the objective function score of the HR collaboration level changes by up to 18%.

For cases in which the best collaboration level is HOR, its objective function score did not decrease to beneath the scores of either the H or HR collaboration levels for small or major changes in the robot sensitivity. Increases in the robot sensitivity will decrease the difference between the objective function scores of the HOR and the R collaboration levels.

For major changes in robot sensitivity, the objective function score of the R collaboration level exceeds that of the HOR collaboration level for cases where the initial difference between the robot and human sensitivities was 1 or less and the best collaboration level will shift to R. For small changes in robot sensitivity, the objective function score was changed by up to 18%.

The sensitivity analysis performed on d'_r indicated that changes in robot sensitivity may shift the best collaboration level from one to another; the shift is to the adjacent/next collaboration level.

The objective function scores of H, HR, and HOR collaboration levels increase with increases in human sensitivity. The R collaboration level is not influenced by the human sensitivity.

For cases in which R is the best collaboration level, the objective function score remains above the scores of all other collaboration levels for small and major decreases in human sensitivity. For intermediate target probability values and for robot sensitivities equal to human sensitivities, the objective function score of the R collaboration level dips below the score of at least one other collaboration level for small increases in human sensitivity. In this case the collaboration level achieving the highest score is HOR.

For cases in which the best collaboration level is HR, the objective function scores remain above the scores of all other collaboration levels for both minor and major changes in the human sensitivity.

For cases in which the best collaboration level is HOR, the objective function score stays above the scores of both the H and HR collaboration levels for small or major changes in human sensitivity. Decreases in the human sensitivity produce corresponding decreases in the difference between the objective function scores of the HOR and the R collaboration levels.

For intermediate target probability values and robot sensitivity equal to human sensitivity, the objective function score of the R collaboration level exceeds the score of the HOR collaboration level for small decreases in human sensitivity.

The sensitivity analysis on d'_h revealed that changes in the human sensitivity values can shift the best collaboration level from one to another; the shift will be between adjacent/next collaboration levels.

For the cases examined in the sensitivity analysis of d'_r and d'_h , the H collaboration level never ranks as the best collaboration level.

5.2.3 Sensitivity analysis of target probability, P_s

The target probability P_s ranged between 0.1 and 0.9. The sensitivity analysis was performed on the optimal values of β_r , β_h , and β_{rh} and evaluated the influence of ± 0.1 deflections on the objective function score and on the best collaboration level.

The objective function score of all four collaboration levels increases with the increase in target probability.

When R is the best collaboration level, the objective function score remains above the scores of the H and HR collaboration levels for small changes in the target probability.

In some cases where the human sensitivity is equal to or higher than the robot sensitivity, the objective function score of the R collaboration level decreases beneath the score of the HOR collaboration level for small changes in the target probability. In those cases the HOR collaboration level achieves the highest score.

When the best collaboration level is HR, even small decreases in the target probability reduce the objective function score of the HR collaboration level to a value below that of the H score. A major increase in the target probability, however, reduces the objective function score of the HR collaboration level to a value less than that of the HOR score.

When the best collaboration level is HOR the objective function score remains above the score of the R collaboration level for minor and major changes in the robot sensitivity. When target probability is low, the objective function score of the HR collaboration level exceeds that of the HOR collaboration level for small decreases in the target probability and the best collaboration level will then shift to HR. In some cases where the target probability is intermediate or high, the objective function score in the HOR collaboration level is reduced to a level below the score for H for major decreases in the target probability.

Sensitivity analysis on target probability shows that changes in the human sensitivity may cause shifts in the best collaboration level, although not necessarily between adjacent/next collaboration levels.

5.3 Summary and conclusions

When increases in target probability, the number of targets increased and the number of non-target objects decreased, the system is influenced less by false alarms and therefore, the probabilities of both hit and of false alarms increase. The likelihood ratios, β_r , β_h and β_{rh} decrease, the operational cost increases, and the objective function score increases.

For all collaboration levels the highest objective function score increases with the increase in human and robot sensitivities.

When the objective function includes operational costs, HR collaboration performs better than HOR when the target probability is low and the robot sensitivity is low. In these cases the number of robot false alarms is high relative to the number of robot hits and in the HOR collaboration level the human requires more time to correct the robot false alarms than to confirm the robot hits. Therefore, in the HOR collaboration level the task time and the operational cost increase and the objective function score decreases.

The H collaboration level is never the best collaboration level probably due to its high operational cost and low hit rate relative to the other collaboration levels. Thus, the collaboration of human and robot in target recognition tasks will always improve the optimal performance of a single human detector .

When robot sensitivities are higher than human sensitivities the best collaboration level is R. At the best collaboration level, the system likelihood ratio and the system sensitivity both decrease while the target probability increases. Moreover, the system sensitivity is never less than the robot sensitivity.

Elimination of operational costs from the objective function will unite the HR and HOR into one collaboration level, since the only differences between the HR and the HOR collaboration level as expressed in the system objective function are in the time parameters and the operational costs. The objective function score increases. The best collaboration level for the objective function excluding the operational costs will be the HOR collaboration level for the entire sensitivity space and for all target probabilities. The combination of both human and robot in the HOR collaboration level increases the sensitivity in most cases and increases the probability of a hit while reducing the probability of false alarms. The system sensitivity for the objective function excluding the operational costs is lower than in the case of the objective function including the operational costs for all target probabilities except for high target probability with high human sensitivity and low robot sensitivity. The overall system sensitivity will always be higher than the human sensitivity.

The sensitivity analysis on the optimal values of the robot and human likelihood ratios, β_r , β_h , and β_{rh} , of the best collaboration levels showed that any change in either direction in the optimal values will decrease the objective function score of the best collaboration level. In some cases, small changes in the optimal values of the likelihood ratios will cause a shift from a collaboration level to the one adjacent to it, except in the case of R, which remains the best collaboration level even for major changes in the optimal values (*i.e.*, $HR \leftrightarrow HOR \rightarrow R$). The sensitivity analysis of d_r shows that small, positive changes in robot sensitivity will increase the objective function score of the best collaboration level and will diminish the differences between the best collaboration level and the adjacent and more autonomous collaboration level. In some cases changes in robot sensitivity may cause the best collaboration level to shift to an adjacent level; however for collaboration levels involving a human, the shift will occur only in one direction, to the more autonomous collaboration level (*i.e.*, $HR \rightarrow HOR \leftrightarrow R$).

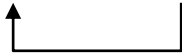
The sensitivity analysis on d_h reveals that small positive changes in human sensitivity increase the objective function score of the best collaboration level unless it is R. In some cases, changes in human sensitivity may cause the best collaboration level to shift to an

adjacent level; however, this occurs between the two highest autonomous levels only, HOR and R (*i.e.*, $HR ; HOR \leftrightarrow R$).

The best collaboration level is never H and the shift to H will never occur when the optimal values of β_r , β_h , β_{rh} , d'_r , and d'_h can change.

A sensitivity analysis on target probability shows that an increase in the target probability can increase the objective function score of the best collaboration level. In some cases, changes in the target probability may shift the best collaboration level from one definition to another; however, the HOR collaboration level can shift directly to the H.

(*i.e.*, $HO \leftarrow HR \leftrightarrow HOR \leftarrow R$).



The sensitivity analysis showed that small changes in the optimal values of the analyzed parameters can cause shifts in the best collaboration level from one to another. Changes in the different parameters can also have different influence on the system stability. An algorithm that will account for system stability and the influence of small changes in the parameters can increase the system performance in real cases where the parameters are drifting around the optimal values. These findings are beyond the scope of this current framework.

6 MELON DETECTION EXPERIMENT

This chapter starts with the description of the apparatus, design and procedure of the melon detection experiment that was conducted. It continues with an extensive presentation of the findings.

6.1 *General*

An experimental system was developed to test and examine different human-robot collaboration levels for a specific target detection task in an agricultural environment. The experiment consists of a series of images taken in a standard melon field in which the participants were asked to identify melons in the field. The melons were partially covered by leaves and had different colors and sizes.

The goals of the experiment are to determine the hit and false alarm rates of the human and the system for different task objectives, collaboration levels, complexity levels, and robot hit and false alarm rates.

The experiment focuses on the detection part; the picking part is not addressed and we do not consider its practical aspects.

Experiment assumptions

Robot detection performance measures are not influenced by the image complexity level, the collaboration level, or by the human and system performances, and therefore, remain constant during the experiment.

Experiment hypotheses

1. When dealing with human-robot collaboration, several factors influence human performance, including image complexity, collaboration level, objective function payoffs, and the robot's performance.
2. The factors influencing system performance are image complexity, collaboration level, objective function weights, robot performance and human performance.
3. Collaboration between human and robot can better improve system performance relative to human or robot performance measures alone.

6.2 *Apparatus and design*

Participants

120 IEM undergraduate students participated in the experiment. The participants were assigned randomly to 10 groups with 12 students in each group. Motivation for high

performance was encouraged through the promise of a monetary award (up to 100 NIS) to 10% of the participants.

Database

Melon images in the field were taken by a video camera mounted on a robotic melon harvester (Figure 15; Edan 1995) moving along a melon row in various illumination conditions. Images were shown on the screen as seen from a camera mounted vertically on the vehicle, facing the ground in the middle of the row. From the video file, single images were manually selected. The images were viewed by a panel of three experts and were classified into three levels of complexities: low, intermediate, and high. The image complexity represents the difficulty level of detecting targets in the image. The location of true targets in each image was identified and saved in a targets database. The image resolution was 640X480 pixels and each pixel represents an area of 4 mm².



Figure 15: Robotic melon harvester (Edan, 1995).

Design

The experimental system consists: i) mouse MMI (man-machine interface) in order to run the experiment on 15 participants at a time in a computer classroom; ii) PC; iii) a program written in Matlab to simulate a working station for target detection in an unstructured environment; and, iv) a database of melon images taken in the field.

In each session participants from all experimental groups (Table 3) were tested, and were seated randomly in the classroom. The participants were divided into ten groups, each of which was given one of two objective function weights (represented by the reward system),

one of two different robot detection performance qualities (high and low), and one of three collaboration levels (H, HR, HOR) as shown in Table 3. The objective function weights of groups 1,3,4,7,8 were to achieve minimum false alarms, defined as $V_H=3$ corresponding to the weight of a single hit and $V_{FA}=-7$ corresponding to the weight of a single false alarm. The objective function weights of groups 2, 5, 6, 9, 10 were to achieve maximum hits, defined as $V_H=7$ and $V_{FA}=-3$. These values of V_H and V_{FA} were selected in order for the participant to understand the importance of the reward. The ratio was a little higher than 2. If the ratio would have been higher, the participants would have tend to disregard the FA influence in the maximum hit reward system or disregard the hit influence in the minimum FA reward system. The values in two cases of the reward system examined were opposite one to another, to create a symmetric response by the participants and the sum of the magnitude of both V_H and V_{FA} values is 10.

There was no time limit for any of the experimental groups and the participants were not rewarded for their detection time ($V_t=0$). The specific values of the robot hit and false alarm rates were chosen so as to examine two different robot qualities.

A target was defined as any yellow or orange melon and the participants' task were to mark all the targets in the images,

Table 3: The experimental groups.

Group no.	Participants ID no.	Collaboration level			Reward system		Robot quality	
		H	HOR	HR	Minimize FA	Maximize Hit	high	low
1	10-19,1001,1002	X			x			
2	20-29,2001,2002	x				x		
3	30-39,3001,3002		x		x		x	
4	40-49,4001,4002		x		x			x
5	50-59,5001,5002		x			x	x	
6	60-69,6001,6002		x			x		x
7	70-79,7001,7002			x	x		x	
8	80-89,8001,8002			x	x			x
9	90-99,9001,9002			x		x	x	
10	100-111			x		x		x

Each group viewed 180 images. The images were divided *a-priori* into three complexity levels: low, intermediate and high, with 60 images in each complexity level. In each image the number of targets varied between zero and four.

The total number of hits and false alarm targets marked by the robot was equal for the low and high robot qualities and in all groups. The total number of targets in each experiment was 235. The 'high quality' robot detected 212 targets (90% hit rate) and 11 false alarms, for a total of 223 marks. The 'low quality' robot detected 118 targets (50% hit rate) and 105 false alarms, for a total of 223 marks. Therefore, in both conditions participants received 223 indications of possible targets. In the experiment, the robot did not perform image processing but the computer picked targets and non-target objects (marked as false alarms) from the database, simulating the robot operation.

All participants received written instructions in which they were informed of the task objective and the reward system payoffs. The participants were not informed of the differing complexity levels or of the robot's quality. The participants were told that the robot detections are not totally reliable. Before the experiment, the participant practiced on a tutorial software for 5 images with "unlimited" time. During the experiment the activities of the human operator, the objects marked, and the time of each action were automatically recorded. Performance measures were calculated from the recorded raw data. The participants received feedback on their performance during the experiment after each image.

The images were arranged in three statistical blocks, numbered 1, 2 and 3, with 60 images in each block. The order of the blocks was identical for all groups and participants. The images within each block were displayed in random order for each group and each subject. The blocks were arranged so in order to examine if there can be a learning effect.

The controls of the experiment were the H collaboration level groups and the R collaboration level. The independent variables within each experimental group were:

- 1) image complexity level, defined as low, intermediate, and high.
- 2) block order.

The independent variables between the groups were:

- 1) The objective function weights (reward system): V_H , V_{FA} . The task objective weights are constant and fixed within each group during the entire experiment.
- 2) Collaboration levels: H, HOR, and HR. The collaboration level is constant and fixed within each group during the entire experiment.
- 3) Robot quality: high - $p_{Hr} = 0.9$, $F_{FA} = 11$, low - $p_{Hr} = 0.5$, $F_{FA} = 105$. The robot quality is constant and fixed within each group during the entire experiment.

In an integrated human-robot system, such as the one investigated here, the measured and calculated variables can be divided into three groups: robot variables, which are part of the independent variables in the experiment and were predetermined; the human variables; and, the system variables, which are parameters that reflect the system as a whole. Both human and system variables are dependant variables in the experiment.

- i. system hit rate (p_{Hs});
- ii. system average false alarms (p_{FAs});
- iii. human hit rate of targets that the robot didn't mark(p_{Hh});
- iv. human average false alarm of objects that the robot did not mark(p_{FAh});
- v. human hit rate of targets marked by the robot (p_{Hrh});
- vi. human false alarm rate of objects marked by the robot (p_{FArh});
- vii. average image time;
- viii. system objective function score (point accumulated, VIs).

6.3 Procedure

The experimental procedure was identical for all participants:

- 1) A group of approximately 15 participants from different experiment groups entered the room in which the experiment was conducted. Each participant was seated in front of one computer. The system was demonstrated and the objective of the experiment, the experimental procedure, and the experimental facilities were explained.
- 2) A short interview was conducted to collect information on the participant's background, occupation, eyesight, and other relevant data for the experiment.
- 3) The participant adjusted the screen and the chair for his or her convenience according to his or her physical dimensions.
- 4) The experimenter described the experiment to the participants, demonstrated what is considered to be a target, a robot hit, and a false alarm, and demonstrated how to work with the experimental system.
- 5) The participants activated a familiarization program of five images in order to provide some practice. The experimenter explained that this is a familiarization program of five images and guided and supervised the participant during the trial.
- 6) After the familiarization, the experimenter ran the experimental program and did not interfere during the experiment. The experiment consisted of 180 images. All system parameters and the participant's actions were automatically recorded during the experiment.

An example of the experimental screen is shown in Figure 16. The image was displayed in the middle of the screen. Objects in the image could appear in four states: 1) unrecognized and therefore unmarked, 2) object is recommended by the robot to be a target denoted by a red frame around the object, 3) the object is marked and acquired as a target by the robot or the human, denoted by a red frame and a black cross. The human can move the mouse to a spot on the image and click on it to: i) acquire a new target, ii) acquire a target already recommended by the robot, iii) eliminate a target that was acquired by the robot or by the human. When done, in order to continue to the next image in the block, the human clicks on the “next” button on the left side of the screen. The participant can only scroll through the images.

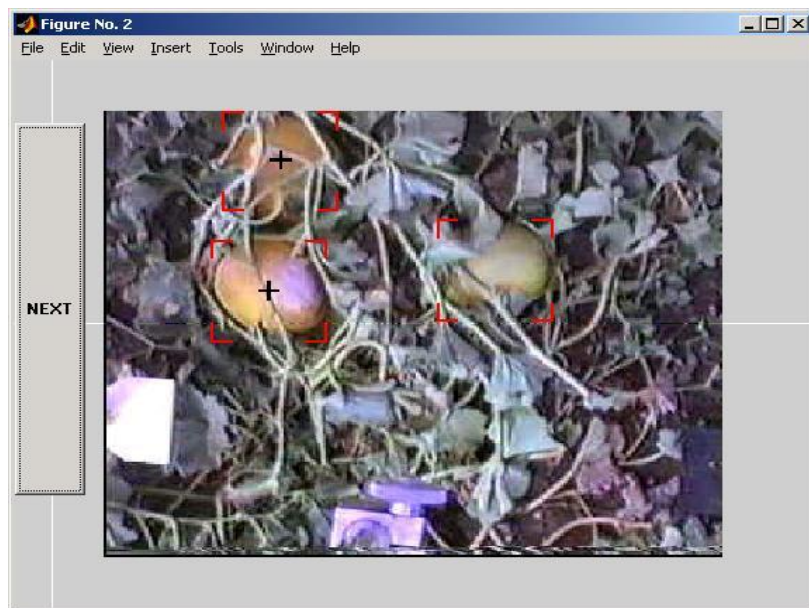


Figure 16: An example for the display during the experiment.

Between the images, the participants received information about their current performance (Figure 17). The information includes the current objective function score (score), the last image number of hits (Detections), the last image number of false alarms (False) and the last image number of missed targets (Misses).

- 7) At the end of the experiment, the computer showed the score the participant achieved during the experiment and filled out a questionnaire about the completed experiment.
- 8) After the participant left the room the experimenter prepared the experimental system for the next participant.



Figure 17: Information windows between images.

6.4 Results

6.4.1 General

Statistical analysis of the experimental results included: analysis of the system performance and analysis of the human performance. System performance analysis includes hits, false alarms, time, and score of the objective function. Human performance analysis is done on human hits and false alarms of objects already marked by the robot, human hits and false alarms of objects that were not marked by the robot, and human sensitivity. Analyses examined the influence of the block, the image complexity, the reward, the level of cooperation, and the robot quality on the system and human performances. Statistical analyses, comprising repeated measures analysis of variance, Fisher LSD post-hoc comparison, and general linear model of univariate tests of significance, were all performed with Statistica™ 7 on a personal computer.

The results are arranged as follows: each dependent variable is presented and discussed separately, at first the general findings and a table of "the repeated measures analysis of variance" is given followed by analyses of the main findings. The first part of the results (section 6.4.2) deals with system performance and includes system detection performance (section 6.4.2.1), analysis of system hit (p_{Hs} , section 6.4.2.1.1), analysis of system false alarm (section 6.4.2.1.2), analysis of the system operation time (section 6.4.2.2), points accumulated (objective function score section 6.4.2.2) and conclusions from the system performance part (section 6.4.2.4). The second part (section 6.4.3) deals with human performance. It includes analysis of: p_{Hrh} (section 6.4.3.1), p_{Hh} (section 6.4.3.2), p_{FArh} (section 6.4.3.3), human false

alarms that the robot did not mark, F_{FAh} (section 6.4.3.4), $d'h$ calculated based on p_{Hrh} and p_{FArh} (section 6.4.3.5) and conclusions (section 6.4.3.6). in addition in appendix XIII Analysis of β_{rh} for objects that were marked by the robot are presented.

6.4.2 System efficiency for different levels of automation and different stimulus complexities

6.4.2.1 Detection Performance

6.4.2.1.1 Analysis of System hit as a function of level of cooperation, block, image complexity, robot performance, reward.

The experiment included two groups of H collaboration levels, one for each reward type, and four groups of the HR and HOR collaboration levels, two for the reward types and two for the robot quality levels. To perform the statistical analyses for all collaboration levels, the robot quality variable and level of cooperation variables were rescaled into one group variable with 5 levels (H, HOR-high, HOR-low, HR-high, HR-low) named NewGroup. Analysis of each performance measure was executed in two stages, the first, an analysis on the NewGroup, the second an analysis of the collaboration levels excluding the H collaboration level groups. In this analysis, the collaboration level and the robot quality were independent variables.

6.4.2.1.1.1 Analysis with groups as the independent variable (combining all levels of cooperation).

Statistical analysis of the system hits as a function of the reward and the experimental group on all images showed that the reward and the NewGroup had significant effects (Table 4).

Table 4: The repeated measures analysis of variance results.

	DoF	MS	F	p
{1}Rewards	1, 110	0.134	4.63	0.034
{2}NewGroup	4, 110	0.150	5.18	0.001
Rewards*NewGroup	4, 100	0.016	0.54	N.S.
{3}BLOCK	2, 220	0.135	17.22	0.000
BLOCK*Rewards	2, 220	0.008	0.99	N.S.
BLOCK*NewGroup	8, 220	0.005	0.66	N.S.
BLOCK*Rewards*NewGroup	8, 220	0.010	1.27	N.S.
{4}COMPLEXITY	2, 220	1.564	232.12	0.000
COMPLEXITY*Rewards	2, 220	0.000	0.01	N.S.
COMPLEXITY*NewGroup	8, 220	0.013	1.98	0.050
COMPLEXITY*Rewards*NewGroup	8, 220	0.011	1.60	N.S.
BLOCK*COMPLEXITY	4, 440	0.069	19.45	0.000
BLOCK*COMPLEXITY*Rewards	4, 440	0.002	0.52	N.S.
BLOCK*COMPLEXITY*NewGroup	16, 440	0.005	1.38	N.S.
3*4*1*2	16, 440	0.003	0.77	N.S.

The reward system had a significant effect. Overall the hit probability was smaller (.88) when the aim was to minimize false alarms, compared to when the aim was to maximize hits (.91). Thus, people seemed to have considered the reward structure and increased their tendency to detect targets if they were rewarded for detection.

The experimental group also had a significant effect. The mean results and the results of post-hoc comparisons between the five groups are shown in Table 5 for the system hit values. The difference between the control H group and the HOR group with high robot quality was marginally significant ($p < .1$). A significant difference exists in system performance between low levels of automation (HO-R) with a 'low quality' robot and the other groups.

Table 5: Post-hoc comparisons between the five Newgroups.

	HO	HOR-high	HR-high	HOR-low	HR-low
system hit rate	0.898	0.926	0.912	0.897	0.855
HR-low	0.010	0.000	0.001	0.013	

There was a significant effect of the level of complexity. Hit rates were highest when stimuli had low complexity (.97), somewhat lower with intermediate complexity (.89) and lowest with high complexity stimuli (.83).

There was a significant difference between the blocks; the hit rates in the first block (.89) and the second block (.88) were similar but not significant. The difference between the last block (.92) and the prior two blocks was highly significant ($p < .001$). This can be explained by the significant Block*Complexity interaction (Figure 18). Apparently in the high complex images the stimuli in block 2 were more difficult, and lead to lower hit rates than the high complex stimuli in the other blocks. There was no significant difference between the blocks in the low complex stimuli (Table 6), Also, there was no significant difference between blocks 1 and 2 in the intermediate complex stimuli.

Complexity interacted with the experimental group. The differences between the groups were small and non-significant for low-complexity stimuli and increased for intermediate and especially high-complexity stimuli. In the intermediate-complexity stimuli and the high-complexity stimuli there was a significant difference between the HR-low experimental group and the experimental groups of high robot quality (HOR-high/HR-high). In the high-complexity stimuli there was significant difference between the HR and HOR collaboration levels. The system hit rate in each experimental group was significantly different between the three complexity levels of stimuli. In each complex stimulus the HOR collaboration level with the high robot quality group achieved the highest system hit rate. The HR collaboration level with the low robot quality group achieved the lowest hit rate (Figure 19).

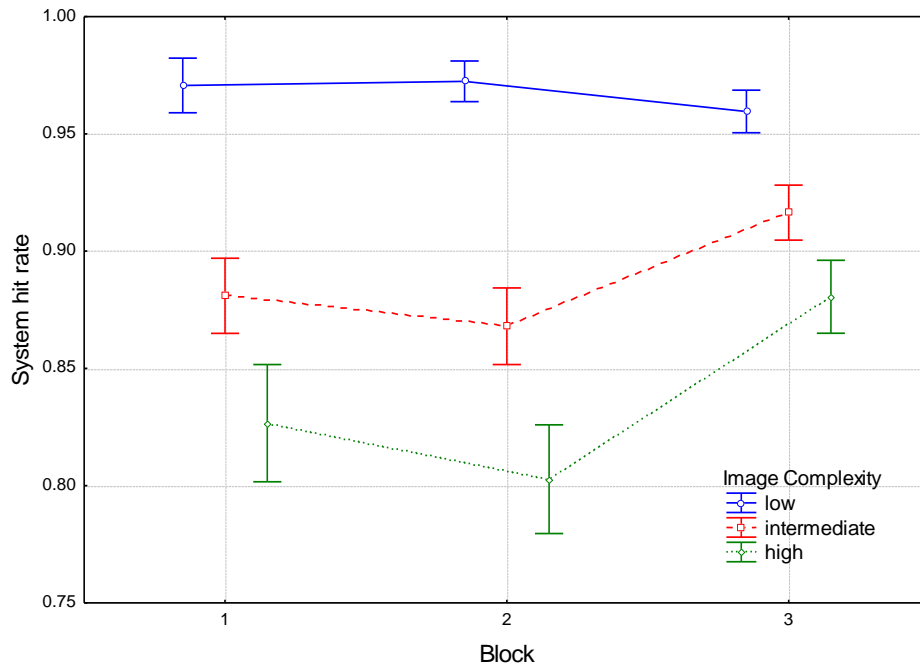


Figure 18: Probability of Hit for the blocks as a function of the stimulus complexity.

Table 6: Post-hoc comparisons between the Block*Complexity combinations.

		Block 1	Block 1	Block 1	Block 2	Block 2	Block 2	Block 3	Block 3	Block 3
Complexity		low	Inter.	high	low	Inter.	high	low	Inter.	high
System hit rate		0.971	0.881	0.827	0.972	0.868	0.803	0.960	0.916	0.881
Block 1	Low		0.000	0.000	N.S.	0.000	0.000	N.S.	0.000	0.000
Block 1	Inter.	0.000		0.000	0.000	0.092	0.000	0.000	0.000	N.S.
Block 1	High	0.000	0.000		0.000	0.000	0.002	0.000	0.000	0.000
Block 2	Low	N.S.	0.000	0.000		0.000	0.000	0.094	0.000	0.000
Block 2	Inter.	0.000	0.092	0.000	0.000		0.000	0.000	0.000	N.S.
Block 2	High	0.000	0.000	0.002	0.000	0.000		0.000	0.000	0.000
Block 3	Low	N.S.	0.000	0.000	0.094	0.000	0.000		0.000	0.000
Block 3	Inter.	0.000	0.000	0.000	0.000	0.000	0.000	0.000		0.000
Block 3	High	0.000	N.S.	0.000	0.000	N.S.	0.000	0.000	0.000	

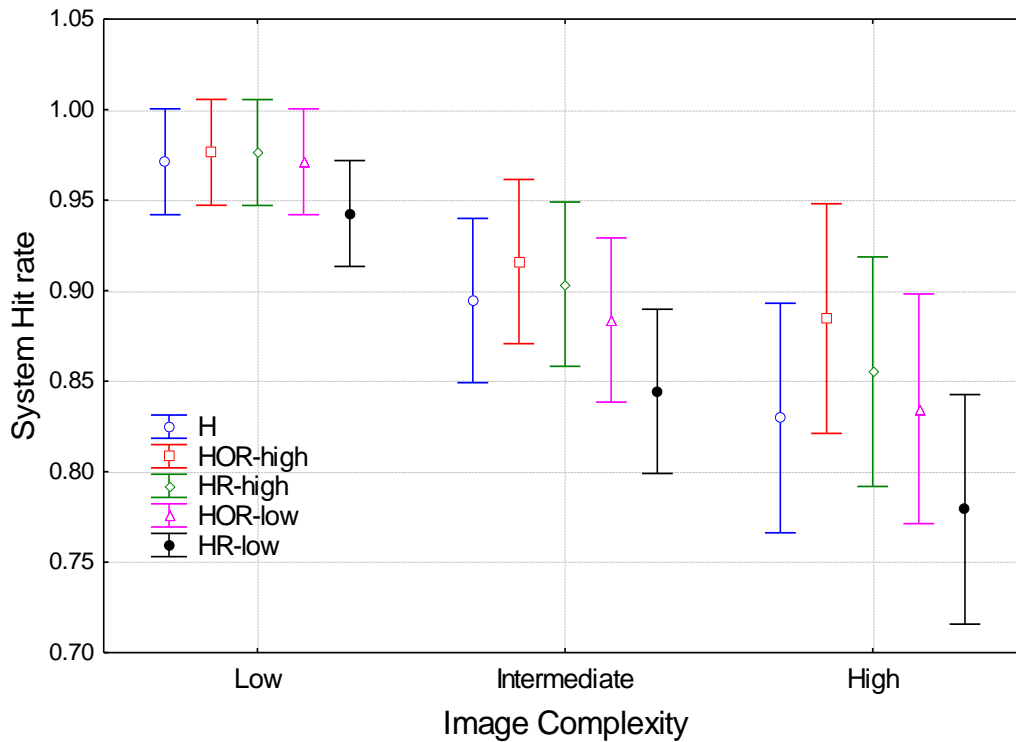


Figure 19: Probability of a Hit for the five experimental groups as a function of the stimulus complexity.

6.4.2.1.1.2 Analysis with cooperation level and robot performance as independent variables for all cooperation levels except H.

Overall the probability was significantly smaller (.88) when the automation level was high (HOR), compared to low automation level, HR, (.91). The central finding here was that any level of automation (HOR/HR) with a 'low quality' robot impairs hit performance, compared to cases without automation.

Also the effect of robot quality was highly significant ($p < .01$). The average system hit probability for a system with a 'high quality' robot was .92, almost 5% higher than for a system with a 'low quality' robot.

Table 7 shows the statistical output of the repeated measures analysis of variance performed on the experimental results.

The influence of the Complexity*Robot quality interaction is shown in Figure 20. The system hit probability is significantly reduced with the increase of the stimulus complexity, for both low and 'high quality' robots ($p < .01$). In addition, for each complex stimulus, the system performance of the 'high quality' robot was higher than for the 'low quality' robot. This difference was found to be significant for intermediate and high stimulus complexities ($p < .05$). For low image complexity the system hit probabilities were similar for both low and 'high quality' robots and no significance was found.

Table 7: The repeated measures analysis of variance results.

	DoF	MS	F	p
{1}Collaboration	1, 88	0.164	5.03	0.027
{2}Rewards	1, 88	0.071	2.17	N.S.
{3}Robot quality	1, 88	0.394	12.06	0.001
Collaboration*Rewards	1, 88	0.006	0.19	N.S.
Collaboration*Robot quality	1, 88	0.040	1.23	N.S.
Rewards*Robot quality	1, 88	0.032	0.98	N.S.
Collaboration*Rewards*Robot quality	1, 88	0.006	0.17	N.S.
{4}BLOCK	2, 176	0.097	11.28	0.000
BLOCK*Collaboration	2, 176	0.003	0.29	N.S.
BLOCK*Rewards	2, 176	0.004	0.42	N.S.
BLOCK*Robot quality	2, 176	0.010	1.11	N.S.
BLOCK*Collaboration*Rewards	2, 176	0.016	1.89	N.S.
BLOCK*Collaboration*Robot quality	2, 176	0.007	0.81	N.S.
BLOCK*Rewards*Robot quality	2, 176	0.006	0.72	N.S.
4*1*2*3	2, 176	0.011	1.27	N.S.
{5}COMPLEXITY	2, 176	1.207	164.21	0.000
COMPLEXITY*Collaboration	2, 176	0.014	1.95	N.S.
COMPLEXITY*Rewards	2, 176	0.003	0.43	N.S.
COMPLEXITY*Robot quality	2, 176	0.035	4.71	0.010
COMPLEXITY*Collaboration*Rewards	2, 176	0.003	0.42	N.S.
COMPLEXITY*Collaboration*Robot quality	2, 176	0.000	0.00	N.S.
COMPLEXITY*Rewards*Robot quality	2, 176	0.002	0.22	N.S.
5*1*2*3	2, 176	0.020	2.72	0.068
BLOCK*COMPLEXITY	4, 352	0.063	17.66	0.000
BLOCK*COMPLEXITY*Collaboration	4, 352	0.010	2.69	0.031
BLOCK*COMPLEXITY*Rewards	4, 352	0.002	0.57	N.S.
BLOCK*COMPLEXITY*Robot quality	4, 352	0.001	0.33	N.S.
4*5*1*2	4, 352	0.001	0.32	N.S.
4*5*1*3	4, 352	0.005	1.27	N.S.
4*5*2*3	4, 352	0.003	0.93	N.S.
4*5*1*2*3	4, 352	0.004	1.04	N.S.

The mean results and the results of post-hoc comparisons between Complexity and Robot quality interaction are shown in Table 8.

A similar analysis was performed on the influence of the Complexity*collaboration-level*BLOCK interaction (Figure 21). The system hit probability was found to be significantly reduced with the increase of the stimulus complexity for both lower and higher automation levels for each block ($p < .01$). In all the blocks and the stimulus complexities, the system hit rate was higher for the high automation level (HOR) than for the low automation level (HR), except for block 1 and low stimuli complexities where the hit rates for both automation levels were similar. The differences between the lower and higher automation levels were found to be insignificant for all complexity stimuli and blocks.

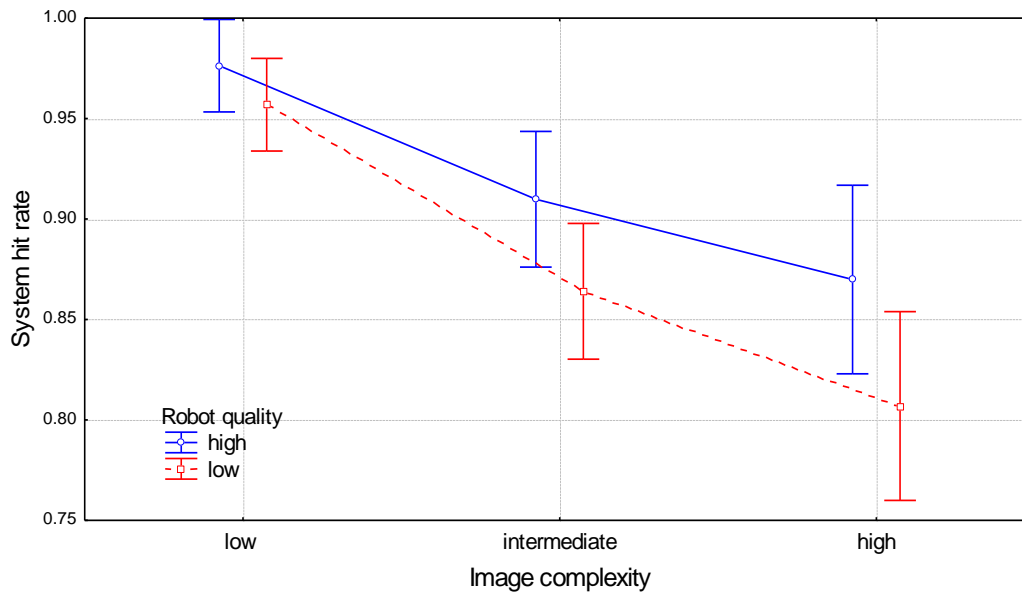


Figure 20: Probability of a hit for the two robot quality levels as a function of the stimulus complexity.

Table 8: post-hoc comparisons between the Complexity*Robot-quality combinations.

		high robot quality	high robot quality	high robot quality	low robot quality	low robot quality	low robot quality
	COMPLEXITY	low	Inter.	high	low	Inter.	high
	system hit rate	0.976	0.910	0.870	0.957	0.864	0.807
high robot quality	low		0.000	0.000	N.S.	0.000	0.000
high robot quality	intermediate	0.000		0.000	0.002	0.034	0.000
high robot quality	high	0.000	0.000		0.000	N.S.	0.004
low robot quality	low	N.S.	0.002	0.000		0.000	0.000
low robot quality	intermediate	0.000	0.034	N.S.	0.000		0.000
low robot quality	high	0.000	0.000	0.004	0.000	0.000	

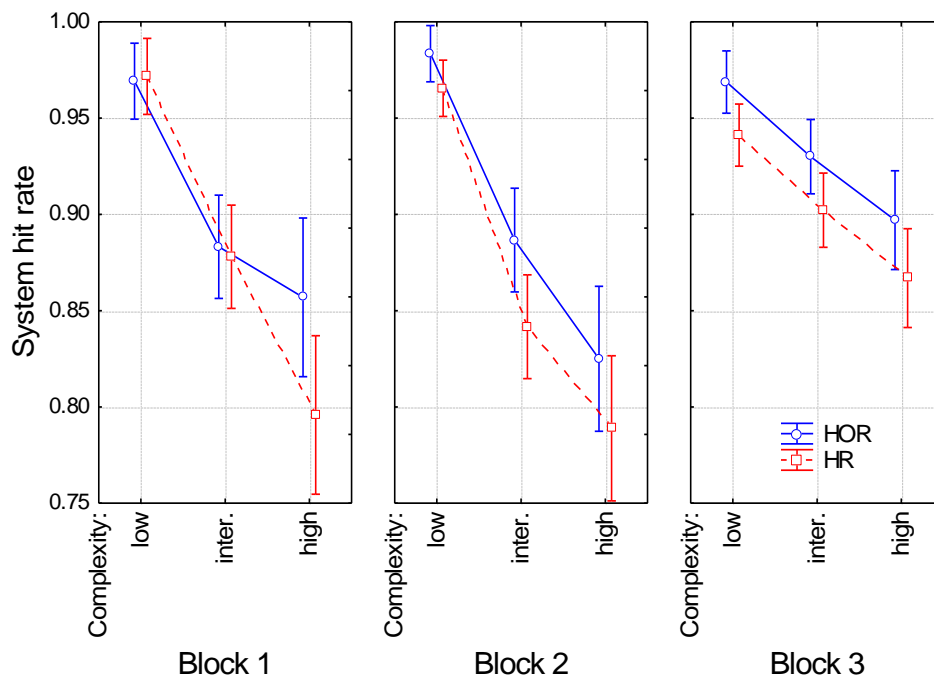


Figure 21: Probability of a hit for the two automation levels as a function of the stimulus complexity and block number.

6.4.2.1.2 Analysis of system false alarms as a function of level of cooperation, block, image complexity, robot performance, reward.

System false alarms (FA) are events during which the system marks non-target objects in the images. System FA can occur by human marks of non-target objects or robot marks of non-target objects that are confirmed by the human.

6.4.2.1.2.1 Analysis with groups as the independent variable (combining all levels of cooperation).

Table 9 shows the statistical output of the repeated measures analysis of variance performed on the experiment results.

To compare the number of false alarms for different complexity stimuli and blocks, the overall number of false alarms (FA) was divided by the number of images with the same stimulus and block, and the result was defined as a normalized false alarm. The normalized FA was smaller (.0935) when the aim was to minimize false alarms, as compared to when the aim was to maximize hits (.107). Although the effect was not statistically significant, people seemed to consider the reward structure and increased their attention to reduce the number of FA if they were rewarded for minimizing false alarms.

Table 9: The repeated measures analysis of variance results.

	DoF	MS	F	p
{1}Rewards	1, 110	0.050	1.1782	N.S.
{2}NewGroup	1, 110	0.069	1.6205	N.S.
Rewards*NewGroup	4, 110	0.013	0.3186	N.S.
{3}BLOCK	2, 220	0.127	9.4873	0.000
BLOCK*Rewards	2, 220	0.001	0.0881	N.S.
BLOCK*NewGroup	8, 220	0.006	0.4831	N.S.
BLOCK*Rewards*NewGroup	8, 220	0.007	0.5531	N.S.
{4}COMPLEXITY	2, 220	0.254	51.0036	0.000
COMPLEXITY*Rewards	2, 220	0.004	0.7789	N.S.
COMPLEXITY*NewGroup	8, 220	0.008	1.5614	N.S.
COMPLEXITY*Rewards*NewGroup	8, 220	0.006	1.1827	N.S.
BLOCK*COMPLEXITY	4, 440	0.110	26.0176	0.000
BLOCK*COMPLEXITY*Rewards	4, 440	0.004	1.0455	N.S.
BLOCK*COMPLEXITY*NewGroup	16, 440	0.005	1.2404	N.S.
3*4*1*2	16, 440	0.003	0.6850	N.S.

In the NewGroup*Complexity interaction, post-hoc comparison analysis showed that the difference between the low complexity and the other two complexities was highly significant ($p < .01$). There was no significance difference between the intermediate and high complexity stimuli.

There was a significant difference between the blocks. The highest value of the normalized FA was in the first block (.116), and the lowest value was in the last block (.0794), implying that there can be a learning effect.

The difference between the block interactions with the image complexity stimuli was highly significant ($p < .001$). For the low image complexity the normalized FA value was the lowest for all blocks while the highest was achieved for the high complexity stimuli in the first block. The normalized FA rate reduced between block 1 and block 3 for low and high complex stimuli (Figure 22). The normalized FA rate of the intermediate complexity stimuli was similar but the standard deviation was reduced, which indicates that the subjects were more uniform and clear about their FA selections.

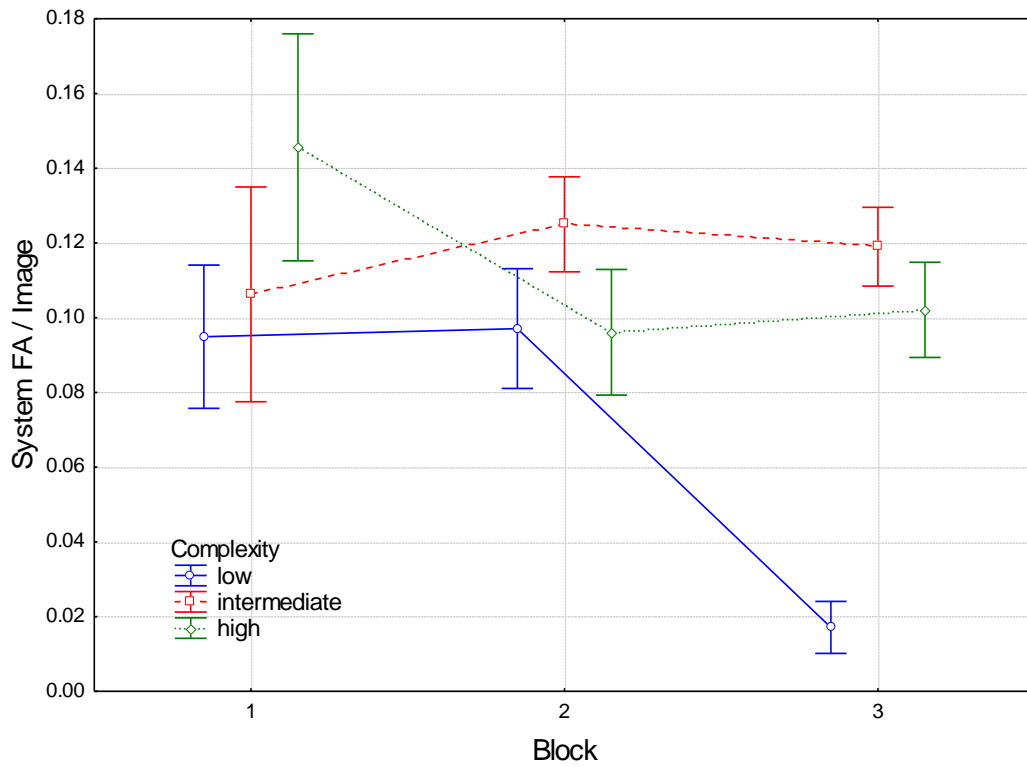


Figure 22: Normalized false alarm rate for the three blocks as a function of the stimulus complexity.

6.4.2.1.2.2 Analysis with cooperation level and robot performance as independent variables for all cooperation levels except H.

Table 10 shows the statistical output of the repeated measures analysis of variance performed on the experiment results. The system FA was significantly different for the different blocks and different image complexities levels. The block*complexity interaction was had a significant effect as well. The complexity*robot quality interaction had a marginally significant effect ($p = .052$).

Table 10: The repeated measures analysis of variance results.

	DoF	MS	F	p
{1}Collaboration	1, 88	0.085	1.6607	N.S.
{2}Rewards	1, 88	0.028	0.5576	N.S.
{3}Robot quality	1, 88	0.119	2.3311	N.S.
Collaboration*Rewards	1, 88	0.029	0.5661	N.S.
Collaboration*Robot quality	1, 88	0.033	0.6404	N.S.
Rewards*Robot quality	1, 88	0.004	0.0716	N.S.
Collaboration*Rewards*Robot quality	1, 88	0.017	0.3248	N.S.
{4}BLOCK	2, 176	0.115	7.2756	0.001
BLOCK*Collaboration	2, 176	0.007	0.4295	N.S.
BLOCK*Rewards	2, 176	0.001	0.0446	N.S.
BLOCK*Robot quality	2, 176	0.010	0.6071	N.S.
BLOCK*Collaboration*Rewards	2, 176	0.006	0.4014	N.S.
BLOCK*Collaboration*Robot quality	2, 176	0.006	0.3509	N.S.
BLOCK*Rewards*Robot quality	2, 176	0.007	0.4149	N.S.
4*1*2*3	2, 176	0.016	1.0085	N.S.
{5}CMPEXIT	2, 176	0.235	42.0155	0.000
CMPEXIT*Collaboration	2, 176	0.004	0.6613	N.S.
CMPEXIT*Rewards	2, 176	0.007	1.1749	N.S.
CMPEXIT*Robot quality	2, 176	0.017	3.0049	0.052
CMPEXIT*Collaboration*Rewards	2, 176	0.010	1.8173	N.S.
CMPEXIT*Collaboration*Robot quality	2, 176	0.003	0.5501	N.S.
CMPEXIT*Rewards*Robot quality	2, 176	0.007	1.2056	N.S.
5*1*2*3	2, 176	0.003	0.6036	N.S.
BLOCK*CMPEXIT	4, 352	0.071	15.1587	0.000
BLOCK*CMPEXIT*Collaboration	4, 352	0.004	0.8647	N.S.
BLOCK*CMPEXIT*Rewards	4, 352	0.004	0.7872	N.S.
BLOCK*CMPEXIT*Robot quality	4, 352	0.006	1.2169	N.S.
4*5*1*2	4, 352	0.008	1.6577	N.S.
4*5*1*3	4, 352	0.004	0.8733	N.S.
4*5*2*3	4, 352	0.001	0.2588	N.S.
4*5*1*2*3	4, 352	0.001	0.1484	N.S.

6.4.2.2 Operation Time: Mean time for stimuli with a given level of complexity as a function of cooperation level, block, complexity, robot performance, and reward

6.4.2.2.1 Analysis with groups as an independent variable.

Table 11 shows the statistical output of the repeated measures analysis of variance performed on the experiment results.

The rewards system had no significant effect on the image mean time. The block system had a highly significant effect ($p < .001$) on the image mean time. The overall image mean time was 6.60 s for block 1, which was reduced by 75% in block 3. The block*NewGroup interaction was found to be significant and indicated that low robot performances increased

the image mean time in all blocks (Figure 23). The longest image mean time accepted was for the high automation level with low robot quality (HOR-low) in all the blocks. For blocks 2 and 3, it seems that for high robot quality it is better to use the high automation level (HOR), while for low robot quality the low automation level (HR) accomplished a shorter image time. The image mean time for the H experimental group was a value between the two automation levels with high robot quality. For all experimental groups the image mean time decreased with the increase in block number.

Table 11: The repeated measures analysis of variance results.

	DoF	MS	F	p
{1}Rewards	1, 110	0.890	0.063	N.S.
{2}NewGroup	4, 110	22.596	1.608	N.S.
Rewards*NewGroup	4, 110	4.717	0.336	N.S.
{3}BLOCK	2, 220	816.861	302.595	0.000
BLOCK*Rewards	2, 220	0.235	0.087	N.S.
BLOCK*NewGroup	8, 220	5.646	2.091	0.038
BLOCK*Rewards*NewGroup	8, 220	2.038	0.755	N.S.
{4}COMPLEXITY	2, 220	11.787	17.545	0.000
COMPLEXITY*Rewards	2, 220	0.229	0.341	N.S.
COMPLEXITY*NewGroup	8, 220	2.412	3.590	0.001
COMPLEXITY*Rewards*NewGroup	8, 220	0.572	0.851	N.S.
BLOCK*COMPLEXITY	4, 440	11.454	27.964	0.000
BLOCK*COMPLEXITY*Rewards	4, 440	0.393	0.959	N.S.
BLOCK*COMPLEXITY*NewGroup	16, 440	0.434	1.059	N.S.
3*4*1*2	16, 440	0.555	1.356	N.S.

The image mean time increases significantly with increasing stimulus complexity. The overall image mean time for high complexity stimuli (5.05 s) is significantly longer by almost 8% than for the low complexity stimuli (4.69 s). The complexity*NewGroup interaction was found to be significant and showed that low robot performances increased the image mean time for all complexity stimuli and both collaboration levels. The complexity*block interaction was found to be significant and indicated that the image mean time decreased with the increase in the block number, implying the existence of a learning effect (Figure 24). The image mean time increased with the increase in the level of complexity stimuli for blocks 1 and 3. In block 2 the average image time for all three complexity stimuli were similar. A post hoc comparison indicated that the difference between the average image times of all complexity stimuli was significant for block 1. For blocks 2 and 3 there was no significant difference between the intermediate and high-complexity stimuli.

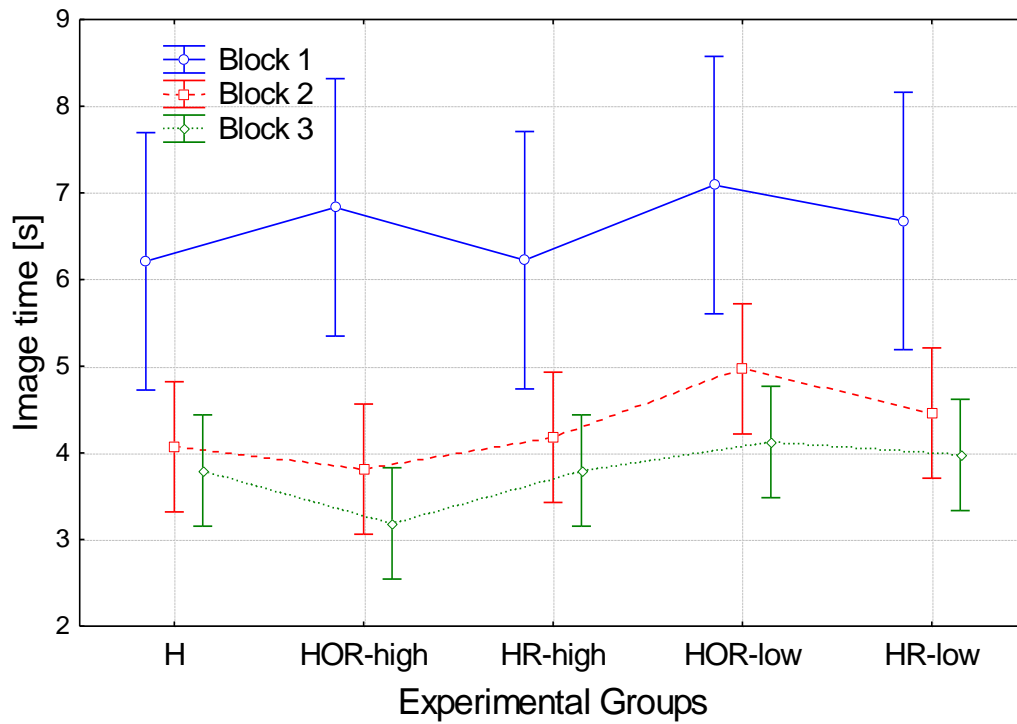


Figure 23: Image mean time for the five experimental groups as a function of the blocks.

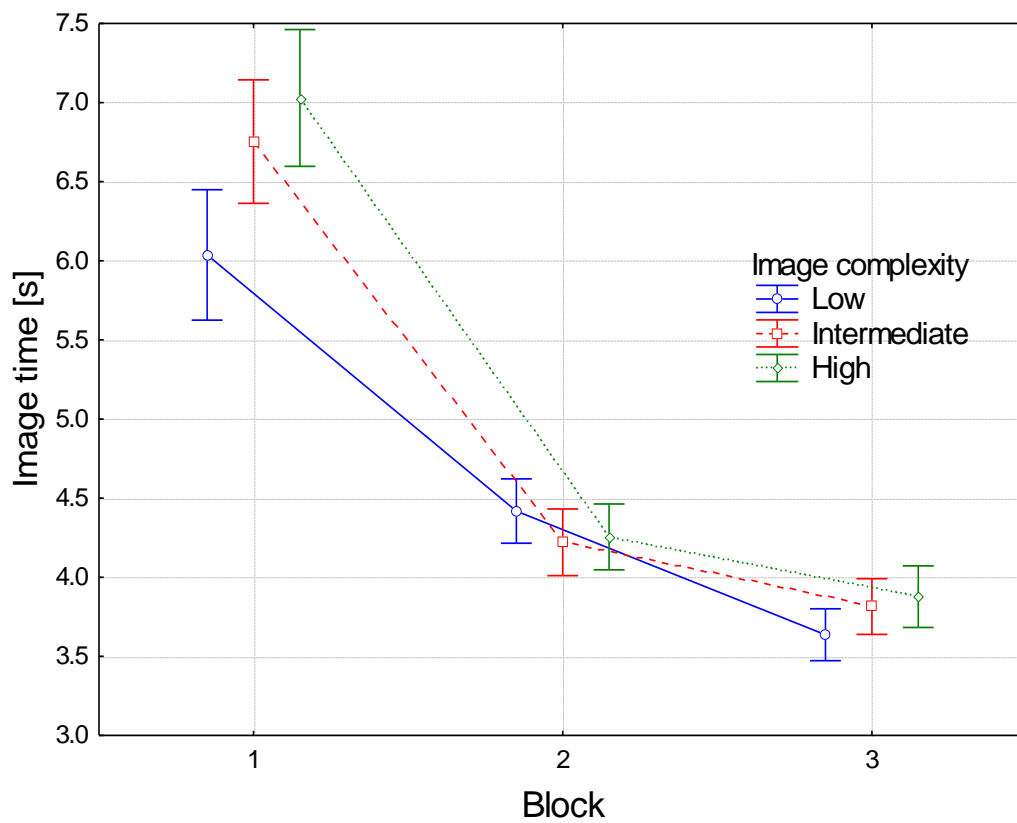


Figure 24: Image mean time for the three blocks as a function of the stimulus complexity.

6.4.2.2.2 Analysis with cooperation level and robot performance as independent variables for all cooperation levels except H.

Table 12 shows the statistical output of the repeated measures analysis of variance performed on the experiment results.

Robot quality levels significantly affected image mean time. The overall average time per image was shorter for the 'high quality' robot (4.67s) than for the 'low quality' robot (5.22 s).

The interaction between the complex stimuli and the automation level produced significant differences. The average time per image for both automation levels increased with increasing image complexity (table 13), but the complexity influenced the HOR automation level more strongly. The difference between the two automation levels was insignificant for the same stimulus complexity (table 13). The difference between low-complexity stimuli and high-complexity stimuli was significant for the same automation level.

Table 12: The repeated measures analysis of variance results.

	DoF	MS	F	p
{1}Collaboration	1, 88	2.995	0.217	N.S.
{2}Rewards	1, 88	0.341	0.025	N.S.
{3}Robot quality	1, 88	63.995	4.636	0.034
Collaboration*Rewards	1, 88	0.057	0.004	N.S.
Collaboration*Robot quality	1, 88	12.456	0.902	N.S.
Rewards*Robot quality	1, 88	18.468	1.338	N.S.
Collaboration*Rewards*Robot quality	1, 88	0.002	0.000	N.S.
{4}BLOCK	2, 176	694.953	271.543	0.000
BLOCK*Collaboration	2, 176	10.031	3.919	0.022
BLOCK*Rewards	2, 176	0.378	0.148	N.S.
BLOCK*Robot quality	2, 176	2.383	0.931	N.S.
BLOCK*Collaboration*Rewards	2, 176	1.224	0.478	N.S.
BLOCK*Collaboration*Robot quality	2, 176	6.222	2.431	0.091
BLOCK*Rewards*Robot quality	2, 176	5.585	2.182	N.S.
4*1*2*3	2, 176	1.151	0.450	N.S.
{5}COMPLEXITY	2, 176	14.697	22.504	0.000
COMPLEXITY*Collaboration	2, 176	4.157	6.365	0.002
COMPLEXITY*Rewards	2, 176	0.029	0.044	N.S.
COMPLEXITY*Robot quality	2, 176	1.526	2.336	0.100
COMPLEXITY*Collaboration*Rewards	2, 176	0.477	0.731	N.S.
COMPLEXITY*Collaboration*Robot quality	2, 176	1.001	1.532	N.S.
COMPLEXITY*Rewards*Robot quality	2, 176	0.956	1.465	N.S.
5*1*2*3	2, 176	0.505	0.773	N.S.
BLOCK*COMPLEXITY	4, 352	8.966	22.597	0.000
BLOCK*COMPLEXITY*Collaboration	4, 352	0.209	0.527	N.S.
BLOCK*COMPLEXITY*Rewards	4, 352	0.220	0.555	N.S.
BLOCK*COMPLEXITY*Robot quality	4, 352	0.511	1.288	N.S.
4*5*1*2	4, 352	0.149	0.376	N.S.
4*5*1*3	4, 352	0.545	1.374	N.S.
4*5*2*3	4, 352	0.885	2.231	0.065
4*5*1*2*3	4, 352	0.515	1.297	N.S.

Table 13: Post-hoc comparisons between the Complexity*Automation-level combinations.

		HOR	HOR	HOR	HR	HR	HR
	COMPLEXITY	low	inter.	high	low	inter.	high
	image time [s]	4.63	5.07	5.31	4.77	4.90	4.98
HOR	low		0.000	0.000	N.S.	N.S.	N.S.
HOR	inter.	0.000		0.010	N.S.	N.S.	N.S.
HOR	high	0.000	0.010		0.044	N.S.	N.S.
HR	low	N.S.	N.S.	0.044		N.S.	0.028
HR	inter.	N.S.	N.S.	N.S.	N.S.		N.S.
HR	high	N.S.	N.S.	N.S.	0.028	N.S.	

6.4.2.3 Points accumulated: Number of points as a function of block, level of cooperation, robot performance, and reward.

6.4.2.3.1 Analysis with groups as an independent variable.

Table 14 shows the statistical output of the repeated measures analysis of variance performed on the experiment results.

Figure 25 shows the Block*Reward interaction. The score levels of the minimizing FA reward are significantly lower ($p<.001$) than the score levels of the maximizing hit reward. Thus, the reward system describes the task orientation, and as such, presents different score scales. When minimizing the FA reward, the score in the last block was significantly higher, by 51% ($p<.001$), than the score in the first block. When maximizing the Hit reward the score in last block was significantly higher, by 36% ($p<.001$), than the score in the first block.

Table 14: The repeated measures analysis of variance results.

	DoF	MS	F	p
Rewards	1, 110	8130629	5367.62	0.000
NewGroup	4, 110	8277	5.46	0.000
Rewards*NewGroup	4, 110	141	0.09	N.S.
BLOCK	2, 220	454443	1081.47	0.000
BLOCK*Rewards	2, 220	54073	128.68	0.000
BLOCK*NewGroup	8, 220	244	0.58	N.S.
BLOCK*Rewards*NewGroup	8, 220	203	0.48	N.S.

The experimental group exhibited a highly significant effect ($p<.001$). The automation levels with low robot quality achieved significantly lower scores than the automation levels with high robot quality and the control H group (Figure 26). There was no significance difference between the automation levels with high robot quality and the control H group, but both of them had higher scores than the H group. The high automation level (HOR) yielded higher scores than the low automation level (HR).

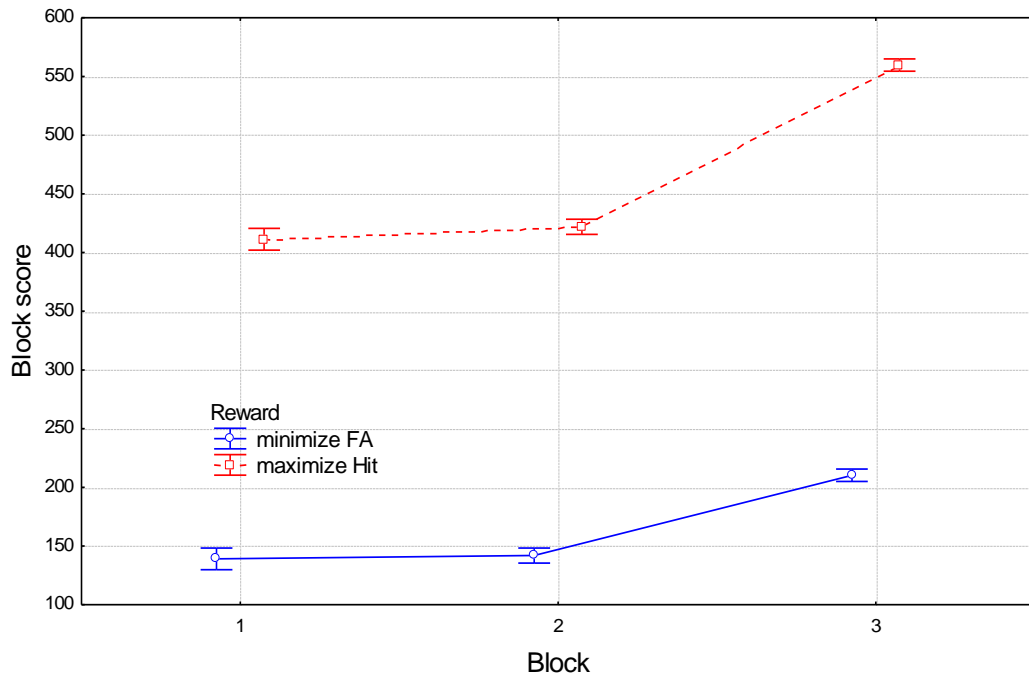


Figure 25: Block score for the three blocks as a function of the reward system.

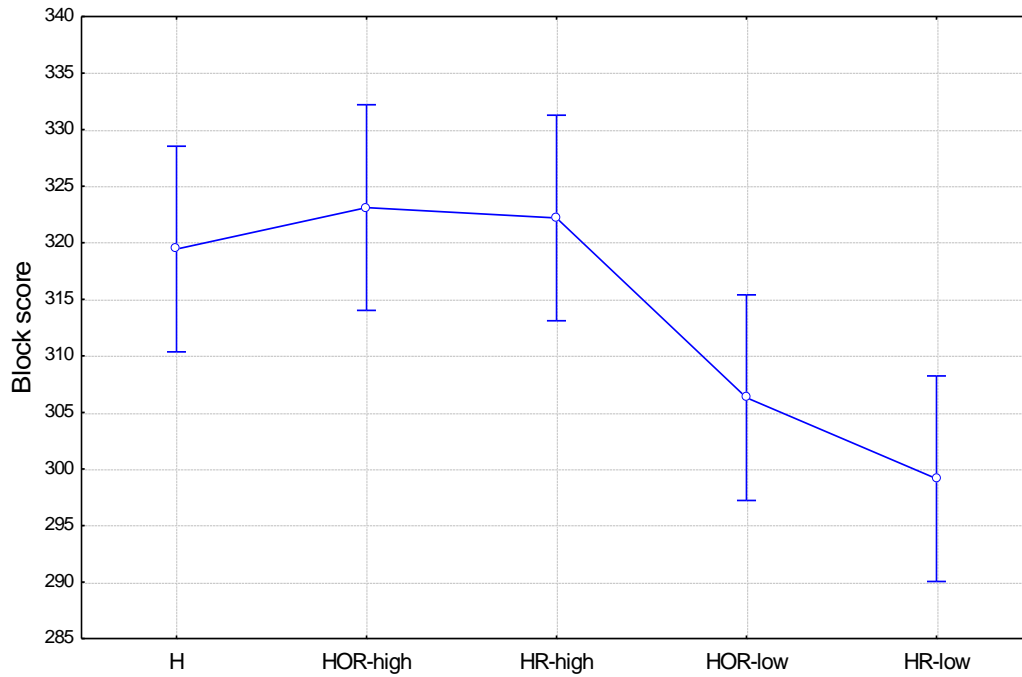


Figure 26: Block score for the five experimental groups.

6.4.2.3.2 Analysis with cooperation level and robot performance as independent variables for all cooperation levels except H.

Table 15 shows the statistical output of the repeated measures analysis of variance performed on the experiment results.

Table 15: The repeated measures analysis of variance results.

	DoF	MS	F	p
{1}Collaboration	1, 88	1176	0.64	N.S.
{2}Rewards	1, 88	6507028	3568.49	0.000
{3}Robot quality	1, 88	28600	15.68	0.000
Collaboration*Rewards	1, 88	17	0.01	N.S.
Collaboration*Robot quality	1, 88	703	0.39	N.S.
Rewards*Robot quality	1, 88	261	0.14	N.S.
Collaboration*Rewards*Robot quality	1, 88	284	0.16	N.S.
{4}BLOCK	2, 176	365182	784.55	0.000
BLOCK*Collaboration	2, 176	229	0.49	N.S.
BLOCK*Rewards	2, 176	43408	93.26	0.000
BLOCK*Robot quality	2, 176	39	0.08	N.S.
BLOCK*Collaboration*Rewards	2, 176	121	0.26	N.S.
BLOCK*Collaboration*Robot quality	2, 176	547	1.18	N.S.
BLOCK*Rewards*Robot quality	2, 176	564	1.21	N.S.
4*1*2*3	2, 176	43	0.09	N.S.

The difference between the low and high robot qualities was significant ($p < .001$). The overall average score of the low robot quality was 302 points. Improving the robot quality increased the system performance by 15%.

6.4.2.4 Conclusions regarding system performance

To represent different task types the reward values were fixed and could not be changed during the task performance. Results indicate that the reward system has a significant effect on the system hit rate, false alarms, and the system objective function score. The system hit rate of participants who were rewarded for maximum hits was higher than for the others; likewise, the system false alarms of participants who were rewarded for minimum FA was lower than for the others. The reward has no influence on the system performance time.

Robot quality has a significant influence on the system hit rate and the system objective function score, which increases with increasing robot quality. Although the increase in robot quality reduces the number of system false alarms, this finding was insignificant. A higher level of automation (HO-R) combined with low robot quality, however, significantly increases the number of false alarms, as compared to no automation (HO). For low robot quality, the increase in the automation level increases detection time, whereas for the 'high quality' robot, the increase in the automation level reduces the detection time. This effect was partially significant. Low robot quality impairs system hit rate and score. When robot quality is low it is better to use no automation at all. As image complexity is increased, however, the

system hit rate decreases, the system false alarms number grows, and the system time increased – all at significant levels.

The block number causes a significant decrease on the system false alarm, a 75% decrease in the system time, and an increase in the experiment score. These results suggest the occurrence of a learning effect during the experiment.

6.4.3 Use of the cues from the robotic system

6.4.3.1 Analysis of p_{Hrh}

6.4.3.1.1 *Comparison of probability of a human hit (p_{Hrh}) for all levels of cooperation when the robot marked a target as a function of robot performance and rewards (combined over all levels of complexity and blocks).*

Table 16 shows the statistical output of the repeated measures analysis of variance performed on the experiment results.

Table 16: The repeated measures analysis of variance results.

	DoF	MS	F	p
Collaboration	1, 88	0.015	4.39	0.039
Rewards	1, 88	0.010	3.01	0.086
Robot quality	1, 88	0.033	9.80	0.002
Collaboration*Rewards	1, 88	0.000	0.09	N.S.
Collaboration*Robot quality	1, 88	0.004	1.23	N.S.
Rewards*Robot quality	1, 88	0.006	1.77	N.S.
Collaboration*Rewards*Robot quality	1, 88	0.001	0.35	N.S.

The automation level exhibited a significant effect on the probability of a hit, which increased with the increase in automation level from .901 for the HR automation level to .926 for the HOR automation level (Figure 27).

Although the reward effect is marginally significant ($p < .09$), people seemed to consider the reward structure and increased their attention to increase the hit probability if they were rewarded for maximum hits (Figure 28).

Robot quality significantly influenced the probability of a hit. The hit probability for high robot quality (.932) exceeded by almost 4% that for the 'low quality' robot (.895). It seems that the participants noticed when robot quality was high and as such they trusted the robot decisions more than when quality was low.

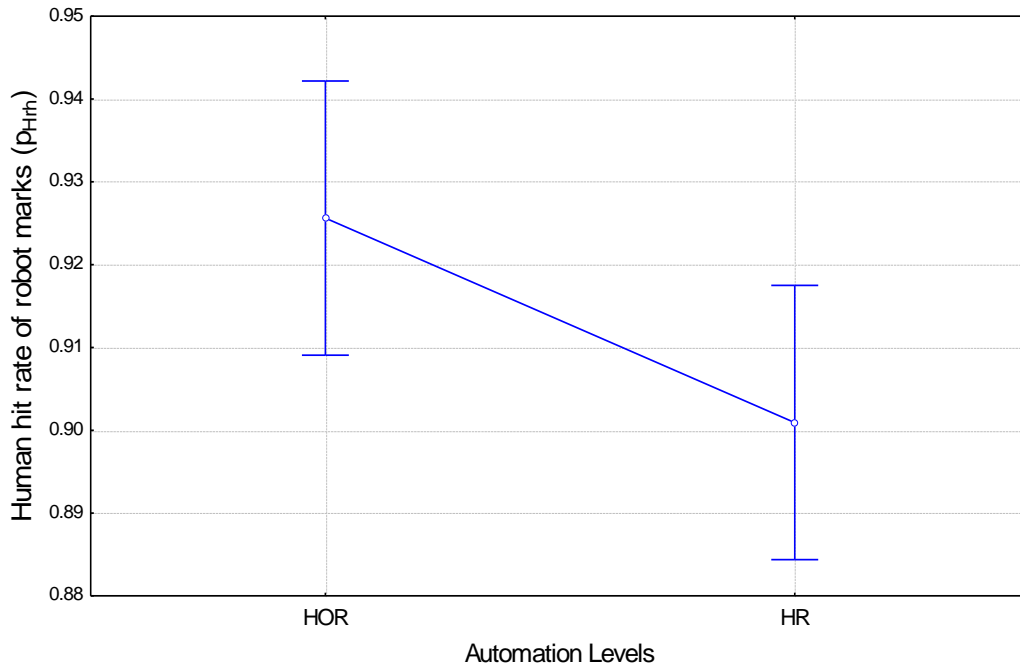


Figure 27: Probability of a human hit of targets marked by the robot as a function of the automation level.

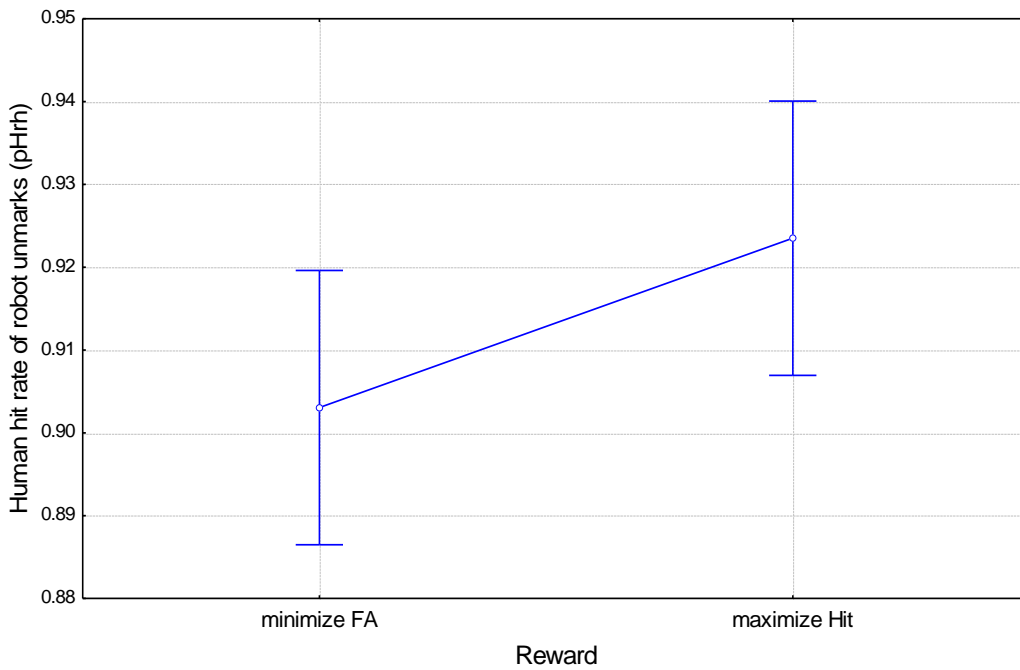


Figure 28: Probability of a human hit of targets marked by the robot as a function of the reward system.

6.4.3.2 Analysis of p_{Hh}

6.4.3.2.1 Comparison of probability of a human hit (p_{Hh}) for all levels of cooperation when the robot did not mark a target as a function of robot performance and rewards (combined over all levels of complexity and blocks).

6.4.3.2.1.1 Analysis with groups as an independent variable

Table 17 shows the statistical output of the repeated measures analysis of variance performed on the experiment results.

Table 17: The repeated measures analysis of variance results.

	DoF	MS	F	p
Rewards	1, 110	0.023	5.74	0.018
NewGroup	4, 110	0.009	2.32	0.061
Rewards*NewGroup	4, 110	0.000	0.06	N.S.

The reward system had a significant effect on the probability of a hit. The human probability for a hit was higher by 3% in the maximum hit reward system (.913) in comparison to the minimum FA reward system (.885).

The experimental group had a marginally significant effect on the probability of a hit. The human hit probability for the low automation level (HR) with low robot quality was significantly lower than the high automation level (HOR) with low robot quality, the high automation level with high robot quality, and the H controlled group. It was also lower with marginal significance ($p < .06$) relative to the low automation level with high robot quality (Figure 29).

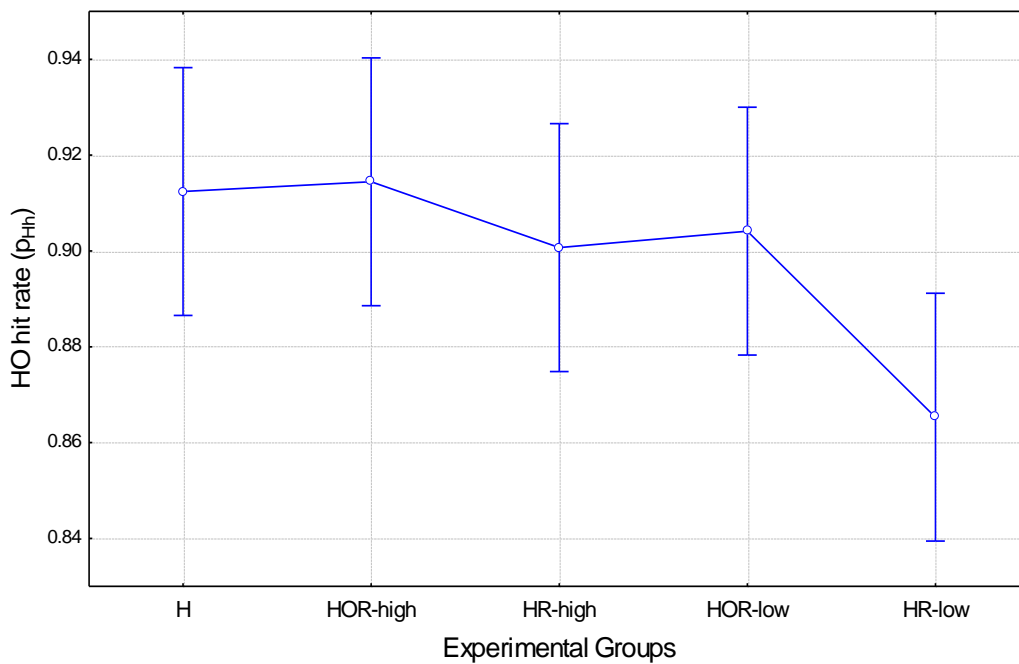


Figure 29: Human hit probability of unmarked targets for the experimental groups.

6.4.3.2.1.2 Analysis with cooperation level and robot performance as independent variables for all cooperation levels except H.

Table 18 shows the statistical output of the repeated measures analysis of variance performed on the experiment results.

Table 18: The repeated measures analysis of variance results.

	DoF	MS	F	p
Collaboration	1, 88	0.017	3.46	0.066
Rewards	1, 88	0.018	3.67	0.059
Robot quality	1, 88	0.013	2.62	N.S.
Collaboration*Rewards	1, 88	0.001	0.13	N.S.
Collaboration*Robot quality	1, 88	0.004	0.79	N.S.
Rewards*Robot quality	1, 88	0.000	0.01	N.S.
Collaboration*Rewards*Robot quality	1, 88	0.000	0.06	N.S.

Figure 30 shows the human probability of a hit for the different automation levels. Results indicate that increases in the automation level increase the human probability of a hit ($p < .07$).

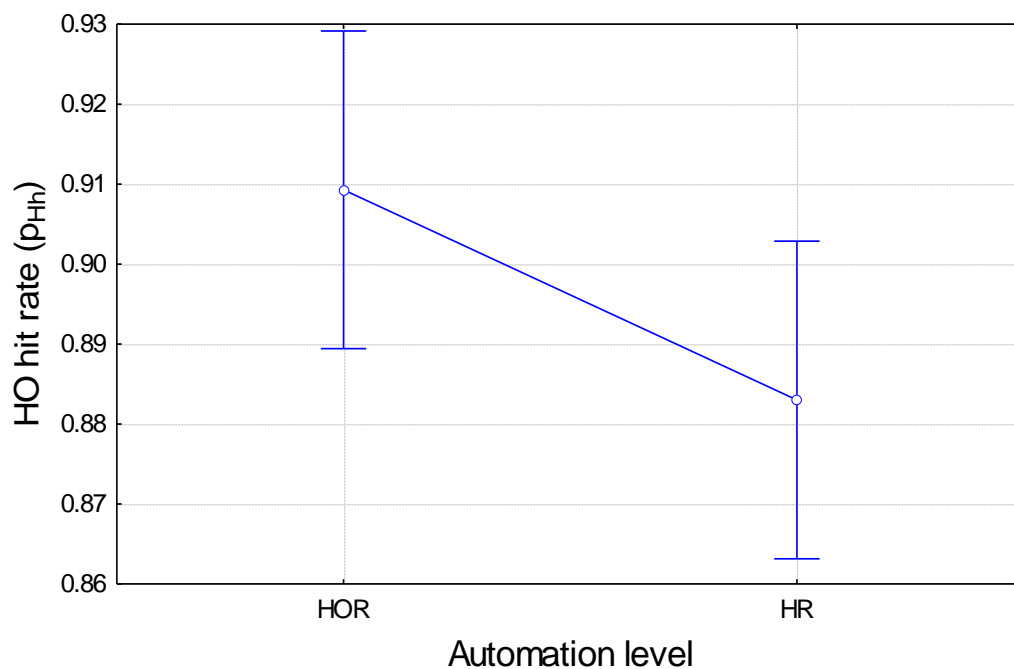


Figure 30: Human hit probability of unmarked targets for the different automation levels.

6.4.3.2.2 *Comparison of probabilities of a human hit (p_{Hh}) for all levels of cooperation when the robot did not mark a target as a function of robot performance, complexity, block, and rewards.*

6.4.3.2.2.1 *Analysis with groups as an independent variable*

When robot quality is high, the number of unmarked targets by the robot is low and therefore, the resolution of the human probability of a hit of a target that was not marked by the robot is very low. Low resolution of the probability of a hit can distort the results and as a

result, the groups with high robot quality were not counted. Table 19 shows the statistical output of the repeated measures analysis of variance performed on the experiment results.

The reward system had a significant effect on the probability of a hit. The overall probability of a hit was lower when the aim was to minimize FA (.86) than when the aim was to maximize the hit (.90).

The difference between the experimental groups was also found to be significant. The probability of a hit for the human when part of the low automation level setup and the 'low quality' robot group (HR-low) was significantly lower (.85) than that for the high automation level (HOR-low) and the control group H (.89, Figure 31).

Table 19: The repeated measures analysis of variance results.

	DoF	MS	F	p
{1}Rewards	1, 66	0.158	5.47	0.022
{2}NewGroup	2, 66	0.120	4.15	0.020
Rewards*NewGroup	2, 66	0.007	0.24	N.S.
{3}BLOCK	2, 132	0.194	19.11	0.000
BLOCK*Rewards	2, 132	0.018	1.79	N.S.
BLOCK*NewGroup	4, 132	0.007	0.66	N.S.
BLOCK*Rewards*NewGroup	4, 132	0.026	2.57	0.041
{4}COMPLEXITY	2, 132	1.196	159.88	0.000
COMPLEXITY*Rewards	2, 132	0.005	0.67	N.S.
COMPLEXITY*NewGroup	4, 132	0.006	0.75	N.S.
COMPLEXITY*Rewards*NewGroup	4, 132	0.017	2.25	0.067
BLOCK*COMPLEXITY	4, 264	0.127	20.73	0.000
BLOCK*COMPLEXITY*Rewards	4, 264	0.004	0.64	N.S.
BLOCK*COMPLEXITY*NewGroup	8, 264	0.012	1.95	0.053
3*4*1*2	8, 264	0.006	0.96	N.S.

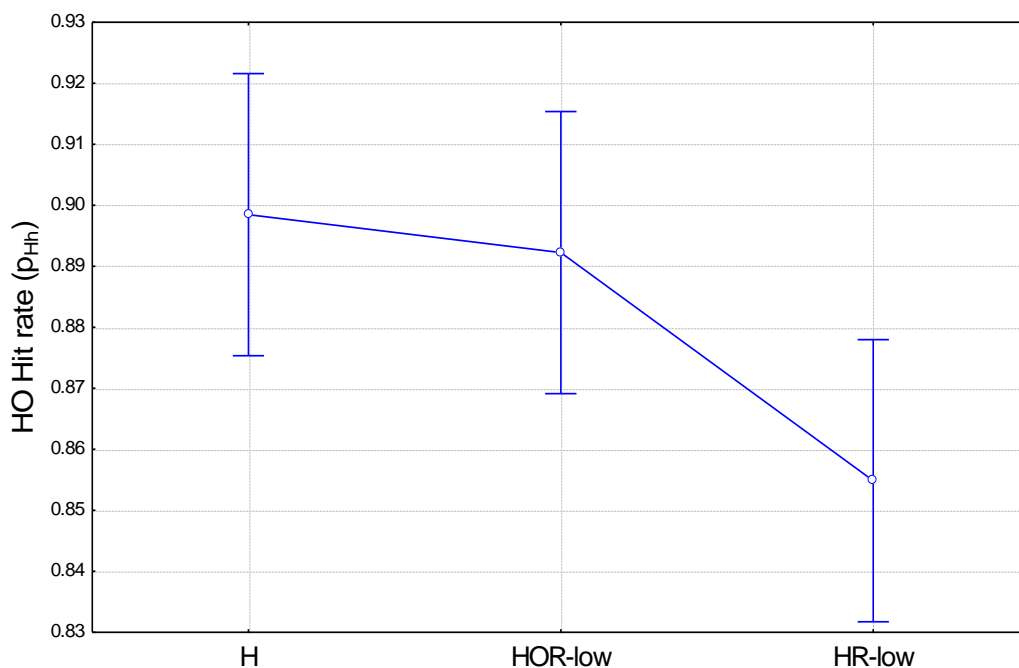


Figure 31: Human hit probability of unmarked targets for the experimental groups.

Image complexity had a strong influence on the human hit probability. Increases in the image complexity decrease the human hit rate (Figure 32). The probability for a human hit in low complexity images was higher by 18% (0.96) than that in the high complexity images (0.81). This effect was found to be highly significant ($p < .001$).

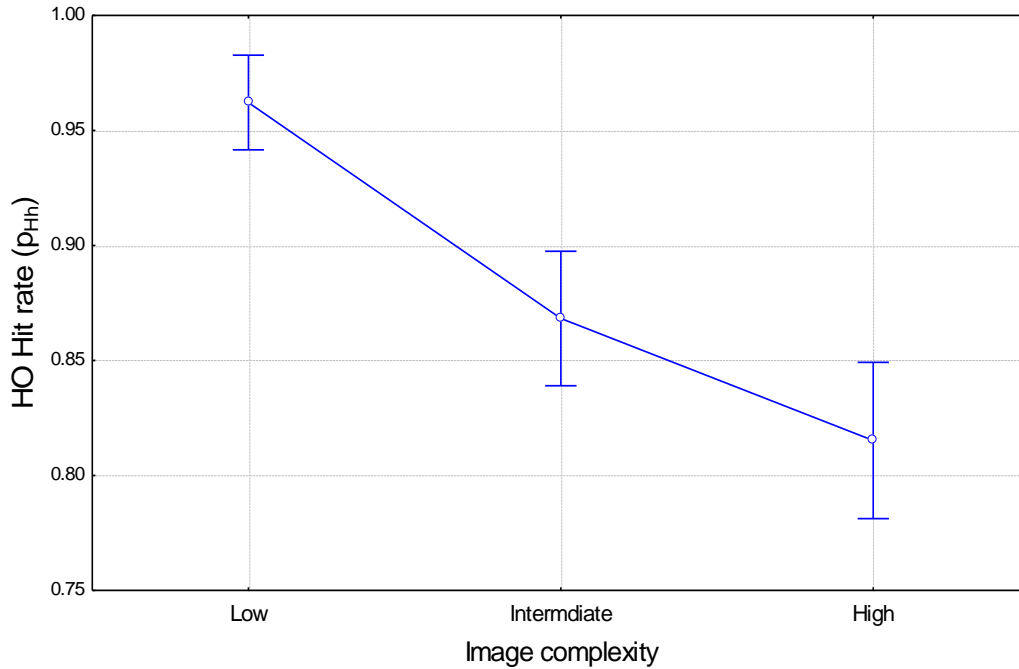


Figure 32: Human hit probability as a function of the image complexity.

6.4.3.3 Analysis of p_{FArh}

6.4.3.3.1 Probability of robot FA that the human approved (p_{FArh}) as a function of the level of cooperation (all, except HO), robot performance, and rewards (combined over all levels of complexity and blocks).

Table 20 shows the statistical output of the repeated measures analysis of variance performed on the experiment results.

Table 20: The repeated measures analysis of variance results.

	DoF	MS	F	p
Collaboration	1, 88	0.207	11.747	0.001
Rewards	1, 88	0.045	2.560	N.S.
Robot quality	1, 88	0.121	6.865	0.010
Collaboration*Rewards	1, 88	0.000	0.007	N.S.
Collaboration*Robot quality	1, 88	0.032	1.831	N.S.
Rewards*Robot quality	1, 88	0.065	3.660	0.059
Collaboration*Rewards*Robot quality	1, 88	0.001	0.071	N.S.

The automation level had a highly significant effect ($p < .001$) on the human FA probability for objects that were already marked by the robot. The FA probability increased with the increase in the automation level (Figure 33) such that the probability of FA was more than 70% higher for the HOR automation level (.225) in comparison to the HR automation level (.132). It seems that when the system was more automatic the participants tend to approve its decisions regarding FA.

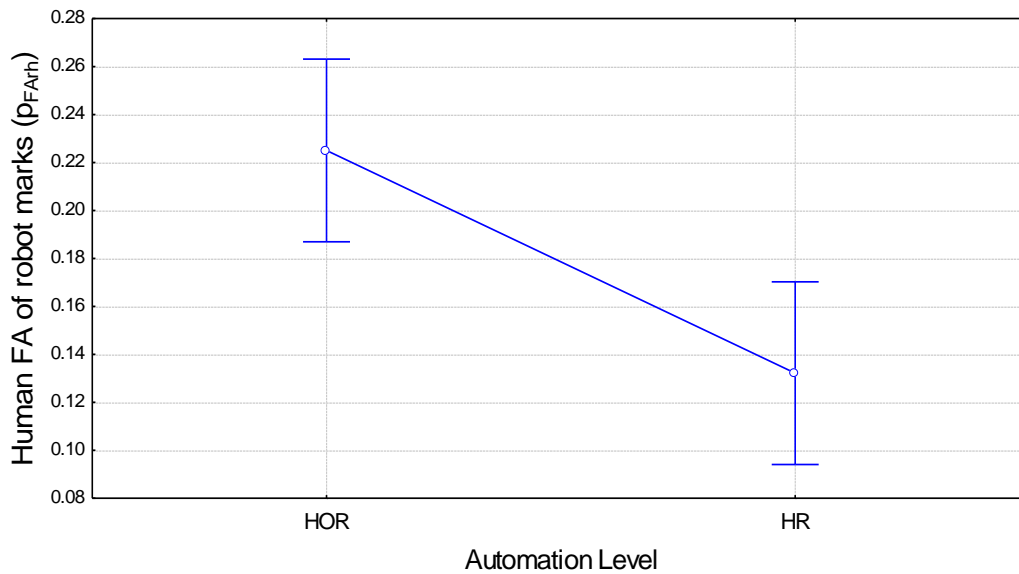


Figure 33: The probability of FA of objects already marked by the robot as a function of the automation level.

Figure 34 shows that the increase in robot quality increases the probability of FA of objects already marked by the robot. This finding fits the behavior of the number of FA of objects unmarked by the robot and could be explained by examining the number of robot hits and FA marks. A 'low quality' robot marks many objects as FA and forces the human to check each one since the number of FA is illogical. In addition, we assumed earlier that the participants recognized the robot quality during the experiment and knew that they cannot rely on the robot marks. The 'high quality' robot marks very few FA, the human trusts the robot decisions, and therefore, does not correct the FA marks of the 'high quality' robot at the same rate as for the 'low quality' robot.

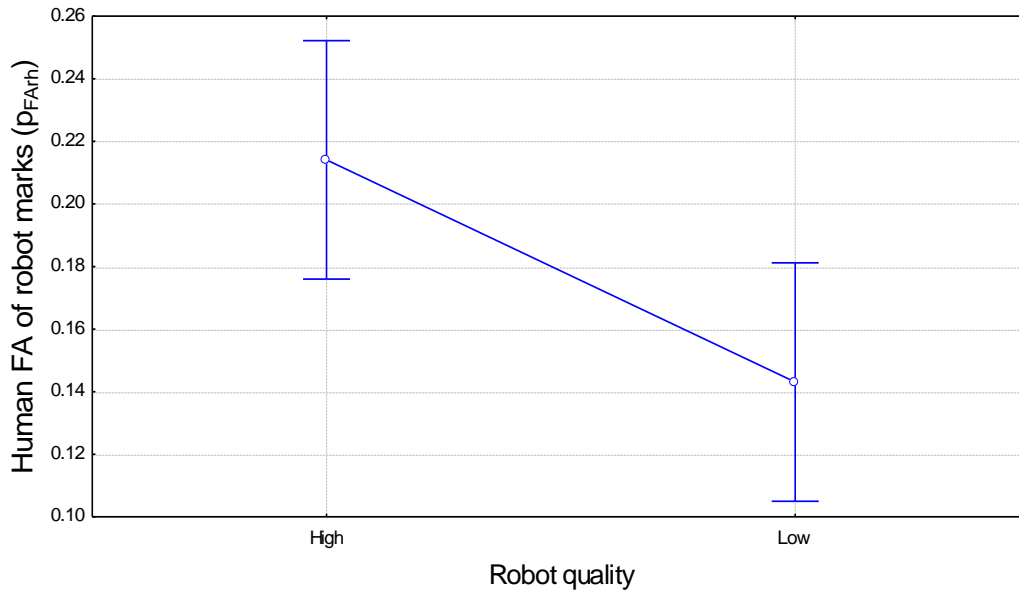


Figure 34: The probability of FA of objects already marked by the robot as a function of the robot quality.

6.4.3.4 Analysis of human FA that the robot did not mark (F_{FAh})

6.4.3.4.1 Comparison of human FA that the robot did not mark for all levels of cooperation as a function of robot performance, complexity, block, and rewards.

6.4.3.4.1.1 Analysis with groups as an independent variable

Table 21 shows the statistical output of the repeated measures analysis of variance performed on the experiment results.

Table 21: The repeated measures analysis of variance results.

	DoF	MS	F	p
{1}Rewards	1, 110	0.059	2.383	N.S.
{2}NewGroup	4, 110	0.147	5.967	0.000
Rewards*NewGroup	4, 110	0.013	0.508	N.S.
{3}BLOCK	2, 220	0.086	9.174	0.000
BLOCK*Rewards	2, 220	0.003	0.367	N.S.
BLOCK*NewGroup	8, 220	0.006	0.632	N.S.
BLOCK*Rewards*NewGroup	8, 220	0.006	0.646	N.S.
{4}COMPLEXITY	2, 220	0.082	24.402	0.000
COMPLEXITY*Rewards	2, 220	0.000	0.080	N.S.
COMPLEXITY*NewGroup	8, 220	0.015	4.496	0.000
COMPLEXITY*Rewards*NewGroup	8, 220	0.003	0.818	N.S.
BLOCK*COMPLEXITY	4, 440	0.081	33.008	0.000
BLOCK*COMPLEXITY*Rewards	4, 440	0.003	1.155	N.S.
BLOCK*COMPLEXITY*NewGroup	16, 440	0.011	4.617	0.000
3*4*1*2	16, 440	0.003	1.039	N.S.

Although the reward had no significant effect ($p=.12$), it seems that the participant's awareness of the reward increased their tendency to detect targets when they were rewarded for detection. The number of false alarms that were not marked by the robot and were marked by the human was 26.7% smaller when the reward was to minimize FA (.056) as compared to when they were rewarded for maximum hits (.071). The effect of the experimental group was highly significant ($p<.001$). The control H group attained the highest normalized FA value (Figure 35).

Figure 36 shows the average normalized FA for the different blocks. The normalized FA declined significantly with each block ($p<.001$), indicating the possible existence of a learning effect. The confidence intervals were also reduced with each block, which could also indicate that the human decisions became progressively more uniform. Image complexity also had a highly significant effect as evidenced by the increase in the number of normalized FA that corresponded with the increase in image complexity (Figure 37).

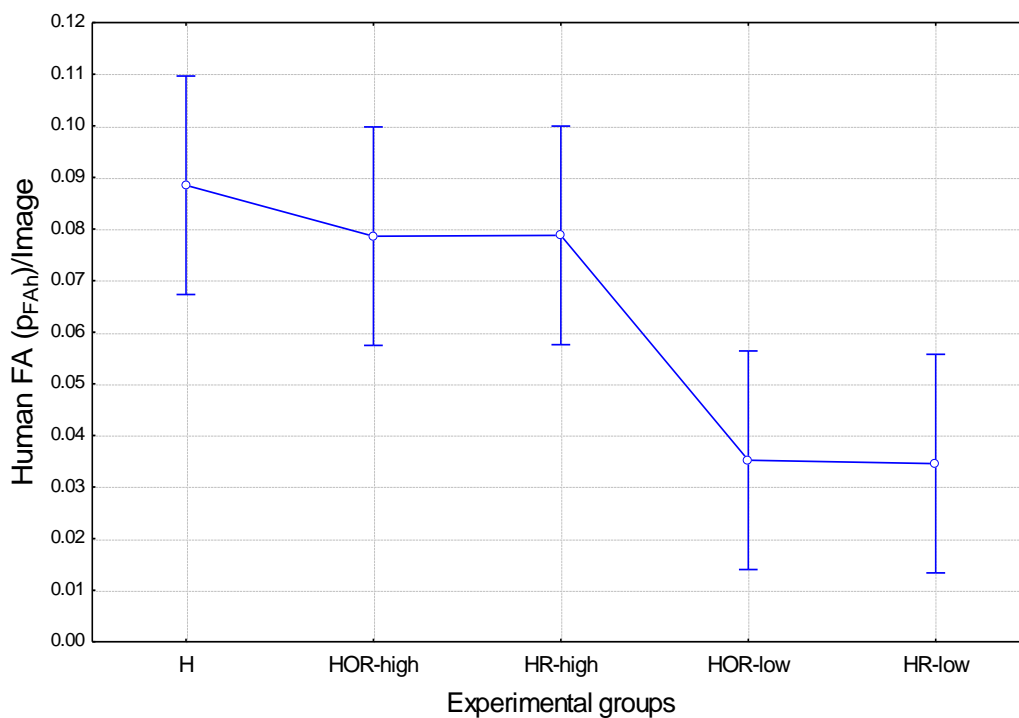


Figure 35: Human normalized false alarm as a function of the experimental group.

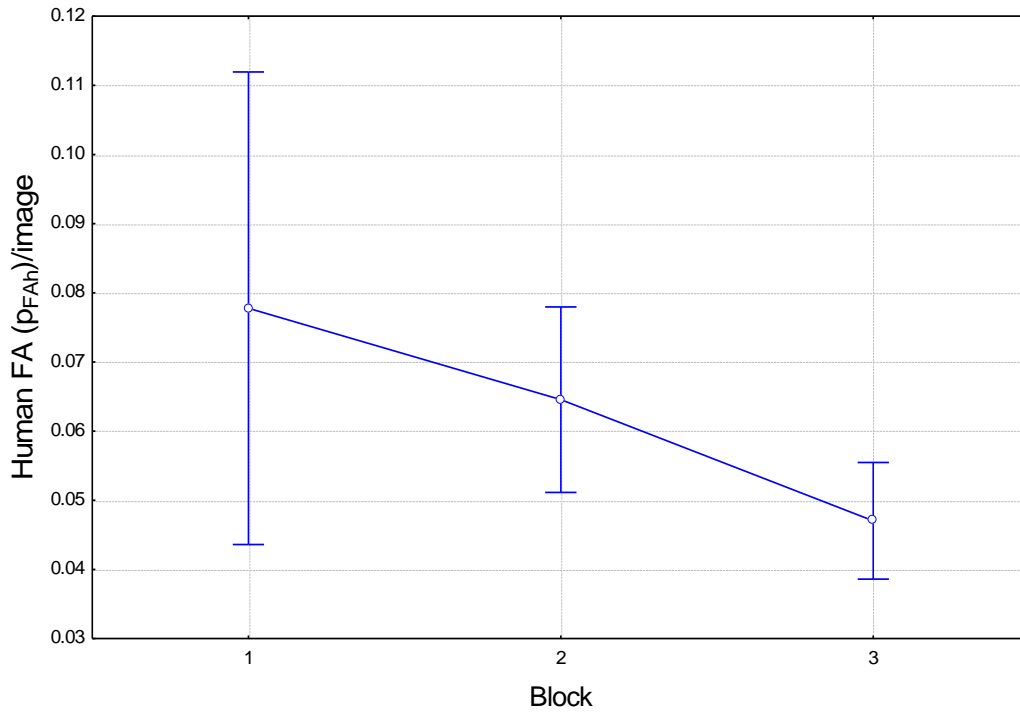


Figure 36: Human normalized false alarm as a function of the block number.

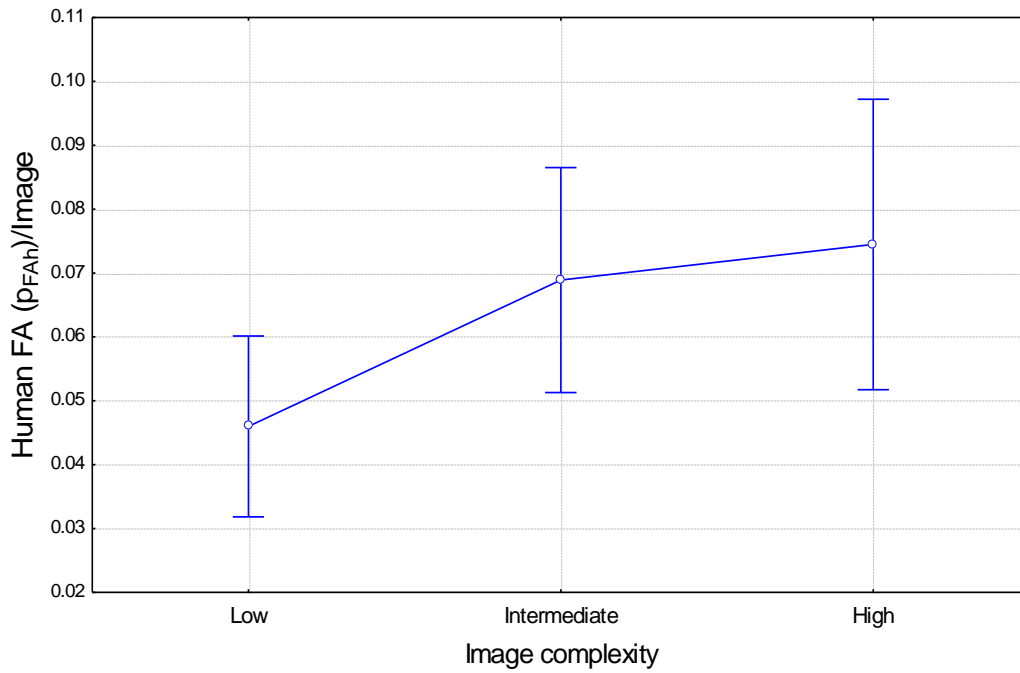


Figure 37: Human normalized false alarm as a function of image complexity.

6.4.3.4.1.2 Analysis with cooperation level and robot performance as independent variables for all cooperation levels except H.

Table 22 shows the statistical output of the repeated measures analysis of variance performed on the experiment results.

Table 22: The repeated measures analysis of variance results.

	DoF	MS	F	p
{1}Collaboration	1, 88	0.000	0.000	N.S.
{2}Rewards	1, 88	0.036	1.248	N.S.
{3}Robot quality	1, 88	0.415	14.339	0.000
Collaboration*Rewards	1, 88	0.022	0.759	N.S.
Collaboration*Robot quality	1, 88	0.000	0.001	N.S.
Rewards*Robot quality	1, 88	0.016	0.544	N.S.
Collaboration*Rewards*Robot quality	1, 88	0.009	0.304	N.S.
{4}BLOCK	2, 176	0.075	6.979	0.001
BLOCK*Collaboration	2, 176	0.002	0.140	N.S.
BLOCK*Rewards	2, 176	0.002	0.213	N.S.
BLOCK*Robot quality	2, 176	0.011	1.052	N.S.
BLOCK*Collaboration*Rewards	2, 176	0.002	0.233	N.S.
BLOCK*Collaboration*Robot quality	2, 176	0.006	0.515	N.S.
BLOCK*Rewards*Robot quality	2, 176	0.006	0.518	N.S.
4*1*2*3	2, 176	0.016	1.486	N.S.
{5}COMPLEXITY	2, 176	0.063	17.577	0.000
COMPLEXITY*Collaboration	2, 176	0.002	0.500	N.S.
COMPLEXITY*Rewards	2, 176	0.001	0.257	N.S.
COMPLEXITY*Robot quality	2, 176	0.051	14.187	0.000
COMPLEXITY*Collaboration*Rewards	2, 176	0.009	2.505	0.085
COMPLEXITY*Collaboration*Robot quality	2, 176	0.001	0.173	N.S.
COMPLEXITY*Rewards*Robot quality	2, 176	0.000	0.057	N.S.
5*1*2*3	2, 176	0.001	0.167	N.S.
BLOCK*COMPLEXITY	4, 352	0.046	18.905	0.000
BLOCK*COMPLEXITY*Collaboration	4, 352	0.001	0.585	N.S.
BLOCK*COMPLEXITY*Rewards	4, 352	0.002	0.818	N.S.
BLOCK*COMPLEXITY*Robot quality	4, 352	0.031	12.790	0.000
4*5*1*2	4, 352	0.007	2.836	0.024
4*5*1*3	4, 352	0.001	0.350	N.S.
4*5*2*3	4, 352	0.000	0.144	N.S.
4*5*1*2*3	4, 352	0.001	0.426	N.S.

The graph (Figure 38) indicates that increase in robot quality led to a corresponding 119% increase in the number of normalized FA, a result that was found to be highly significant. One possible explanation for this phenomenon could be that the 'low quality' robot marks large numbers of false alarms, leaving very few false alarm objects for the human.

There was no significant difference between automation levels (HOR vs. HR). It appears that the automation level did not influence the number of normalized human false alarms that were not marked by the robot, and the difference in the number of normalized FA between the two automation levels was less than 0.4%.

The interaction between image complexity and robot quality produced a significant effect (Figure 39), as evidenced by the gradually increasing number of false alarms by the 'high quality' robot corresponding with the increasing image complexity.

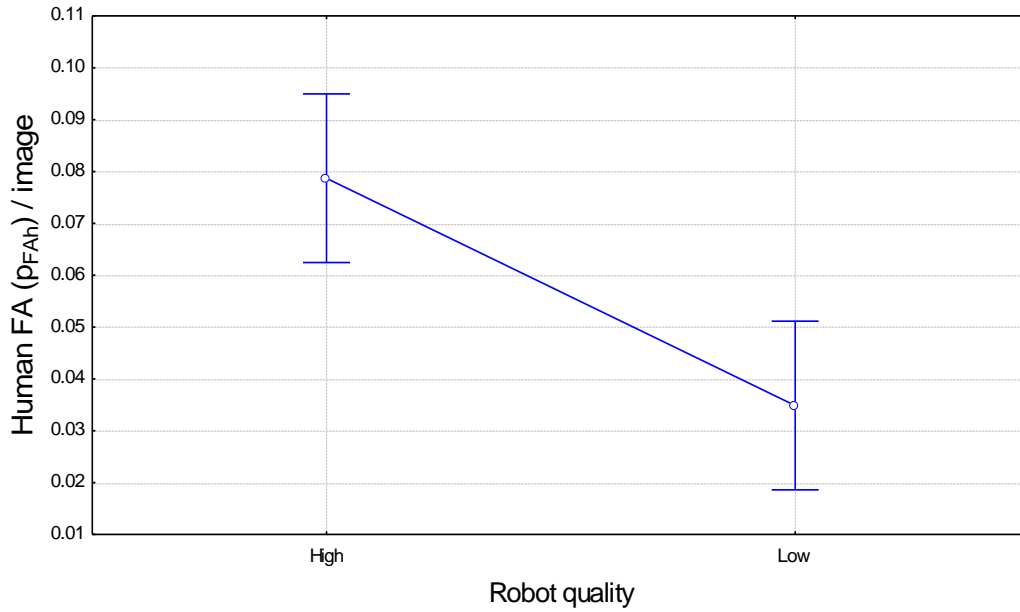


Figure 38: Normalized human FA as a function of the robot quality.

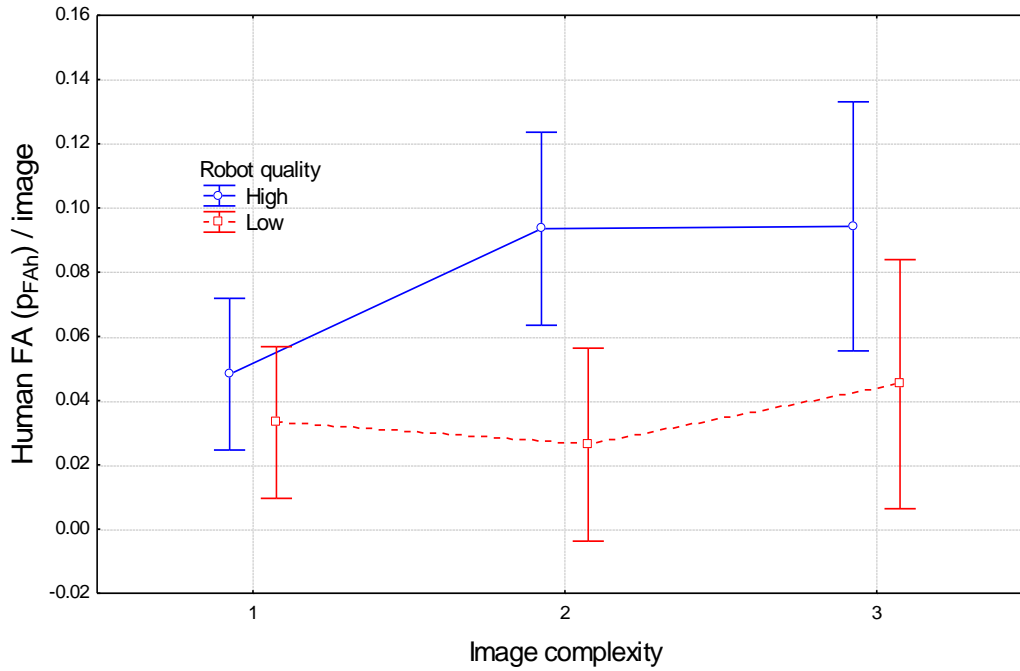


Figure 39: Human normalized FA for the two robot qualities as a function of the image complexity.

6.4.3.5 Analysis of d'_h

6.4.3.5.1 Analysis of d' for objects that were marked by the robot. Here we can compute p_{Hi} and p_{FA} for the human, and accordingly compute d' . The independent variables will be level of cooperation (all, except HO), robot performance, and rewards (combined over all levels of complexity and blocks).

The sensitivity parameter d' is a function of the hit and false alarm probabilities (chapter 4). The probabilities are transferred into distribution standard deviation values (Z). When the FA probability is zero, its theoretical Z value is $-\infty$ and the value of d' is ∞ . In the experiment, only a few participants avoided marking any robot false alarms, resulting in a FA probability of 0. Since these results were achieved due to the finite number of robot FA and it is impossible to statistically analyze results with infinite values, for those few cases we determine the Z value to be -4 (in standard deviation units). The calculated FA probability for that value is 0.0000317, which can be regarded as zero for our purposes. The analysis was also performed to calculate the FA probability of Z values equal to -3 and -6 and showed similar results.

The human sensitivity (d'_h) in this section was calculated based on the results of the measured human hit and FA probability for objects that were already marked by the robot (p_{Hrh} and p_{FArh} respectively).

Table 23 shows the statistical output of the univariate tests of significance performed on the experiment results.

Table 23: The univariate tests of significance results.

	DoF	MS	F	p
Collaboration	1, 88	4.109	4.834	0.031
Rewards	1, 88	7.176	8.443	0.005
Robot quality	1, 88	5.241	6.166	0.015
Collaboration*Rewards	1, 88	0.848	0.997	N.S.
Collaboration*Robot quality	1, 88	3.647	4.291	0.041
Rewards*Robot quality	1, 88	3.288	3.869	0.052
Collaboration*Rewards*Robot quality	1, 88	1.271	1.496	N.S.

The sensitivity (d') decreased with the increase in the automation level (Figure 40). The sensitivity for the low automation level (HR; 2.9) was 17% higher than the sensitivity of the high automation level (HOR; 2.48). Both the probability of a human hit and false alarm of objects marked by the robot decreased with the increase in the automation level, but the probability of false alarm decreased more drastically. These results could indicate that the participants were more sensitive and paid more attention to the task and the robot marks in the low automation level (HR).

The reward system had a significant effect on participant sensitivity (d'), as evidenced by the participant's higher sensitivity under the maximum hit reward system relative to the minimum FA reward system (Figure 41). It could be that the participants were simply better able to confirm the robot hits as opposed to eliminate its false alarms. In a similar fashion, an

increase in participant sensitivity was noticed when aiming for target detection than for false alarm elimination.

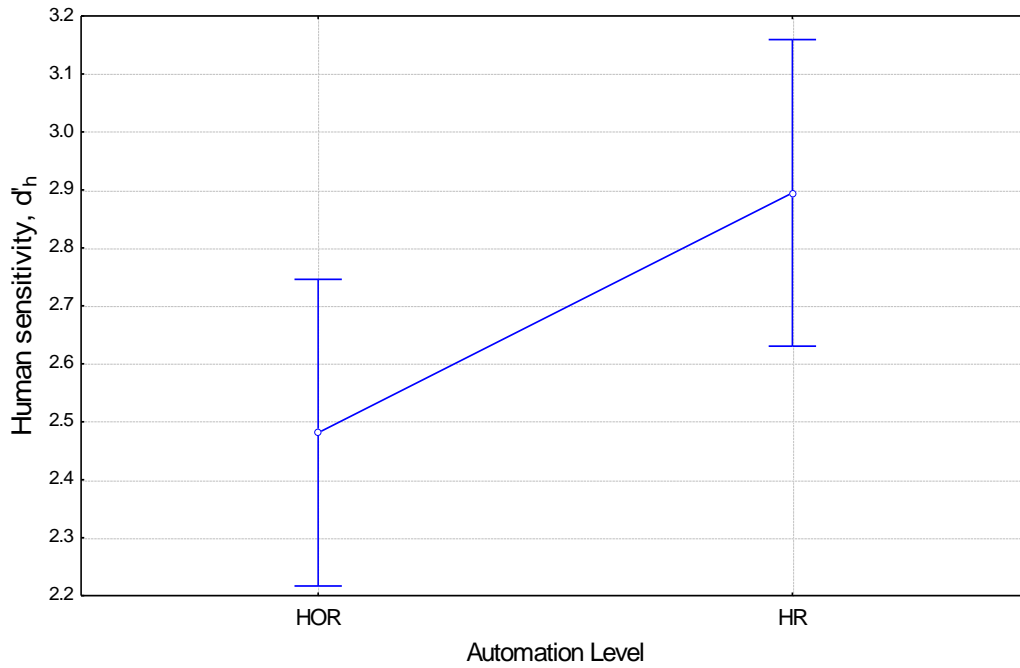


Figure 40: The human sensitivity for objects marked by the robot as a function of the automation level.

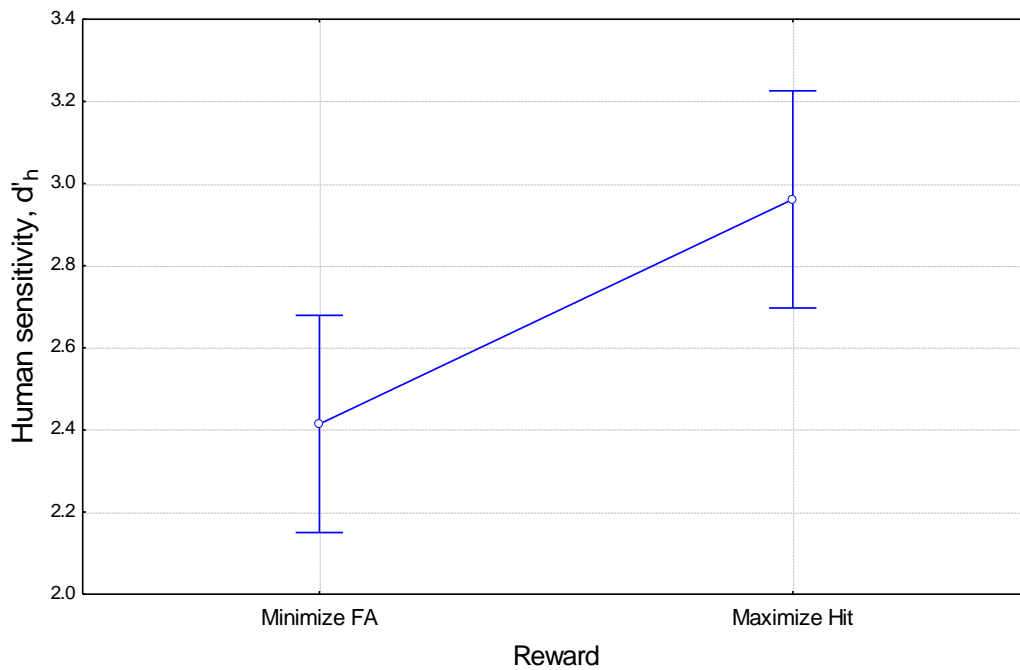


Figure 41: The human sensitivity for objects marked by the robot as a function of the reward system.

Figure 42 shows the influence of robot quality on human sensitivity. The human sensitivity for objects marked by the robot increases with the increase in robot quality. The human sensitivity for high robot quality was significantly increased by 19% (2.92) in comparison to the human sensitivity for low robot quality (2.45). The increase in robot quality

could be presented as an increase in robot sensitivity that, in turn, can increase human sensitivity.

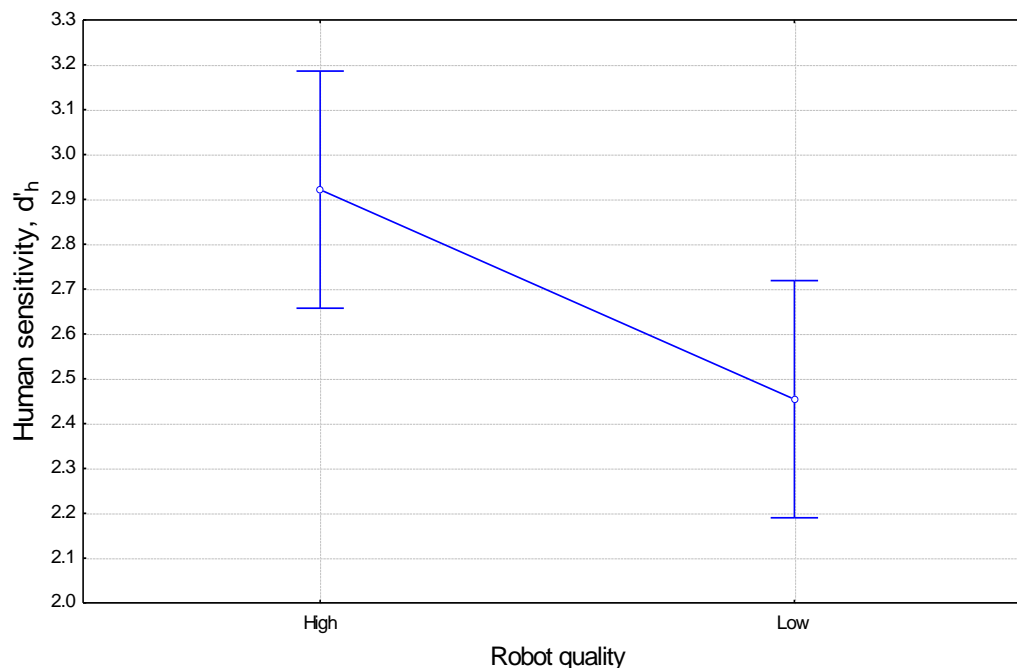


Figure 42: The human sensitivity for objects marked by the robot as a function of robot quality.

Table 24: Post-hoc comparisons between the automation level*rewards combinations.

		HOR	HOR	HR	HR
		min FA	max Hit	min FA	max Hit
	human sensitivity	2.30	2.66	2.53	3.26
HR	Reward: max Hit	0.001	0.026	0.007	

Human sensitivity for both reward systems was higher at the low automation level (Figure 43) but human sensitivity in the maximum hit reward system was more influenced by the automation level than in the minimum FA reward system.

A significant effect was produced by the interaction between automation level and robot quality. Figure 44 shows that for the 'high quality' robot human sensitivity is reduced with increasing automation level. Human sensitivity for the low automation level (3.2) and the high automation level (2.52) show a 32% reduction. Automation levels of the 'low quality' robot have no influence on human sensitivity (2.45). The results of post-hoc comparisons between the two automation levels and the two robot qualities show that there are significant differences between the automation levels of the 'high quality' robot (Table 25) and no significant differences between the automation levels of the 'low quality' robot.

The effect of robot quality-reward system interaction (Figure 45) was marginally significant ($p < .055$). In the maximum hit reward system human sensitivity increased with the

increase in robot quality. In the minimum FA reward system robot quality had no effect on human sensitivity.

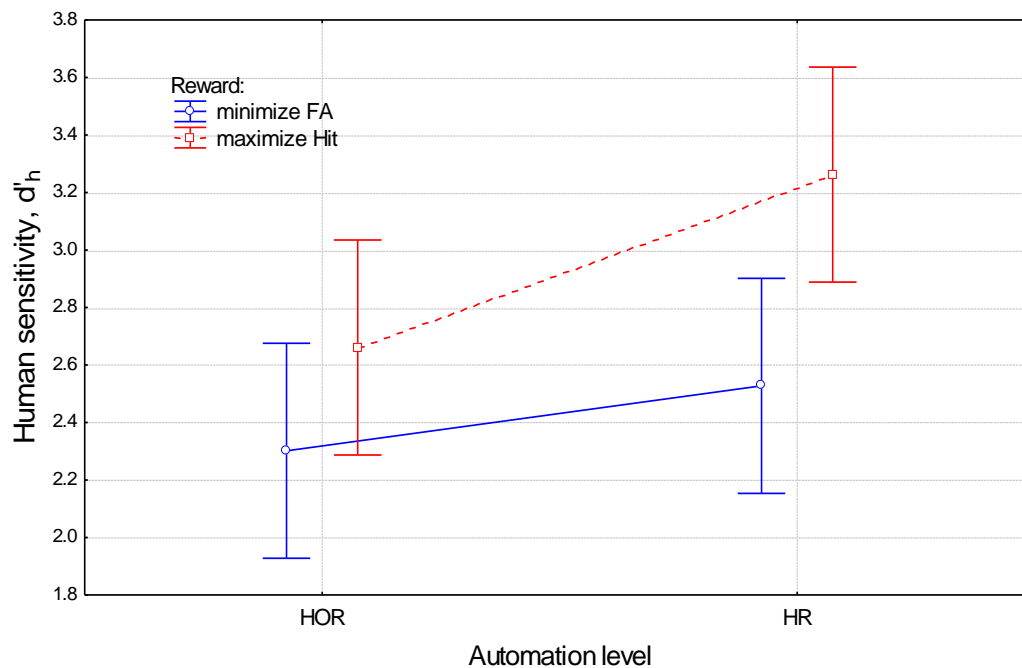


Figure 43: The human sensitivity for objects marked by the robot as a function of the automation level and reward system.

Table 25: Post-hoc comparisons between the automation level*robot quality combinations.

		HOR	HOR	HR	HR
	Robot quality	high	low	high	low
	Human sensitivity	2.52	2.44	3.32	2.47
HOR	High		N.S.	0.003	N.S.
HOR	Low	N.S.		0.001	N.S.
HR	High	0.003	0.001		0.002
HR	Low	N.S.	N.S.	0.002	

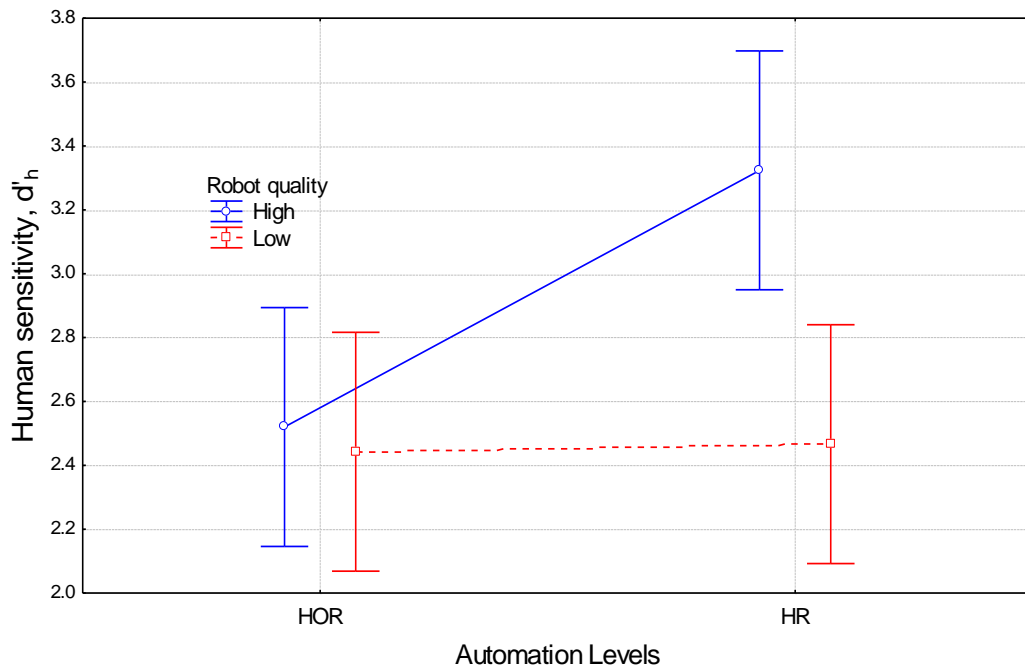


Figure 44: The human sensitivity for objects marked by the robot as a function of the automation level and robot quality.

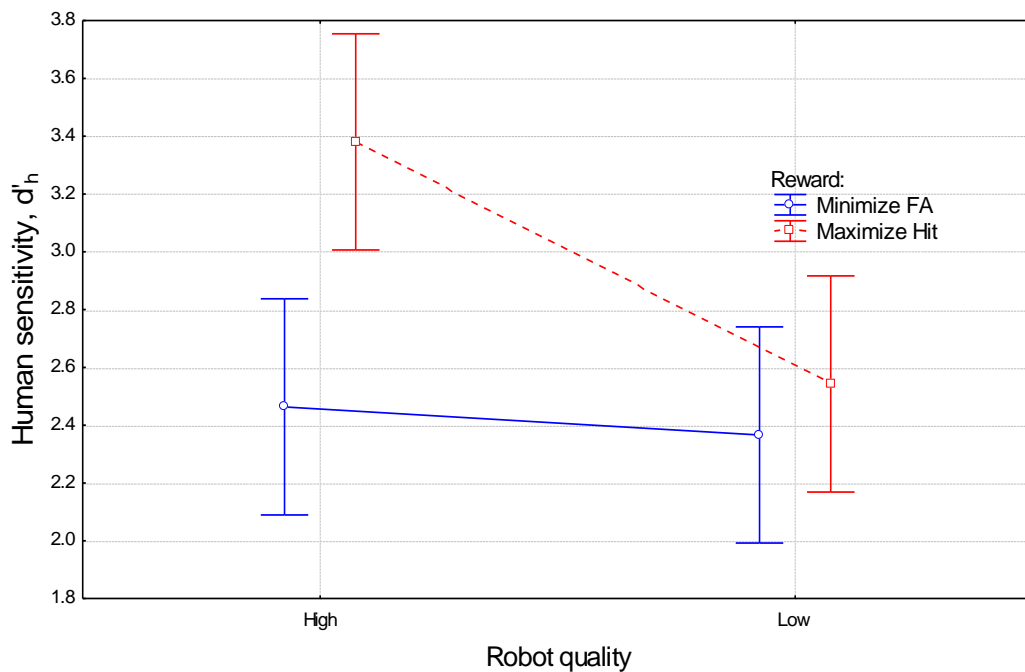


Figure 45: The human sensitivity for objects marked by the robot as a function of the reward system and robot quality.

6.4.3.6 Conclusions regarding cues from the robotic system

Conclusions of the analysis of the human performances focus on the influences of level of cooperation, stimulus difficulty, learning, and strategy changes due to different rewards.

The statistical analysis showed that the reward system has a marginally significant effect on the human hits of the robot marks (P_{Hrh}), a significant affect on the human hits of the

objects the robot did not mark (P_{Hh}), and the human sensitivity (d'_h). The human hit rates, P_{Hrh} and P_{Hh} , of participants who were rewarded for maximum hits were higher than for the participants who were rewarded for minimum FA; likewise, the human sensitivity of participants who were rewarded for maximum hits was higher than for those who were rewarded for FA. It appears that the participants internalize the reward structure, whether it was to minimize the number of false alarms or to maximize the number of hits, and they focus their attention according to the reward.

Robot quality has a significant influence on the human hits of the robot marks (P_{Hrh}), the human false alarms of the robot marks (P_{FArh}), the human false alarms of the objects the robot did not mark (P_{FAh}), and the human sensitivity. Increasing robot quality increased the system objective function score of the experiment. Increase in robot quality increases the values of P_{Hrh} , P_{FArh} , P_{FAh} and human sensitivity. It seems that during the experiment the participants perceived the robot quality and relied on the robot decisions when its quality was high. Additionally, although robot quality did not significantly effect the human hits of the objects the robot did not mark (P_{Hh}), at the low automation level (HR) a decrease in robot quality reduces P_{Hh} and the HOR collaboration level achieves the highest values of P_{Hh} .

Image complexity significantly influenced the human hits and false alarms of the objects the robot did not mark (P_{Hh} and P_{FAh}). Increases in the image complexity decrease P_{Hh} and increase P_{FAh} .

The automation level had a significant effect on the human hits and on the false alarms of the objects the robot marked (P_{Hrh} and P_{FArh}). Increasing the automation level increases P_{Hrh} and P_{FArh} . It seems that for the high automation levels the participant tends to accept the robot decisions. Furthermore, the human sensitivity of the participants who had the 'high quality' robot decreased with the increase in the automation level. This finding indicates that the increase in robot quality reduces both human control and human sensitivity.

The block number had a significant effect on the number of human false alarms for objects the robot did not mark (P_{FAh}). The values and the confidence intervals of P_{FAh} decreased with the increase in block number. This suggests a learning effect.

7 DISCUSSION

In this thesis, four collaboration levels based on Sheridan's levels of automation (1978) were defined in this thesis for a target recognition task of an integrated human-robot system. Though specific collaboration levels were defined for different types of human-robot systems and tasks in other studies, to the best of our knowledge no previous research dealt with collaboration levels for target recognition. Tsuji and Tanaka (2005) investigated a tracking task where the human and the machine act simultaneously. Bruemmer et al. (2005) and Hughes and Lewis (2005) developed different automation levels for a human-robot vehicle in an indoor exploration task. Graves and Czarnecki (2000) described a scale of five human-robot interaction levels for a telerobotic behavior based system. Between these applications each collaboration level differs by nature, scale, structure, and number of levels, and it is unfit for and inapplicable to the present research. Only the manual and fully autonomous levels have similar characteristics since they consist of a single collaborator, and there is no cooperative activity. Furthermore, specific collaboration levels for the task and the specific type of integrated human-robot system investigated in this work were never structured or presented. Since physical platforms and sensors vary significantly from system to system (Edan and Nof, 2000) and also the task and the environment can differ for different cases, the collaboration levels must be well matched to the specific task and system in order to achieve good system performance.

In addition, to the best of our knowledge, mathematical modeling of the collaboration levels and quantification of its influence on system performance has not yet been conducted. Graves and Czarnecki (2000) defined a general logical expression related to system behavior, but they did not define an explicit expression and hence, could not evaluate the influence of different collaboration levels on system performance. To investigate the different collaboration levels and their influence on system performance, an objective function was developed and a numerical analysis performed. The mathematical analysis indicated that the difference between the investigated collaboration levels that include both human and robot (defined as HR and HOR in this research) is expressed only in the human operational parameters related to time (t_{Hh} , t_{FAh} , t_{Hrh} and t_{FArh}). Hence, the only difference between the HR and the HOR collaboration levels is structured in their operational cost. Although it was defined that the required human decision time for target or non-target objects is equal in all cases, for the HR collaboration level the motoric time is added to the human decision time required to confirm a robot hit (t_{Hrh}) and in the HOR collaboration it is added to the human decision time required to reject a robot false alarm (t_{FArh}). Since the time parameters only

appear in the operational cost part of the objective function expression (equations 10-11), when omitting the operational cost there is no difference between the HR and HOR collaboration levels – they become one collaboration level in the objective function. Although the actual operations in the HR and HOR collaboration levels are different, final system performance will be the same. This results from the objective function definitions and indicates the significance of the operational costs.

The objective function integrates the system's operational costs and detection performance measures, thereby resulting in a better estimation of system performance. Since the operational cost of each system is unique, different systems will result in different performances for the same task. Thus, the objective function must be fitted for a specific system to ensure evaluation accuracy.

The objective function enables to rank and compare different systems. The influence of different human, robot, task, and environment parameters on system performance can be evaluated. However, in many cases some of the parameters are unknown *a priori*, such as target probability or human and robot sensitivities. These could be estimated according to previous data collected from similar environments, human and robot performances, or through calibration between withered forms of the objective function of an experiment. This is achievable by equalizing experimental results to the objective function score and extracting the unknown parameters according to the collaboration level and other known parameters.

In this thesis a methodology to determine the best collaboration level was developed. It makes it possible to improve system performance when environmental conditions are known *a priori* by determining the optimal human and robot parameters and the best collaboration level. These developments enable adaptation of an integrated human-robot system to a specific task and environment.

Extensive research was conducted in selecting the best performance measures and the best sensors in autonomous mobile robot systems. Different methods have been developed and implemented for binary parallel detection systems to optimize detection (Hall, 1992). Performance evaluation of sensory algorithms is usually based on either experiments in real environments or theoretical analysis (Brooks and Iyengar, 1998; HoseinNezhad et al., 2002; Luo and Kay, 1989; Ribo and Pinz, 2001). The first approach is problematic in unstructured and dynamic environments, since it is impossible to repeat experiments under identical conditions (Cohen, 2005). The second approach requires explicit assumptions concerning the nature of sensory information, a hard concept to implement since it is usually difficult to characterize sensory performance in unstructured environments (Cohen, 2005).

In our research we encountered similar questions concerning evaluation and optimization of human-robot system performance. We can optimize system performance by using the appropriate collaboration level, which influences the significance of the performance measures. For the H collaboration level, the robot performance measures are uncounted and vice versa in the R collaboration level. Each of the HR and HOR collaboration levels assign a different influence to the operational cost. Likewise, system performance and the best-fit collaboration level were evaluated by numerical and experimental analysis.

Assigning the quantified task and environmental parameters and the defined human and robot sensitivity ranges to the objective function and the best collaboration level methodology enables effective and optimal system design, development of a simple robotic subsystem, reduction of system operational costs, and improved robustness and system performance. The methodology enables system designers to predict the performance of a developed system and to determine the best-fit collaboration levels *a priori*.

Both the objective function and the methodology were developed assuming that all parameters are constant and do not change during task execution. This assumption is unrealistic since many of the parameters are expected to change with time and should be influenced by learning or fatigue effects. During the learning process the human must adjust to the environment, the task, and the system, his sensitivity and decision quality of the cutoff point will be relatively low resulting in poor performance. Likewise, fatigue or tediousness will also reduce human performance. The parameters can also change according to other parameters such as human modes or problems with robotic subsystem calibration. These phenomena are not considered in the current objective function and methodology. Investigation of these behaviors and expression of the objective function parameters as time dependant variables could result in a more accurate evaluation.

Changing from one collaboration level to another, based on changes in the human, robot and environment parameters will enable the system to deal with more dynamic and complex conditions and to keep the system performance. However, dealing with this extension, requires consideration of all changing parameters.

In addition, we assumed that there is no direct influence of the robot performance measures on the human performance measures and vice versa. In other words, low robot hit rate does not necessary cause low or high human hit rate. However, in realistic conditions where the robot actions are visible to the human, the robot performance (*e.g.*, quality and reliability) can be evaluated by the human and influence his performance (Maltz and Shinar, 2003). Our experimental results indicated that when the human estimates that robot performance is high, he will rely on the robot and will less question the robot decisions.

Due to the vast number of independent parameters and the interactions between the parameters, prediction of system performance and the best collaboration level is comprehensive and not obvious. In the presented research we demonstrated the use of the objective function and the methodology to determine the best collaboration level for a specific environment, task and system parameters through numerical analysis. This methodology could be expanded for other environments, tasks and systems and will result in different solutions. Changes in values of several parameters that interact such as probability of robot hit, probability of human hit of robot marks, target probability, payoff ratio, time and additional parameters will influence system performance and the best collaboration level in an unexpected manner. Hence, it is important to perform a numerical analysis of the objective function on the desired parameters to estimate system performance.

Application of modified signal detection theory enabled to reduce the number of parameters and to enhance the researchers' control on the human and robot basic characteristics such as sensitivity and cutoff point (decision) on behalf of loosing control on each detection performance measures individually. For example, a change in the human sensitivity will change both human hit and false alarm rates. An increase of the robot cutoff point value will decrease the robot hit and false alarm rates and the ratio between them.

Sensitivity analysis on the human, robot, environment and task parameters indicates that small changes in the optimal values can shift the best collaboration level from one to another. In dynamic realistic conditions, the control and sensors resolution and accuracy are low and the optimal values of the objective function parameters are unknown precisely and cannot be retained durably. This could cause a difference between the actual values and the expected values and change the actual system performances. In such cases a different collaboration level other than the best collaboration level determined by the optimal values can obtain better system performance. Since the actual values are unstable and distributed in the vicinity of the expected optimal values, an algorithm that will take into account the distribution of the value combined with the objective function and the methodology to determine the best collaboration could achieve better system performance for realistic cases. Instead of placing the expected optimal value in the objective function and the methodology, the mean of the actual values or the distribution of the actual values could be placed to achieve higher system performance. The objective function and the methodology must be modified in order to be able to account for data such as distribution or biased values. For instance if we find that the values of a specific parameter has a Gaussian distribution around its theoretical optimal value, and since the influence on the system performance is not symmetric, placing the specific distribution

will yield more accurate evaluation of the system performance and the best collaboration level.

Experimental results indicated that although the participants' performances were not optimal, they significantly reacted to the different robot, task and environmental parameters. Experimental results were consistent with the numerical analysis results. Both in the experiment and the numerical analysis an increase in robot quality, (*i.e.*, increase in robot sensitivity), increased system performance (the final score) for all collaboration levels that included a robot, and increase in the payoff ratio reduced system performance for all collaboration levels. Similar results were obtained for the best collaboration level. Numerical analysis of the objective function excluding the operational cost showed that the integrated HR/HOR is the best collaboration level. In the experiment the best collaboration levels were found to be HOR and HR. In conclusion, the experimental results support qualitatively the objective function numerical analysis; the objective function and the methodology can predict system performance and the best collaboration level.

The unstructured environment is characterized by environmental disturbances and fuzzy definitions of targets. This causes problems in quantification of the number of non-target objects or target probability in the experiment. Performance measures such as the probability of false alarms cannot be calculated. Hence, only part of the human and robot performance measures and the environmental parameters could be evaluated and compared to the numerical analysis. A method that can estimate the number of non-target objects or the target probability could enable full comparison between the numerical analysis of the objective function and experimental results and could pave the way for a system that could control robot performance. Moreover, this could provide the human with on-line feedback to reach optimal system performance. Development of advanced pattern recognition algorithms to determine the number of objects in unstructured environments is beyond the objective of this work.

8 CONCLUSIONS and FUTURE WORK

8.1 Conclusions

A comprehensive process was designed and undertaken to evaluate the influence of different collaboration levels on the performance of an integrated human-robot system for target recognition tasks in different cases. It includes the development of collaboration levels and an objective function to measure system performance. The objective function was evaluated using numerical and experimental analyses.

The collaboration levels were designed for target recognition tasks in unstructured environments, and they were based on Sheridan's (1978) ten levels of automation. Although the collaboration levels were adjusted for the specific system type and task, they were similar to other scale levels used in other systems and for other tasks (Bruemmer et al., 2005; Hughes and Lewis, 2005; Graves and Czarnecki, 2000). The collaboration levels enable the human operator to collaborate with the robot at four different levels, from manual to fully autonomous. This enables the operation by a human operator in accordance with the robot's design to achieve optimal performance. It was found that the difference between the collaboration levels that include both human and robot (in this research these were defined as HR and HOR) is expressed only in the time parameters of the objective function. Therefore, omitting the operational cost from the objective function unites HR and HOR into one collaboration level.

The objective function enables the determination of the expected value of system performance, given the characteristics of the human, the robot, the task, and the environment. It was defined as the weighted sum of the performance measures. The performance measures used in this research were similar to those used in other studies and included hit and false alarm rates (Maltz, 2000; Swet et al., 2000; Filippidis et al., 2000; Sun et al. 2004; Pei and Lai, 2001; Gao and Hinders, 2005; Liu and Haralick, 2002) and detection time (Steinfeld et al., 2006). The weights allow for the objective function to be adapted to different systems, tasks, and environments, to rank and compare different systems, and to analyze the influence of human, robot, task, and environment parameters, and different collaboration levels on system performance. A modified version of signal detection theory for a human-robot integrated system was applied to simplify and describe the objective function parameters through the human and robot basic characteristics (sensitivity and decision of cutoff point).

The numerical analysis investigated the influence of the human and robot basic characteristics, the task and environment parameters, and different human-robot collaboration levels on the system objective function. Furthermore, it enabled determination of the optimal

human and robot basic characteristics and the best collaboration level for different task and environment parameters.

Numerical analysis results indicate that the best system performance, the optimal performance measures values, and the best collaboration level depend on the task, the environment, human and robot parameters, and the system characteristics. Since the number of independent parameters is vast and, in addition, there are interactions between the parameters, the prediction of the system performance and the optimal solution is comprehensive and not obvious. However, it can be determined through investigation of the objective function. The findings indicate that for the tested cases H is never the best collaboration level for the optimal solution, probably due to its high operational cost and low hit rate relative to the other collaboration levels. Thus, collaboration of human and robot in target recognition tasks will always improve the optimal performance of a single human detector. In addition, for the optimal solution of the objective function including operational cost, the best collaboration level is R when robot sensitivity is higher than human sensitivity. Moreover, the overall system sensitivity never decreases beneath the robot sensitivity.

The sensitivity analyses illustrate the influence of small variations, in the human and robot optimal values and in the environmental parameters, on the objective function and on the best collaboration level. Results indicate that small changes in the optimal values can cause shifts in the best collaboration levels from one to another but the shift is always to an adjacent level. A sensitivity analysis of the environmental target probability parameter showed that small changes in the optimal value can shift the best collaboration level from one to another and in some cases that shift leads directly to H. This finding can be exploited for the design and operation of integrated human-robot systems under dynamic and realistic conditions where the true value of the parameters is unknown and the resolution and accuracy are low, or in cases where the parameters are dynamic and drifting around their expected values.

The experiments included a thorough investigation of the objective function via the different weights for the performance measures, the different collaboration levels, the various robot qualities, and assorted environments. Statistical analyses highlighted the importance of robot quality, collaboration level, and environment on the system performance, and the significance of the weighted human, robot, environmental, and performance measures on the best collaboration level.

Experimental results indicated that although the participants' performances were not optimal, they reacted significantly to the different robot task and environment parameters, and their results are consistent with the results of the numerical analysis of the objective function

excluding the operational cost. Due to the unknown number of total objects, targets and non-targets, only part of the human and robot performance measures and the environmental parameters could be evaluated and compared to the numerical analysis.

Throughout the development, great care was taken to quantify the independent parameters and the results and to validate the theoretical findings with the experiment. The objective function was developed in such a way as to facilitate a comparison of different systems, environments, and tasks.

The methodology developed can help analyze *a priori* the performance of an integrated human-robot system for target recognition tasks and for determining the best collaboration level for optimal performance. In addition, the research investigated the influence of different collaboration levels under various tasks, different human and robot parameters, and changing environmental conditions. The system performance can be simulated and adjusted to the task and the environment. The advantage of this method is that it can be conducted off-line and even in the absence of an actual system, and it allows the comprehensive survey of the influence of various parameters on system performance. System designers can use these methodologies to develop a well adapted, integrated human-robot system for target recognition tasks in unstructured environments. Furthermore, this methodology can be used to analyze system performance during the task performance, and to recommend the best collaboration and the human performance on-line.

The limitations of the research are due to two factors. The first factor is the requirement for the human, robot, and environment parameters to be known *a priori* in order to achieve accurate estimation. In the absence of *a priori* data, prediction accuracy depends on the estimation quality of the parameters. The second factor is that in order to simplify the development of the objective function with signal detection theory, we assumed that the target and non-target objects are normal and with identical distributions. The variables that are influenced by the distribution type are the human and robot different hit and false alarm probabilities (equations 1, 3-8) and the value of the optimal β s. When the S and N distributions are not normal, the probabilities will have to be recalculated according to the new distributions and equations 1, 3-8 will have to be modified to fit the new distributions instead of the normal distribution. However, the collaboration levels, the objective function formation, the methodology to determine the best collaboration level are not influenced by the S or N distribution type.

8.2 *Future research*

Many research areas remain open for the future expansion of this work.

Objective function

The currently analyzed objective function consists of hit, false alarm, and operational cost elements. We propose the following points for future work on the objective function to fit it to more realistic cases:

- Modeling of the various human decision times in the operational cost part according to signal detection theory. We assume that the time to detect depends on the cutoff point and the distance between the specific object distribution value and the cutoff point. The closer the object distribution value is to the cutoff point, the time to detect it will be longer.
- Assimilating signal detection theory with different target and non-target distributions into the objective function. The target and non-target distributions should be fitted to the real distribution in realistic and specific unstructured environments.
- Include time dependency of the objective function parameters to emulate learning and fatigue phenomena or other time dependant influences. The basic human characteristics will be described as time dependent variables based on the results of learning and fatigue experiments. The basic robot characteristics will be described as time dependant variables according to the mean time between calibrations and setup of the specific robotic subsystem.
- Investigate the combined influence of small changes in the independent parameters. For example, the combined influence of small changes in both human and robot sensitivities.

Methodology

Currently the methodology determines the best collaboration level based on static conditions. We suggest:

- Develop an algorithm that will consider the influence of small changes in the parameter values that was found in the sensitivity analysis according to a distribution function of the variation. Each parameter probably has its unique distribution function that is influenced by the

environment and the task. The distribution function of the parameters variation can be determined through experiments.

- The methodology and the objective function parameters must be known *a priori* to accurately predict system performance and the best collaboration level. Hence, it is important to develop a model that predicts the environment parameters according to the statistical data of different tasks and environments.
- Develop a methodology that will include dynamic shifting between collaboration levels to maintain maximum system performance despite changes in the parameter values during the task performance and a rule-based algorithm to shift between collaboration levels based on human, robot, task, and environmental parameters and limitations.

Experiments

In future research additional and comprehensive experiments are suggested:

- Conducting an experiment to examine the learning and fatigue effects on both human and system performance.
- Conducting an experimental research to assess all time variables.
- An experiment for investigating the effect of shifting between collaboration levels should be conducted. Many questions can be asked concerning the shift manner: who decides on the shift, human, robot, or is it a collaborative decision? How many levels can be shifted at one time, what parameters should be considered in the shift and what should the frequencies of the shift be?

9 REFERENCES

- Al-Mouhamed M.A. Toker O. and Al-Harthy A. 2005. A 3-D vision-based man-machine interface for hand-controlled telerobot. *IEEE Transactions on Industrial Electronics* 52(1): 306 - 319.
- Al-Jumaily, A.A.S. and Amin, S.H.M. 2000. Blending multi-behaviors of intelligent reactive navigation for legged walking robot in unstructured environment. *Proceedings of TENCON 2*: 297-302.
- Alchanatis V., Ridet L., Hetzroni A. and Yaroslavsky L. 2005. Weed detection in multi-spectral images of cotton fields. *Computers and Electronics in Agriculture* 47 (3): 243-260.
- Aracil R., Ferre M., Hernando M., Pinto E. and Sebastian J. M. 2003. Telerobotic system for live-power line maintenance: ROBTET. *Control Engineering Practice* 10(11): 1271-1281.
- Ara'ujo R. and de Almeida A.T. 1999. Learning Sensor-Based Navigation of a Real Mobile Robot in Unknown Worlds. *IEEE Transactions on Systems, Man and Cybernetics*, part B, 29(2): 164–178.
- Arena P., Di Giamberardino P., Fortuna L., La Gala F., Monaco Muscato S., Rizzo G., A. and Ronchini R.. 2004. Toward a mobile autonomous robotic system for Mars exploration. *Planetary and Space Science* 52(1-3): 23-30.
- Ayrulu B. and Barshan B. 2001. Neural networks for improved target differentiation and localization with sonar. *Neural Networks* 14(3): 355-373
- Aviram G. and Rotman S.R. 2000. Evaluation of human detection performance of targets embedded in natural and enhanced infrared images using image metrics. *Optical Engineering*. 39(4): 885-896.
- Balakirsky S., Messina E., Schlenoff C., Smith S. and Uschold M. 2004. Knowledge representation for a trash collecting robot: results from the 2004 AAAI Spring Symposium. *Robotics and Autonomous Systems* 49(1-2): 7-12.
- Banerjee A., Banerjee P., DeFanti T, Dodds B. and Curtis J.R. 2000. A behavioral layer architecture for telecollaborative virtual manufacturing operations. *IEEE Transactions on Robotics and Automation*. 16 (3): 218-227.
- Banerjee A., Burlina P. and Chellappa R. 1999. Adaptive target detection in foliage-penetrating SAR images using alpha-stable models. *IEEE Transactions On Image Processing*. 8(12): 1823-1831.
- Bar A., Edan E. and Alper Y. 1996. Robot transplanting: simulation and adaptation. ASAE paper no. 96-3008. ASAE, St. Joseph, MI.
- Beam S.E., Miles G.E. and Treece G.J. 1991. Robotic transplanting: simulation, design, performance tests. ASAE paper no. 91-7027. ASAE, St. Joseph, MI.
- Bechar A. and Edan Y. 2003. Human-robot collaboration for improved target recognition of agricultural robots. *Industrial Robot* 30(5): 432-436.
- Bechar, A., Edan Y. and Meyer J. 2004. An Objective Function for Performance Measurement of Human-Robot Target Recognition Systems in Unstructured Environments. *International Conference on Systems, Man and Cybernetics*, IEEE SMC Paper No. 520 The Hague, The Netherlands.
- Belkhouche B. and Belkhouche F. 2005. Modeling and controlling a robotic convoy using guidance laws strategies. *IEEE Transactions on Systems, Man and Cybernetics*, Part B 35(4): 813 – 825.

- Benady M. and Miles G.E. 1992. locating melons for robotic harvesting using structured light. ASAE paper no. 92-7021. ASAE, St. Joseph, MI.
- Benyahia I. and Potvin J.Y. 1998. Decision Support for Vehicle Dispatching Using Genetic Programming. IEEE Transactions on Systems, Man and Cybernetics, part A. 28(3): 306-314.
- Bhanu B., Lin Y.Q., Jones G. and Peng J. 2000. Adaptive target recognition. Machine Vision And Applications. 11(6): 289-299.
- Bicho E., Mallet P. and Schoner G. 2000. Target representation on an autonomous vehicle with low-level sensors. International Journal of Robotic Research 19(5): 424-447.
- Billingsley P. F. 2000. Morphometric analysis of *Rhodnius prolixus* (Hemiptera: Reduviidae) midgut cells during blood digestion. Tissue and Cell 20(2): 291-301.
- Birk A. and Kenn H. 2002. RoboGuard, a teleoperated mobile security robot. Control Engineering Practice 10(11): 1259-1264.
- Brooks, R. R. and Iyengar S. S. 1998. Multi-sensor fusion. Prentice Hall, New York, NY.
- Brown, G.K. 2002. Mechanical harvesting systems for the Florida citrus juice industry. ASAE Paper No. 021108. ASAE, St. Joseph, MI.
- Brown C.D. and Davis H.T. 2006. Receiver operating characteristics curves and related decision measures: A tutorial. Chemometrics and Intelligent Laboratory Systems 80(1): 24-38.
- Bruemmer D.J., Few D. A., Boring R.A., Marble J.A., Walton M.C. and Nielsen C.W. 2005. Shared Understanding for Collaborative Control. IEEE Transactions on Systems, Man and Cybernetics: Part A 35(4): 494-504.
- Bulanon, D.M., Kataoka, T., Zhang, S., Ota, Y. and Hiroma, T. 2001. Optimal thresholding for the automatic recognition of apple fruits. ASAE Paper No. 01-3133.
- Carelli R. and Freire E.O. 2003. Corridor navigation and wall-following stable control for sonar-based mobile robots. Robotics and Autonomous Systems 45(3-4): 235-247.
- Ceres R., Pons J.L., Jimenez A.R., Martin J.M. and Calderon L. 1998. Design and implementation of an aided fruit-harvesting robot (Agribot). Industrial Robots. 25(5): 337-346.
- Chakravarthy A. and Ghose D. 1998. Obstacle Avoidance in a Dynamic Environment: A Collision Cone Approach. IEEE Transactions on Systems, Man and Cybernetics, part A. 28(5): 562-574.
- Chang Y.C., Song G.S. and Hsu S.K. 1998. Automatic extraction of ridge and valley axes using the profile recognition and polygon-breaking algorithm. Computers and Geosciences 24(1): 83-93.
- Cheng Y.D., O'Toole A.J. and Abdi H. 2001. Classifying adults' and children's faces by sex: computational investigations of subcategorical feature encoding. Cognitive Science 25(5): 819-838.
- Cherif M. 1999. Motion planning for all-terrain vehicles: A physical modeling approach for coping with dynamic and contact interaction constraints. IEEE Transactions on Robotics and Automation 15 (2): 202-218.
- Chirikjian, G.S., Zhou Y. and Suthakorn, J. 2002. Self-replicating robots for lunar development. IEEE/ASME Transactions on Mechatronics 7(4): 462- 472.
- Cohen O. 2005. Grid-map based sensor fusion for autonomous mobile robots. PhD thesis. Department of Industrial Engineering and Management, Ben-Gurion University of the Negev. Israel.

- Deb, K. Thiele, L. Laumanns, M. and Zitzler, E. 2002. Scalable multi-objective optimization test problems. Proceedings of the 2002 Congress on Evolutionary Computation. 1: 825-830. Honolulu, HI, USA.
- Dollarhide R.L. and Agah A. 2003. Simulation and control of distributed robot search teams. Computers and Electrical Engineering 29(5): 625-642.
- Dobrusin, Y., Edan Y., Grinspan J., Peiper U.M. and Hetzroni A. 1992. Real-time image processing for robotic melon harvesting, ASAE paper No. 92-3515, ASAE St. Joseph, MI.
- Du Q. and Ren H. 2002. Real-time constrained linear discriminant analysis to target detection and classification in hyperspectral imagery. Pattern Recognition. In press.
- Edan Y., Flash T., Shmulevich I. And Peiper U.M. 1990. An algorithm defining the motions of a citrus picking robot. Journal of Agricultural Research. Academic press. 46(4): 259-273.
- Edan Y., Flash T., Shmulevich I. And Sarig Y. 1991. Near minimum time task planning algorithm for fruit picking robots. IEEE Transaction on Robotics and Automation. 7(1): 48-56.
- Edan Y. 1995. Design of an autonomous agricultural robot. Applied Intelligence. 5 (1): 41-50.
- Edan Y. and Bechar A. 1998. Multi-Purpose Agricultural Robot. Proceeding of The Sixth IASTED International Conference, Robotics And Manufacturing, Banff, Canada. pp. 205-212.
- Edan Y, Miles G.E. 1993. Design of an agricultural robot for harvesting melons. Transaction of the ASAE 36 (2): 593-603.
- Edan, Y., 1999. Food and agricultural robots. In The Handbook of Industrial Robotics: 1143-1155, Second Edition. Ed.: S.Y. Nof. John Wiley and Sons, New York, NY.
- Ethier, S., Wilson, W.J. and Hulls, C. 2002. Telerobotic part assembly with shared visual servo control. IEEE International Conference on Robotics and Automation, Proceedings. ICRA 4: 3763 – 3768.
- Everett S. and Dubey R. 1998. Human-Machine Cooperative Telerobotics Using Uncertain Sensor and Model Data. Proceedings of the IEEE International Conference on Robotics and Automation. Leuven, Belgium. pp. 1615-1622.
- Farahvash P. and Boucher T.O. 2004. A multi-agent architecture for control of AGV systems. Robotics and Computer-Integrated Manufacturing 20(6): 473-483.
- Flann N.S., Moore K.L. and Ma L. 2002. A small mobile robot for security and inspection operations. Control Engineering Practice 10(11): 1265-1270 .
- Filippidis, A. Jain, L.C. Martin, N . 2000. Multisensor data fusion for surface land-mine detection. IEEE Transactions on Systems, Man and Cybernetics, Part C 30(1): 145 – 150.
- Fletcher L., Loy G., Barnes N. and Zelinsky A. 2005. Correlating driver gaze with the road scene for driver assistance systems. Robotics and Autonomous Systems 52: 71–84.
- Forero M.G., Sroubek F. and Cristóbal G. 2004. Identification of tuberculosis bacteria based on shape and color. Real-Time Imaging 10(4): 251-262.
- Gao W. and Henders M.K. 2005. Mobile robot sonar interpretation algorithm for distinguishing trees from poles. Robotics and Autonomous Systems 53(2): 89-98.
- Garcia E. and de Santos P.G. 2004. Mobile-robot navigation with complete coverage of unstructured environments. Robotics and Autonomous Systems 46(4): 195-204.
- Gerrish J.B., Stockman G.C., Mann L. and Hu G. 1986. path finding by image processing in agricultural fields operations. ASE paper 86-1455. SAE Trans. 95(5), SAE, Warrendale, PA.

- Gilmore J.F. 1991. Knowledge-based target recognition system evolution. *Optical Engineering*. 30(5): 557-570.
- Gonzalez-Galvan E.J., Cruz-Ramirez S.R., Seelinger M.J., Cervantes-Sanchez J.J. 2003. An efficient multi-camera, multi-target scheme for the three-dimensional control of robots using uncalibrated vision. *Robotics and Computer-Integrated Manufacturing* 19(5): 387-400.
- Gowadia V., Farkas C. and Valtorta M. 2005. PAID: A Probabilistic Agent-Based Intrusion Detection system. *Computers and Security* 24(7): 529-545.
- Grand d'Esnon A., pellenc R., Rabatel G., Journeau A. and Aldon M. 1985. Magali a self propelled robot to pick apples. ASAE paper no. 87-037. ASAE, St. Joseph, MI.
- Guida G. and Lamperti G. 2000. AMMETH: A methodology for requirements analysis of advanced human-system interfaces. *IEEE Transactions on Systems, Man and Cybernetics*, part A. 30 (3): 298-321.
- Graves A.R. and Czarnecki C. 2000. Design Patterns for Behavior-Based Robotics. *IEEE Transactions on Systems, Man and Cybernetics*, Part A, 30(1): 36-41.
- Hall D.L. 1992. Mathematical techniques in multisensor data fusion, Artech House Inc.
- Hannan, M.W., T.F. Burks. 2004, Current Developments in Robotic Harvesting of Citrus, ASAE Paper No. 043087. ASAE, St. Joseph, MI.
- Hasegawa, T., Nakagawa, K. and Murakami, K. 2004. Toward on- line transition to autonomous teleoperation from master-slave manipulation. *IEEE International Conference on Robotics and Automation*, 2004. Proceedings of ICRA 4: 3715 - 3720.
- Harrel R.C. and Levi P. 1988. Vision controlled robots for automatic harvesting of citrus. AGENG paper no. 88-426. International Conference on Agricultural Engineering.
- Harrel R.C., Adsit P.D., Munilla R.D. and Slaughter D.C. 1990. Robot picking citrus. *Robotica* 8: 269-278.
- Hill H., Schyns F. G. and Akamatsu S. 1997. Information and viewpoint dependence in face recognition. *Cognition* 62(2): 201-222.
- Hirukawa H., Matsui T., Onda H. Takase K., Ishiwata Y., and Konaka K. 1997. Prototypes of Teleoperation Systems via a Standard Communication Protocol with a Standard Human Interface. *Proceeding of ICRA 97*. pp.1028-1033.
- Hoffman R., Fitzpatrick K., Ollis M., Pangles H., Pilarski T. and Stentz A. 1996. DEMETER: An autonomous alfalfa harvesting system. ASAE paper no. 963005. ASAE, St. Joseph, MI.
- Hannaford, B. and Jee-Hwan Ryu. 2002. Time-domain passivity control of haptic interfaces. *IEEE Transactions on Robotics and Automation* 18(1): 1-10.
- HoseinNezhad R., Moshiri B. and Asharif M. R. 2002. Sensor fusion for ultrasonic and laser arrays in mobile robotics. *IEEE Sensors 2002*, The 1st IEEE International Conference on Sensors, Orlando, Florida, USA, June 12-14: 1682-1689.
- Hughes S.B. and Lewis M. 2005. Task-Driven Camera Operations for Robotic Exploration. *IEEE Transactions on Systems, Man and Cybernetics: Part A* 35(4): 513-522.
- Ip Y.L. and Rad A.B. 2004. Incorporation of Feature Tracking into Simultaneous Localization and Map Building via Sonar Data. *Journal of Intelligent and Robotic Systems* 39(2): 149 – 172.
- Itoh T., Kosuge K. and Fukuda T. 2000. Human– Machine Cooperative Telemanipulation with Motion and Force Scaling Using Task- Oriented Virtual Tool Dynamics. *IEEE Transactions on Robotics and Automation*. 16(5): 505–516.

- Ivanisevic I. and Lumelsky V. 1997. A Human - Machine Interface for Teleoperation of Arm Manipulators in a Complex Environment. Tech. Report RL-97006. Robotics Lab, University of Wisconsin-Madison, Madison, Wisconsin, USA.
- Iwahashi N. 2003. Language acquisition through a human-robot interface by combining speech, visual, and behavioral information. *Information Sciences* 156(1-2): 109-121.
- Jean J., Liang X., Drozd B., Tomko K. and Wang Y. 2001. Automatic Target Recognition with Dynamic Reconfiguration. *Journal of VLSI Signal Processing* 25: 39-53.
- Jee-Hwan R., Dong-Soo K. and Hannaford, B. 2004. Stable teleoperation with time-domain passivity control. *IEEE Transactions on Robotics and Automation* 20(2): 365 – 373.
- Jiminez, A.R., R. Ceres and J.L. Pons. 2000. Vision system based on a laser range-finder applied to robotic fruit harvesting. *Machine Vision and Applications* 11(6):321-329.
- Jing X.J. 2005. Behavior dynamics based motion planning of mobile robots in uncertain dynamic environments. *Robotics and Autonomous Systems* 53(2): 99-123.
- Kofman, J., Xianghai Wu, Luu, T.J. and Verma, S. 2005. Teleoperation of a robot manipulator using a vision-based human-robot interface. *IEEE Transactions on Industrial Electronics* 52(5): 1206-1219.
- Kawamura N., Namikawa K., Fujiura T. and Ura M. 1985. Study on agricultural robot (III) Detection and detaching devices of fruits. (IV) Improvement of manipulator of fruit harvesting robot. Research report on Agricultural Machinery. No. 15. Kyoto University, Japan.
- Kawamura N., Namikawa K., Fujiura T. and Ura M. 1987. Study on agricultural robot (VII) Hand of fruit harvesting robot. (VIII) Sigling manipulator. Research report on Agricultural Machinery. No. 17. Kyoto University, Japan.
- Kazaz I., S. Gan-Mor (1993). Leader cable architecture for guidance of agricultural vehicles. ASAE paper No. 931056. ASAE, St. Joseph, MI.
- Khadraoui D., Debain C. and Rouveure R. 1998. Vision-based control in driving assistance of agricultural vehicles. *International Journal of Robotics Research* 17(10): 1040-1054.
- Kidono K., Miura J. and Shirai Y. 2002. Autonomous visual navigation of a mobile robot using a human-guided experience. *Robotics and Autonomous Systems* 40(2-3): 121-130.
- Kim W.S., Hannaford B. and Bejczy A.K. 1992. Force reflection and shared compliant control in operating telemanipulators with time delay, *IEEE Transactions on Robotics and Automation*. 8:176-185.
- Kim H. J. and Shim D. H. 2003. A flight control system for aerial robots: algorithms and experiments. *Control Engineering Practice* 11(12): 1389-1400.
- Kirlik, A., Plamondon, B.D., Lytton, L., Jagacinski, R.J. and Miller, R.A. 1993. Supervisory control in a dynamic and uncertain environment: laboratory task and crew performance. *IEEE Transactions on Systems, Man and Cybernetics*, 23(4), pp. 1130-1138.
- Klas N. and Rolf J. 1999. Integrated architecture for industrial robot programming and control. *Robotics and Autonomous Systems* 29(4): 205-226.
- Kofman, J., Xianghai W., Luu, T.J. and Verma, S. 2005. Teleoperation of a robot manipulator using a vision-based human-robot interface. *IEEE Transactions on Industrial Electronics* 52(5): 1206 – 1219.
- Kondo N., Nishitsuji Y. and Ling P.P. 1996. Visual feedback guided robotic cherry tomato harvesting. *Transactions of the ASAE* 39 (6): 2331-2338.
- Kondo H. and Ura T. 2004. Navigation of an AUV for investigation of underwater structures. *Control Engineering Practice* 12(12): 1551-1559.

- Kosuge K. 1990. Control of single-master multi-slave manipulator system using VIM. IEEE International Conference on Robotics and Automation Proceeding: 1172–1177.
- Ku C.H. and Tsai W.H. 1999. Obstacle Avoidance for Autonomous Land Vehicle Navigation in Indoor Environments by Quadratic Classifier. IEEE Transactions on Systems, Man and Cybernetics, Part B. 29(3): 416-439.
- Kuchar, J. K. 1996. Methodology for Alerting-System Performance Evaluation. AIAA Journal of Guidance, Control and Dynamics 19(2): 438-444.
- Lacomme P., Prins C. and Ramdane-Chérif W. 2005. Evolutionary algorithms for periodic arc routing problems. European Journal of Operational Research 165(2): 535-553.
- Lam, H.K. and Leung, F.H.F. 2005. Stability analysis of fuzzy control systems subject to uncertain grades of membership. IEEE Transactions on Systems, Man and Cybernetics, Part B. 35(6): 1322-1325.
- Liang M. and Palakal M.J. 2002. Airborne sonar target recognition using artificial neural network. Mathematical and Computer Modelling. 35(3-4): 429-440.
- Ling P.P., Tai Y.W. and Ting K.C. 1990. vision guided robotic seedling transplanting. ASAE paper no. 90-7520. ASAE, St. Joseph, MI.
- Liu G. and Haralick R.M. 2002. Optimal matching problem in detection and recognition performance evaluation. Pattern Recognition 35(10): 2125-2139.
- Lopez-Juarez, I and Howarth, M. 2002. Knowledge acquisition and learning in unstructured robotic assembly environments. Information Sciences. 145(1-2): 89-111.
- Luo R. C. and Kay M. G. 1989. Multisensor integration and fusion in intelligent systems, IEEE Transactions on Systems Man, and Cybernetics, 19(5): 901-931.
- Luk B.L., Cooke D.S., Arthur S.G., Collie A. and Chen S. 2005. Intelligent legged climbing service robot for remote maintenance applications in hazardous environments. Robotics and Autonomous Systems 53(2): 142-152.
- Maltz M. 2000. Decision modeling for a target acquisition task. Optical Engineering. 39 (9): 2581-2584.
- Maltz M. and Meyer J. 2001. Use of Warnings in an Attentionally Demanding Detection Task. Human Factors. 43 (2): 217-226.
- Maltz M. and Shinar D. 2003. New alternative methods of analyzing human behavior in cued target acquisition. Human Factors 45(2):281-95.
- Matthies L., Xiong Y., Hogg R., Zhu D., Rankin A., Kennedy B., Hebert M., MacLachlan R., Won C., Frost T., Sukhatme G., McHenry M. and Goldberg S. 2002. A portable, autonomous, urban reconnaissance robot. Robotics and Autonomous Systems 40(2-3): 163-172.
- Matthews J. W., Rosenberger F. U., Bosch W. R., Harms W. B. and Purdy J. A. 1996. Real-time 3D dose calculation and display: A tool for plan optimization. International Journal of Radiation Oncology, Biology, Physics 36(1): 159-165.
- Matlab. 1995. The Mathworks, Inc., South Narick, MA 01760.
- Meyer J and Kuchar J.K. 2006. Maximal Benefits and Possible Costs of Alerting Systems. In preparation.
- Michaud, F., Audet, J., Letourneau, D., Lussier, L., Theberge-Turmel, C. and Caron, S. 2001. Experiences with an autonomous robot attending AAI. IEEE Intelligent Systems 16(5): 23-29.
- Millan A.A.J. and Floreano D. 1999. Efficient learning of variable-resolution cognitive maps for autonomous indoor navigation. IEEE Transactions on Robotics and Automation 15 (6): 990-1000.

- Mouaddib E.M. and Marhic B. 2000. Geometrical Matching for Mobile Robot Localization. *IEEE Transactions on Robotics and Automation* 16(5): 542–552.
- Neira J., Tardós J.D., Horn J. and Schmidt G. 1999. Fusing Range and Intensity Images for Mobile Robot Localization. *IEEE Transactions on Robotics and Automation* 15(1): 76–84.
- Ng K.C. and Trivedi M.M. 1998. A Neuro-Fuzzy Controller for Mobile Robot Navigation and Multirobot Convoying. *IEEE Transactions on Systems, Man and Cybernetics, part B.* 28(6): 829-840.
- Oboe R. and Fiorini P. 1998. A design and control environment for Internet-based telerobotics. *International Journal of Robotic Research* 17 (4): 433-449.
- Ogasawara T., Hirukawa H., Kitagaki K., Onda H., Nakamura A. and Tsukune H. 1998. A Telerobotics System for Maintenance Tasks Integrating Planning Functions Based on Manipulation Skills. *Proceedings of the IEEE International Conference on Robotics and Automation.* Leuven,Belgium: 1870-1876.
- Olson C.F. 2000. Probabilistic self-localization for mobile robots. *IEEE Transactions on Robotics and Automation* 16 (1): 55-66.
- Oriolo G., Ulivi G. and Vendittelli M. 1998. Real- Time Map Building and Navigation for Autonomous Robots in Unknown Environments. *IEEE trans. Sys. Man cyber.* 28(3): 316-333.
- Parasuraman R., Sheridan T.B. and Wickens C.D. 2000. A Model for Types and Levels of Human Interaction with Automation. *IEEE Transactions on Systems, Man and Cybernetics, part A.* 30(3): 286-197.
- Patnaik L.M. and Rajan K. Target detection through image processing and resilient propagation algorithms. *Neurocomputing.* 35: 123-135.
- Pei S.C. and Lai C.L. 2001. A morphological approach of target detection on perspective plane. *Signal Processing* 81(9): 1975-1984.
- Penin L.F., Aracil R., Ferre M., Pinto E., Hernando M. and Barrientos A. 1998. Telerobotic system for live power lines maintenance: ROBTET. *Proceedings of the IEEE International Conference on Robotics and Automation.* Leuven, Belgium. pp. 2210-2115.
- Perzanowski, D., Schultz, A.C., Adams, W., Marsh, E. and Bugajska, M. 2001. Building a multimodal human-robot interface. *IEEE Intelligent Systems* 16(1): 16 – 22.
- Peshkin M.A., Colgate J.E., Wannasuphprasit W., Moore C.A., Gillespie R.B. and Akella P. 2001. Cobot architecture. *IEEE Transactions on Robotics and Automation* 17 (4): 377-390.
- Peungsungwal, S. Pungsiri, B. Chamnongthai, K. and Okuda, M. 2001. Autonomous robot for a power transmission line inspection. *IEEE International Symposium on Circuits and Systems* 3: 121 – 124.
- Pons J.L., Ceres R. and Jimenez A.R. 1996. mechanical design of fruit picking manipulator. Improvement of dynamic behavior. *IEEE Int. Conference on Robot. Automat.* Minneapolis. pp. 969-974.
- Ponweiser W., Vincze M. and Zillich M. 2005. A software framework to integrate vision and reasoning components for Cognitive Vision Systems. *Robotics and Autonomous Systems* 52: 101–114.
- Pook P.K. and Ballard D.H. 1996. Deictic human/robot interaction. *Robotics and Autonomous Systems* 18(1-2) : 259-269.
- Potts G.F. and Tucker D.M. 2001. Frontal evaluation and posterior representation in target detection. *Cognitive Brain Research* 11(1): 147-156.

- Plebe, A. and G. Grasso. 2001. Localization of spherical fruits for robotic harvesting. *Machine Vision and Applications*. 13(2): 70-79.
- Radix C.L., Robinson P., Nurse P. 1999. Extension of Fitts law to modeling motion performance in man-machine interfaces. *IEEE Transactions on Systems, Man and Cybernetics* 29 (2): 205-209.
- Raghavan V., Molineros J. and Sharma R. 1999. Interactive evaluation of assembly sequences using augmented reality. *IEEE Transactions on Robotics and Automation* 15 (3): 435-449.
- Raju G.J. 1989. Design issues in 2-port network models of bilateral remote manipulation. in *Proceedings of IEEE International Conference on Robotics and Automation*: 1316–1321.
- Ribo M. and Pinz A. 2001. A comparison of three uncertainty calculi for building sonar based occupancy grids, *International Journal of Robotics and Automation Systems* 35: 201-209.
- Robinson, D. E., & Sorkin, R. D. 1985. A contingent criterion model of computer assisted detection. In R. Eberts & C. G. Eberts (Eds.) *Trends in Ergonomics/Human Factor II*, pp. 75-82. North Holland: Amsterdam
- Rodriguez G. and Weisbin C.R. 2003. A New Method to Evaluate Human-Robot System Performance. *Autonomous Robots* 14: 165–178.
- Roy D. 2005. Semiotic schemas: A framework for grounding language in action and perception. *Artificial Intelligence* 167(1-2): 170-205.
- Rosenblatt J., Williams S. and Durrant-Whyte H. 2002. A behavior-based architecture for autonomous underwater exploration. *Information Sciences*, Volume 145, Issues 1-2, August 2002, Pages 69-87.
- Rucci M., Edelman G.M. and Wray J. 1999. Adaptation of Orienting Behavior: From the Barn Owl to a Robotic System. *IEEE Transactions on Robotics and Automation*. 15(1): 96–110.
- Sano A., Fujimoto H. and Tanaka M. 1998. Gain-Scheduled Compensation for Time Delay of Bilateral Teleoperation Systems. *Proceedings of the IEEE International Conference on Robotics and Automation*. Leuven, Belgium: 1916-1923.
- Scholtz, J.C., Antonishek, B. and Young, J.D. 2005. Implementation of a situation awareness assessment tool for evaluation of human-robot interfaces. *IEEE Transactions on Systems, Man and Cybernetics, Part A* 35(4): 450 – 459.
- Schmitter E. 1995. Automatic grain-size determination and classification of iron carbides with neural nets. *Steel research*. 66(10): 449-453.
- Se, S., Lowe, D.G., Little, J.J. 2005. Vision-based global localization and mapping for mobile robots. *IEEE Transactions on Robotics* 21(3): 364 – 375.
- Sevila F. and Baylou P. 1991. The principles of robotics in agriculture and Horticulture, In: *Progress in Agricultural Physics and Engineering*, C.A.B. International, Bedford, U.K.: 119-147.
- Salter T., Dautenhahn K. and Boekhorst R. 2006. Learning about natural human–robot interaction styles. *Robotics and Autonomous Systems* 54: 127–134.
- Sheridan T.B. and Verplank W.L. 1978. Human and Computer Control of Undersea Teleoperators, MIT Man-Machine Systems Laboratory. Cambridge, MA, Tech. Rep.
- Sheridan T. B. 1989. Telerobotics, *Automatica* 25(4): 487-507.
- Sheridan T.B. 1992. Telerobotics, Automation and Supervisory Control. Cambridge, MA. MIT Press.

- Sidenbladh H., Kragic, D. and Christensen, H.I. 1999. A person following behavior for a mobile robot. Proceedings of the 1999 IEEE International Conference on Robotic and Automation. pp. 670-675.
- Speich, J.E. and Goldfarb, M. 2005. An implementation of loop-shaping compensation for multidegree-of-freedom macro-microscaled telemanipulation. IEEE Transactions on Control Systems Technology 13(3): 459 – 464.
- St-Amant R. 1999. User interface affordances in a planning representation. Hum.-Comput. Interact. 14 (3): 317-354.
- Stanczyk B. and Buss, M. 2004. Development of a telerobotic system for exploration of hazardous environments. IEEE/RSJ International Conference on Intelligent Robots and Systems, Proceedings 3: 2532 – 2537.
- Steinfeld A. 2004. Interface lessons for fully and semi-autonomous mobile robots. ICRA 3: 2752 – 2757.
- Sun Z., Bebis G. and Miller R. 2004. Object detection using feature subset selection. Pattern Recognition 37(11): 2165-2176.
- Swets J.A. Dawes R.M. and Monahan J. 2000 .Better Decisions Through Science. Scientific American :82-87
- Synergy. 2001. Human engineering consideration in operation of telerobotic armored vehicle. Company report. Israel. (In Hebrew).
- Thrun, S., Thayer, S., Whittaker, W., Baker, C., Burgard, W., Ferguson, D., Hahnel, D., Montemerlo, D., Morris, A., Omohundro, Z., Reverte, C. and Whittaker W. 2004. Autonomous exploration and mapping of abandoned mines. IEEE Robotics and Automation Magazine 11(4): 79-91.
- Thuilot, B., Cariou, C., Martinet, P., Berducat, M.2002. Automatic guidance of a farm tractor relying on a single CP-DGPS. Autonomous Robots 13(1): 53-71.
- Tsuji T. and Tanaka Y. 2005. Tracking Control Properties of Human–Robotic Systems Based on Impedance Control. IEEE Transactions on Systems, Man and Cybernetics: Part A 35(4): 523-535.
- Tsourveloudis N.C., Valavanis K.P. and Hebert T. 2001. Autonomous Vehicle Navigation Utilizing Electrostatic Potential Fields And Fuzzy Logic. IEEE Transactions on Robotics and Automation 17(4): 490-497.
- Torii T. 2000. Research in autonomous agriculture vehicles in Japan. Computers and Electronics in Agriculture 25(1-2): 133-153.
- Van Erp J.B.F. and Van Veen H.A.H.C. 2004. Vibrotactile in-vehicle navigation system. Transportation Research Part F: Traffic Psychology and Behaviour 7(4-5): 247-256.
- Van Henten E. J., Van Tuijl B. A. J., Hemming J., Kornet J. G., Bontsema J. and Van Os E. A. 2003. Field Test of an Autonomous Cucumber Picking Robot. Biosystems Engineering, Volume 86, Issue 3, November 2003, Pages 305-313.
- Venkataramani, K., Qidwai, S., Vijayakumar, B.V.K. 2005. Face authentication from cell phone camera images with illumination and temporal variations. IEEE Transactions on Systems, Man, and Cybernetics, Part C. 35(3): 411-418.
- Wang M. and Liu J. N.K. 2005. Interactive control for Internet-based mobile robot teleoperation. Robotics and Autonomous Systems 52(2-3): 160-179.
- Wilson, M. and Neal, H. 2001. Diminishing returns of engineering effort in telerobotic systems. IEEE Transactions on Systems Man and Cybernetics, Part A 31(5): 459-465.
- Xiao-Gang W., Moallem, M. and Patel, R.V. 2003. An Internet-based distributed multiple-telerobot system. IEEE Transactions on Systems Man and Cybernetics, Part A 33(5): 627-634.

- Xu Y., Song J., Nechyba M.C. and Yam Y. 2002. Performance evaluation and optimization of human control strategy. *Robotics and Autonomous Systems* 39 (2002): 19–36.
- Yamashita J. and Kondo N. 1992. Agricultural robots (1): vision sensing systems. ASAE paper no. 92-3517. ASAE, St. Joseph, MI.
- Ye Y.M. and Tsotsos J.K. 1999. Sensor planning for 3D object search. *Computer Vision And Image Understanding*. 73(2): 145-168.
- Yokokoji Y. and Yoshikawa T. 1994. Bilateral control of master-slave manipulators for ideal kinesthetic coupling—Formulation and experiment. *IEEE Transactions on Robotics and Automation* 10: 605–620.

10 APPENDIXES

Appendix I: Transformation of the probability function from X to Z

In order to describe the problem in standard deviation units rather than in the actual units that suits just the specific case, the probability functions are transformed from the actual units, X, to standard deviation units, Z.

$$f_s(x) = \frac{1}{\sigma_s \sqrt{2\pi}} e^{-\frac{(x-\mu_s)^2}{2\sigma_s^2}}$$

$$P_M(x) = \int_{-\infty}^x f_s(x) dX = \frac{1}{\sigma_s \sqrt{2\pi}} \int_{-\infty}^x e^{-\frac{(x-\mu_s)^2}{2\sigma_s^2}} dX$$

$$Z = \frac{X - \mu_s}{\sigma_s} \Rightarrow X = \sigma_s \cdot Z + \mu_s$$

$$\frac{dX}{dZ} = \sigma_s \Rightarrow dX = \sigma_s \cdot dZ$$

$$x = \sigma_s \cdot Z_s + \mu_s$$

$$P_M(Z_s) = \frac{1}{\sigma_s \sqrt{2\pi}} \int_{-\infty}^{Z_s} e^{-\frac{(\sigma_s \cdot Z_s + \mu_s - \mu_s)^2}{2\sigma_s^2}} \sigma_s dZ = \frac{\sigma_s}{\sigma_s \sqrt{2\pi}} \int_{-\infty}^{Z_s} e^{-\frac{(Z_s)^2}{2}} dZ = \frac{1}{\sqrt{2\pi}} \int_{-\infty}^{Z_s} e^{-\frac{(Z_s)^2}{2}} dZ$$

Appendix II: Expression of Z as a function of β and d'

The standard deviation unit, Z, can be expressed by the likelihood ratio, β , between the signal and noise density functions in the cut off point x, and the distance between the means of the signal and noise distributions, which is the sensitivity parameter, d' .

$$i) \quad d' = Z_N - Z_s$$

$$ii) \quad \ln(\beta) = -\frac{1}{2}(Z_s^2 - Z_N^2)$$

$$i) \Rightarrow Z_s = Z_N - d'$$

$$\Rightarrow ii) \quad \ln(\beta) = -\frac{1}{2}((Z_N - d')^2 - Z_N^2) = -\frac{1}{2}(Z_N^2 - 2Z_N d' + d'^2 - Z_N^2) = -\frac{1}{2}(d'^2 - 2Z_N d') = Z_N d' - \frac{d'^2}{2}$$

$$Z_N d' = \ln(\beta) + \frac{d'^2}{2} \Rightarrow$$

$$\Rightarrow \begin{aligned} Z_N &= \frac{\ln(\beta)}{d'} + \frac{d'}{2} \\ Z_s &= \frac{\ln(\beta)}{d'} - \frac{d'}{2} \end{aligned}$$

Appendix III: Development of optimal β s for human-robot systems without operational costs

In human-robot systems there are three β s: one β of the robot (β_r) and two β s of the human, the first β for the already detected object by the robot (β_{rh}) and the second for the undetected objects (β_h).

$$Z_S = x - \mu_S$$

$$Z_N = x - \mu_N$$

$$d' = \mu_S - \mu_N = x - Z_S - (x - Z_N) \Rightarrow d' = x - Z_S - x + Z_N \Rightarrow d' = Z_N - Z_S$$

$$\beta = \frac{f_S(Z_S)}{f_N(Z_N)} = \frac{\left(\frac{e^{-\frac{Z_S^2}{2}}}{\sqrt{2\pi}} \right)}{\left(\frac{e^{-\frac{Z_N^2}{2}}}{\sqrt{2\pi}} \right)} = e^{\left(\frac{-Z_S^2}{2} + \frac{Z_N^2}{2} \right)} = e^{-\frac{1}{2}(Z_S^2 - Z_N^2)} \Rightarrow \ln(\beta) = \ln\left(e^{-\frac{1}{2}(Z_S^2 - Z_N^2)} \right) \Rightarrow \ln(\beta) = -\frac{1}{2}(Z_S^2 - Z_N^2)$$

$$\beta^* = \frac{1 - P_S}{P_S} \cdot \frac{-V_{FA}}{V_H} \quad (\text{Swets et al., 2000})$$

$$\beta_{rh}^* = \frac{1 - P_{rh}}{P_{rh}} \cdot \frac{-V_{FA}}{V_H}$$

$$p_{rh} = \frac{p_S \cdot p_{Hr}}{p_S \cdot p_{Hr} + (1 - p_S) \cdot p_{FAr}}$$

$$\begin{aligned} \beta_{rh}^* &= \frac{1 - \left(\frac{p_S \cdot p_{Hr}}{p_S \cdot p_{Hr} + (1 - p_S) \cdot p_{FAr}} \right)}{\left(\frac{p_S \cdot p_{Hr}}{p_S \cdot p_{Hr} + (1 - p_S) \cdot p_{FAr}} \right)} \cdot \frac{-V_{FP}}{V_{TP}} = \frac{\cancel{p_S \cdot p_{Hr}} + (1 - p_S) \cdot p_{FAr} - \cancel{p_S \cdot p_{Hr}}}{p_S \cdot p_{Hr} + (1 - p_S) \cdot p_{FAr}} \cdot \frac{-V_{FP}}{V_{TP}} = \\ &= \frac{(1 - p_S) \cdot p_{FAr}}{p_S \cdot p_{Hr} + (1 - p_S) \cdot p_{FAr}} \cdot \frac{-V_{FP}}{V_{TP}} = \frac{(1 - p_S) \cdot p_{FAr}}{\cancel{p_S \cdot p_{Hr}} + (1 - p_S) \cdot p_{FAr}} \cdot \frac{\cancel{p_S \cdot p_{Hr}} + (1 - p_S) \cdot p_{FAr} - \cancel{p_S \cdot p_{Hr}}}{p_S \cdot p_{Hr}} \cdot \frac{-V_{FP}}{V_{TP}} = \\ &= \frac{(1 - p_S) \cdot p_{FAr}}{p_S \cdot p_{Hr}} \cdot \frac{-V_{FP}}{V_{TP}} = \left[\frac{1 - p_S}{p_S} \cdot \frac{-V_{FP}}{V_{TP}} \right] \cdot \frac{p_{FAr}}{p_{Hr}} = \beta^* \cdot \frac{p_{FAr}}{p_{Hr}} \\ &\Rightarrow \beta_{rh}^* = \beta^* \cdot \frac{p_{FAr}}{p_{Hr}} \end{aligned}$$

$$\beta_h^* = \frac{1 - P_h}{P_h} \cdot \frac{-V_{FA}}{V_H}$$

$$\begin{aligned}
p_h &= \frac{p_S \cdot (1 - p_{Hr})}{p_S \cdot (1 - p_{Hr}) + (1 - p_S) \cdot (1 - p_{FAr})} \\
\beta_h^* &= \frac{1 - \frac{p_S \cdot (1 - p_{Hr})}{p_S \cdot (1 - p_{Hr}) + (1 - p_S) \cdot (1 - p_{FAr})}}{\frac{p_S \cdot (1 - p_{Hr})}{p_S \cdot (1 - p_{Hr}) + (1 - p_S) \cdot (1 - p_{FAr})}} \cdot \frac{-V_{FP}}{V_{TP}} = \frac{\cancel{p_S \cdot (1 - p_{Hr})} + (1 - p_S) \cdot (1 - p_{FAr}) - \cancel{p_S \cdot (1 - p_{Hr})}}{p_S \cdot (1 - p_{Hr}) + (1 - p_S) \cdot (1 - p_{FAr})} \cdot \frac{-V_{FP}}{V_{TP}} = \\
&= \frac{\frac{(1 - p_S) \cdot (1 - p_{FAr})}{p_S \cdot (1 - p_{Hr}) + (1 - p_S) \cdot (1 - p_{FAr})}}{\frac{p_S \cdot (1 - p_{Hr})}{p_S \cdot (1 - p_{Hr}) + (1 - p_S) \cdot (1 - p_{FAr})}} \cdot \frac{-V_{FP}}{V_{TP}} = \\
&= \frac{(1 - p_S) \cdot (1 - p_{FAr})}{\cancel{p_S \cdot (1 - p_{Hr})} + (1 - p_S) \cdot (1 - p_{FAr})} \cdot \frac{\cancel{p_S \cdot (1 - p_{Hr})} + (1 - p_S) \cdot (1 - p_{FAr})}{p_S \cdot (1 - p_{Hr})} \cdot \frac{-V_{FP}}{V_{TP}} = \frac{(1 - p_S) \cdot (1 - p_{FAr})}{p_S \cdot (1 - p_{Hr})} \cdot \frac{-V_{FP}}{V_{TP}} = \\
&= \frac{1 - p_S}{p_S} \cdot \frac{-V_{FP}}{V_{TP}} \cdot \frac{(1 - p_{FAr})}{(1 - p_{Hr})} = \beta^* \cdot \frac{(1 - p_{FAr})}{(1 - p_{Hr})} \Rightarrow \\
\Rightarrow \quad \beta_h^* &= \beta^* \cdot \frac{(1 - p_{FAr})}{(1 - p_{Hr})}
\end{aligned}$$

The human optimal β_s for human robot systems are functions of the optimal β of a single detector system (which depends on the payoff values) and the hit and false alarm probabilities of the robot in a human-robot system case. The hit and false alarm probabilities of the robot are determined by the β and d' of the robot itself (expressed in Z of the robot).

Appendix IV: Human optimal hit and false alarm in human-robot systems

Description of the optimal hit and false alarm probabilities of the human according to Z_{Sr} of the robot.

$$Z_{S_{rh}}^* = \frac{\ln(\beta_{rh}^*)}{d'_h} - \frac{d'_h}{2} = \frac{\ln\left(\beta^* \cdot \frac{p_{FA_r}}{p_{H_r}}\right)}{d'_h} - \frac{d'_h}{2} = \frac{\ln(\beta^*)}{d'_h} + \frac{\ln(p_{FA_r})}{d'_h} - \frac{\ln(p_{FA_r})}{d'_h} - \frac{d'_h}{2}$$

$$\text{definition : } C_1 = \frac{\ln(\beta^*)}{d'_h} - \frac{d'_h}{2}$$

$$\Rightarrow Z_{S_{rh}}^* = \frac{\ln\left(\frac{p_{FA_r}}{p_{H_r}}\right)}{d'_h} + C_1$$

$$Z_{N_{rh}}^* = \frac{\ln(\beta_{rh}^*)}{d'_h} + \frac{d'_h}{2} = \frac{\ln\left(\beta^* \cdot \frac{p_{FA_r}}{p_{H_r}}\right)}{d'_h} + \frac{d'_h}{2} = \frac{\ln(\beta^*)}{d'_h} + \frac{\ln\left(\frac{p_{FA_r}}{p_{H_r}}\right)}{d'_h} + \frac{d'_h}{2}$$

$$\text{definition : } C_2 = \frac{\ln(\beta^*)}{d'_h} + \frac{d'_h}{2}$$

$$\Rightarrow Z_{N_{rh}}^* = \frac{\ln\left(\frac{p_{FA_r}}{p_{H_r}}\right)}{d'_h} + C_2$$

$$Z_{S_h}^* = \frac{\ln(\beta_h^*)}{d'_h} - \frac{d'_h}{2} = \frac{\ln\left(\beta^* \cdot \frac{1-p_{FA_r}}{1-p_{H_r}}\right)}{d'_h} - \frac{d'_h}{2} = \frac{\ln(\beta^*)}{d'_h} + \frac{\ln(1-p_{FA_r})}{d'_h} - \frac{\ln(1-p_{FA_r})}{d'_h} - \frac{d'_h}{2}$$

$$Z_{S_h}^* = \frac{\ln\left(\frac{1-p_{FA_r}}{1-p_{H_r}}\right)}{d'_h} + C_1$$

$$Z_{N_h}^* = \frac{\ln(\beta_h^*)}{d'_h} + \frac{d'_h}{2} = \frac{\ln\left(\beta^* \cdot \frac{1-p_{FA_r}}{1-p_{H_r}}\right)}{d'_h} + \frac{d'_h}{2} = \frac{\ln(\beta^*)}{d'_h} + \frac{\ln\left(\frac{1-p_{FA_r}}{1-p_{H_r}}\right)}{d'_h} + \frac{d'_h}{2}$$

$$\Rightarrow Z_{N_h}^* = \frac{\ln\left(\frac{1-p_{FA_r}}{1-p_{H_r}}\right)}{d'_h} + C_2$$

$$p_{H_r} = 1 - \frac{1}{\sqrt{2\pi}} \int_{-\infty}^{Z_{S_r}} e^{-\frac{Z^2}{2}} dZ$$

$$p_{FA_r} = 1 - \frac{1}{\sqrt{2\pi}} \int_{-\infty}^{Z_N} e^{-\frac{Z^2}{2}} dZ = 1 - \frac{1}{\sqrt{2\pi}} \int_{-\infty}^{Z_S + d'_r} e^{-\frac{Z^2}{2}} dZ$$

$$p_{H_{th}} = 1 - \frac{1}{\sqrt{2\pi}} \int_{-\infty}^{Z_{S_{th}}^*} e^{-\frac{Z^2}{2}} dZ = 1 - \frac{1}{\sqrt{2\pi}} \int_{-\infty}^{\frac{\ln\left(\frac{p_{FA_r}}{p_{H_r}}\right)}{d'_h} + C_1} e^{-\frac{Z^2}{2}} dZ$$

$$p_{FA_{th}} = 1 - \frac{1}{\sqrt{2\pi}} \int_{-\infty}^{Z_{N_{th}}^*} e^{-\frac{Z^2}{2}} dZ = 1 - \frac{1}{\sqrt{2\pi}} \int_{-\infty}^{\frac{\ln\left(\frac{p_{FA_r}}{p_{H_r}}\right)}{d'_h} + C_2} e^{-\frac{Z^2}{2}} dZ$$

$$p_{H_h} = 1 - \frac{1}{\sqrt{2\pi}} \int_{-\infty}^{Z_{S_h}^*} e^{-\frac{Z^2}{2}} dZ = 1 - \frac{1}{\sqrt{2\pi}} \int_{-\infty}^{\frac{\ln\left(\frac{1-p_{FA_r}}{1-p_{H_r}}\right)}{d'_h} + C_1} e^{-\frac{Z^2}{2}} dZ$$

$$p_{FA_h} = 1 - \frac{1}{\sqrt{2\pi}} \int_{-\infty}^{Z_{N_h}^*} e^{-\frac{Z^2}{2}} dZ = 1 - \frac{1}{\sqrt{2\pi}} \int_{-\infty}^{\frac{\ln\left(\frac{1-p_{FA_r}}{1-p_{H_r}}\right)}{d'_h} + C_2} e^{-\frac{Z^2}{2}} dZ$$

Appendix V: PAPER: Human-robot collaboration for improved target recognition of agricultural robots

By

Avital Bechar and Yael Edan

ABSTRACT

Automatic target recognition in agricultural harvesting robots is characterized by low detection rates and high false alarm rates due to the unstructured nature of both the environment and the objects. To improve detection human-robot collaboration levels were defined and implemented. The collaboration level is defined as the level of system autonomy or the level at which the human operator (HO) interacts with the system. Experimental results on images taken in the field indicate that collaboration of HO and robot increases detection and reduces the time required for detection.

1. INTRODUCTION

The advent of agricultural robots is the potential of raising the quality of the fresh produce, lowering production costs and reducing the drudgery of manual labor (Edan, 1999). Despite the tremendous amount of robotic applications in industry, very few robots are operational in agriculture production.

Robots perform well in industrial environments where working conditions are somehow constant, structured and predictable. Unstructured environments such as agriculture are characterized by rapid changes in time and space. The terrain, soil, vegetation landscape, visibility, illumination and other atmospheric conditions vary in rates of seconds to months in time and by meters in space. Developing a robot for the agricultural environment is a difficult task because of the unpredictable location of targets that are difficult to locate (due to the natural variability in size, shape, color and texture) and since the terrain, the landscape, the atmospheric conditions and other environment parameters are unstructured, uneven and continuously change.

Although technological feasibility of many agricultural robots has been proven, commercial application of robots in complex agriculture applications is still unavailable. The main limiting factors are production inefficiencies and lack of economic justification (Edan, 1999). Production inefficiency is caused by problems in fruit identification (75-85%), low cycle times of 3-4 seconds per fruit and the inability to autonomously deal with obstacles. To overcome the complex agricultural environment, the robotic system must be complex and robust resulting in a costly system.

The main problem in fruit recognition is due to shading, occlusion and variations in the fruit properties and changing illuminations properties. Several technologies for fruit detection have been explored, including vision (Sevila & Baylou, 1991), infra-red (Dobrusin *et al.*, 1992), and structured light (Benady *et al.*, 1992; Yamashita and Kondo, 1992), but with each of these techniques only 85% of the fruits were identified (Edan, 1999). Introducing a Human-Operator (HO) into the system can help improve its performance and simplify the robotic system (Kirlik *et al.*, 1993; Ceres *et al.*, 1998; Khadraoui *et al.*, 1998; Sidenbladh *et al.*, 1999; Itoh *et al.*, 2000).

The objective of the research was to define and implement human-robot collaboration levels for target recognition in agricultural environments. The collaboration level is defined as the level of system autonomy or the level at which the human operator (HO) interacts with the system. To evaluate the proposed collaboration levels an experiment was performed on images taken by a robotic melon harvester.

2. HUMAN-ROBOT COLLABORATION LEVELS

Four basic levels for HO-Robot collaboration were defined, implemented, tested and evaluated. The collaboration levels were defined corresponding to the four major degrees of autonomy in multi-target recognition tasks developed by Sheridan's (1978) scale of "action selection and automation of decision": i) **HO**: The HO detects and marks the desired target solely, compatible to level 1 in Sheridan's scale; ii) **HO-Rr**: The HO marks targets, aided by recommendations from an automatic detection algorithm, *i.e.*, the targets are automatically marked by a robot detection algorithm, the HO acknowledges the robot true detections, ignores the false detections and marks the targets missed by the robot, this level is compatible to levels 3-4 in Sheridan's scale; iii) **HO-R**: targets are identified automatically by the robot detection algorithm; the HO assignment is to cancel the false detections and mark the targets missed by the robot system, compatible to levels 5-7 in Sheridan scale; and iv) **R**: the targets are marked automatically by the system, compatible to level 10 in Sheridan's scale.

3. METHODOLOGY

3.1 Experimental Design

The experimental setup consisted of a Pentium-III computer, Philips 15" touch screen and Matlab 5.2 software for image processing, simulation of the HO-Robot system and data acquisition. The experiment consisted of three sets corresponding to the different HO-Robot collaboration levels, HO, HO-Rr and HO-R. Eleven engineers (males and females) aged 26-33 participated in the experiment. Each subject, in each set was explained and trained on three images before tested. Each set was initiated by five additional randomly selected images. The training images and these five images were not considered in the data analysis. For each set, the sequence of images was determined randomly and displayed for all the subjects in the same random order. The sequence of the sets was determined randomly for each subject.

3.2 Experimental Setup

Real images were taken in the field from a video camera mounted on a robotic melon harvester (Edan et al., 1996) moving along a melon row. Singulated melon images on the screen as seen from a camera mounted vertically on the vehicle, facing the ground in the middle of the row were manually selected. The following criteria were defined for target selection: i) melon color is yellow to orange in the majority of the visible area; and, ii) no visual damage is observed on the melon. Ninety images were manually classified by a panel of two into three complexity levels and saved into a database. Complexity was defined based on the visibility, contrast, and number of objects in each image. The panel also determined the total number of melons in each image and this served as the reference for the actual number of melons. For each complexity level the images were randomly divided into the three sets, resulting in thirty images for each set with ten images for each complexity level. The number of melons in each set was approximately 50. The automatic detection algorithm for melon detection (corresponding to the R collaboration level) was based on an algorithm developed by Bechar *et al.* (2000).

Images (Fig. 1) were displayed on the screen in a random order. In the first three sets (the HO strategies) the images were displayed on the screen and the HO detected and marked melons suitable for harvest. The HO marked the melons and scrolled to the next image using a touch screen by pressing the melon location or buttons on the screen. In the R strategy, all 90 images were analyzed by the image processing algorithm solely.



Figure A-46: Screen display in the HO-Rr experiment as viewed by the HO (original image in color). 1 - signed with Rr, 2 – signed with HO cross.

3.3 Performance Measurements

The following parameters were automatically measured and acquired during the experiment: the number of true melons in each image, the number of melons detected / the number of false detections by the HO and the robot, the time and coordinates of each HO operation and the type of operation (*e.g.*, marking melons, unmarking melons, next image).

The performance measures calculated for each collaboration level included the number of true and false detections of the HO and the robot, and time per image.

Comparison between the collaboration levels was calculated separately for each performance measure using the statistical t-test for a significance of $\alpha=0.1$.

4. RESULTS AND DISCUSSION

The average time per set for the HO and the HO-Rr strategies was 179 and 180 seconds respectively (Fig. 2) with no significant statistical difference.

The average time for the HO-R strategy was 20% shorter with significant statistical difference ($\alpha=0.1$).

The automatic detection algorithm (R) yielded 80% true detections (Fig. 3) with 8% false detections of the total number of melons (Fig. 4). Highest detection was achieved for the HO-Rr strategy (94.1% with S.D of 4%). The HO collaboration level resulted in the lowest detection percentage ($90.6 \pm 3.9\%$). Collaboration between HO and robot significantly increases detection percentages of the HO by almost 4% (HO-R), ($\alpha=0.1$).

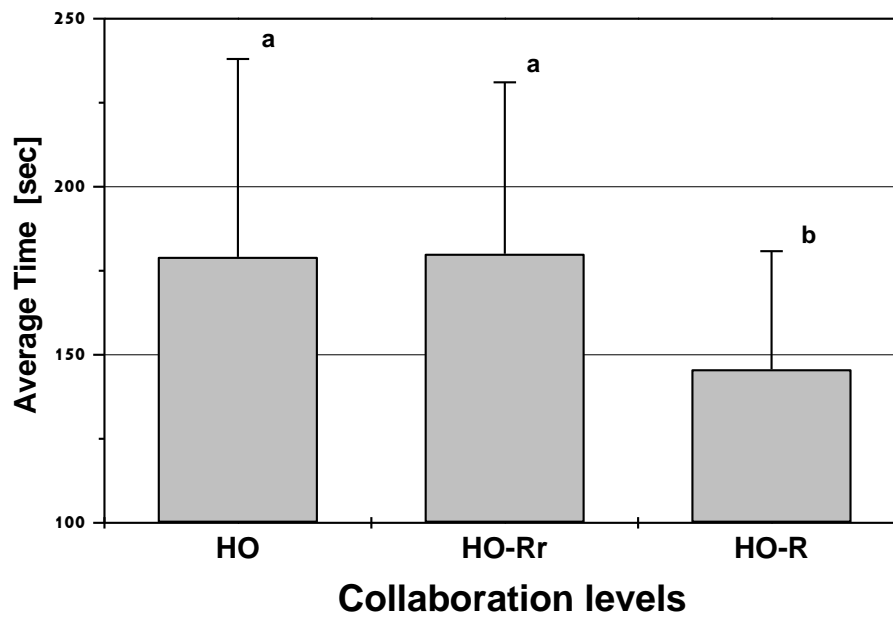


Figure A-47: Average time per set for the three HO collaboration levels (30 images with a total number of 50 melons). The different letters represent different populations according to 90% significance of difference.

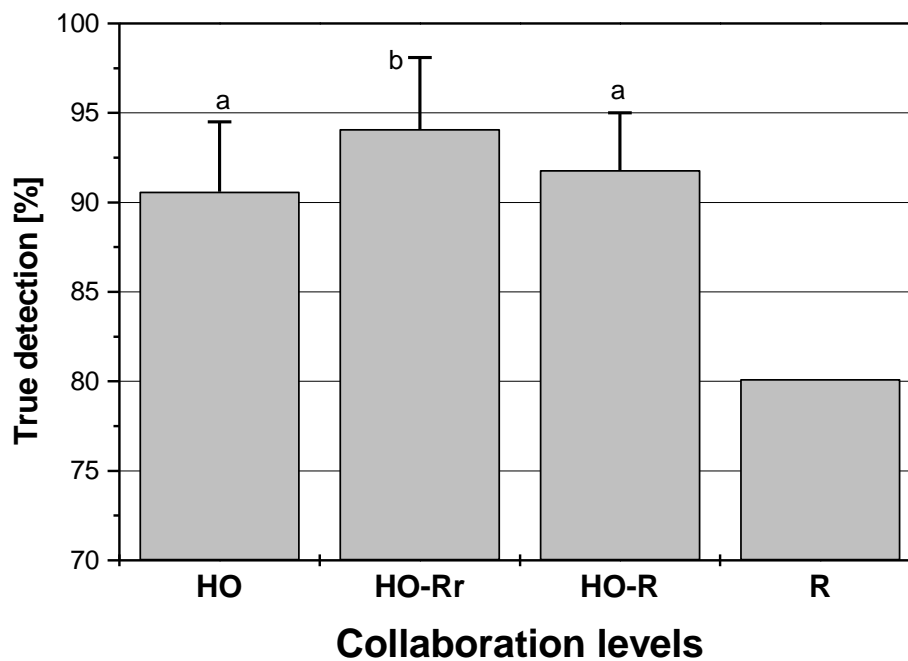


Figure A-48: True and false detection percentages. The error bars represent the standard deviation. The different letters represent different populations according to 90% significance of difference.

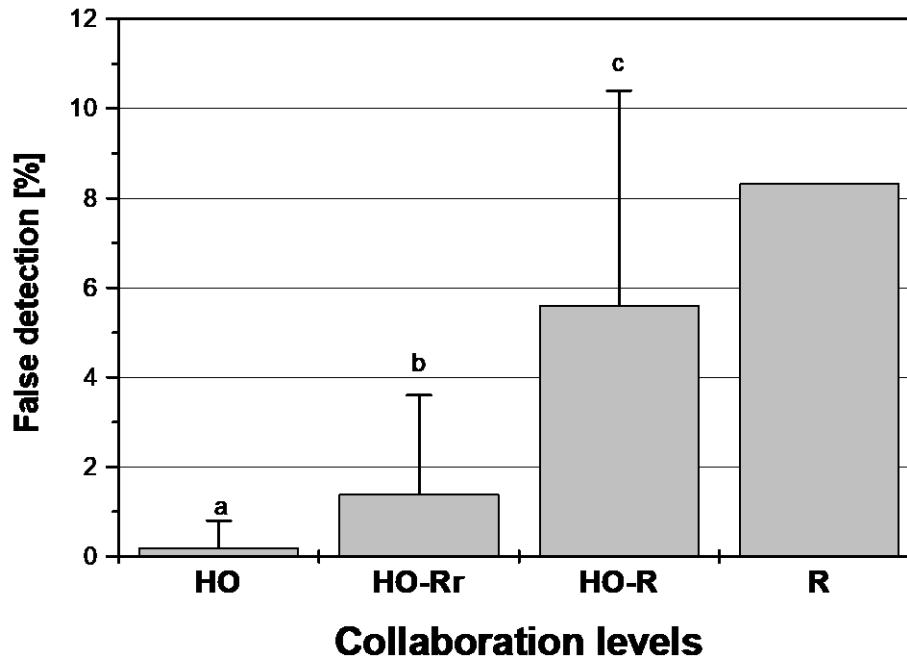


Figure A-49: True and false detection percentages. The error bars represent the standard deviation. The different letters represent different populations according to 90% significance of difference.

Best detection results for the easy and medium complexity levels were achieved by the HO-Rr strategy (Fig. 5: 100% and 97.5% respectively). Best detection results for the difficult complexity level were achieved in the HO-R strategy (87.5%). Detection percentage reduces as the complexity of the image increases. However, this decrease is much more rapid in the HO collaboration level (from 95.7% in the easy level to 80.7% in the difficult level). When the HO assists with the robot, detection percentage is improved by 4.5% - 7% as compare to the HO alone and by 8% - 20% as compared to the robot alone.

5. CONCLUSIONS AND SUMMARY

Four different human-robot collaboration levels were proposed and developed for a target recognition task. Collaboration of HO and robot increases detection by 4% when compared to a human operator alone (HO) and by 14% when compared to a fully autonomous system. This results in high detection rates (average of 94% and up to 100%) and can help overcome the limitations of full autonomous systems, in which detection success is relatively lower (75-85% on average).

In addition, when compared to the HO alone, detection times of integrated systems are reduced by 20%. Typical robotic harvesting rates are assumed to be 2s/fruit. Although this is better than manual picking rates (assumed to be around 10s/fruit) economic analysis indicates that even if the cost of manual labor increases by 50% the development cost will just break even (Edan, 1999). However, by harvesting with a robot the quality of the fruit harvested is improved as compared to manual picking (Edan, 1999). In addition, if due to technological developments the picking and production efficiencies increase, agricultural robots might be the harvesting machines of the future. Integration of a human operator that works together with the robot harvester is one way to achieve this in parallel to decreasing system complexity thereby further enhancing economic feasibility.

The best collaboration method depends on image complexity and the human operator performance. Future underway research is aimed at developing an algorithm to automatically select the best collaboration level (Bechar, 2002) since environmental conditions, visibility parameters and human performance continuously change. However, the adjustment required from the human operator to switch to a new collaboration level must also be considered. The exact switching time (to be determined automatically by the algorithm) must therefore aim to provide optimal performance of the whole system including transitions.

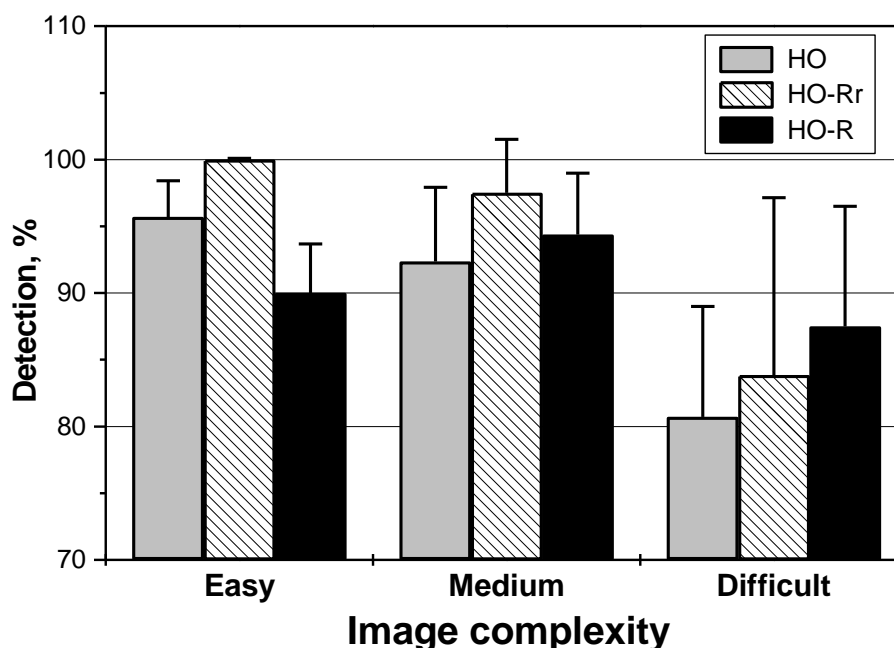


Figure A-50: Melon detection percentages for different complexity levels. The error bars represent the standard deviation.

6. ACKNOWLEDGMENTS

This research was partially supported by the BGU Paul Ivanier Center for Robotics Research and Production Management.

7. REFERENCES

- Bechar, A., Edan, Y., Meyer, J., Rotman, M. and Friedman, L. (2000), "Human-machine collaboration for melons detection", ASAE Paper No. 003143, ASAE Annual International Meeting, Milwaukee, Wisconsin.
- Bechar, A. (2002), "PhD. Proposal", Department of Industrial Engineering and Management, Ben-Gurion University of the Negev, Beer-Sheva, Israel 84105.
- Benady, M. and Miles, G.E. (1992), "locating melons for robotic harvesting using structured light", ASAE paper no. 92-7021, ASAE, St. Joseph, MI.
- Ceres, R., Pons, J. R., Jimenez, A.R., Martin, J.M. and Calderon, L. (1998), "Design and Implementation of an Aided Fruit-Harvesting Robot (Agribot)", *Industrial Robot*, 25(5), pp. 337-346.
- Dobrusin, Y., Edan, Y., Grinspan, J., Peiper, U.M. and Hetzroni, A. (1992), "Real-time image processing for robotic melon harvesting", ASAE Paper No. 92-3515, ASAE St. Joseph, MI, 49085.

Edan, Y., Miles, G.E., Flash, T. I., Wolf, J., Grinspun, Y. and Peiper, U.M. (1996). "The robotic melon harvester", *Service Robot* 2(1): 10-15.

Edan, Y. (1999), "Food and agricultural robots. In *The Handbook of Industrial Robotics*:", 1143-1155, Second Edition. Ed.: S.Y. Nof. John Wiley and Sons, New York, NY.

Itoh, T., Kosuge, K. and Fukuda, T. (2000), "Human-Machine cooperative telemanipulation with motion and force scaling using task-oriented virtual tool dynamics", *IEEE Transactions on Robotics and Automation*. 16(5), pp. 505-516.

Khadraoui, D., Debain, C., Rouveure, R., Martinet, P., Bonton, P. and Gallice, J. (1998), "Vision based control in driving assistance of Agricultural vehicles", *The Int. J. of Robotic Research*, 17(10), pp. 1040-1054.

Kirlik, A., Plamondon, B.D., Lytton, L., Jagacinski, R.J. and Miller, R.A. (1993), "Supervisory control in a dynamic and uncertain environment: laboratory task and crew performance", *IEEE Transactions on Systems, Man, and Cybernetics*, 23(4), pp. 1130-1138.

Sevila, F. and Baylou, P. (1991), "The principles of robotics in agriculture and Horticulture", *Progress in Agricultural Physics and Engineering*, C.A.B. International, Bedford, U.K.: 119-147.

Sidenbladh, H., Kragic, D. and Christensen, H.I. (1999), "A person following behavior for a mobile robot", *Proceedings of the 1999 IEEE International Conference on Robotics and Automation*, pp. 670-675.

Yamashita, J. and Kondo, N. (1992), "Agricultural robots (1): vision sensing systems", ASAE paper no. 92-3517, ASAE, St. Joseph, MI.

Appendix VI: Analysis of Non Optimal Cases

Analysis of the objective function, V_{Is} , was performed for i) the robot likelihood ratio, β_r , ii) the human likelihood ratio of targets the robot already detected, β_{rh} , and iii) human likelihood ratio of targets the robot did not detect, β_h . The analysis was performed on different target probability conditions, P_s , different human and robot sensitivities, d'_h and d'_r respectively and different payoff value ratio, V_{AR} .

10.1.1 Analysis of β_h and β_{rh}

The parameters in the analysis were determined to be: $N=1000$ objects; $V_H=50$; $V_{AR}=-1$ (and therefore $V_{FA}=-50$); $V_C=-2$ and $V_t=-2000 \text{ hr}^{-1}$. The human sensitivity was set to $d'_h=2$ and the robot sensitivity was set to $d'_r=2$. The target probability was set to $P_s=0.5$. The decision time for all human time parameters was determined to be $t_D=5 \text{ s/object}$ and the human motoric time was set to $t_M=2 \text{ s/(detected object)}$. The robot time was set to $t_r=0.01 \text{ s/object}$. The logarithm of the robot likelihood ratio, β_r , was set to -2 .

HO collaboration level

Figure A-51 shows the HO hit probability for different human sensitivities (d'_h) and human cutoff points (β_h). The results indicate that the probability for hit increase with increase in the human sensitivity and with decrease in the human likelihood ratio.

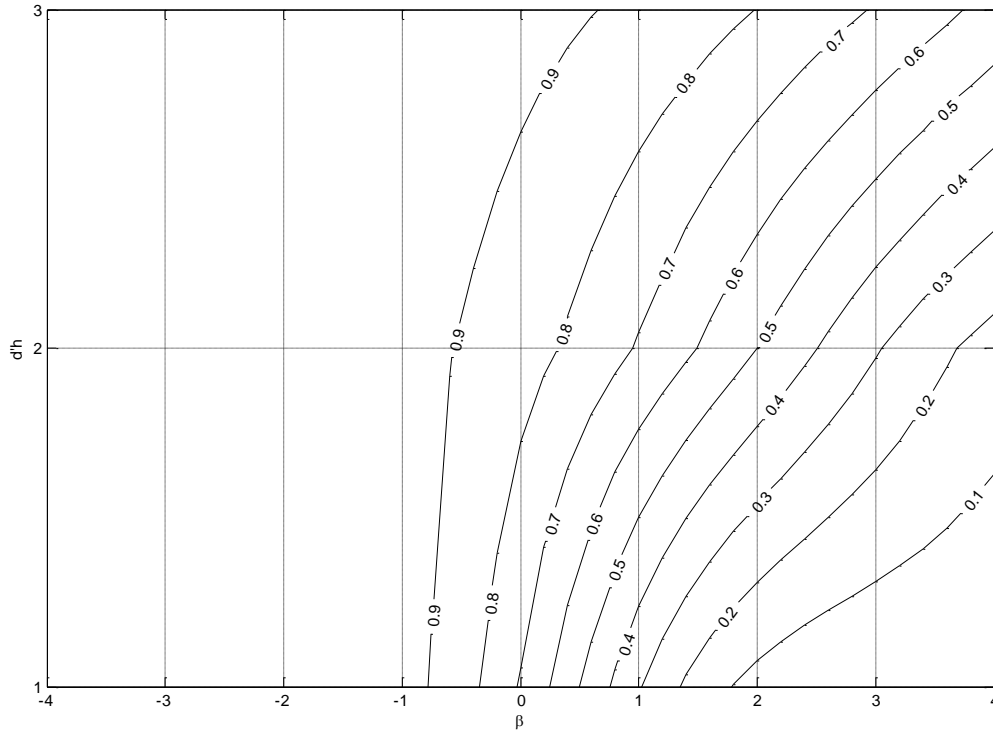


Figure A-51: Human hit probability.

The task time, t_s , of the HO collaboration level is increased with the decrease in the logarithm of the likelihood ratio, β_h . The task time is increased with the increase in the human sensitivity

when β_h is negative and increased with the decrease in the human sensitivity when β_h is positive. When β_h is equal to zero the human sensitivity has no influence on the task time (Figure A-52).

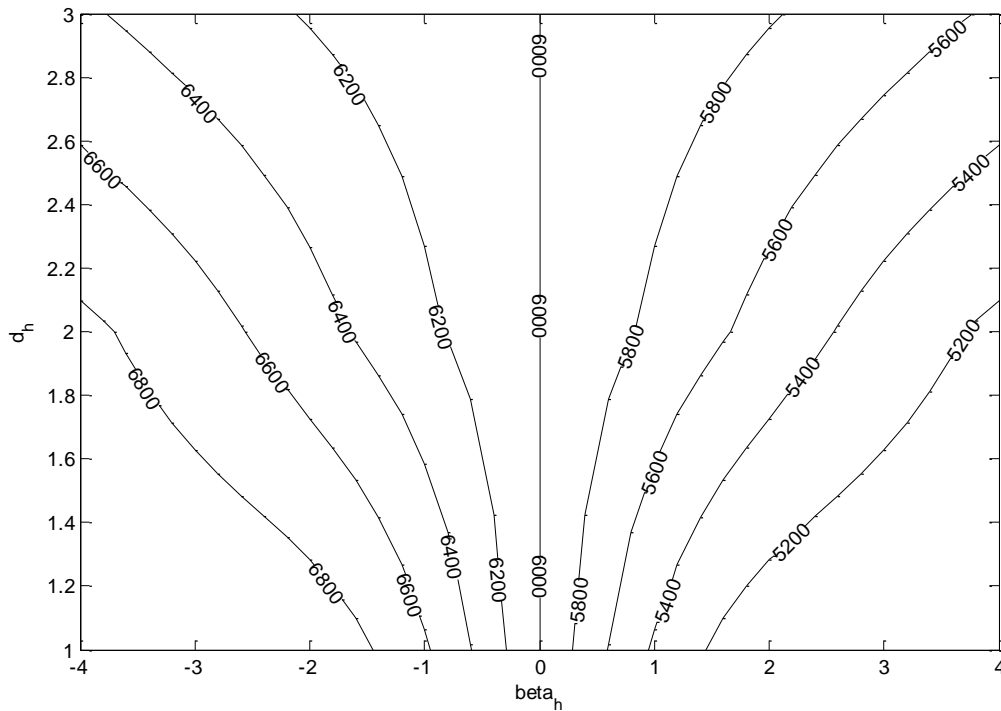


Figure A-52: HO task time.

Figure A-53 shows the Objective function for HO collaboration level versus the likelihood ratio, β_h , and the human sensitivity, d_h . For the entire range the system objective function score is increased with the increase in the human sensitivity. The maximum objective function score achieved for positive and small β_h values.

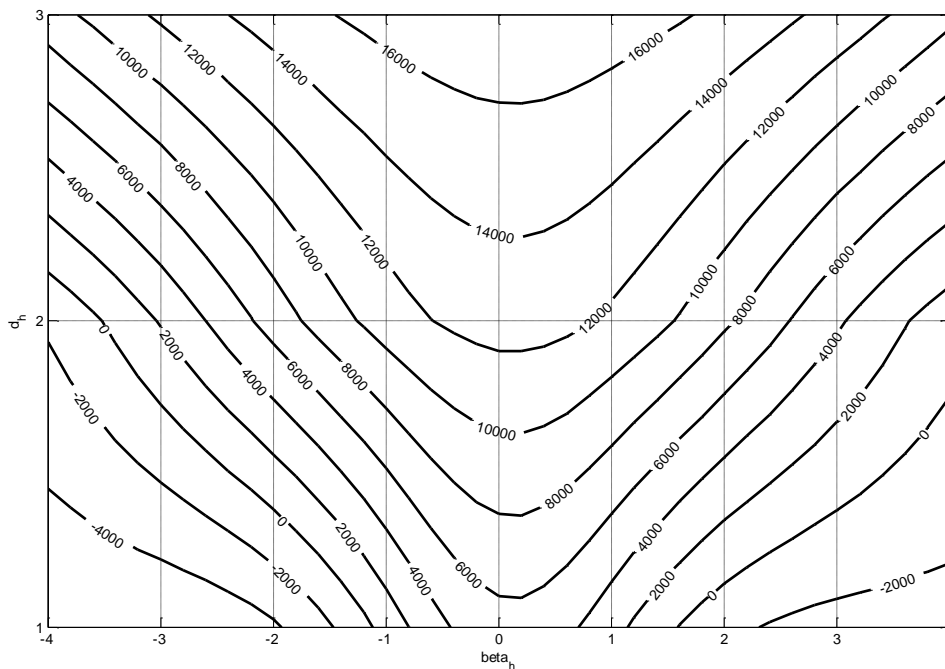


Figure A-53: Objective function for HO collaboration level.

The value of the robot likelihood ratio, β_r , have no influence of the system performance, the task time, the probability of hit and the objective function score in the HO collaboration level.

HO-Rr collaboration level

Figure A-54 shows the hit probability for different human likelihood ratio of targets the robot already detected, β_{rh} , and human likelihood ratio of targets the robot did not detect, β_h . The results indicate that the probability for hit increase with decrease of β_{rh} , nevertheless the value of β_h have only little influence on the probability of hit.

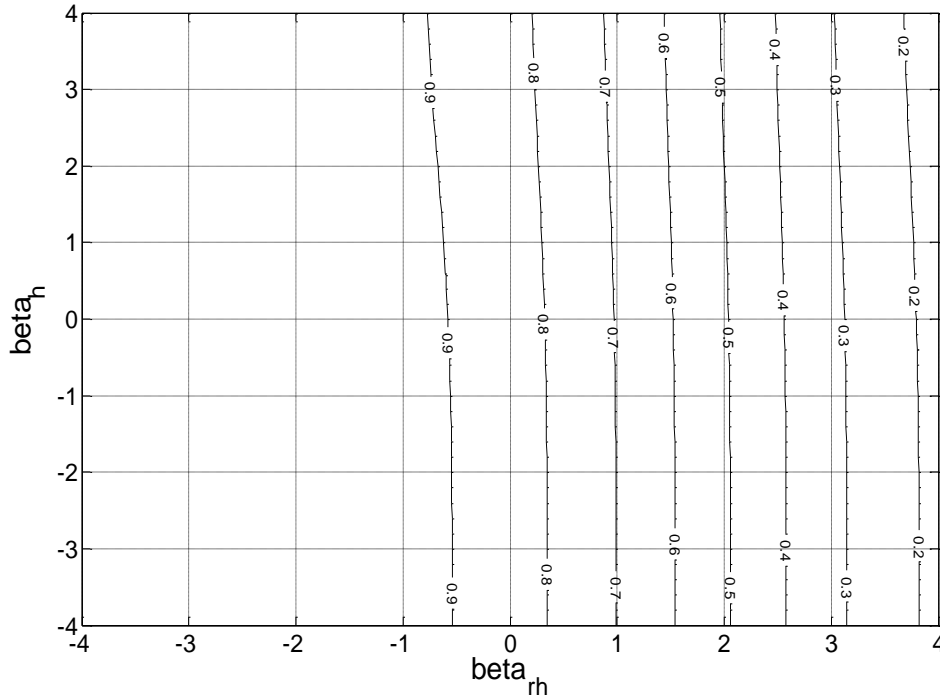


Figure A-54: Hit probability for HO-Rr collaboration level.

The task time, t_s , of the HO-Rr collaboration level is increased with the decrease in the likelihood ratio, β_h and β_{rh} . However, positive values of the logarithm of β_h have small effect on the task time (Figure A-55). This occurs since for high β_h values the influence of the human is reduced, the number of marked objects is reduced and therefore the time reduces. This phenomenon does not happen for the β_{rh} since this parameter is linked to the robot likelihood ratio, β_r , which in this case its logarithm is negative.

Figure A-56 shows the objective function score for different β_h , and β_{rh} values. The objective function score increases with the increase in the β_h values. Although, for positive values of the logarithm of β_h the effect on the objective function score is small. Analysis of the β_h parameter indicates that the maximum objective function score is achieved for positive small β_{rh} values. The global maximum of the system objective function for this case exists for the highest value of β_h and positive small β_{rh} values.

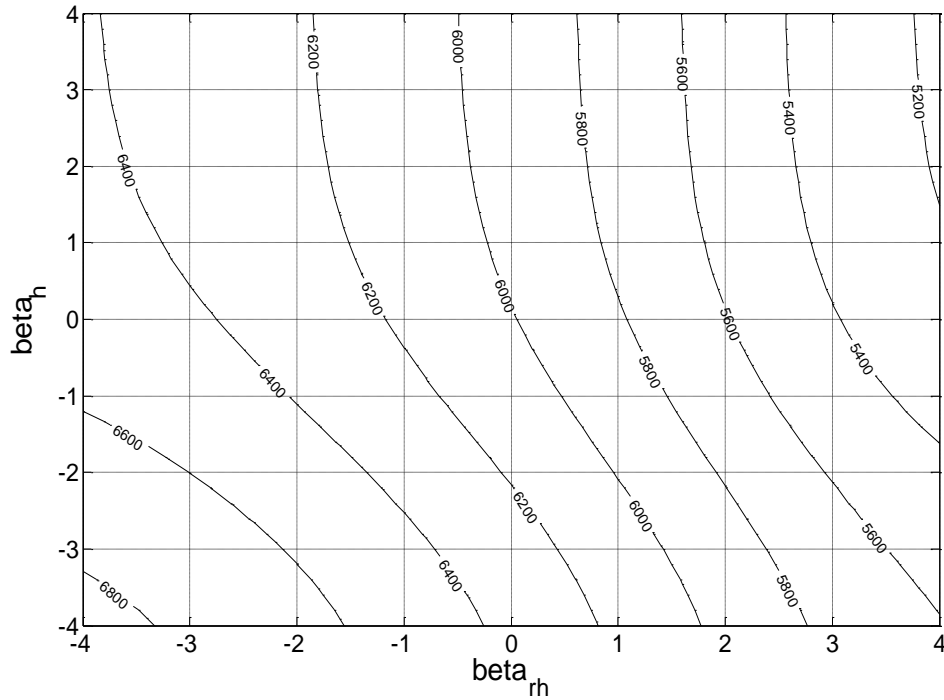


Figure A-55: HO-Rr task time.

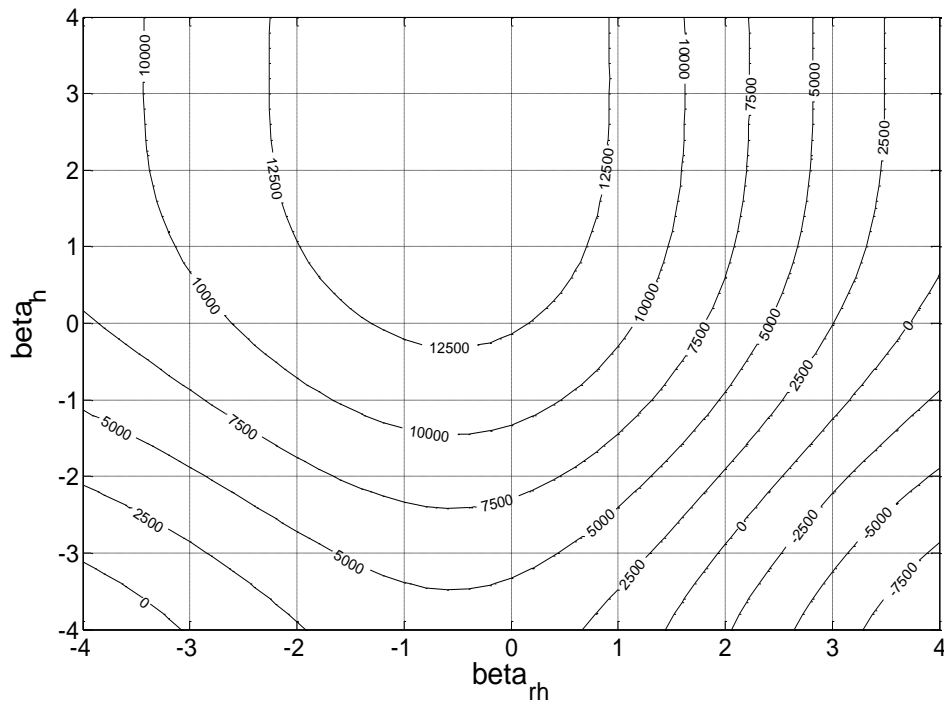


Figure A-56: Objective function for HO-Rr collaboration level.

HO-R collaboration level

The difference between the HO-Rr and the HO-R collaboration levels appear in the operational cost part, therefore the probability of hit will be identical to the HO-Rr collaboration level as shown in Figure A-54. The task time, t_s , of the HO-R collaboration level is increased with the decrease in the likelihood ratio, β_h and the increase in β_{rh} . However, positive values of the logarithm of β_h have little effect on the task time (Figure A-57). This

occurs since for high β_h values the influence of the human is reduced, the number of marked objects is reduced and therefore the task time reduces. This phenomenon does not happen for the β_{rh} since this parameter is linked to the robot likelihood ratio, β_r , which in this case its logarithm, is negative and its influence is significant. There is an opposite influence of the β_{rh} on the task time for the HO-Rr and HO-R collaboration levels due to the nature of the collaboration level. In the HO-Rr collaboration level the human marks each robot target he identifies as a target and therefore the task time increases with the increase in the β_{rh} . In the HO-R collaboration level the human marks each robot target he identifies as a false target and therefore the task time increases with the decrease in the β_{rh} .

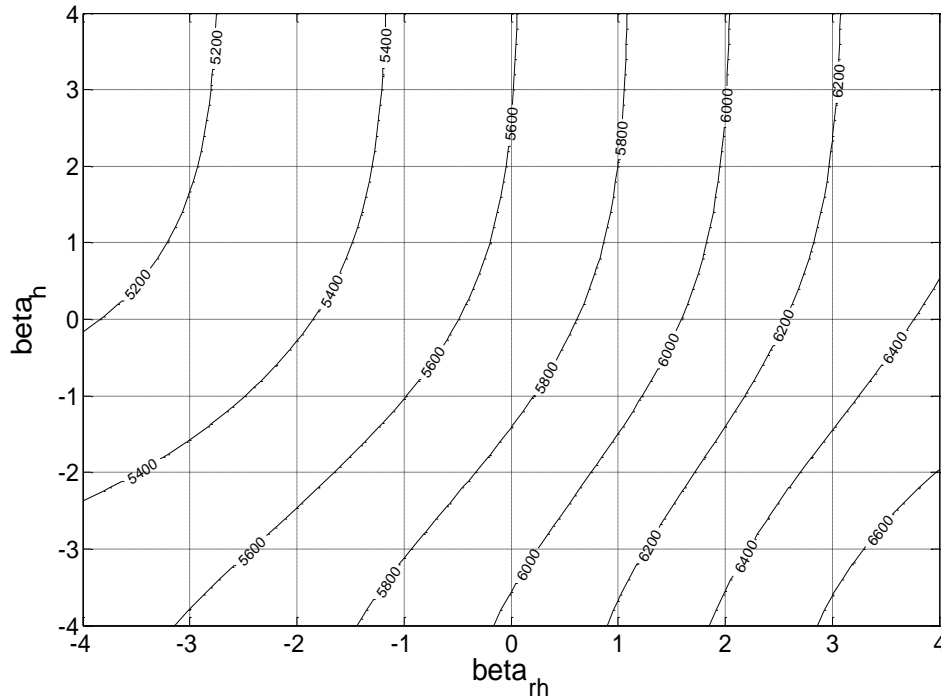


Figure A-57: HO-R task time.

Figure A-58 shows the objective function score for different β_h , and β_{rh} values. The objective function score increases with the increase in the β_h values. Although, for positive values of the logarithm of β_h the effect on the objective function score is small. Analysis of the β_h parameter indicates that the maximum objective function score achieved for positive small β_{rh} values. The global maximum of the system objective function for this case exists for the highest value of β_h and positive small β_{rh} values.

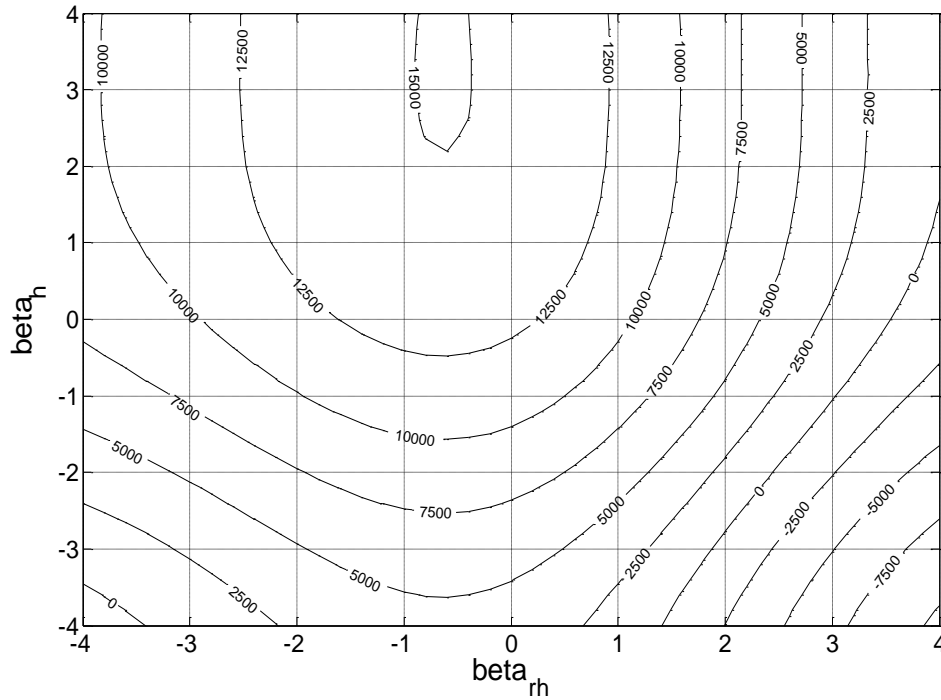


Figure A-58: Objective function for HO-R collaboration level.

Best Collaboration Level

Figure A-59 shows the objective function score of all four collaboration levels. Each surface represents different collaboration level. The surface created from the intersection of all four collaboration level surfaces represents the maximum objective function score for each β_h and β_{rh} combination (Figure A-59 and Figure A-60). The R collaboration level surface is normal to the z axis since this collaboration level is not influence by β_h or β_{rh} . The HO collaboration level is not influenced by β_{rh} and there for it surface changed only as a function of β_h .

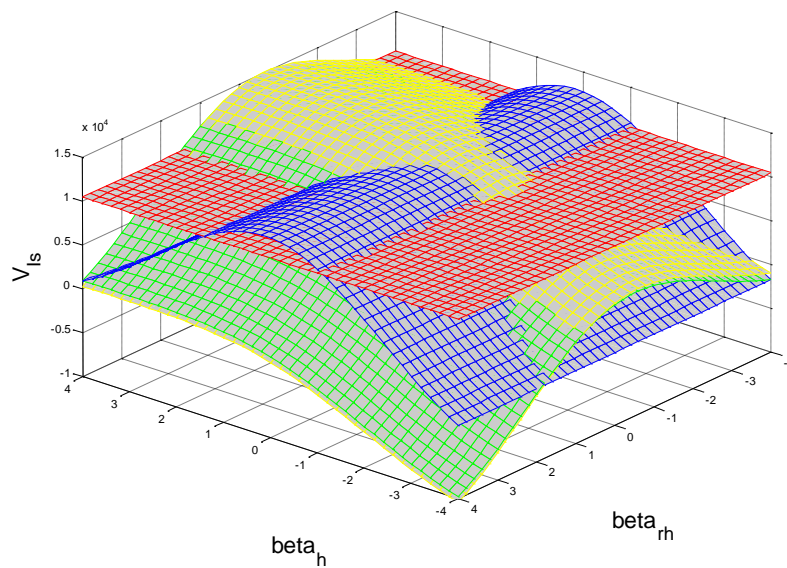


Figure A-59: the objective function for the four collaboration levels. HO – blue, HO-Rr – green, HO-R yellow and R – red.

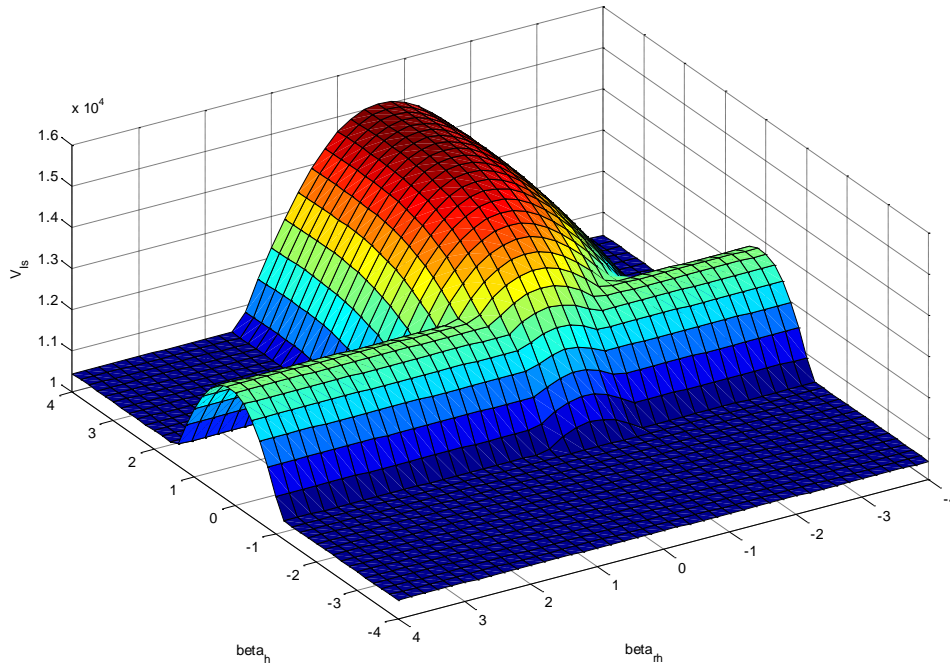


Figure A-60: Maximum objective function score.

The collaboration level which achieved the highest score in the system objective function, for each β_h and β_{rh} is the best collaboration value for those combinations. Figure A-61 shows a best collaboration level map for different β_h and β_{rh} . Each zone is dominated by a single collaboration level.

In the given case, each of the four collaboration levels achieves best results in different zone. There are coordinates which the best collaboration level changes from R to HO and vice versa without transferring through the intermediate HO-R or HO-Rr collaboration levels. This example shows us that there are cases that the best collaboration level could be solely manual or autonomous. Different task objectives and different system objective function properties will produce different best collaboration maps.

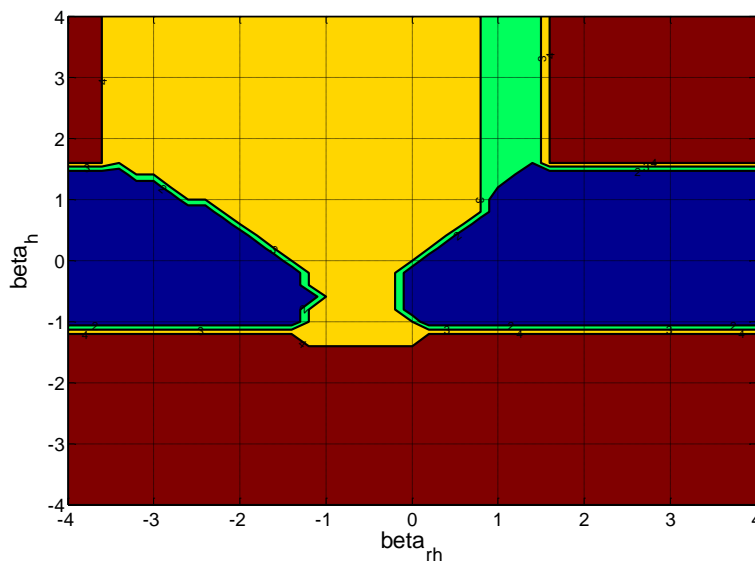


Figure A-61: Best collaboration level map for different β_h and β_{rh} values. HO – blue, HO-Rr – green, HO-R yellow and R – red.

Figure A-62 shows the maximum objective function score for different β_h , and β_{rh} values as a combination of all four collaboration levels. The highest score achieved in the HO-R collaboration level for high β_h and β_{rh} value of small negative.

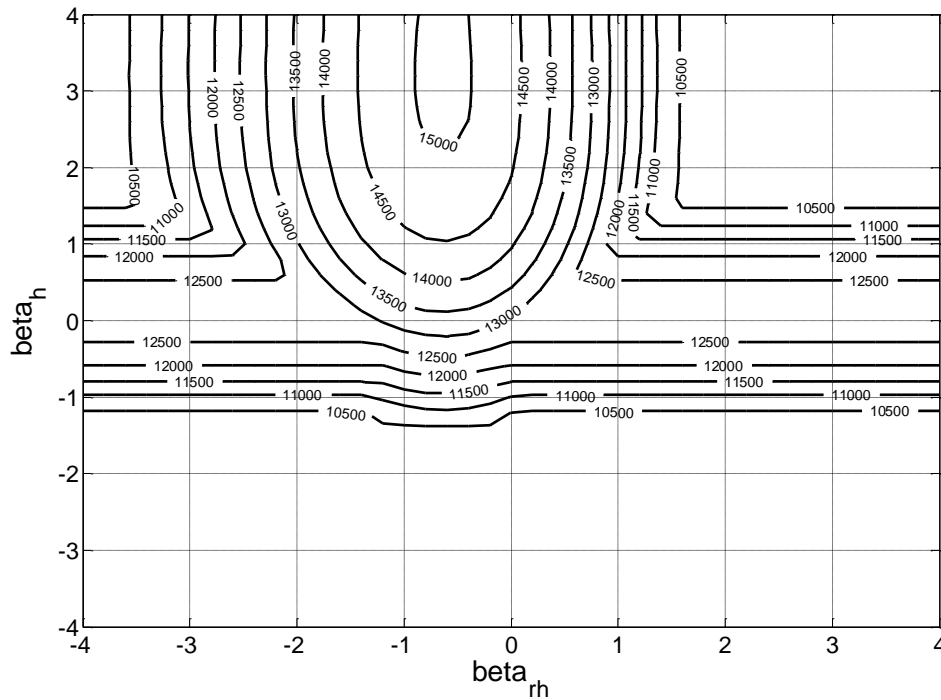


Figure A-62: System objective function score for best collaboration level.

10.1.2 Analysis of β_r

The parameters in the analysis were determined to be: $N=1000$ objects; $V_H=50$; $V_{AR}=-1$ (and therefore $V_{FA}=-50$); $V_C=-2$ and $V_t=-2000 \text{ hr}^{-1}$. The human sensitivity was set to $d'_h=2$ and the robot sensitivity was set to $d'_r=2$. The target probability was set to $P_s=0.5$. The decision time for all human time parameters was determined to be $t_D=5 \text{ s/object}$ and the human motorial time was set to $t_M=2 \text{ s/(detected object)}$. The robot time was set to $t_r=0.01 \text{ s/object}$.

R collaboration level

Figure A-63 shows the R objective function score for different robot sensitivities (d'_r) and robot cutoff points (β_r). The results indicate that the objective function score increase with increase in the robot sensitivity. The maximum score for each robot sensitivity appears for a very small positive value of the logarithm of β_r .

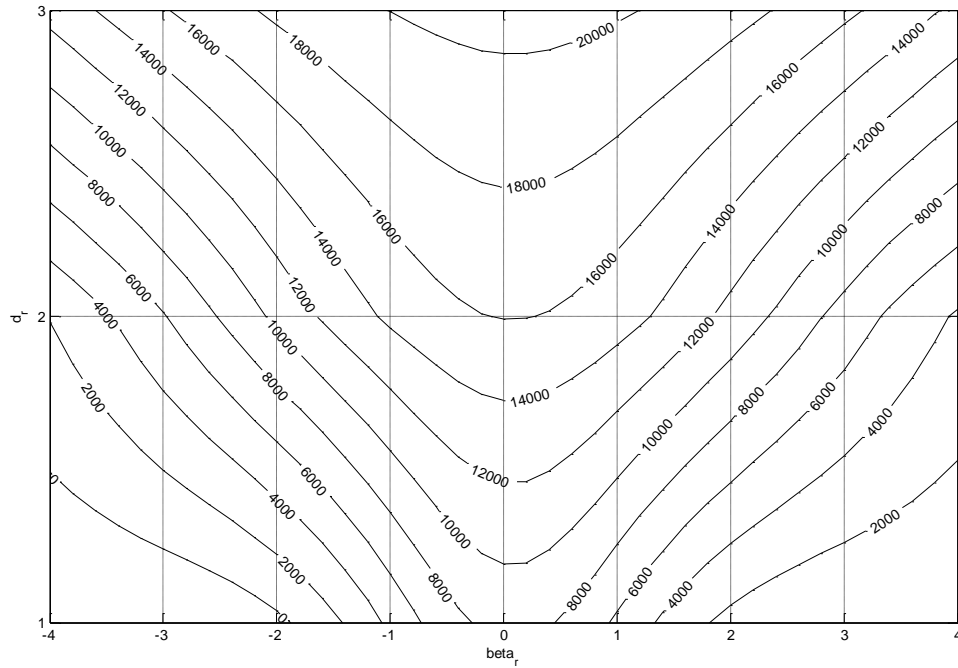


Figure A-63: Objective function for R collaboration level.

HO-Rr collaboration level

Figure A-64 shows the probability of hit in the HO-Rr collaboration level. For very small values of the logarithm of β_r there is no influence of the β_h on the hit probability which increase with the decrease in the value of the logarithm of β_{rh} . With the increase in the value of β_r the influence of β_h increase and the influence of β_{rh} decrease on the probability of hit. The increase in the value of the logarithm of β_r reduces the "weight" of the robot in the system and reduces the robot probability for hit and therefore the influence of β_{rh} on the probability on hit, which depends on β_r , reduced.

Figure A-65 shows the task time in the HO-Rr collaboration level. For very small values of the logarithm of β_r there is little influence of the β_h on the task time. The task time increases with the decrease in the value of the logarithm of β_{rh} . With the increase in the value of β_r the influence of β_h increase and the influence of β_{rh} decrease on the task time.

Figure A-66 shows the system objective function score in the HO-Rr collaboration level. For very small values of the logarithm of β_r , the objective function score increase with the increase in the value of β_h . The maximum objective function score achieved for negative small values of the logarithm of β_{rh} and the influence of β_h is more dominant than of β_{rh} . For high values of the logarithm of β_r , the objective function score increase with the decrease in the value of β_{rh} . The maximum objective function score achieved for positive small values of the logarithm of β_h and the influence of β_{rh} is more dominant than of β_r . the objective function score achieve its global maximum for value of the logarithm of β_r which is positive and close to zero.

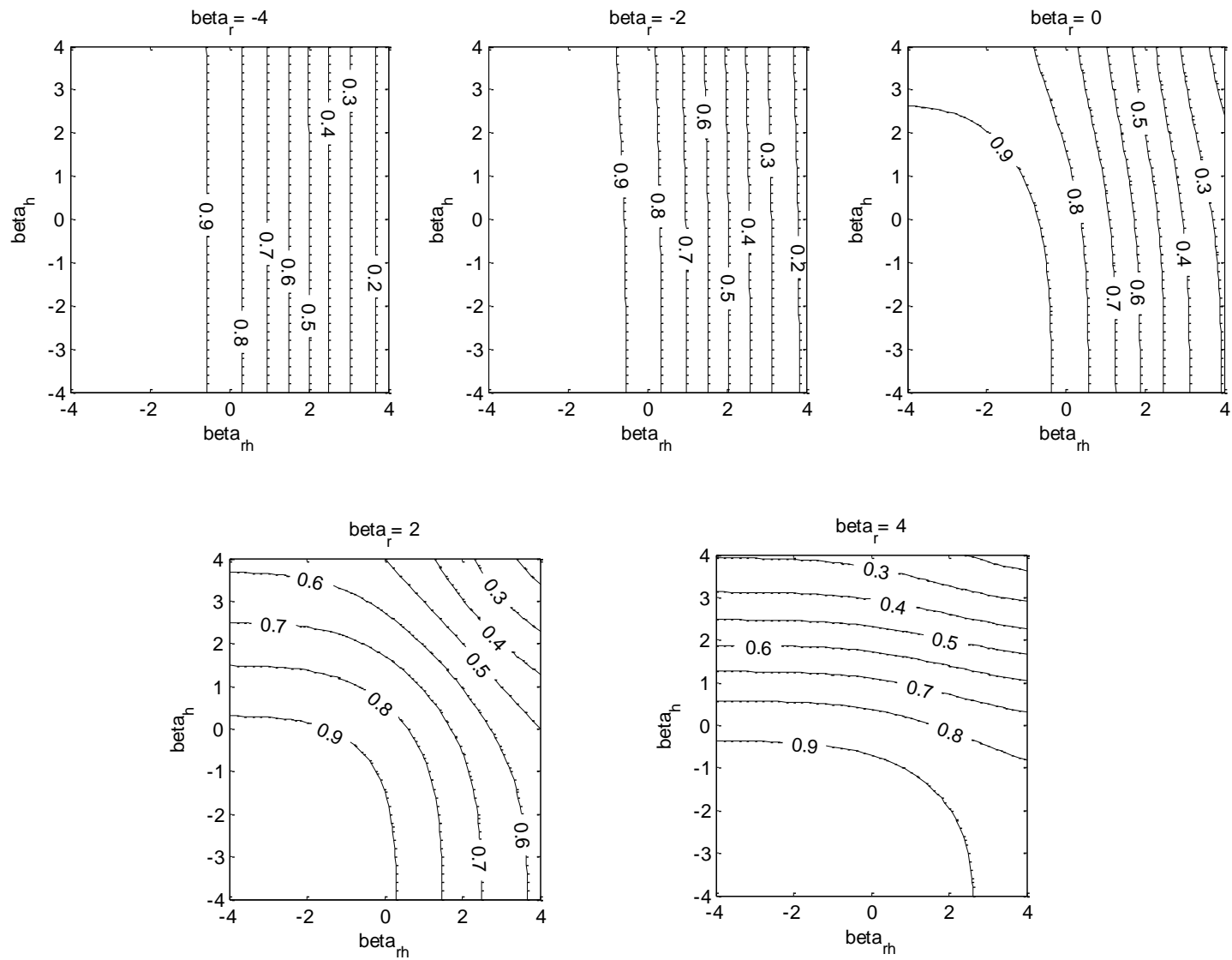


Figure A-64: Probability of hit for HO-Rr collaboration level.

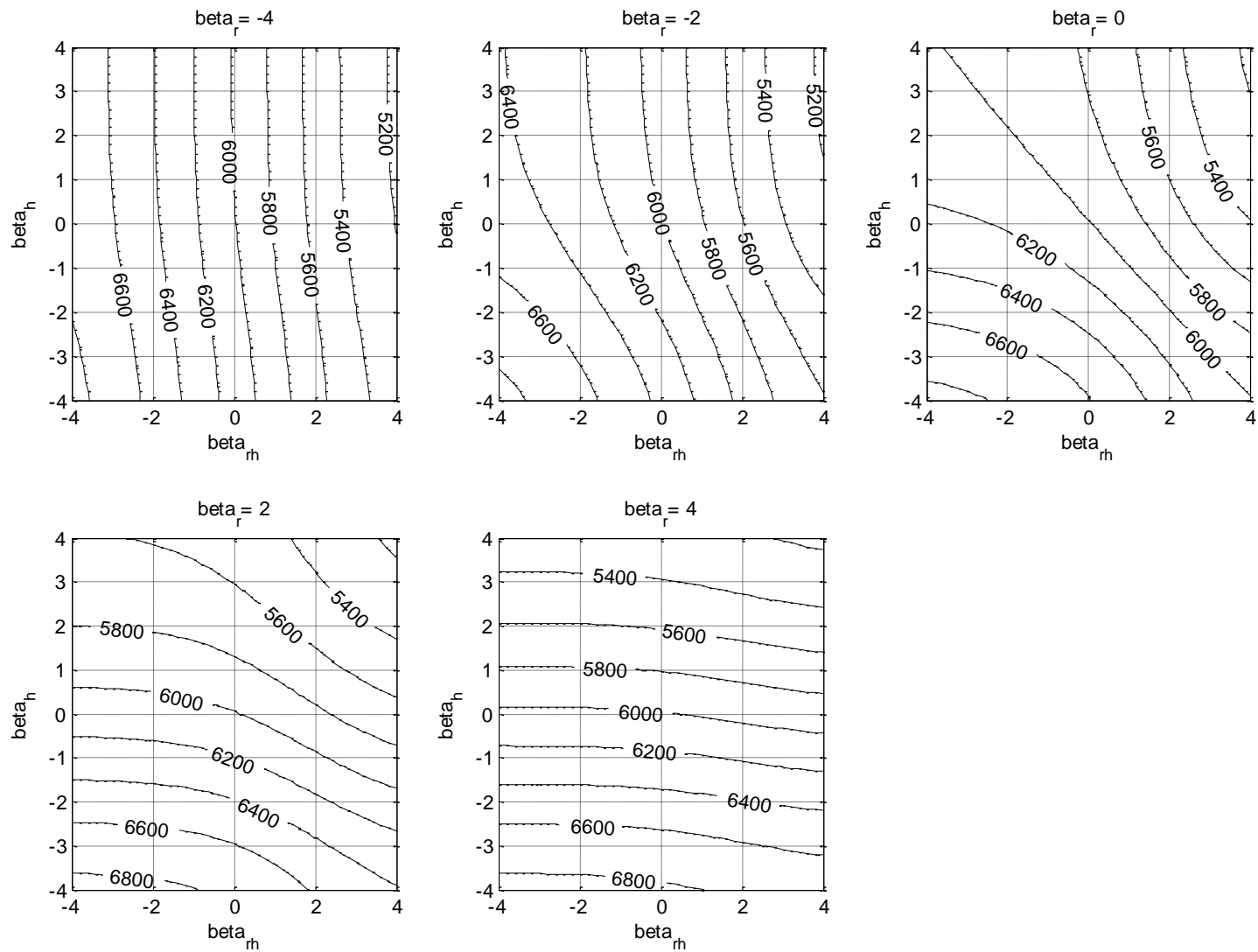


Figure A-65: HO-Rr task time.

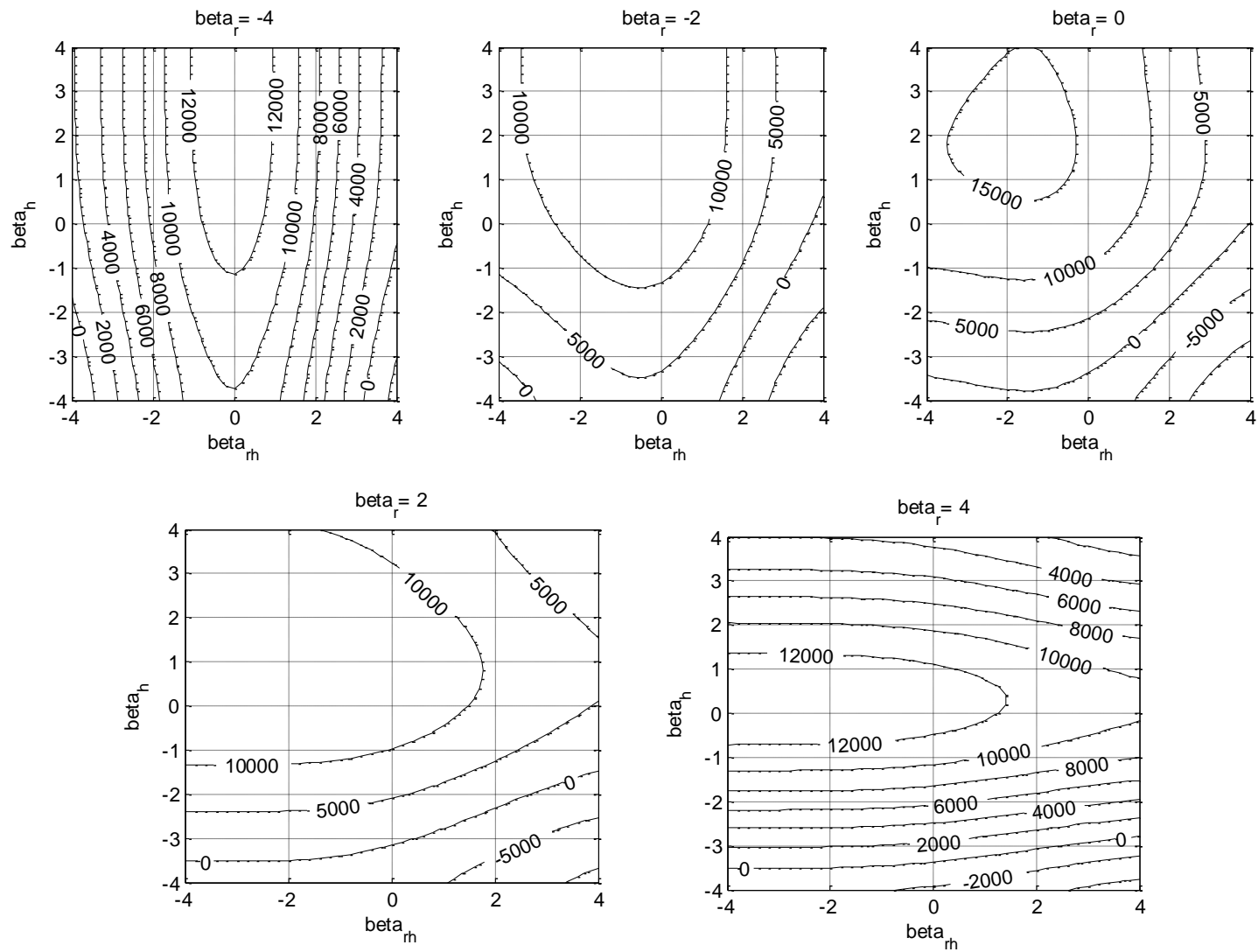


Figure A-66: Objective function for HO-Rr collaboration level.

HO-R collaboration level

Figure A-67 shows the task time in the HO-R collaboration level. For very small values of the logarithm of β_r there is little influence of the β_h on the task time. The task time increases with the increase in the value of the logarithm of β_{rh} . With the increase in the value of β_r the influence of β_h increase and the influence of β_{rh} decrease on the task time, and the task time increase with the decrease in the value of β_h . The increase in the value of the logarithm of β_r reduces the "weight" of the robot in the system and reduces the number of marked objects by the robot and therefore the influence of β_{rh} on the task time, which depends on β_r , reduced.

Figure A-68 shows the system objective function score in the HO-R collaboration level. For very small values of the logarithm of β_r , the objective function score increase with the increase in the value of β_h . The maximum objective function score achieved for negative small values of the logarithm of β_{rh} and the influence of β_h is more dominant than of β_{rh} . For high values of the logarithm of β_r , the objective function score increase with the decrease in the value of β_{rh} . The maximum objective function score achieved for positive small values of the logarithm of β_h and the influence of β_{rh} is more dominant than of β_h . The objective function score achieve its global maximum for value of the logarithm of β_r which is negative and close to zero.

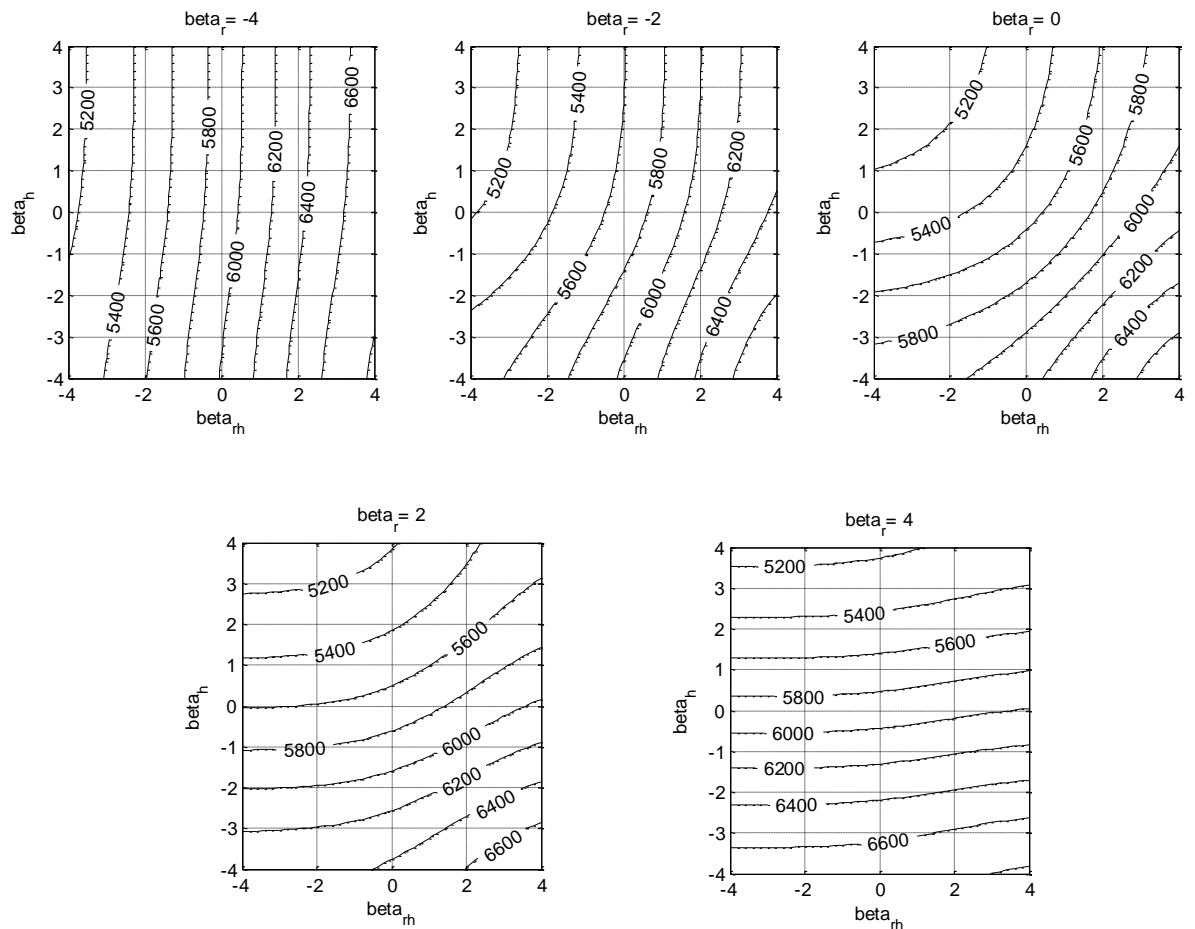


Figure A-67: HO-R collaboration level task time.

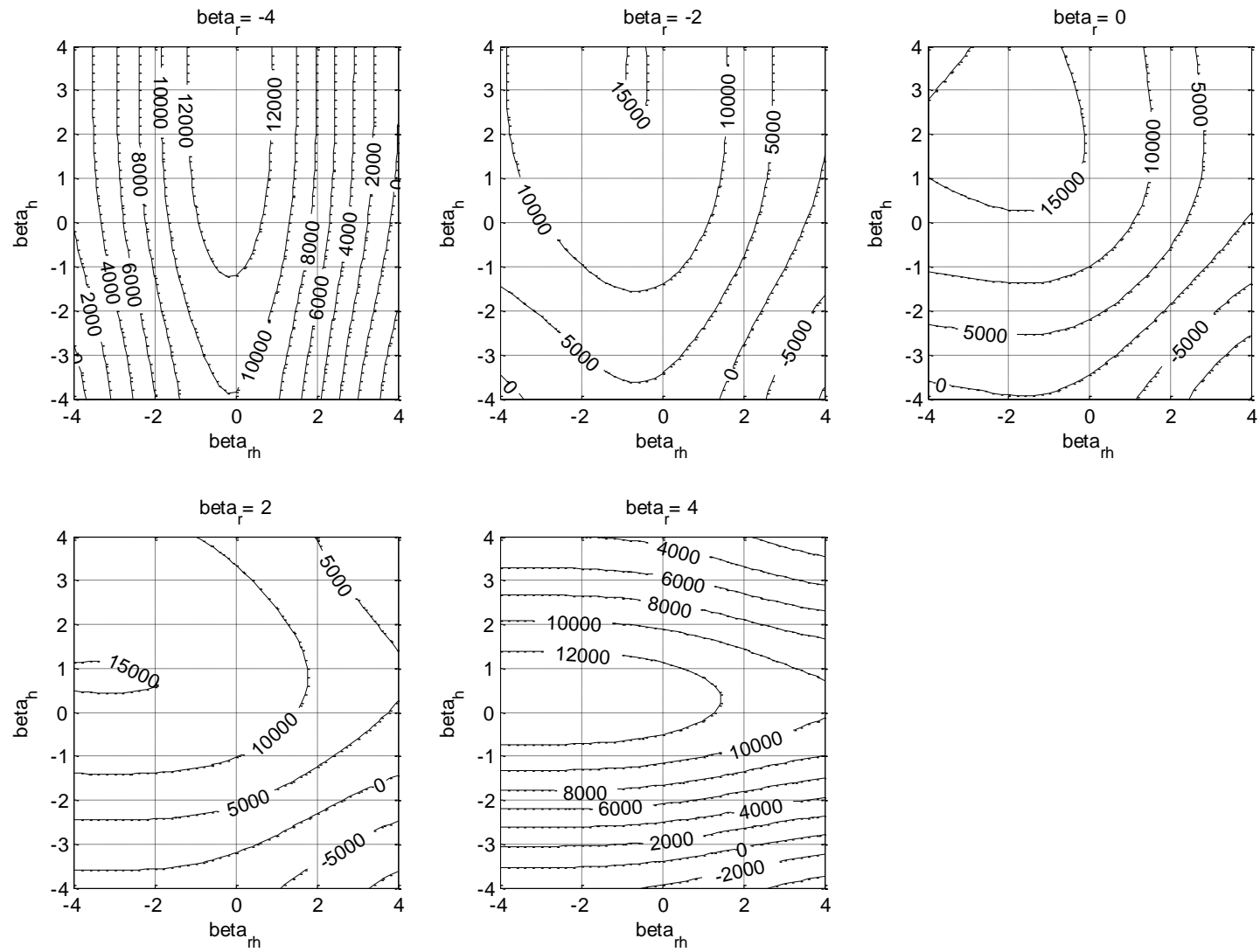


Figure A-68: Objective function for HO-R collaboration level.

Best Collaboration Level

The collaboration level which achieved the highest score in the system objective function, for each β_h and β_{rh} is the best collaboration value for those combinations. Figure A-69 shows a best collaboration level map for different β_h and β_{rh} and for different β_r . Each zone is dominated by a single collaboration level. The R collaboration level is dominant in most of the area when the value of the logarithm of β_r is around zero. The HO-R collaboration level is dominant in part of the area that the value of the logarithm of β_{rh} is negative in negative and positive values of the logarithm of β_r . The HO-Rr collaboration level is dominant in small part of the area that the value of the logarithm of β_{rh} is positive in negative and positive values of the logarithm of β_r . The HO collaboration level is dominant in part of the area that the value of the logarithm of β_h is around zero in negative and positive values of the logarithm of β_r .

Figure A-70 shows the maximum objective function score for different β_h , β_{rh} and β_r values as a combination of all four collaboration levels. Each value of β_r creates different pattern which depends on the best collaboration level map.

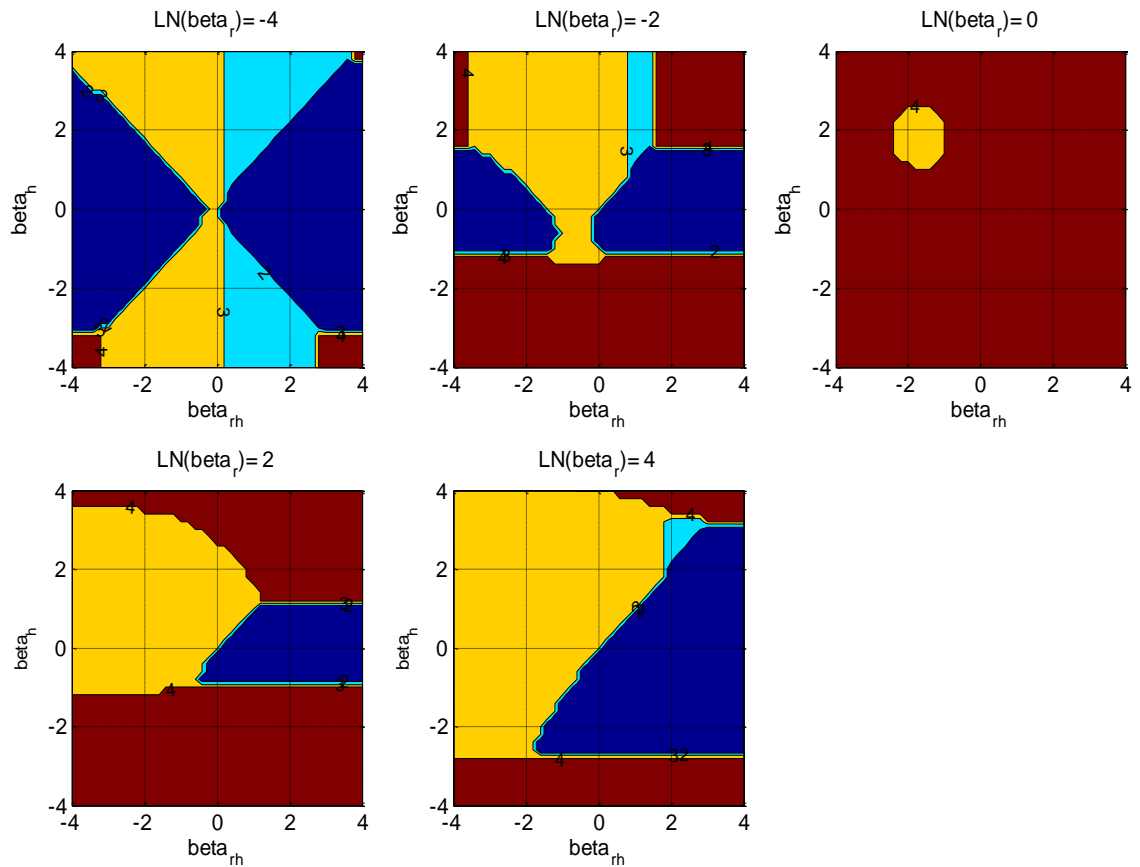


Figure A-69: Best collaboration level.

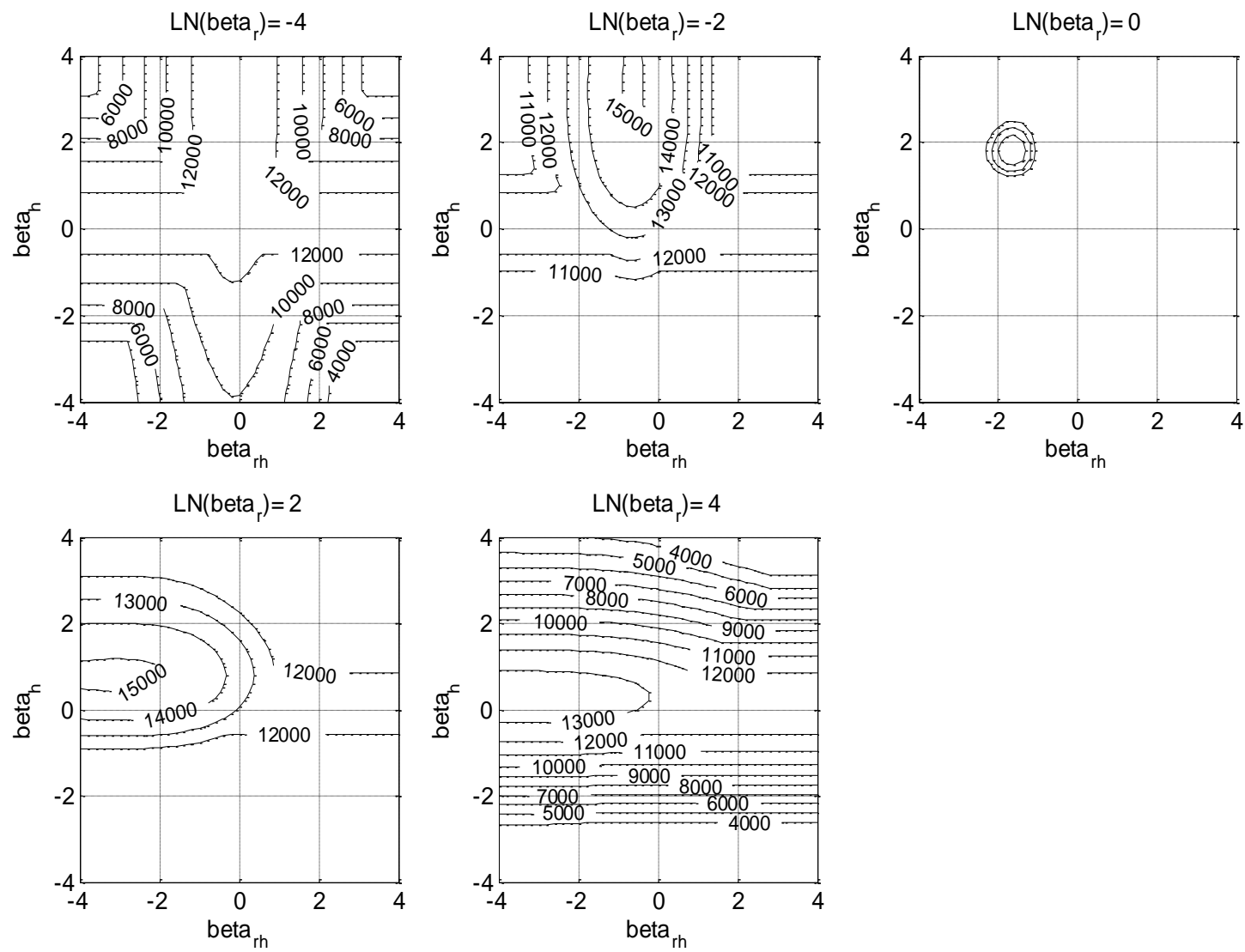


Figure A-70: Objective function.

Conclusions

In the HO collaboration level in order to increase the probability of hit the value of the likelihood ratio β_h has to be decreased and the human sensitivity has to be increased. The objective function score increase with the increase in the human sensitivity but for each human sensitivity there is an optimal β_h of the maximum objective function score.

In the R collaboration level in order to increase the probability of hit the value of the likelihood ratio β_r has to be decreased and the robot sensitivity has to be increased. The objective function score increase with the increase in the robot sensitivity but for each robot sensitivity there is an optimal β_r of the maximum objective function score.

The probability of hit is the same for the HO-Rr and HO-R collaboration levels. The increase in β_r will increase influence of β_{rh} and reduce the influence of β_h on the probability of hit and the task time for both HO-Rr and HO-R collaboration levels. For the objective function score, the increase in the value of β_r will reduce the optimal value of β_h and β_{rh} .

The best collaboration level for β_r of around zero is the R collaboration level and it is dominating most of the area. An Increase or decrease in β_r will decrease the zone in which the R collaboration level is the best collaboration level and the dominating zone of all other collaboration levels will increase. For high values of β_r , which represents small involvement of the robot in the detection process, the best collaboration level in most of the area is the HO-R.

10.1.3 Analysis of Ps

The target probability, P_s , represent the environment and sensors characteristics. High target probability represents environments with high number of objects that can be observed by the system sensors. Low target probability represents environments with low number of objects that can be observed by the system sensors. The parameters in the analysis were determined to be: $N=1000$ objects; $V_H=50$; $V_{AR}=-1$ (and therefore $V_{FA}=-50$); $V_C=-2$ and $V_t=-2000 \text{ hr}^{-1}$. The human sensitivity was set to $d'_h=2$ and the robot sensitivity was set to $d'_r=2$. The decision time for all human time parameters was determined to be $t_D=5 \text{ s/object}$ and the human motoric time was set to $t_M=2 \text{ s/(detected object)}$. The robot time was set to $t_r=0.01 \text{ s/object}$.

HO collaboration level

The HO probability of hit is not influence by the target probability, P_s , and it is identical to the probability of hit that shown in Figure A-51.

Figure A-71 shows the task time as a function of the human sensitivity and human likelihood ratios, β_h , for different target probabilities ($P_s = 0.2, 0.5, 0.8$). For all target probability values the task time increase with the decrease in the value of the logarithm of β_h due to the increase in the hit and false alarms marks. For each target probability, there is a specific value of the logarithm of β_h were above it the task time is increasing with the increase in the human sensitivity and beneath it the task time is decreasing with the increase in the human sensitivity. This specific value is decreasing with the increase in the target probability. At the proximity of the specific value, the influence of the human sensitivity on the task time is minor. The specific value of the logarithm of β_h is zero for target probability of 0.5. For target probabilities lower than 0.5, the task time is decreasing rapidly with the increase in β_h until β_h reaches the specific value. After passing the specific value the task time decrease moderate. For target probabilities higher than 0.5, the task time is decreasing moderate with the increase in β_h until β_h reaches the specific value. After passing the specific value the task time decrease sharply.

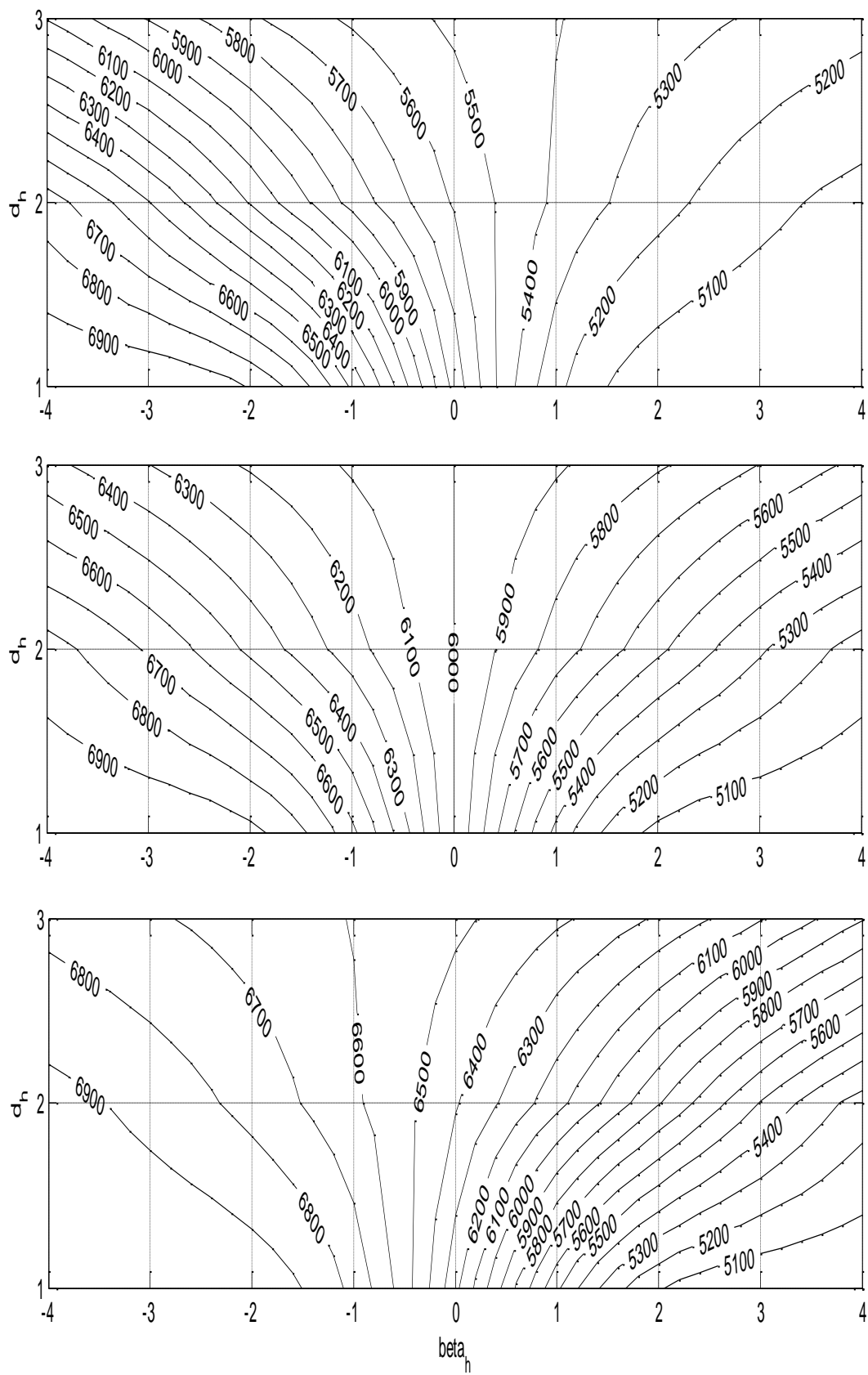


Figure A-71: Task time.

Figure A-72 shows the objective function score as a function of the human sensitivity and human likelihood ratios, β_h , for different target probabilities ($P_s = 0.2, 0.5, 0.8$). The objective function score increase with the increase in the target probability since the number of targets increase. For all target probability values, the objective function score increase with the increase in the human sensitivity. The value of β_h of the objective function maximum score is decreasing with the increase in the target probability for all human sensitivities.

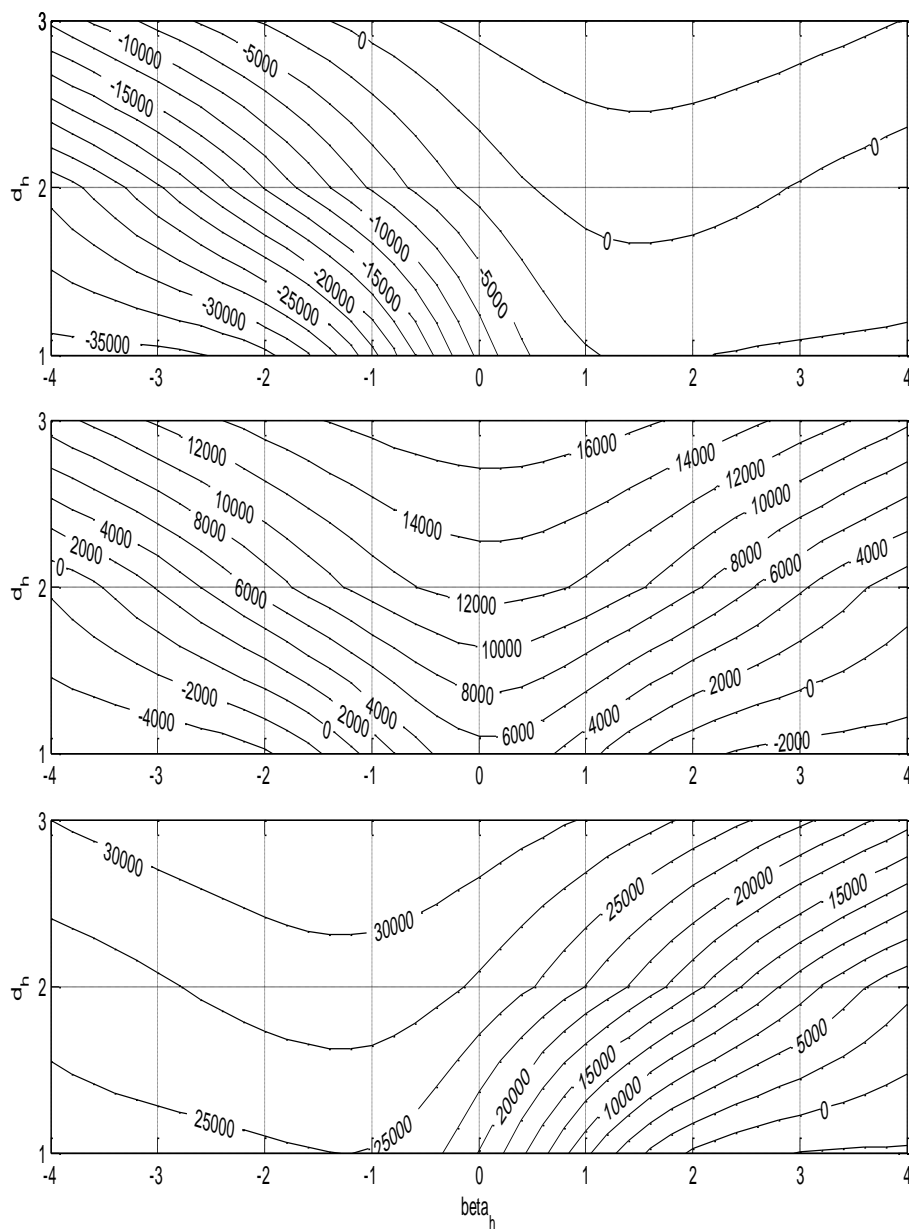


Figure A-72: Objective function.

R collaboration level

The same phenomena that were found for the objective function behavior in the HO collaboration level are shown in the R collaboration level.

The objective function score increase with the increase in the target probability (Figure A-73). For all target probability values, the objective function score increase with the increase in the robot sensitivity. The value of β_r of the objective function maximum score is decreasing with the increase in the target probability for all robot sensitivities.

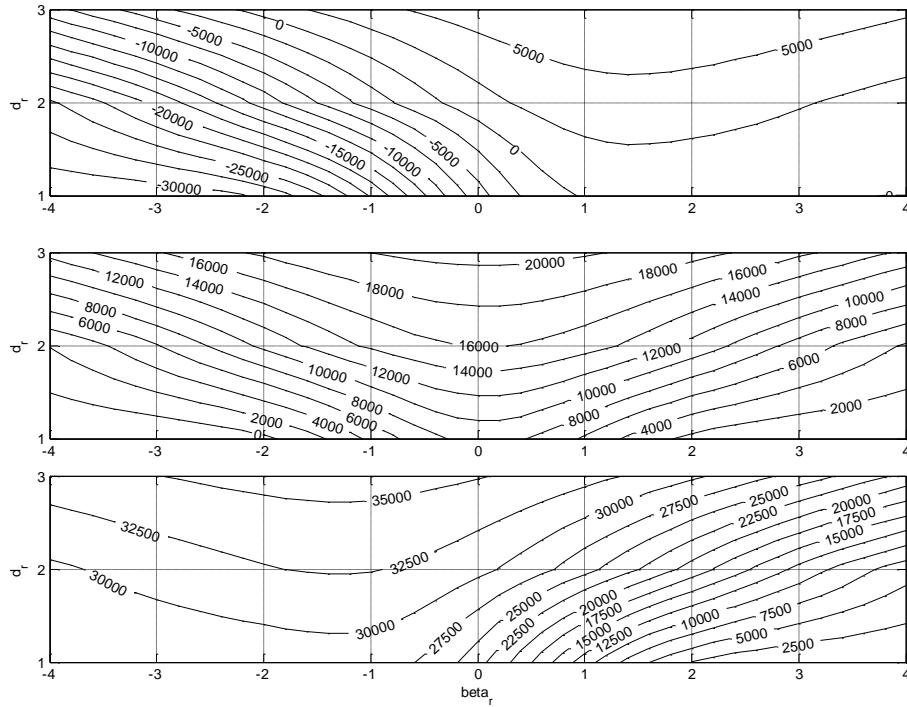


Figure A-73: objective function.

HO-Rr collaboration level

The task time of the HO-Rr collaboration level decrease with the increase in the values of the logarithm of β_h and β_{rh} (Figure A-74). The increase in the value of the logarithm of β_r reduces the influence of the values of β_{rh} on the task time since the increase in β_r reduces the number of object marked by the robot and therefore the number of object that were confirmed by the human. The increase in the target probability will increase the number of objects marked by the system and therefore increase the task time. In addition high target probability magnify the influence of the above parameters and the changes of the above

Increase in target probability will increase the objective function score due to the increase in the number of marked objects by the entire system (Figure A-75). The values of β_h and β_{rh} of the maximum objective function score is reduced with reduce in the target probability. For low β_r values the increase of the target probability will have stronger effect on the value of β_{rh} than β_h and vise versa for high values of β_r . High values of β_r have less weight on the objective function score and therefore β_{rh} which is linked to β_r is less influenced.

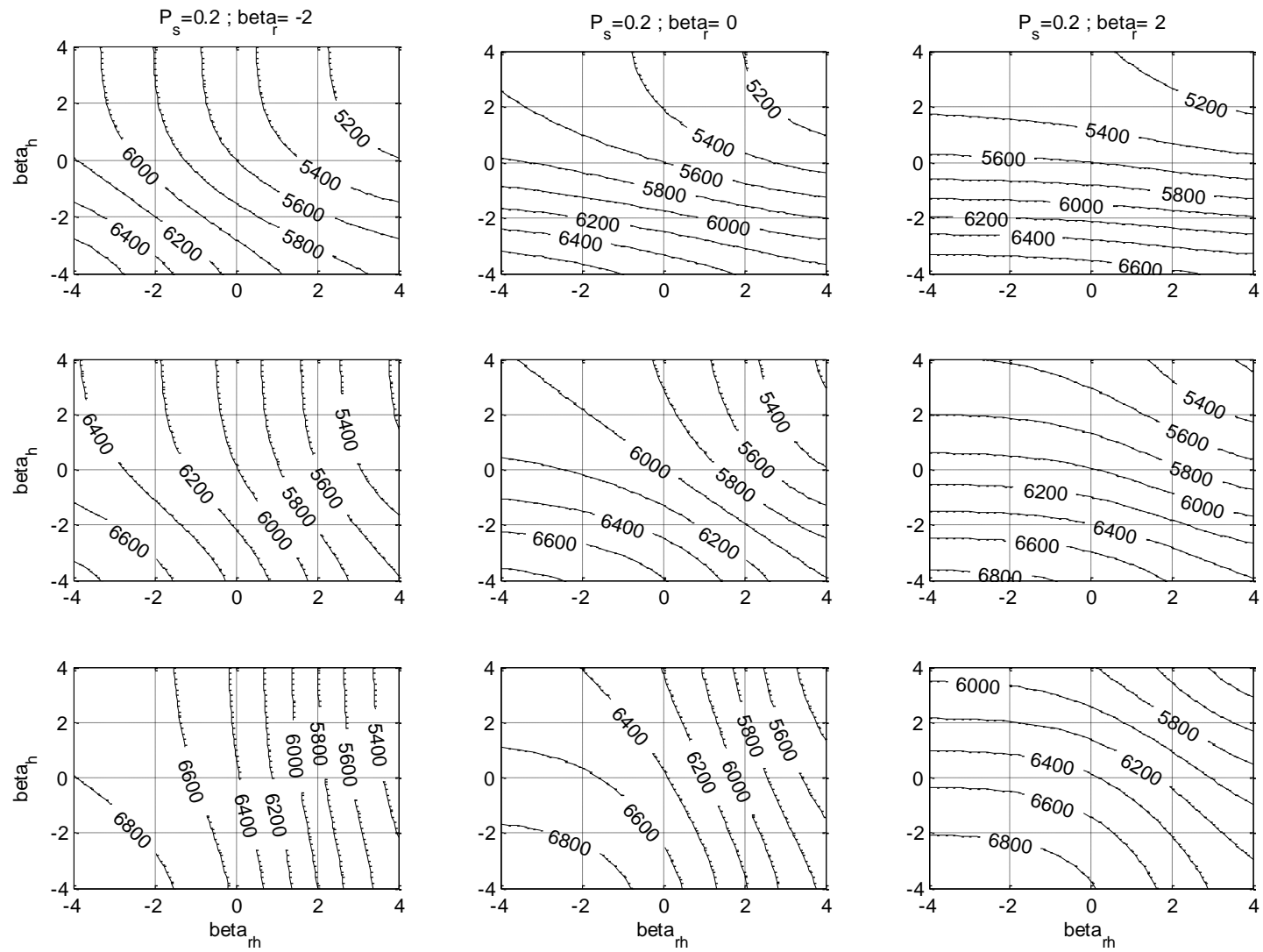


Figure A-74: Task time.

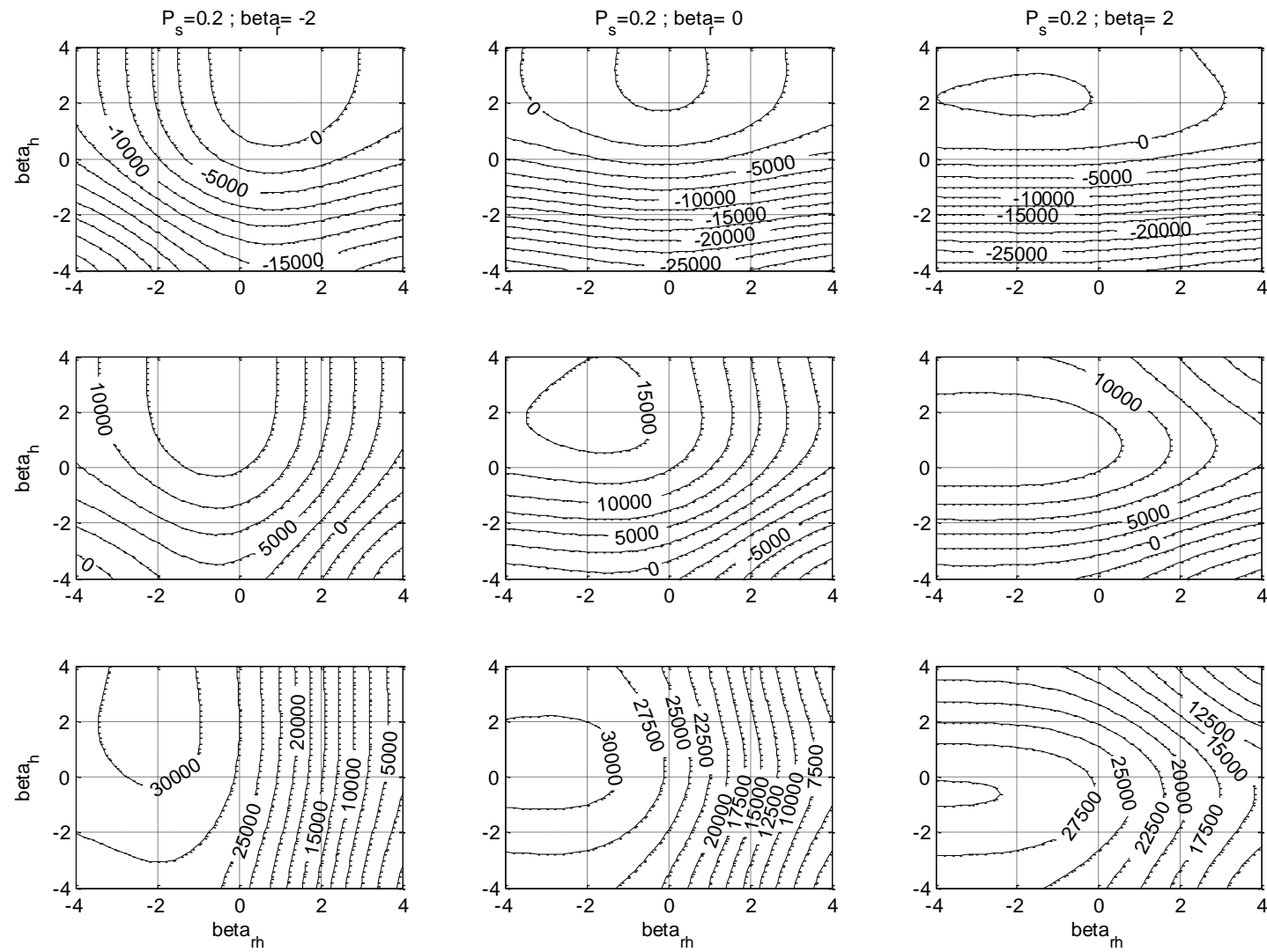


Figure A-75: Objective function.

HO-R collaboration level

The same effects that were observed in the HO-Rr collaboration level are appears in the HO-R collaboration level.

The task time of the HO-R collaboration level decrease with the increase in the values of the logarithm of β_h and β_{rh} (Figure A-76). The increase in the value of the logarithm of β_r reduces the influence of the values of β_{rh} on the task time since the increase in β_r reduces the number of object marked by the robot and therefore the number of object that were confirmed by the human. The increase in the target probability will increase the number of objects marked by the system and therefore increase the task time. In addition high target probability magnify the influence of the above parameters and the changes of the above

Increase in target probability will increase the objective function score due to the increase in the number of marked objects by the entire system (Figure A-77). The values of β_h and β_{rh} of the maximum objective function score is reduced with reduce in the target probability. For low β_r values the increase of the target probability will have stronger effect on the value of β_{rh} than β_h and vise versa for high values of β_r . High values of β_r have less weight on the objective function score and therefore β_{rh} which is linked to β_r is less influenced.

Best Collaboration Level

Figure A-78 shows a best collaboration level map for different β_h , β_{rh} , for β_r equal -2 (left column), 0 (middle column) and +2 (right column) and for target probability equal to 0.2 (upper row), 0.5 (middle row) and 0.8 (lower row).

In most cases the increase in target probability will not drastically change the domination zones of the different collaboration levels, and the highest objective function score will be achieved by the same collaboration level. However, the values of β_h and β_{rh} of the maximum score will become smaller. A change in the domination zone of the collaboration levels and in the collaboration level which achieve the highest score will occur in cases that the objective function score of several collaboration levels are similar and the changes in the objective function score resulting by the change in the target probability can drastically change the ratio between them.

Figure A-79 shows the maximum objective function score as a combination of all four collaboration levels for different β_h , β_{rh} for β_r equal -2 (left column), 0 (middle column) and +2 (right column) and for target probability equal to 0.2 (upper row), 0.5 (middle row) and 0.8 (lower row).

Each value of β_r creates different pattern which depends on the best collaboration level map. The objective function score increase with the increase in target probability.

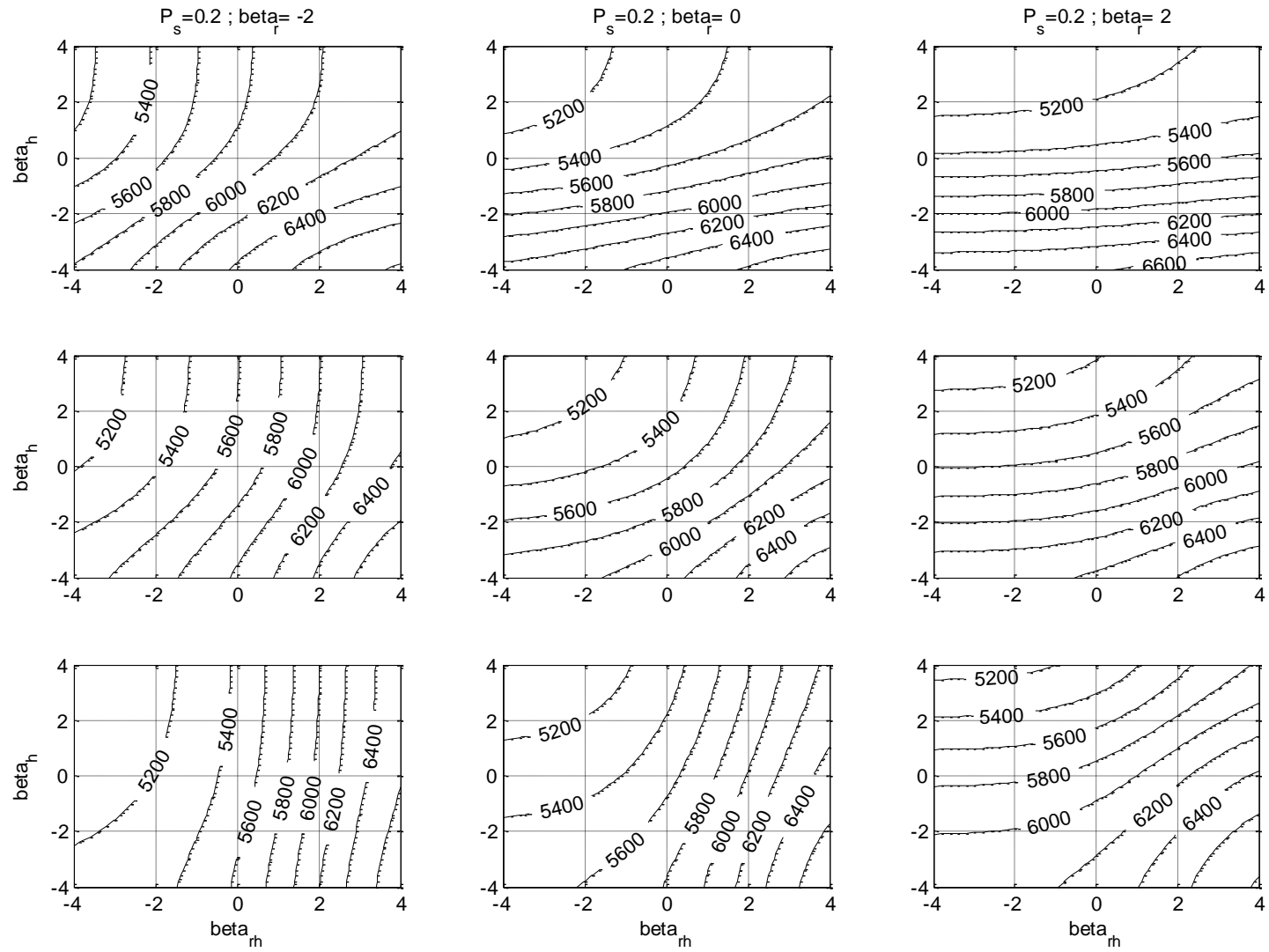


Figure A-76: Task time.

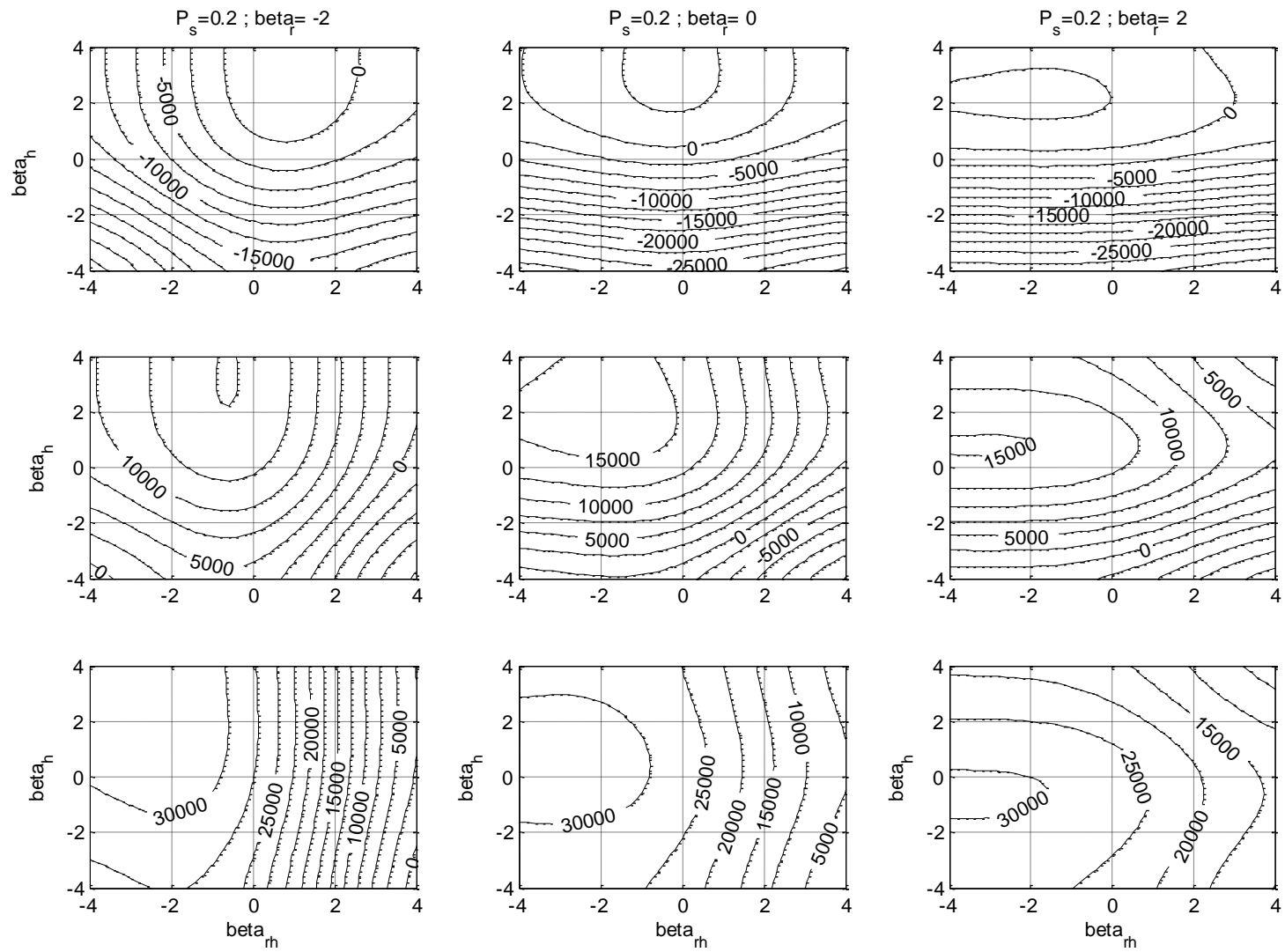


Figure A-77: Objective function.

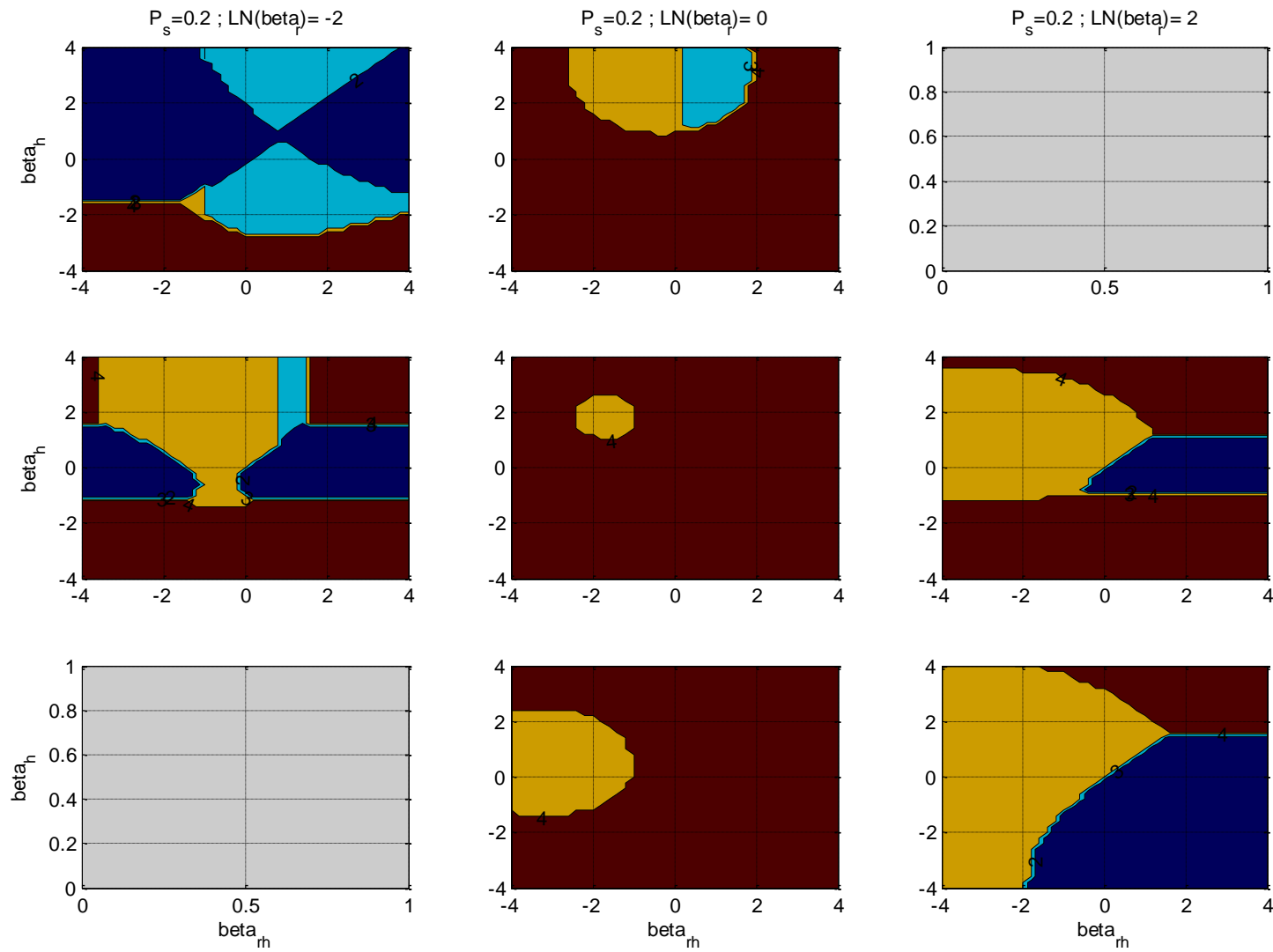


Figure A-78: Best collaboration levels.

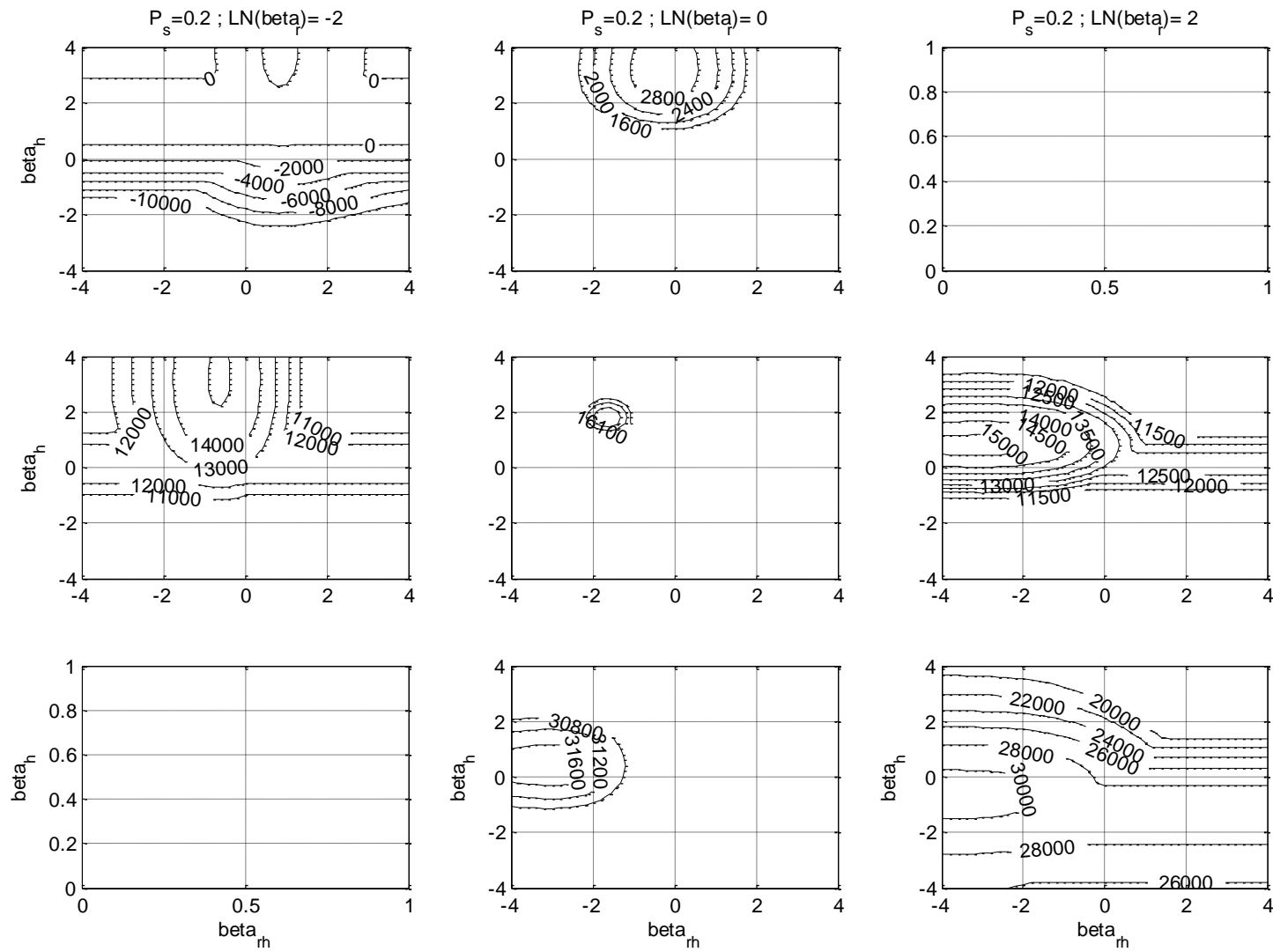


Figure A-79: Objective function.

Conclusions

The probability of hit is not influence by the target probability, P_s . In the HO and R collaboration level, the value of the critical β_h that the human or robot sensitivity has no influence on the task time is decreased with the increase in the target probability. The objective function score increase with the increase in the target probability and the optimal β_h and β_r of the maximum score, decrease with the increase in target probability.

For HO-Rr and HO-R collaboration levels the target probability has similar influence on the task time and the objective function score. The task time increase with the increase of the target probability and it became more affected by the value of β_{rh} and less affected by the value of β_h . the objective function score increase with the increase in the target probability and the optimal β_h and β_r of the maximum score decreased with the increase in the target probability.

10.1.4 Analysis of d'_r

The robot sensitivity, d'_r , indicates the robot ability to distinguish between true targets (signal) and false targets (noise). The parameters in the analysis were determined to be: $N=1000$ objects; $V_H=50$; $V_{AR}=-1$ (and therefore $V_{FA}=-50$); $V_C=-2$ and $V_t=-2000 \text{ hr}^{-1}$. The human sensitivity was set to $d'_h=2$. The target probability was set to $P_s=0.5$. The decision time for all human time parameters was determined to be $t_D=5 \text{ s/object}$ and the human motoric time was set to $t_M=2 \text{ s/(detected object)}$. The robot time was set to $t_r=0.01 \text{ s/object}$.

Since in the HO collaboration the robot is not involved in the task execution, the robot sensitivity has no influence on the human performance.

The robot sensitivity influence the objective function score in the R collaboration level is shown in chapter 3.2.1 and figure 30

HO-Rr collaboration level

Figure A-80 shows system probability for hit for different β_h , β_{rh} , for β_r equal -2 (left column), 0 (middle column) and +2 (right column) and for robot sensitivity equal to 1 (upper row), 2 (middle row) and 3 (lower row). The robot sensitivity has little influence on the system probability of hit for low values of β_r since in low β_r values the robot probability of hit is close to 1 for all robot sensitivities. For high values of β_r the low robot sensitivity yield low robot hit probability thus, β_{rh} has less effect on the system performance, however the high robot sensitivity yield high robot hit probability, most of the targets are marked by the robot and therefore β_{rh} has grate effect on the system performance and β_h has less influence of the system probability of hit.

Although the task time is effected from the human performance, it is also influenced by the robot sensitivity since it affects the human performance. The task time increase with the decrease in β_h and β_{rh} . For low β_r values, the influence of β_h increase with increase in robot sensitivity (Figure A-81). For high β_r values, the influence of β_{rh} increase with increase in robot sensitivity.

Figure A-82 shows the objective function score for different robot sensitivities. The system objective function score increase with the increase in the robot sensitivity. For low β_r values, the β_{rh} value of the maximum score reduces with the increase of the robot sensitivity. For high β_r values, the β_h value of the maximum score reduces with the increase of the robot sensitivity.

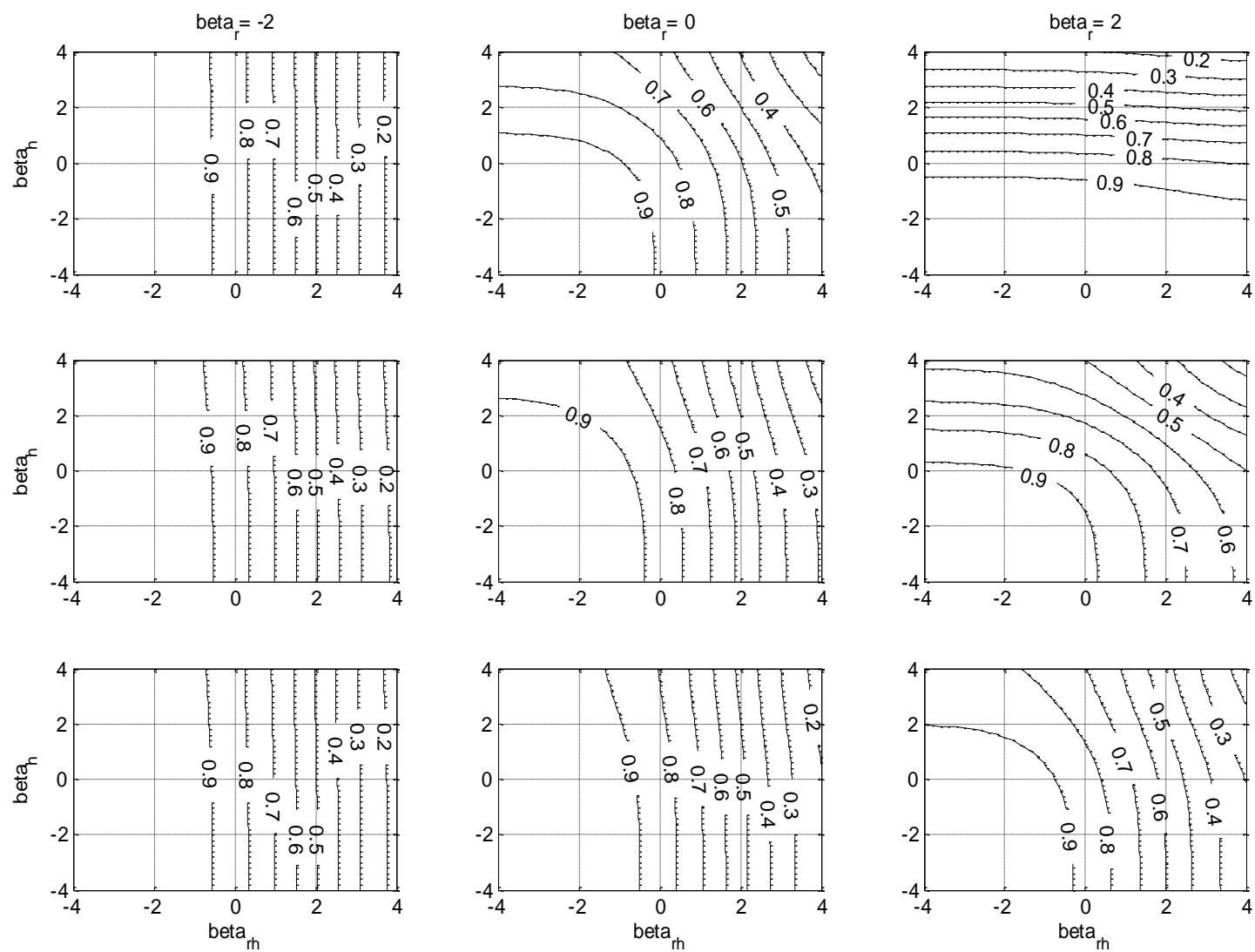


Figure A-80: Probability of hit.

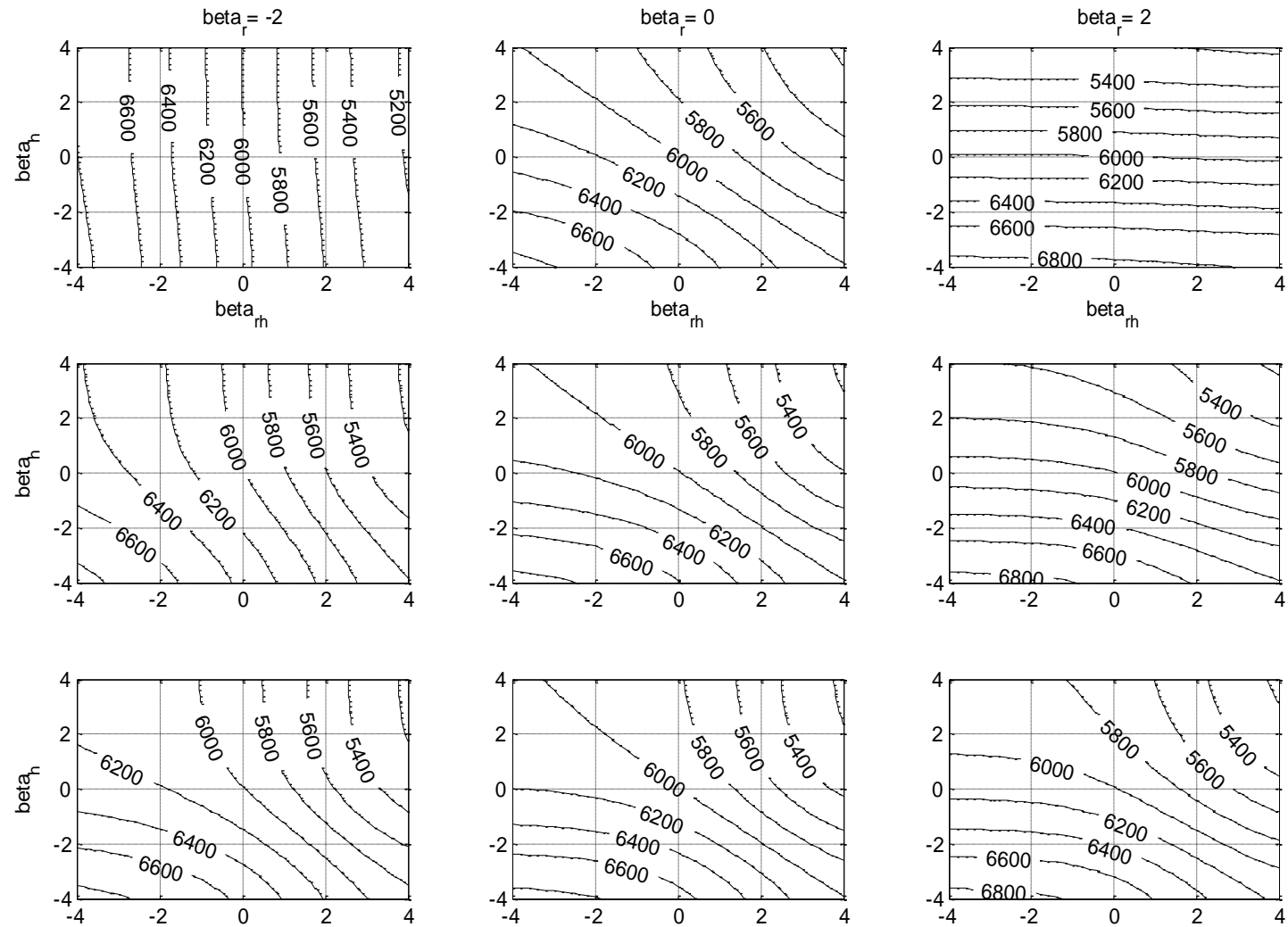


Figure A-81: Task time.

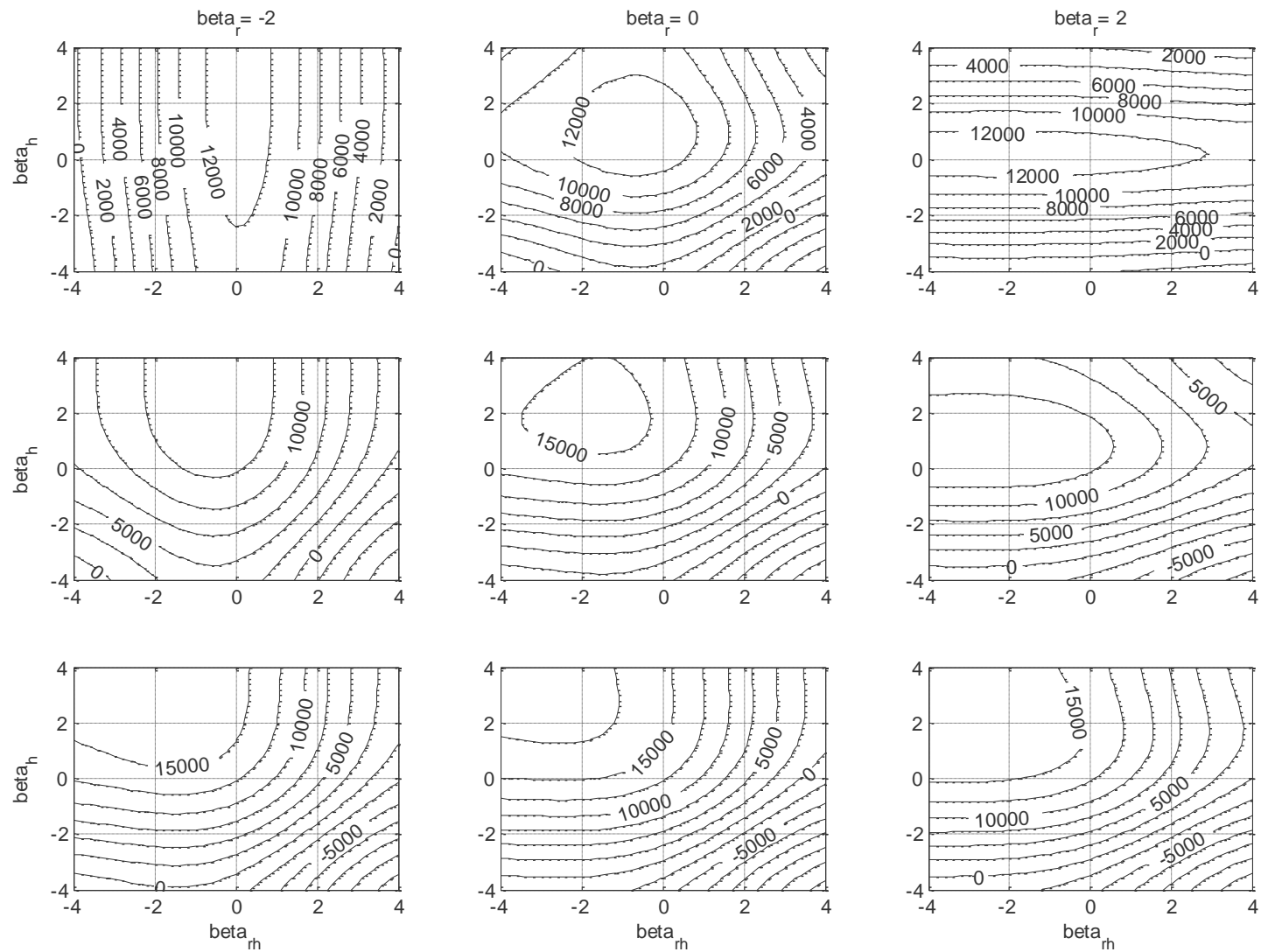


Figure A-82: Objective function.

HO-R collaboration level

Although the task time is effected from the human performance, it is also influenced from the robot sensitivity since it affects the human performance. In the HO-R collaboration level the task time increase with the decrease in β_h and the increase in β_{rh} . For low β_r values, the influence of β_h increase with increase in robot sensitivity (Figure A-83). For high β_r values, the influence of β_{rh} increase with increase in robot sensitivity.

Figure A-84 shows the objective function score for different robot sensitivities. The system objective function score increase with the increase in the robot sensitivity. For low β_r values, the β_{rh} value of the maximum score reduces with the increase of the robot sensitivity. For high β_r values, the β_h value of the maximum score increases with the increase of the robot sensitivity.

Best Collaboration Level

Figure A-85 shows a best collaboration level map for different β_h , β_{rh} , for β_r equal -2 (left column), 0 (middle column) and +2 (right column) and for robot sensitivity equal to 1 (upper row), 2 (middle row) and 3 (lower row).

The increase in the robot sensitivity has no influence on the objective function score of the HO collaboration level, small incensement on the score of the HO-Rr and HO-R collaboration levels and high influence on the score of the R collaboration level. Therefore the increase in the robot sensitivity will increase the zone dominated by the R collaboration level until the best collaboration level for the entire area will be the R collaboration level.

Figure A-86 shows the maximum objective function score as a combination of all four collaboration levels for different β_h , β_{rh} for β_r equal -2 (left column), 0 (middle column) and +2 (right column) and for robot sensitivity equal to 1 (upper row), 2 (middle row) and 3 (lower row). The increase in the robot sensitivity will increase the objective function score on the entire area and will increase the value of the maximum score. The β_h and β_{rh} values of the maximum score will not change a lot with the increase in the robot sensitivity up to a certain sensitivity in which the R collaboration level will be the best collaboration level for the entire area and the maximum score will be identical for the entire area.

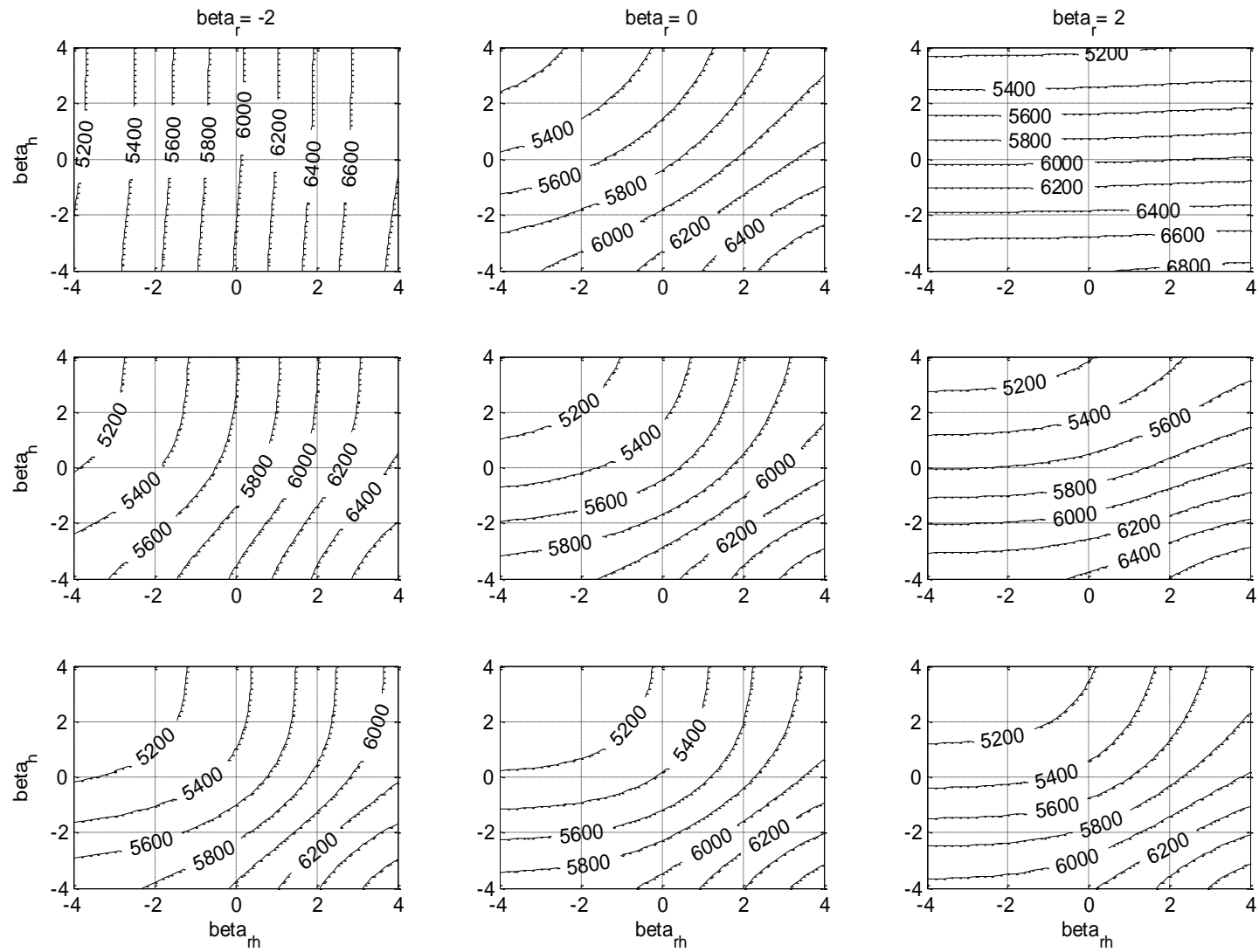


Figure A-83: Task time.

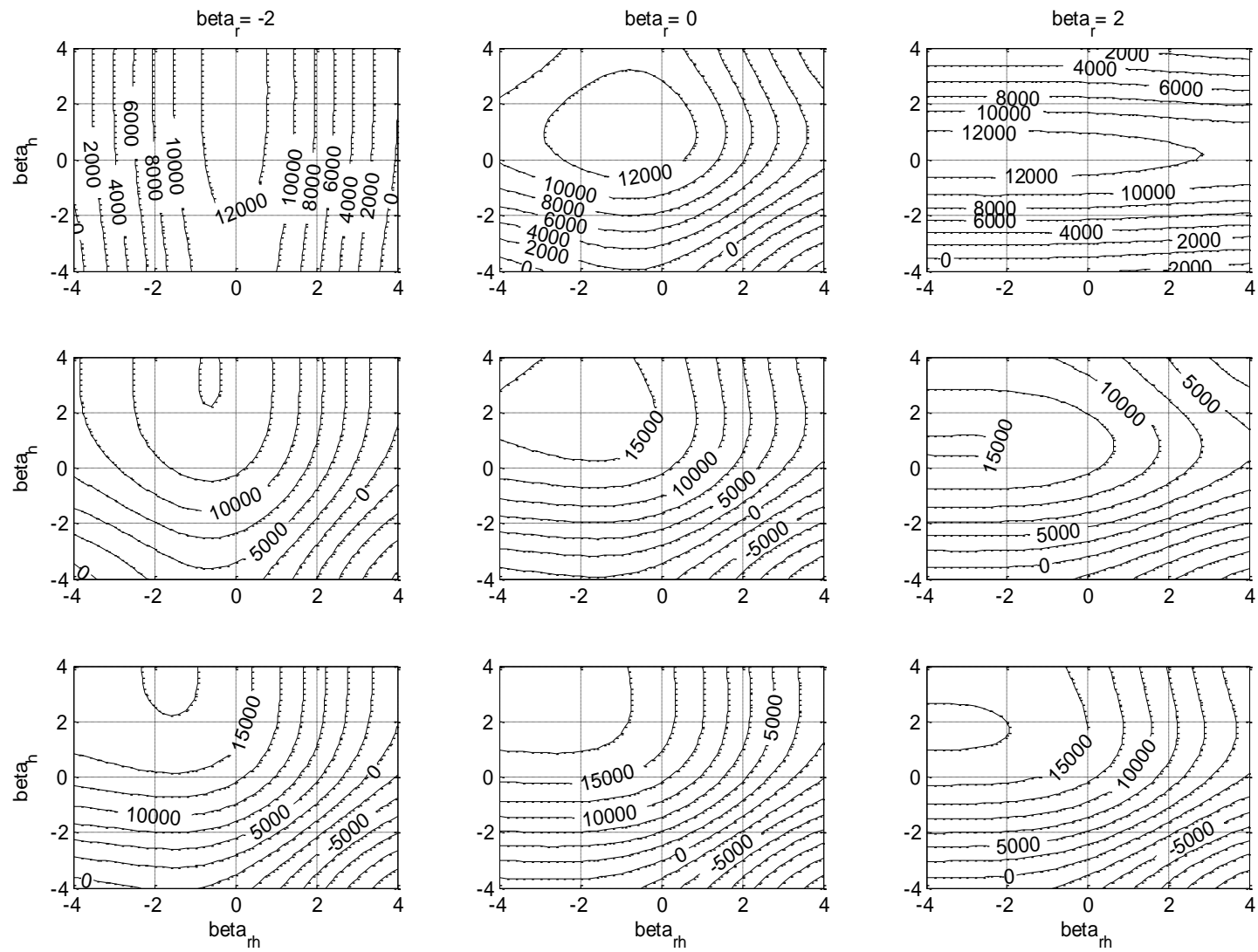


Figure A-84: Objective function.

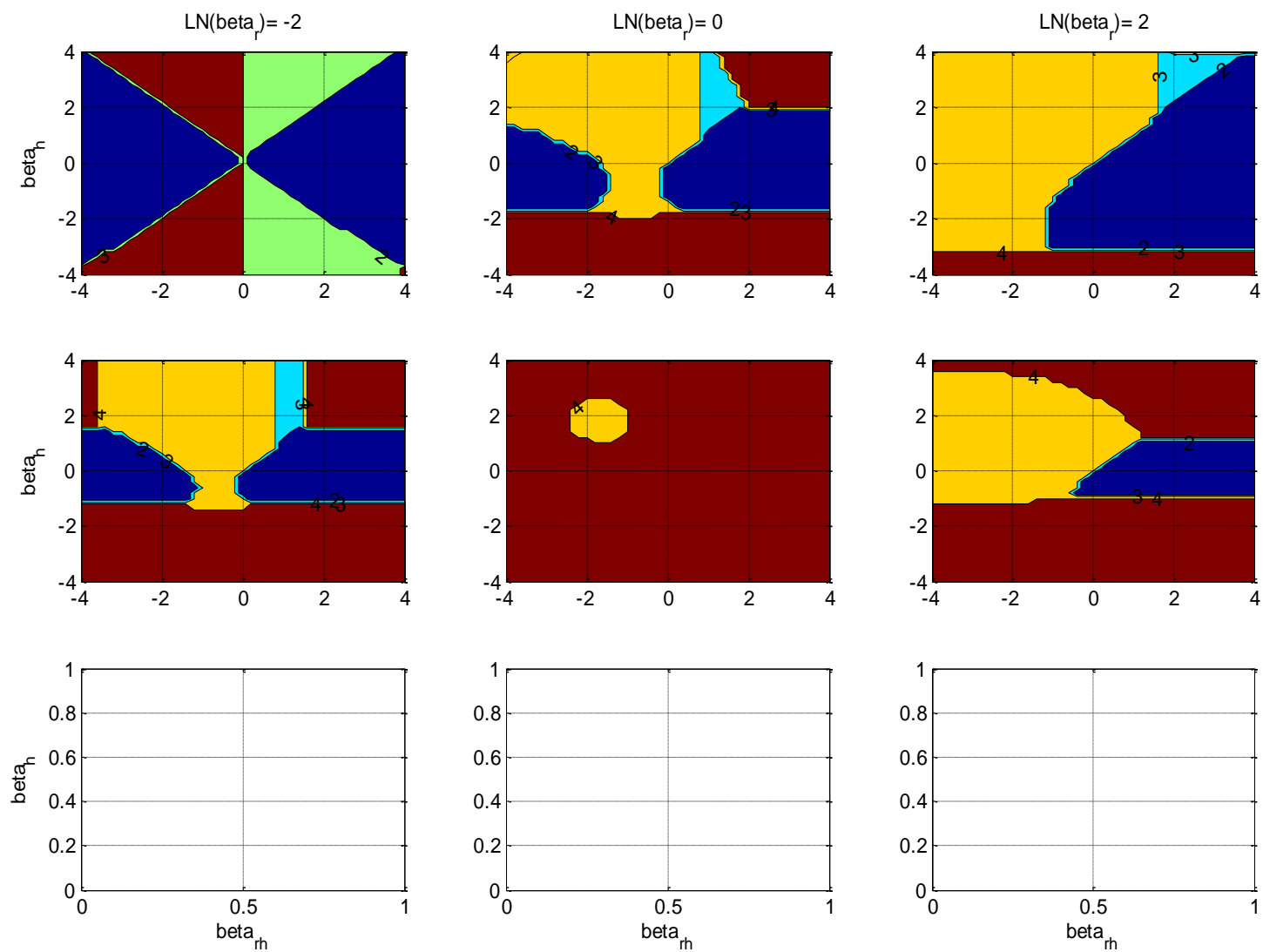


Figure A-85: Best collaboration level.

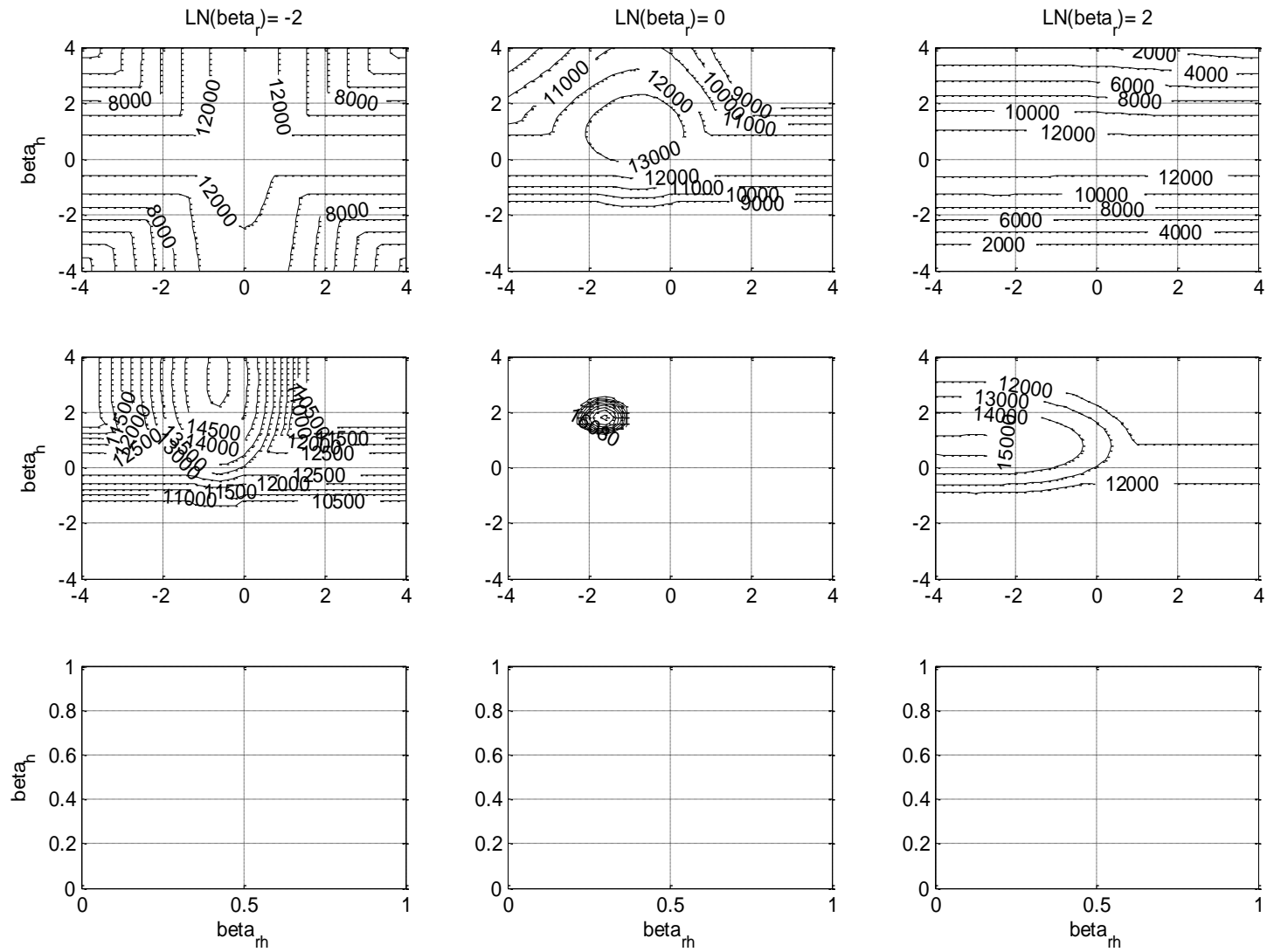


Figure A-86: Max objective function.

Conclusions

The robot sensitivity indicates the robot ability to distinguish between true targets (signal) and false targets (noise) and improves the performance of the robot in a human-robot system.

In the R collaboration level the increase in the robot sensitivity will increase the probability of hit and the objective function score.

In the HO-Rr and HO-R collaboration level the robot sensitivity have negligible influence on the system probability of hit for low β_r values. For normal and high values of β_r the system probability of hit and the objective function score can even decrease with the increase in the robot sensitivity in cases that the human detection of objects marked by the robot is low and the human detection of objects that the robot didn't detect is high. The maximum score of the objective function increase with the increase in the robot sensitivity.

The domination zone of the R collaboration level is increased with the increase in the robot sensitivity although the maximum score achieved in the R collaboration level only when it is dominating the entire area.

10.1.5 Analysis of d'_h

The human sensitivity, d'_h , indicates the human ability to distinguish between true targets (signal) and false targets (noise). The parameters in the analysis were determined to be: $N=1000$ objects; $V_H=50$; $V_{AR}=-1$ (and therefore $V_{FA}=-50$); $V_C=-2$ and $V_t=-2000 \text{ hr}^{-1}$. The robot sensitivity was set to $d'_r=2$. The target probability was set to $P_s=0.5$. The decision time for all human time parameters was determined to be $t_D=5 \text{ s/object}$ and the human motoric time was set to $t_M=2 \text{ s/(detected object)}$. The robot time was set to $t_r=0.01 \text{ s/object}$.

Since in the R collaboration the human is not involved in the task execution, the human sensitivity has no influence on the robot performance.

The human sensitivity influence the objective function score in the HO collaboration level is shown in chapter 3.2.1.

HO-Rr collaboration level

Figure A-87 shows system probability for hit for different β_h , β_{rh} , for β_r equal -2 (left column), 0 (middle column) and +2 (right column) and for human sensitivity equal to 1 (upper row), 2 (middle row) and 3 (lower row). For low values of β_r the increase in human sensitivity increase the system probability of hit, though, β_h has little influence on the system probability of hit for any human sensitivity since in low β_r values the robot probability of hit is close to 1 for all human sensitivities which leaves very few objects that are unmarked by the robot and therefore β_r influence is minimal. For high values of β_r the increase in human sensitivity increase the system probability of hit. There is an equal effect of β_h and β_{rh} on the probability of hit.

The human sensitivity influence directly the human performance and by that the task time. The task time increase with the decrease in β_h and β_{rh} . For low β_r values, the influence of β_h decrease with increase in human sensitivity (Figure A-88). For high β_r values, the influence of β_{rh} decrease with increase in human sensitivity.

Figure A-89 shows the objective function score for different human sensitivities. The system objective function score increase with the increase in the human sensitivity. The β_h and β_{rh} values of the maximum objective function score are not changing with the increase in human sensitivity. The pattern of the objective function for different β_h and β_{rh} is not changed and it seems as an enlargement of the area of the maximum score.

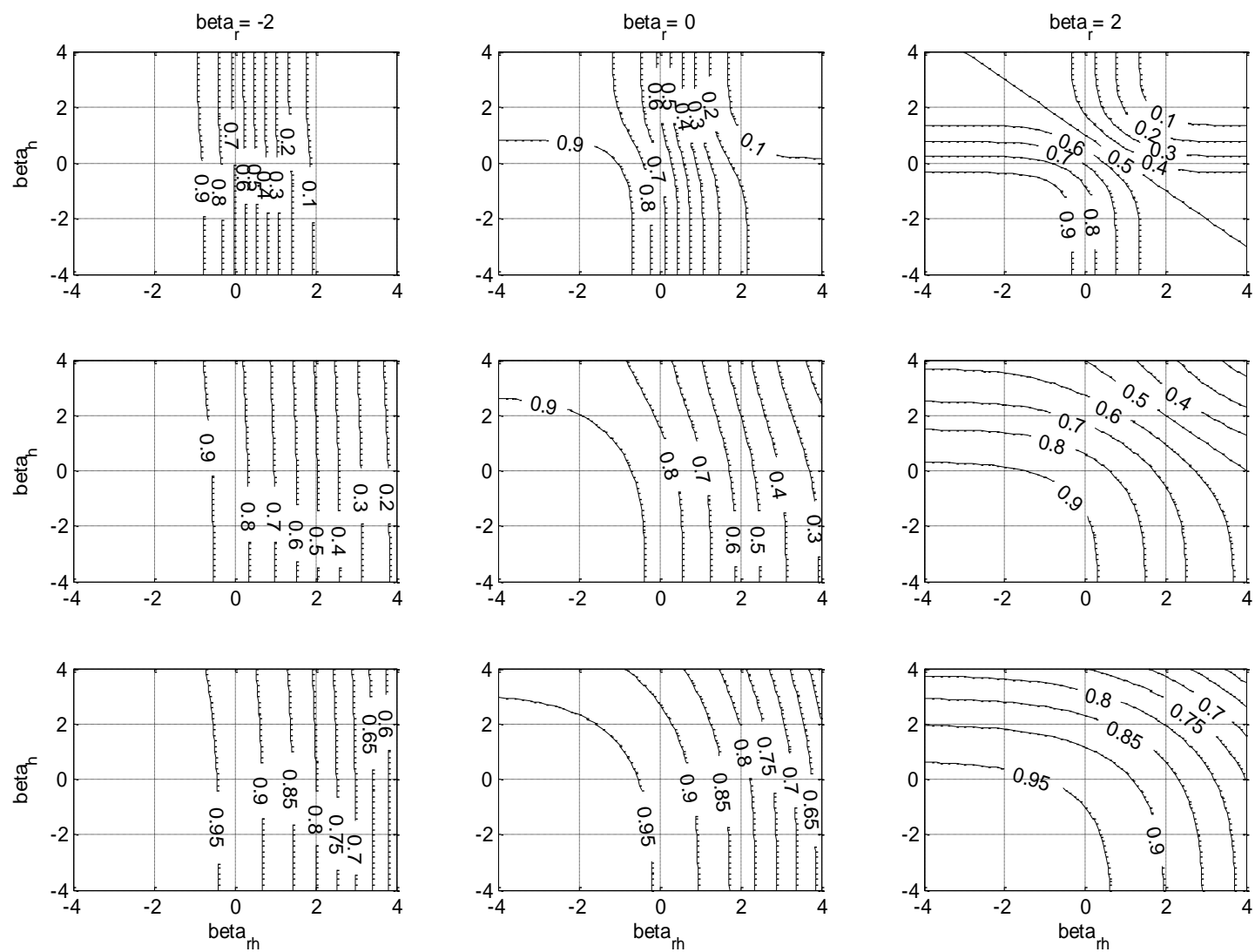


Figure A-87: Probability of hit.

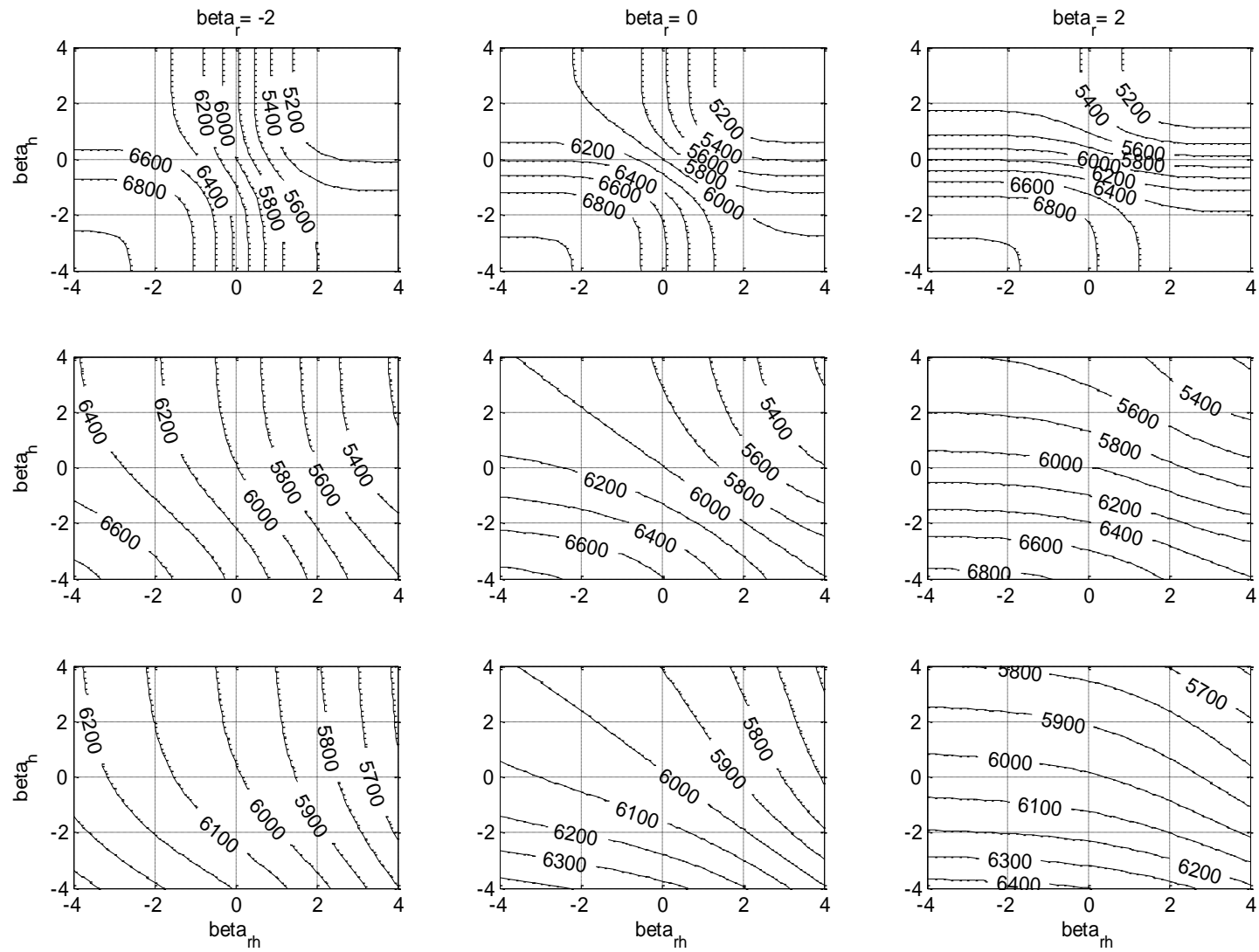


Figure A-88: Task time.

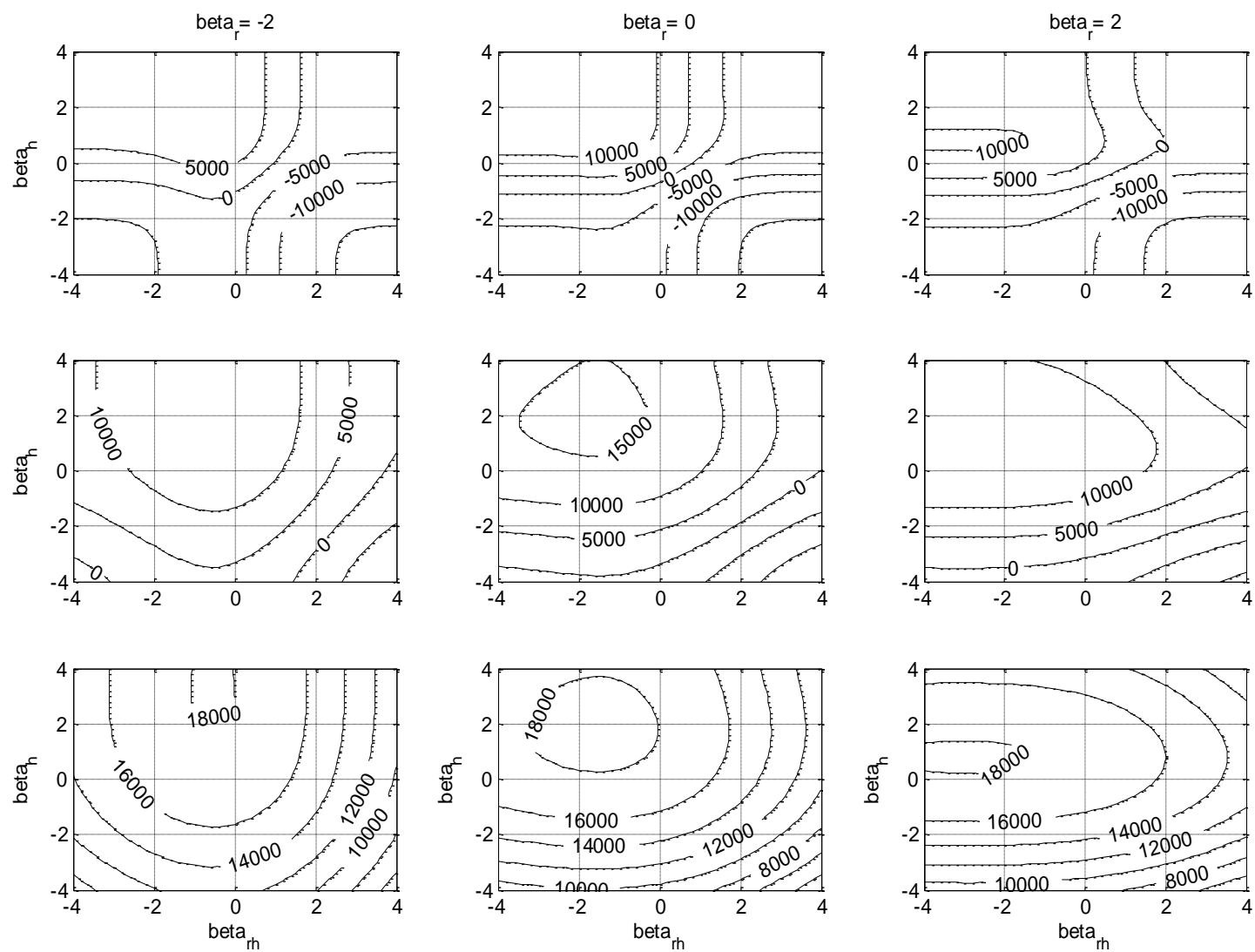


Figure A-89: Objective function.

HO-R collaboration level

The probability of hit will be identical to the HO-Rr collaboration level as shown in figure 40. In the HO-R collaboration level the task time increase with the decrease in β_h and the increase in β_{rh} . For low β_r values, the influence of β_h on the task time decrease and the influence of β_{rh} increase with increase in human sensitivity (Figure A-90). For high β_r values, the influence of β_{rh} decrease and the influence of β_h increase with increase in human sensitivity.

Figure A-91 shows the objective function score for different human sensitivities. The system objective function score increase with the increase in the human sensitivity. The β_h and β_{rh} values of the maximum objective function score are not changing with the increase in human sensitivity. The pattern of the objective function for different β_h and β_{rh} is not changed and it seems as an enlargement of the area of the maximum score.

Best Collaboration Level

Figure A-92 shows a best collaboration level map for different β_h , β_{rh} , for β_r equal -2 (left column), 0 (middle column) and +2 (right column) and for human sensitivity equal to 1 (upper row), 2 (middle row) and 3 (lower row).

The increase in the human sensitivity has no influence on the objective function score of the R collaboration level, small increase on the score of the HO-Rr and HO-R collaboration levels and high influence on the score of the HO collaboration level. Therefore increase in human sensitivity increase the zone dominated by the HO, HO-Rr and HO-R collaboration levels and reduce the zone dominated by the R collaboration level. For human sensitivities that are lower than the robot sensitivity, the best collaboration level for the entire area will be the R collaboration level.

Figure A-93 shows the maximum objective function score as a combination of all four collaboration levels for different β_h , β_{rh} for β_r equal -2 (left column), 0 (middle column) and +2 (right column) and for human sensitivity equal to 1 (upper row), 2 (middle row) and 3 (lower row). The increase in the human sensitivity will increase the objective function score on the entire area and will increase the value of the maximum score. The β_h and β_{rh} values of the maximum score will not change a lot with the increase in the human sensitivity except for cases were the R collaboration level is the best collaboration level for the entire area and the entire area will have the maximum score.

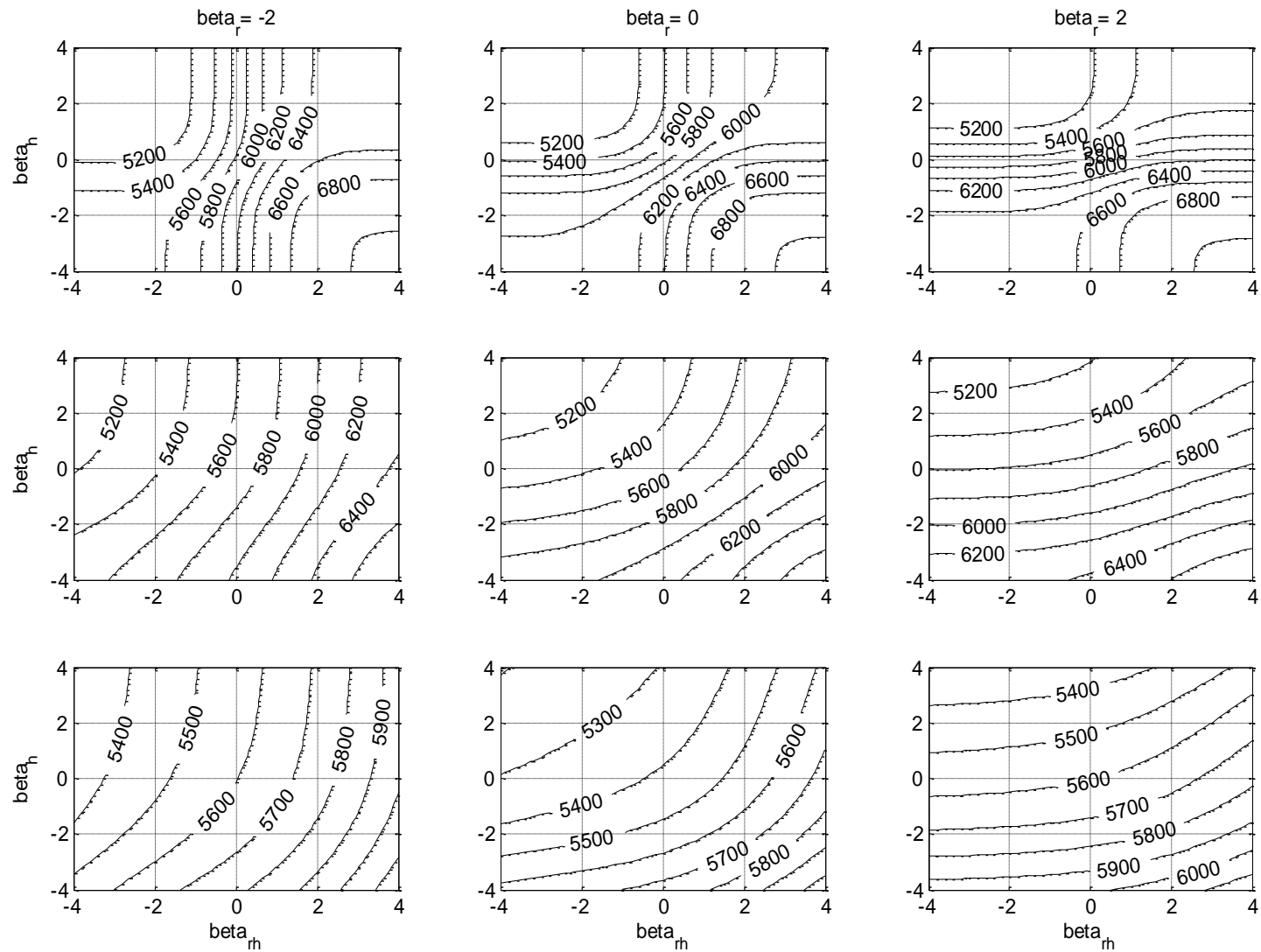


Figure A-90: Task time.

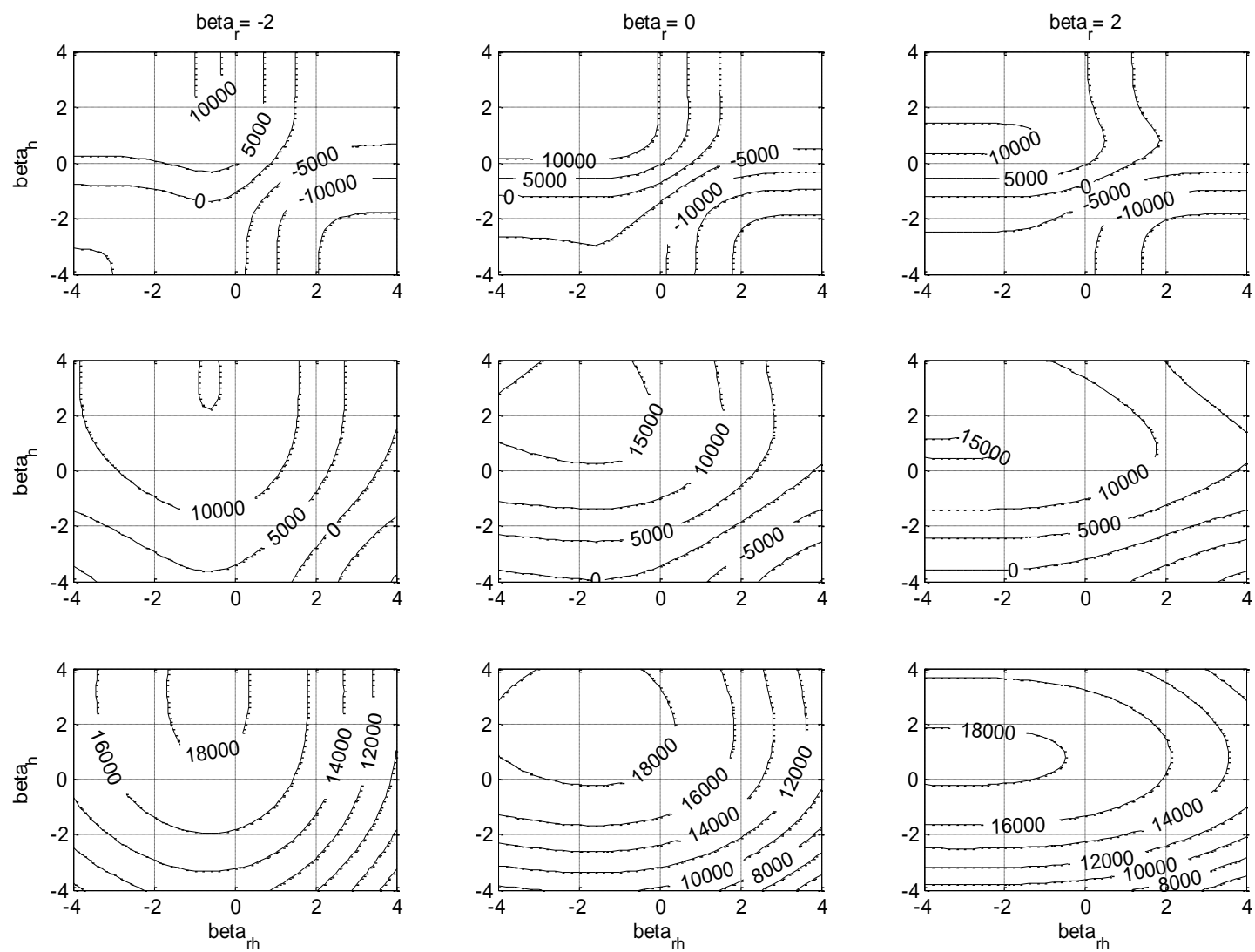


Figure A-91: Objective function.

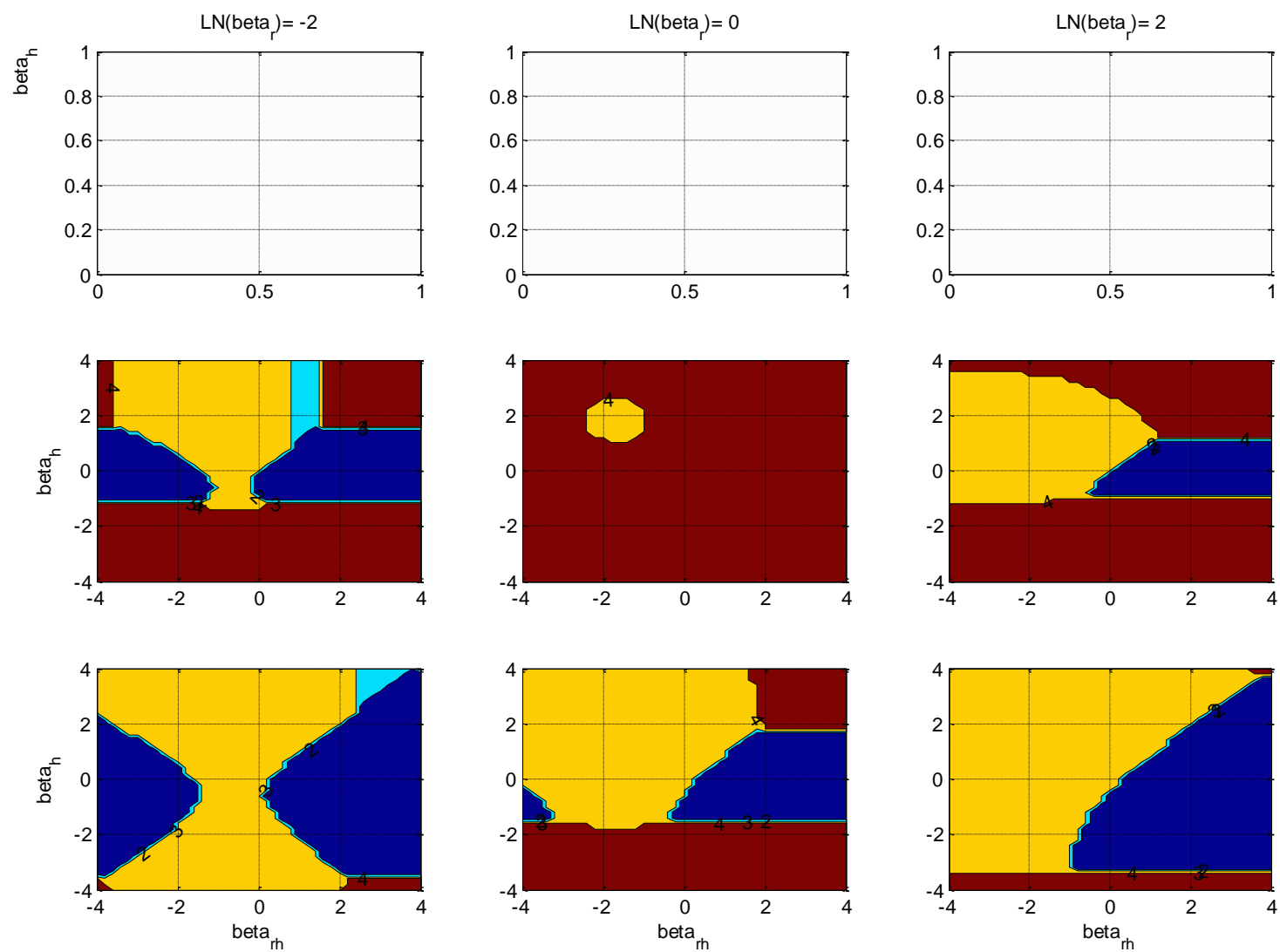


Figure A-92: best collaboration level domination map.

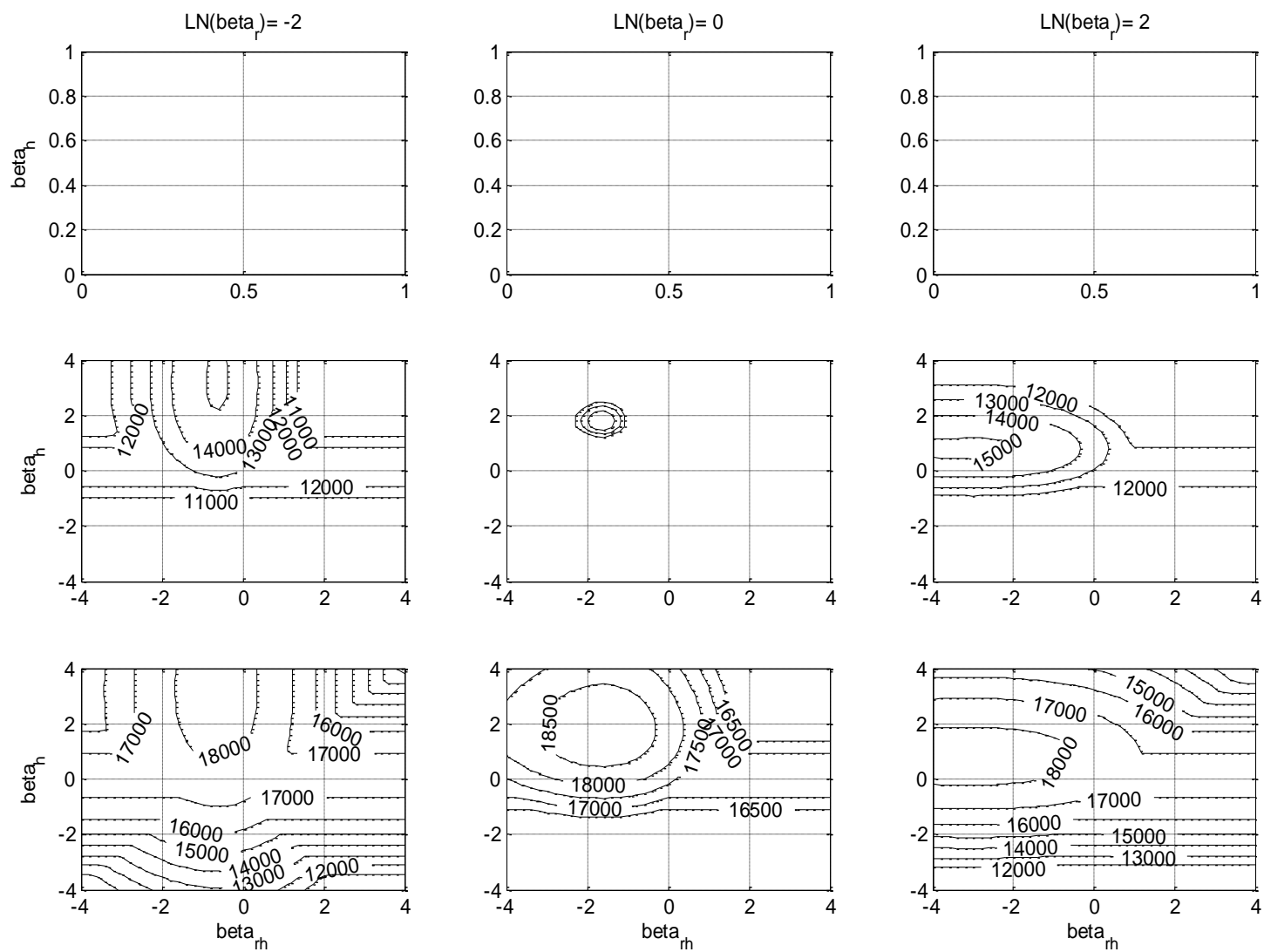


Figure A-93: Maximum objective function score.

Conclusions

The human sensitivity indicates the human ability to distinguish between true targets (signal) and false targets (noise) and improves the performance of the human in a human-robot system.

In the HO collaboration level the increase in the human sensitivity will increase the probability of hit and the objective function score.

The human sensitivity influence directly the human performance and by that the task time. In the HO-Rr and HO-R collaboration level the human sensitivity have negligible influence on the system probability of hit, for low β_r values. For normal and high values of β_r the system probability of hit increases with the increase in the human sensitivity. The task time reduces with the increase in the human sensitivity and the objective function score increase with the increase in the human sensitivity. The maximum score of the objective function increase with the increase in the robot sensitivity. The optimal values of β_h and β_{rh} do not changed with the increase in the human sensitivity.

Increase in human sensitivity increase the best collaboration level zone dominated by the HO, HO-Rr and HO-R collaboration levels and reduce the zone dominated by the R collaboration level.

10.1.6 Analysis of V_{AR}

The payoff ratio, V_{AR} , represent the type of the task through the value ratio of V_{FA} and V_H . High payoff ratio corresponds to high false alarm cost and low hit reward. Low payoff ratio corresponds to low false alarm cost and high hit reward. Task with high payoff ratios will have less tolerance for false alarms and less rewarding for hits. Task with low payoff ratios will be very rewarding for hits and tolerance for false alarms. The parameters in the analysis were determined to be: $N=1000$ objects; the target probability was set to $P_s=0.5$; $V_H=50$; $V_C=-2$ and $V_t=-2000 \text{ hr}^{-1}$. The human sensitivity was set to $d'_h=2$ and the robot sensitivity was set to $d'_r=2$. The decision time for all human time parameters was determined to be $t_D=5 \text{ s/object}$ and the human motoric time was set to $t_M=2 \text{ s/(detected object)}$. The robot time was set to $t_r=0.01 \text{ s/object}$.

The payoff ratio influence only the false alarm cost and the objective function score, hence the HO probability of hit and the task time are not effected by the payoff ratio value. The probability of hit and the task time are identical to those shown earlier.

HO collaboration level

Figure A-94 shows the objective function score as a function of the human sensitivity and human likelihood ratios, β_h , for different payoff ratio values ($V_{AR} = 0.1, 1, 10$). The objective function score decrease with the increase in the payoff ratio since the cost of the false alarms is reduced. For all payoff ratio values, the objective function score increase with the increase in the human sensitivity. The β_h value of the objective function maximum score is increasing with the increase in the payoff ratio for all human sensitivities.

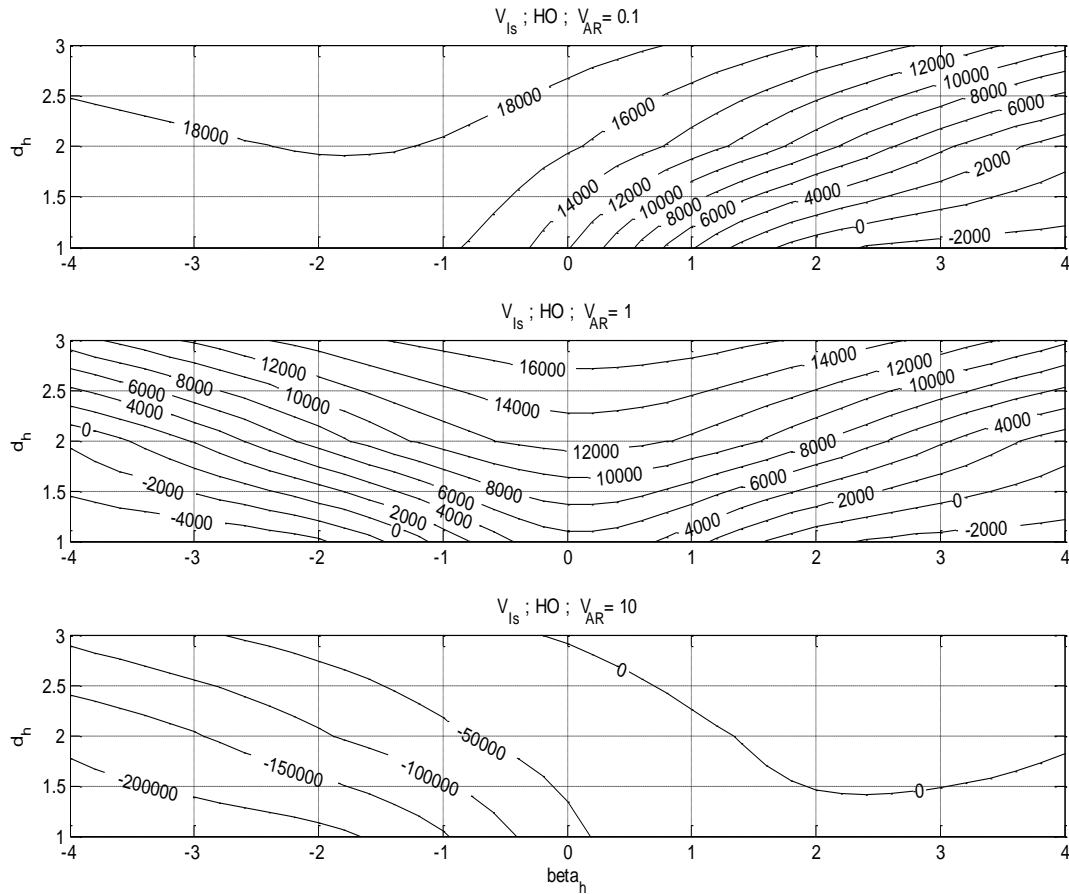


Figure A-94: Objective function score.

R collaboration level

The same phenomena that were found for the objective function behavior in the HO collaboration level are shown in the R collaboration level (Figure A-95).

The objective function score decrease with the increase in the payoff ratio since the cost of the false alarms is reduced. For all payoff ratio values, the objective function score increase with the increase in the human sensitivity. The β_h value of the objective function maximum score is increasing with the increase in the payoff ratio for all human sensitivities.

HO-Rr collaboration level

Figure A-96 shows the system objective function for different β_h , β_{rh} , for β_r equal -2 (left column), 0 (middle column) and +2 (right column) and for payoff ratio equal to 0.1 (upper row), 1 (middle row) and 10 (lower row).

Increase in payoff ratio will decrease the objective function score due to the increase in the false alarm cost (Figure A-96). The values of β_h and β_{rh} of the maximum objective function score is increased with increase in the payoff ratio in order to decrease the number of marked objects and thus reduce the false alarm cost.

For low β_r values the increase in the value of β_{rh} is faster than the increase in the value of β_h . This could be explained by the small number of objects marked by the human (of objects that were not marked by the robot before) in comparison to the number of objects marked by the robot and there for the influence of β_{rh} on the objective function score is grater than β_h and the

number of objects already marked by the robot must be reduced more than the number of objects that were marked firstly by the human.

For high β_r values the increase in the value of β_h is faster than the increase in the value of β_{rh} since the number of objects marked by the robot is few and the influence of β_{rh} is little.

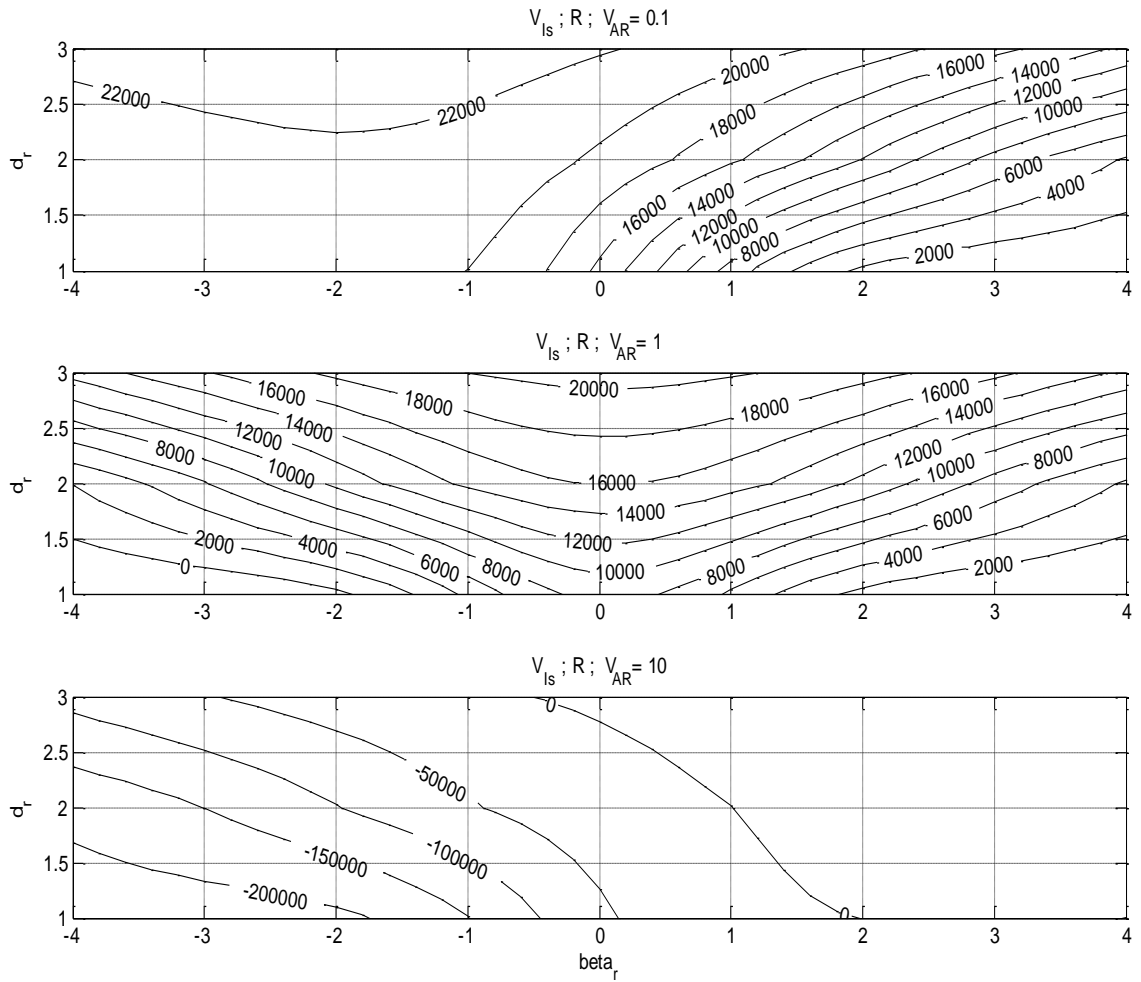


Figure A-95: Objective function score.

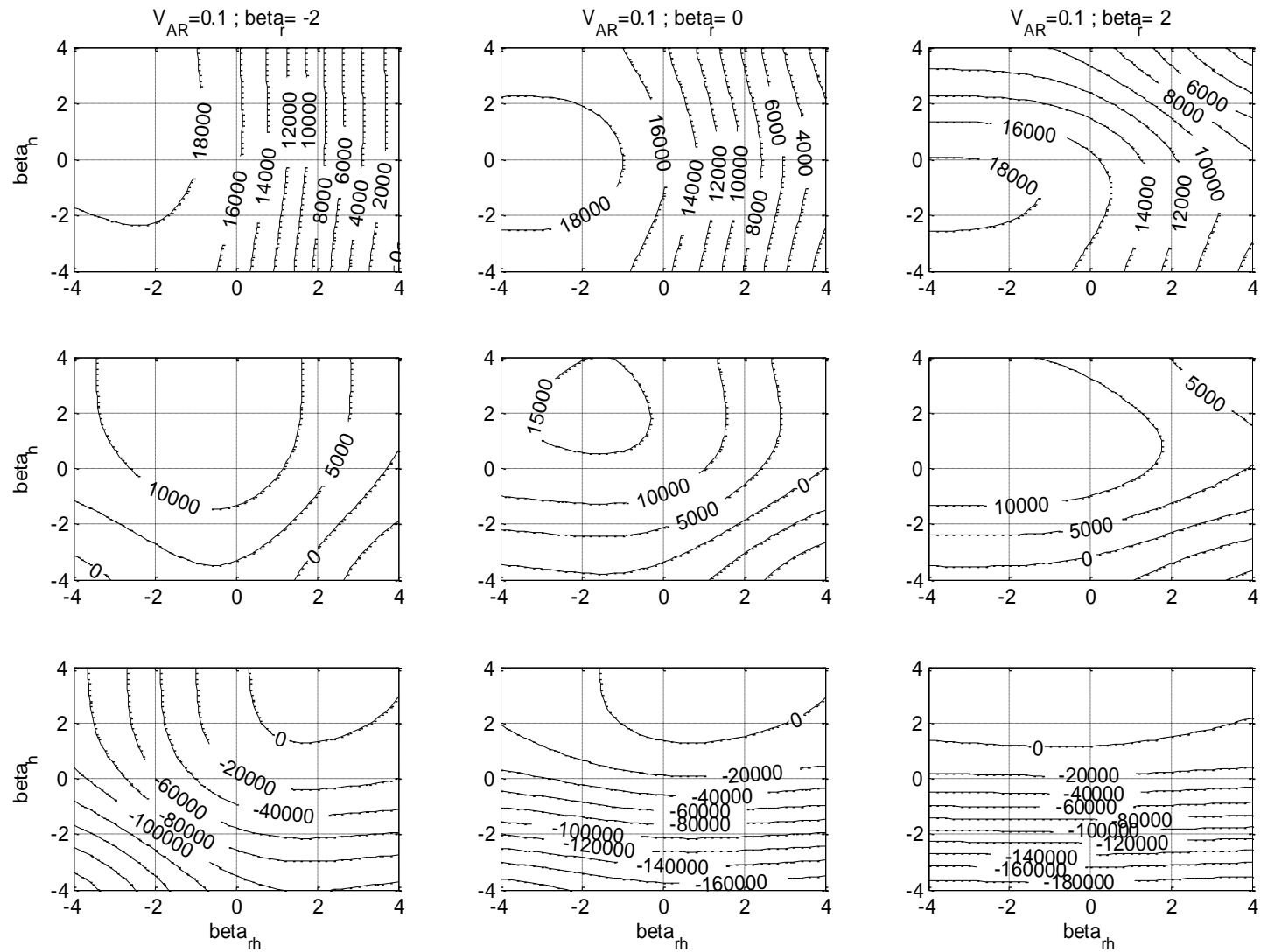


Figure A-96: Objective function score.

HO-Rr collaboration level

Figure A-97 shows the system objective function for different β_h , β_{rh} , for β_r equal -2 (left column), 0 (middle column) and +2 (right column) and for payoff ratio equal to 0.1 (upper row), 1 (middle row) and 10 (lower row).

Increase in payoff ratio will decrease the objective function score due to the increase in the false alarm cost (Figure A-97). The values of β_h and β_{rh} of the maximum objective function score is increased with increase in the payoff ratio in order to decrease the number of marked objects and thus reduce the false alarm cost.

For low β_r values the increase in the value of β_{rh} is faster than the increase in the value of β_h . This could be explained by the small number of objects marked by the human (of objects that were not marked by the robot before) in comparison to the number of objects marked by the robot and there for the influence of β_{rh} on the objective function score is greater than β_h and the number of objects already marked by the robot must be reduced more than the number of objects that were marked firstly by the human.

For high β_r values the increase in the value of β_h is faster than the increase in the value of β_{rh} since the number of objects marked by the robot is few and the influence of β_{rh} is little.

Best Collaboration Level

Figure A-98 shows the system objective function for different β_h , β_{rh} , for β_r equal -2 (left column), 0 (middle column) and +2 (right column) and for payoff ratio equal to 0.1 (upper row), 1 (middle row) and 10 (lower row).

The increases in the payoff ratio is reducing the objective function score for all four collaboration levels and change the domination zones of each collaboration level. For low β_r values the domination zone of R collaboration level is decreased with the increase in the payoff ratio and the domination zones of HO and HO-Rr collaboration levels increase. For high β_r values the domination zone of R collaboration level is increase with the increase in the payoff ratio and the domination zones of HO and HO-R collaboration levels decrease. The HO-Rr collaboration level is not appearing as best collaboration level for high β_r values.

Figure A-99 shows the maximum objective function score as a combination of all four collaboration levels for different β_h , β_{rh} for β_r equal -2 (left column), 0 (middle column) and +2 (right column) and for payoff ratio equal to 0.1 (upper row), 1 (middle row) and 10 (lower row). The increase in the human sensitivity decreases the objective function score on the entire area and decrease the value of the maximum score. The values of β_h and β_{rh} of the maximum objective function score is increased with increase in the payoff ratio in order to decrease the number of marked objects and thus reduce the false alarm cost.

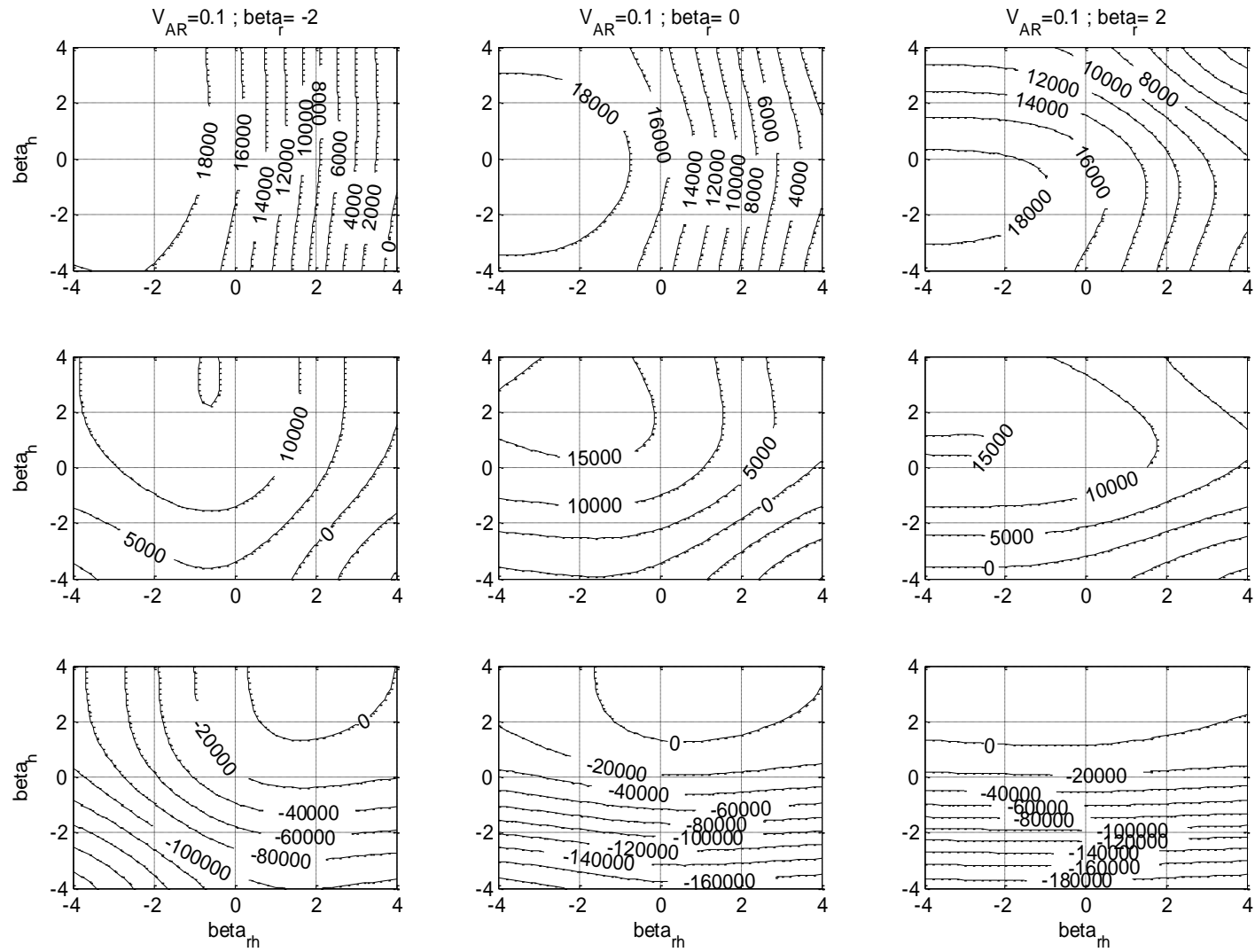


Figure A-97: Objective function score.

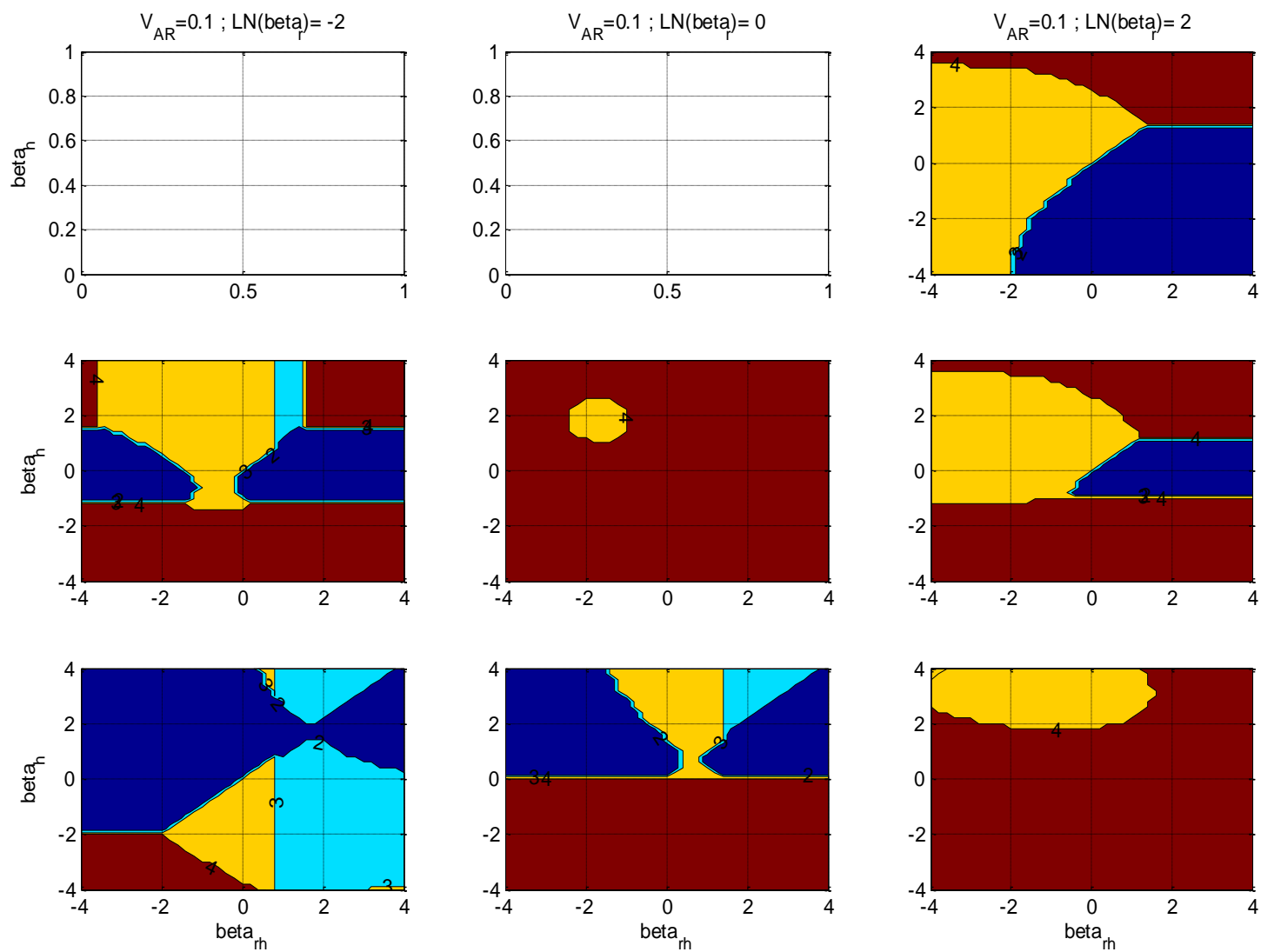


Figure A-98: Best collaboration level.

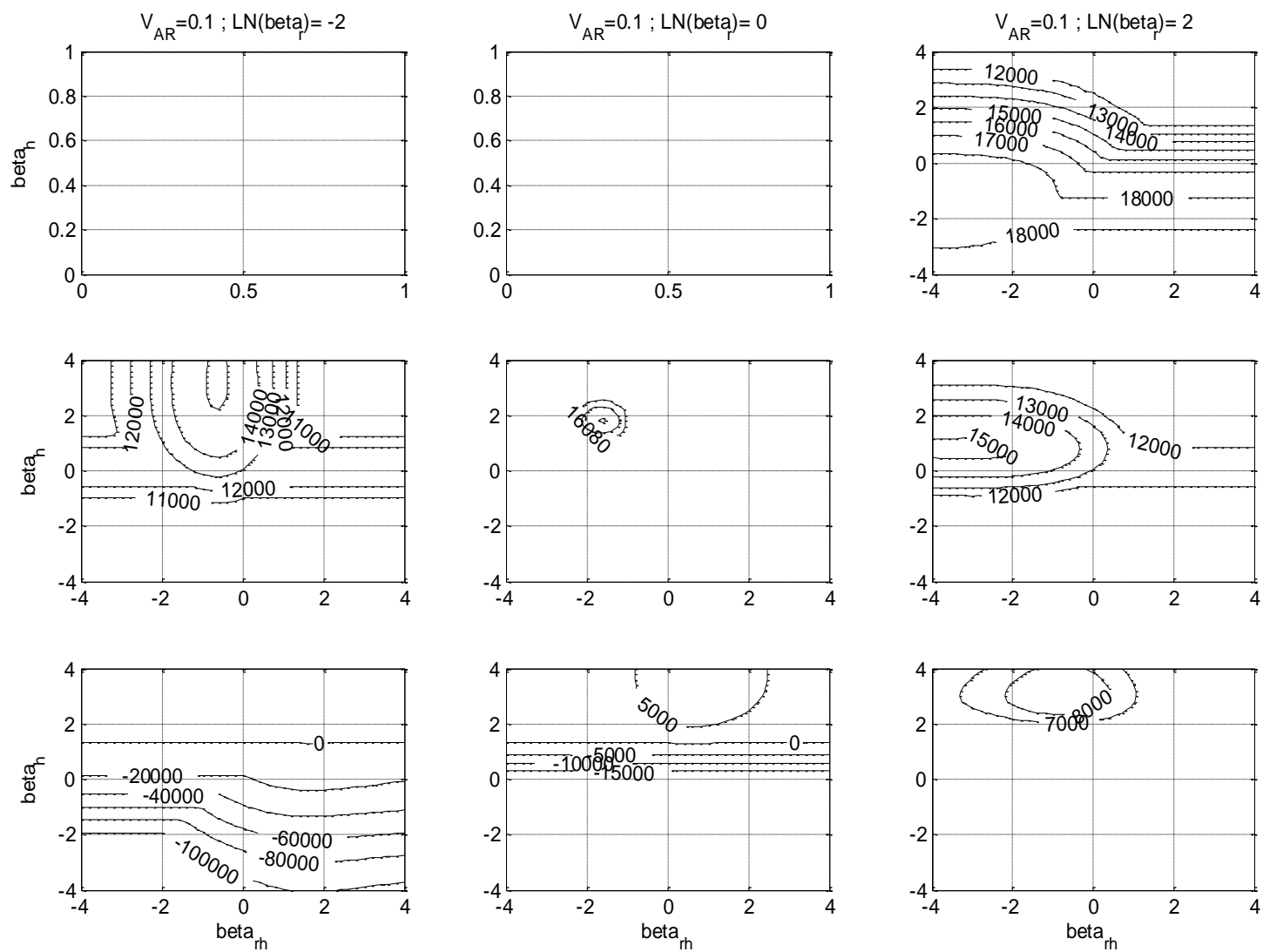


Figure A-99: Maximum objective function score.

Conclusions

The payoff ratio, V_{AR} , represent the type of the task through the value ratio of V_{FA} and V_H . High payoff ratio corresponds to high false alarm cost and low hit reward. Low payoff ratio corresponds to low false alarm cost and high hit reward. Task with high payoff ratios will have less tolerance for false alarms and less rewarding for hits. Task with low payoff ratios will be very rewarding for hits and tolerance for false alarms.

For all collaboration levels the objective function score decrease with the increase in the payoff ratio since the cost of the false alarms is reduced. The optimal β_h value of the objective function maximum score is increasing with the increase in the payoff ratio.

The optimal β_h and β_{th} values of the maximum objective function score is increased with increase in the payoff ratio in order to decrease the number of marked objects and thus reduce the false alarm cost.

10.1.7 Analysis of V_H and V_{FA}

The reward of a single hit, V_H , is representing the type and quality of identified target. Since the cost of a single false alarm, V_{FA} , is related to V_H through the payoff ratio the increase in V_H , will increase V_{FA} and therefore the objective function will increase although not is the same proportion.

10.1.8 Analysis of V_C and V_t

The operational cost of one of object recognition (hit or false alarm), V_C , is representing the cost required to perform a single detection. Increase in V_C , will increase the operational cost value and decrease the objective function score in proportion to the number of objects recognized for all collaboration levels.

The time cost, V_t , represent the time expenses in target recognition task. Increase in V_t , will increase the operational cost value and decrease the objective function score.

10.1.9 Analysis of t_D and t_M

Increase in the decision time, t_D , will increase the operational cost value and decrease the objective function score in proportion to the number of objects equally for the HO, HO-Rr and HO-R collaboration level. On the R collaboration level the decision time have no influence. Increase in the motoric time, t_M , will increase the operational cost value and decrease the objective function score in proportion to the number of human marks or cancellation of the robot marks, depends if the collaboration level is HO, HO-Rr or HO-R. The motoric time have no influence on the R collaboration level.

Appendix VII: The experimental simulator program

HOMarkalone2.m: The main program for the HO collaboration level

```
% in this program the HO mark by himself without the aid of the robot.
clear
clc
close all

sn=input('subject s/n= ');
%sn=2
add=input('add= ');
sub=input('sub= ');
% Call for the tutorial
exptutorial

exlearningHO

scrsz = get(0,'ScreenSize');
A=figure('Position',[1 1 scrsz(3) scrsz(4)])

tic
t2=[cputime,toc,0,0,0,0,0];
HOlogger=[];
allimagesdb=[];
scorestr='SCORE: 0';
ttstr=['Detection: 0'];
tfstr=['False: 0'];
ftstr=['Missed: 0'];
corner=55
score=0;

% imgorder=[11 38 71 90 112 25 8 65 5 40 68 7 33 67 10 61 104 74 95 91 109 44 82 23 14 22 49 92 29 81 30
56 64 60 88];

% Block - the list of all images (about 60 images per block)
load Block

tcross=zeros(21);
tcross(1:21,10:12)=1;
tcross(10:12,1:21)=1;

% Generating 3 blocks with random image order for each subject
% at the end the image order vector called imglist
for j=1:3
    temp_Block=Block(j,:);
    Block_L=length(temp_Block);
    for k=1:Block_L
        temp_size=length(temp_Block);
        randimgplace=floor(rand*temp_size)+1;
        imgorder((j-1)*Block_L+k)=temp_Block(randimgplace);
        if randimgplace==1
            temp_Block=temp_Block(2:temp_size);
        elseif randimgplace==temp_size
            temp_Block=temp_Block(1:temp_size-1);
        else
            temp_Block=[temp_Block(1:randimgplace-1),temp_Block(randimgplace+1:temp_size)];
        end
    end
end
```

```

end

imgorder_L=length(imgorder)

%reading the images directory
ImageDirs=['C:\My Documents\Matlab\Experiments2000\Melons\IMAGES\']
%ImageDirs=['f:\matlab\work\Experiments2000\melons\images\']

load melondatabase

% the format of t2 is: [cputime,time,x,y,fn,command type,stage]
% in command type: 0 - no command, 1 - inserting to database already marked melon,
% 2 - detecting and inserting to database, 3 - deleting detected melon, 4 - unknown yet.
t2=[t2;cputime,toc,0,0,0,0,1];
signs(1:21,1:3)=1;

%Do the following loop for all directories that contain images
for dr=1:1
    % Get filenames of images
    % d=dir(ImageDirs(dr,:));
    % [NumberOfFiles,Dummy]=size(d);
    % NumberOfFiles

    for i=1:imgorder_L
        A2=[];
        imagenumber=imgorder(i);
        mdn=(find(melondatabase(:,4)==imagenumber)); % the lines in the melon DB of the current image
        true_no=length(mdn); %number of true targets
        imgnumbstr=num2str(imagenumber);
        fn=['melon day ',imgnumbstr,'.jpg'];

t2=[t2;cputime,toc,0,0,imagenumber,0,2];
% A=original image
        A=imread(fn,'jpg');
        r=double(A(:,,1))./255;
        g=double(A(:,,2))./255;
        b=double(A(:,,3))./255;
        imagesize=size(r);
        imgsize=[0 0 imagesize];
        rnew=r;
        gnew=g;
        bnew=b;
        A2(:,,1)=rnew;
        A2(:,,2)=gnew;
        A2(:,,3)=bnew;

t2=[t2;cputime,toc,0,0,imagenumber,0,3];

% Call for subroutine which mark the true melons
%Show_targets

t2=[t2;cputime,toc,0,0,imagenumber,0,4];

        figure(2)
        imshow(A2)
        set(A,'Position',[1 1 scrsz(3) scrsz(4)])
%        imshow(rnew,gnew,bnew)
        h = uicontrol('Style','pushbutton','String','NEXT','FontWeight','bold','Position',[2,92,90,400]);
%        h2=uicontrol('Style','text',
'String',scorestr,'FontWeight','bold','HorizontalAlignment','left','Position',[135,10,90,45]);
%        h3=uicontrol('Style','text','String',ttstr,'FontWeight','bold','Position',[255,10,90,45]);

```

```

%      h6=uicontrol('Style','text','String',tfstr,'FontWeight','bold','Position',[380,10,90,45]);
%      h7=uicontrol('Style','text','String',ftstr,'FontWeight','bold','Position',[505,10,90,45]);
%      h8=uicontrol('Style','text','String','Maximum: 1170','FontWeight','bold','Position',[10,10,90,45]);

t2=[t2;cputime,toc,0,0,imagenumber,0,5];

% Subroutine in which the HO select and deselect the melon marks
HODetectalone2

% end
end
end

t2=[t2;cputime,toc,0,0,0,0,99];

snstr=num2str(sn);
eval(['save Mmarkalonsubject' snstr ' t2 HOlogger allimagesdb score'])

% call for subroutine expfinal
expfinal

```

HODetectalone2.m: interface subroutine which display the human actions in the HO collaboration level. Called from HOMarkalone2.m

```

clear imagedatabase
clear paralelimagedb

% the format of paralelimagedb is: x and y coordination of the mark done by the robot (without inserting
% to the DB), the image number, time it was issued (0 for detected by the robot), and the status.

% imagedatabase is the melon inserted by the HO.
% the format of imagedatabase is: x and y coordination of the mark, the image number,
% time it was issued (0 for detected by the robot), and the status (0 for detected by the robot,
% 1 for detected by the robot and inserted to the DB by the HO, 2 for detected by the HO and 3
% for deleted by the HO.
imagedatabase=[];

%gx=999;
gy=999;
while gy>0
    [gy gx]=ginput(1)

t2=[t2;cputime,toc,gx,gy,imagenumber,4,11];

% the format of HOlogger is: the image number, x and y coordination of the mark, and
% the time it was issued
HOlogger=[HOlogger;imagenumber,gx,gy,toc];

if gx>=0 & gy>=0 & gx<imagesize(1) & gy<imagesize(2)
    x=round(gx)
    y=round(gy)
    closetarget=[];

% Check if the HO inserted points and if the new mark close to them
if sum(size(imagedatabase))>0
    dxy=[abs(x-imagedatabase(:,1)),abs(y-imagedatabase(:,2))]
    sumline=sum((dxy<55));
    closetarget=find(sumline==2);

```

```

        imagedbdim=size(imagedatabase);
    end

% this part delete the target and line from DB
    if sum(closetarget)>0
        x=imagedatabase(closetarget(1),1);
        y=imagedatabase(closetarget(1),2);

% reorganizing the DB of imagedatabase
        if imagedbdim(1)==closetarget(1)
            imagedatabase=imagedatabase(1:closetarget(1)-1,:);
        else
            imagedatabase(closetarget(1):imagedbdim(1)-1,:)=imagedatabase(closetarget(1)+1:imagedbdim(1),:);
            imagedatabase=imagedatabase(1:imagedbdim(1)-1,:);
        end

        t2=[t2;cputime,toc,x,y,imagenumber,3,11];
% subroutine which unmark the melon detected
        unmarksign
        A2(:,1)=rnew;
        A2(:,2)=gnew;
        A2(:,3)=bnew;
        imshow(A2)
        set(l,'Position',[1 1 scrsz(3) scrsz(4)])
%     imshow(rnew,gnew,bnew)
        h = uicontrol('Style','pushbutton','String','NEXT','FontWeight','bold','Position',[2,92,90,400]);
%     h2=uicontrol('Style','text',
'String',scorestr,'FontWeight','bold','HorizontalAlignment','left','Position',[135,10,90,45]);
%     h3=uicontrol('Style','text','String',ttstr,'FontWeight','bold','Position',[255,10,90,45]);
%     h6=uicontrol('Style','text','String',tfstr,'FontWeight','bold','Position',[380,10,90,45]);
%     h7=uicontrol('Style','text','String',ftstr,'FontWeight','bold','Position',[505,10,90,45]);
%     h8=uicontrol('Style','text','String','Maximum: 1170','FontWeight','bold','Position',[10,10,90,45]);

% this part mark and insert new melon by the HO
        else
            imagedatabase=[imagedatabase;x,y,imagenumber,toc,2];
            t2=[t2;cputime,toc,x,y,imagenumber,2,11];
% subroutine wich mark the melon detected
            MARKSIGN
            A2(:,1)=rnew;
            A2(:,2)=gnew;
            A2(:,3)=bnew;
            imshow(A2)
            set(l,'Position',[1 1 scrsz(3) scrsz(4)])
%     imshow(rnew,gnew,bnew)
            h = uicontrol('Style','pushbutton','String','NEXT','FontWeight','bold','Position',[2,92,90,400]);
%     h2=uicontrol('Style','text',
'String',scorestr,'FontWeight','bold','HorizontalAlignment','left','Position',[135,10,90,45]);
%     h3=uicontrol('Style','text','String',ttstr,'FontWeight','bold','Position',[255,10,90,45]);
%     h6=uicontrol('Style','text','String',tfstr,'FontWeight','bold','Position',[380,10,90,45]);
%     h7=uicontrol('Style','text','String',ftstr,'FontWeight','bold','Position',[505,10,90,45]);
%     h8=uicontrol('Style','text','String','Maximum: 1170','FontWeight','bold','Position',[10,10,90,45]);

        end

    end

end

t2=[t2;cputime,toc,0,0,imagenumber,3,31];

```

```

% call for subroutine which calculate the image score
imagescore

t2=[t2;cputime,toc,0,0,imagenumber,3,32];
% call for display score figure
scorefigure

t2=[t2;cputime,toc,0,0,imagenumber,3,33];

allimagesdb=[allimagesdb;imagedatabase];

t2=[t2;cputime,toc,0,0,imagenumber,3,34];

```

HOMark2.m: The main program for the HO-Rr collaboration level

```

% HO-Rr collaboration level

clear
clc
close all
load FAdatabase

sn=input('subject s/n= ');
add=input('add= ');
sub=input('sub= ');
robothit=input('robot hit= ');
robotfalse=0;
if robothit==0.9
    robotfalse=12;
end
if robothit==0.5
    robotfalse=106;
end
% Call for the tutorial
exptutorial
exlearningHORr

%robothit=0.8 % Robot hit rate
robot_all_tar=[]
HOlogger=[];
allimagesdb=[];
scorestr='SCORE: 0';
ttstr=['Detection: 0'];
tfstr=['False: 0'];
ftstr=['Missed: 0'];
corner=55
score=0;

scrsz = get(0,'ScreenSize');
K=figure('Position',[1 1 scrsz(3) scrsz(4)])

tic
t2=[cputime,toc,0,0,0,0,0];

%imgorder=[11 38 71 90 77 57 79 97 27 2 4 9 34 31 58 19 46 99 17 42 72 16 83 110 21 24 39 43 47 50 101 105
96 102 6 69 75 89 36];

```

```

% Block - the list of all images (about 60 images per block)
load Block

tcross=zeros(21);
tcross(1:21,10:12)=1;
tcross(10:12,1:21)=1;

% Generating 3 blocks with random image order for each subject
% at the end the image order vector called imglist
for j=1:3
    temp_Block=Block(j,:);
    Block_L=length(temp_Block);
    for k=1:Block_L
        temp_size=length(temp_Block);
        randimgplace=floor(rand*temp_size)+1;
        imgorder((j-1)*Block_L+k)=temp_Block(randimgplace);
        if randimgplace==1
            temp_Block=temp_Block(2:temp_size);
        elseif randimgplace==temp_size
            temp_Block=temp_Block(1:temp_size-1);
        else
            temp_Block=[temp_Block(1:randimgplace-1),temp_Block(randimgplace+1:temp_size)];
        end
    end
end
% random

imgorder_L=length(imgorder)

%reading the images directory
ImageDirs=['C:\My Documents\Matlab\Experiments2000\Melons\IMAGES\']
%ImageDirs=['D:\users\avital\phd\Experiments2000\melons\images\']
%ImageDirs=['f:\matlab\work\Experiments2000\melons\images\']

load melondatabase

% the format of t2 is: [cputime,time,x,y,fn,command type,stage]
% in command type: 0 - no command, 1 - inserting to database already marked melon,
% 2 - detecting and inserting to database, 3 - deleting detected melon, 4 - unknown yet.
t2=[t2;cputime,toc,0,0,0,0,1];
signs(1:21,1:3)=1;

f_targets=[]; % vector that contains the numbers of all the false images found by the robot in all the images
temp_f_targets=[]; %a vector that contains the numbers of all the images in Block
st=0;
f_index=0;
    f=1+(118-1)*rand;
    f_num=round(f);

while st==0
    if length(temp_f_targets)==robotfalse
        st=1;
    end
    if st==0
        fnd=0;
        temp_f_targets_L=length(temp_f_targets);
        for i=1: temp_f_targets_L %search for num in vector temp
            if temp_f_targets(i)==f_num
                fnd=1;
            end
        end
    end
end

```

```

end

if fnd==1
    f=1+(118-1)*rand;
    f_num=round(f);
else
    temp_f_targets=[temp_f_targets;f_num];
end
end % if stop==0
end % while stop==0
temp_f_targets_L=length(temp_f_targets);
for i=1: temp_f_targets_L
    f_index=temp_f_targets(i);
    f_targets=[f_targets;FAdatabase(f_index,1:4)];
end

f_targets_L=length(f_targets);
%Do the following loop for all directories that contain images
for dr=1:1
    % Get filenames of images
    % d=dir(ImageDirs(dr,:));
    % [NumberOfFiles,Dummy]=size(d);
    % NumberOfFiles

    for i=1:imgorder_L
        A2=[];
        % paralelimagedb=[];
        imagenumber=imgorder(i);
        mdn=(find(melondatabase(:,4)==imagenumber)); % the lines in the melon DB of the current image
        fdn=(find(f_targets(:,4)==imagenumber)); % the lines in the melon DB of the current image
        true_no=length(mdn); %number of true targets
        Img_R_hit=rand(1,true_no); % the robot hit rate for each melon in the image

        imgnumbstr=num2str(imagenumber);
        fn=['melon day ',imgnumbstr,'.jpg'];

        t2=[t2;cputime,toc,0,0,imagenumber,0,2];
        % A=original image
        A=imread(fn,'jpg');
        r=double(A(:,1))/255;
        g=double(A(:,2))/255;
        b=double(A(:,3))/255;
        imagesize=size(r);
        imgsize=[0 0 imagesize];
        rnew=r;
        gnew=g;
        bnew=b;

        t2=[t2;cputime,toc,0,0,imagenumber,0,3];

        robot_target_n=[];
        robot_f_target_n=[];
        if true_no>0
            robot_target_n=find(Img_R_hit<robothit); % The melons in the image whom succeed the robot hit rate
            robot_all_tar=[robot_all_tar;melondatabase(mdn(robot_target_n),:);
            for j=1:length(robot_target_n)
                x=melondatabase(mdn(robot_target_n(j)),2);
                y=melondatabase(mdn(robot_target_n(j)),3);

% subroutine which mark the melon detected

```

```

        framesign
    end
end

    for w=1:length(fdn)
        x=f_targets(fdn(w),2);
        y=f_targets(fdn(w),3);
% subroutine which mark the false alarms
        framesign
    end
% robot_FA=find(robot_false(:,1)==imgorder(i); % robot_false - the list of all robot false alarms in all the
images
% if robot_FA>0
% img_robot_FA=find(rand(1)<1-robothit-0.05); % The false alarms in the image whom succeed the
robot hit rate
% robot_all_FA=[robot_all_FA;robot_false(robot_FA,:)];
% for j=1:length(robot_target_n)
% x=robot_false(robot_FA(j),2);
% y=robot_false(robot_FA(j),3);
%
% subroutine which mark the false alarms detected
% marksign
% end
% end

t2=[t2;cputime,toc,0,0,imagenumber,0,4];

    A2(:,1)=rnew;
    A2(:,2)=gnew;
    A2(:,3)=bnew;

% figure(2)
    imshow(A2)
    set(K,'Position',[1 1 scrsz(3) scrsz(4)])
% imshow(rnew,gnew,bnew)
    h = uicontrol('Style','pushbutton','String','NEXT','FontWeight','bold','Position',[2,92,90,400]);
% h2=uicontrol('Style','text',
'String',scorestr,'FontWeight','bold','HorizontalAlignment','left','Position',[135,10,90,45]);
% h3=uicontrol('Style','text','String',ttstr,'FontWeight','bold','Position',[255,10,90,45]);
% h6=uicontrol('Style','text','String',tfstr,'FontWeight','bold','Position',[380,10,90,45]);
% h7=uicontrol('Style','text','String',ftstr,'FontWeight','bold','Position',[505,10,90,45]);
% h8=uicontrol('Style','text','String','Maximum: 1170','FontWeight','bold','Position',[10,10,90,45]);

t2=[t2;cputime,toc,0,0,imagenumber,0,5];

% Subroutine in which the HO select and deselect the melon marks
    HOdetect2

% end
end
end

t2=[t2;cputime,toc,0,0,0,0,99];

snstr=num2str(sn);
eval(['save Mmarksubject' snstr ' t2 HOlogger allimagesdb robot_all_tar score f_targets'])

% call for subroutine expfinal
expfinal

```

HOdetect2.m: interface subroutine which display the human actions in the HO-Rr collaboration level. Called from HOMark2.m

```
clear imagedatabase
clear paralelimgedb

% the format of paralelimgedb is: x and y coordination of the mark done by the robot (without inserting
% to the DB), the image number, time it was issued (0 for detected by the robot), and the status.
paralelimgedb=[];

if ~isempty(robot_target_n) %inserting true targets the robot detected
    paralelimgedb=[paralelimgedb;melondatabase(mdn(robot_target_n),2:4)];
    paralelimgedb(:,4:5)=0;
end
if ~isempty(fdn) % inserting false alarms the robot detected
    for w2=1:length(fdn)
        paralelimgedb=[paralelimgedb;f_targets(fdn(w2),2:4),0 0];
    end
    % paralelimgedb(:,4:5)=0;
end
%if ~isempty(img_robot_FA)
% imagedatabase=[imagedatabase;robot_false(robot_FA,2:4)];
% imagedatabase(:,4:5)=0;
%end

% imagedatabase is the melon inserted by the HO.
% the format of imagedatabase is: x and y coordination of the mark, the image number,
% time it was issued (0 for detected by the robot), and the status (0 for detected by the robot,
% 1 for detected by the robot and inserted to the DB by the HO, 2 for detected by the HO and 3
% for deleted by the HO.
imagedatabase=[];

%gx=999;
%gy=999;
while gy>0
    [gy gx]=ginput(1);

t2=[t2;cputime,toc,gx,gy,imagenumber,4,1 1];

% the format of HOlogger is: the image number, x and y coordination of the mark, and
% the time it was issued
HOlogger=[HOlogger;imagenumber,gx,gy,toc];

if gx>=0 & gy>=0 & gx<imagesize(1) & gy<imagesize(2)
    x=round(gx);
    y=round(gy);
    closetarget=[];
    closetomark=[];

% Check if the HO inserted points and if the new mark close to them
if sum(size(imagedatabase))>0
    dxy=[abs(x-imagedatabase(:,1)),abs(y-imagedatabase(:,2))];
    sumline=sum((dxy<55));
    closetarget=find(sumline==2);
    imagedbdim=size(imagedatabase);
end

% Check if the new mark close to the marks made by the computer
if sum(size(paralelimgedb))>0
    fdxy=[abs(x-paralelimgedb(:,1)),abs(y-paralelimgedb(:,2))];
```

```

fsumline=sum((fdxy<55));
closetomark=find(fsumline==2);
fimagedbdim=size(paralelimageb);
end

% this part delete the target and line from DB
if sum(closetarget)>0
    x=imagedatabase(closetarget(1),1);
    y=imagedatabase(closetarget(1),2);

% reorganizing the DB of imagedatabase
    if imagedbdim(1)==closetarget(1)
        imagedatabase=imagedatabase(1:closetarget(1)-1,:);
    else
        imagedatabase(closetarget(1):imagedbdim(1)-1,:)=imagedatabase(closetarget(1)+1:imagedbdim(1),:);
        imagedatabase=imagedatabase(1:imagedbdim(1)-1,:);
    end

% reorganizing the DB of paralelimageb
    if sum(closetomark)>0
        if fimagedbdim(1)==closetomark(1)
            paralelimageb=paralelimageb(1:closetomark(1)-1,:);
        else
            paralelimageb(closetomark(1):fimagedbdim(1)-1,:)=paralelimageb(closetomark(1)+1:fimagedbdim(1),:);
            paralelimageb=paralelimageb(1:fimagedbdim(1)-1,:);
        end
    end

    t2=[t2;cputime,toc,x,y,imagenumber,3,1 1];
% subroutine which unmark the melon detected
    unmarksign
    imshow(rnew,gnew,bnew)
    set(K,'Position',[1 1 scrsz(3) scrsz(4)])
    h = uicontrol('Style','pushbutton','String','NEXT','FontWeight','bold','Position',[2,92,90,400]);

% this part marking the cross sight and inserting it to the database
elseif sum(closetomark)>0
    x=paralelimageb(closetomark(1),1);
    y=paralelimageb(closetomark(1),2);
    t2=[t2;cputime,toc,x,y,imagenumber,1,1 1];
    imagedatabase=[imagedatabase;x,y,imagenumber,toc,1];
% subroutine wich mark cross on the melon detected
    crosssign
    imshow(rnew,gnew,bnew)
    set(K,'Position',[1 1 scrsz(3) scrsz(4)])
    h = uicontrol('Style','pushbutton','String','NEXT','FontWeight','bold','Position',[2,92,90,400]);

% this part mark and insert new melon by the HO
else
    imagedatabase=[imagedatabase;x,y,imagenumber,toc,2];
    t2=[t2;cputime,toc,x,y,imagenumber,2,1 1];
% subroutine wich mark the melon detected
    marksign
    imshow(rnew,gnew,bnew)
    set(K,'Position',[1 1 scrsz(3) scrsz(4)])
    h = uicontrol('Style','pushbutton','String','NEXT','FontWeight','bold','Position',[2,92,90,400]);
end

end
end

```

```

end

t2=[t2;cputime,toc,0,0,imagenumber,3,31];
% call for subroutine which calculate the image score
imagescore

t2=[t2;cputime,toc,0,0,imagenumber,3,32];
% call for display score figure
scorefigure

t2=[t2;cputime,toc,0,0,imagenumber,3,33];

allimagesdb=[allimagesdb;imagedatabase];

t2=[t2;cputime,toc,0,0,imagenumber,3,34];

```

HOMarkandinsert2.m: The main program for the HO-R collaboration level

```

% HO-R collaboration level

clear
clc
close all
load FAdatabase
sn=input('subject s/n= ');

add=input('add= ');
sub=input('sub= ');
robothit=input('robot hit= ');
% Call for the tutorial
exptutorial
exlearningHOR

if robothit==0.9
    robotfalse=12;
end
if robothit==0.5
    robotfalse=106;
end

%robothit=0.8 % Robot hit rate
robot_all_tar=[]
HOlogger=[];
allimagesdb=[];
scorestr='SCORE: 0';
ttstr=['Detection: 0'];
tfstr=['False: 0'];
ftstr=['Missed: 0'];
corner=55
score=0;

scrsz = get(0,'ScreenSize');
l=figure('Position',[1 1 scrsz(3) scrsz(4)])

tic

```

```

t2=[cputime,toc,0,0,0,0,0];

%imgorder=[11 38 71 90 26 32 66 86 106 20 28 53 3 35 63 45 73 94 12 76 108 15 84 62 52 13 48 54 98 18 51
78 59 41 107 70 80 103 93];
%imgorder=[91 10 43 101 89 106 73 12 26 32 66 86 106 20 28 53 3 35 63 45 73 94 12 76 108 15 84 62 52 13
48 54 98 18 51 78 59 41 107 70 80 103 93];

% Block - the list of all images (about 60 images per block)
load Block

tcross=zeros(21);
tcross(1:21,10:12)=1;
tcross(10:12,1:21)=1;

% Generating 3 blocks with random image order for each subject
% at the end the image order vector called imglist
for j=1:3
    temp_Block=Block(j,:);
    Block_L=length(temp_Block);
    for k=1:Block_L
        temp_size=length(temp_Block);
        randimgplace=floor(rand*temp_size)+1;
        imgorder((j-1)*Block_L+k)=temp_Block(randimgplace);
    if randimgplace==1
        temp_Block=temp_Block(2:temp_size);
    elseif randimgplace==temp_size
        temp_Block=temp_Block(1:temp_size-1);
    else
        temp_Block=[temp_Block(1:randimgplace-1),temp_Block(randimgplace+1:temp_size)];
    end
    end
    end
    % random

imgorder_L=length(imgorder)

%reading the images directory
ImageDirs=['C:\My Documents\Matlab\Experiments2000\Melons\IMAGES\']
%ImageDirs=['D:\users\avital\phd\Experiments2000\melons\images\']
%ImageDirs=['f:\matlab\work\Experiments2000\melons\images\']

load melondatabase

% the format of t1 is: [cputime,time,x,y,fn,command type,stage]
% in command type: 0 - no command, 1 - inserting to database already marked melon,
% 2 - detecting and inserting to database, 3 - deleting detected melon, 4 - unknown yet.
t2=[t2;cputime,toc,0,0,0,0,1];
signs(1:21,1:3)=1;

f_targets=[]; % vector that contains the numbers of all the false images
temp_f_targets=[]; % a vector that contains the numbers of all the images in Block
st=0;
f_index=0;
f=1+(118-1)*rand;
f_num=round(f);

while st==0
    if length(temp_f_targets)==robotfalse
        st=1;
    end
end

```

```

if st==0
    fnd=0;
    temp_f_targets_L=length(temp_f_targets);
    for i=1: temp_f_targets_L %search for num in vector temp
        if temp_f_targets(i)==f_num
            fnd=1;
        end
    end

    if fnd==1
        f=1+(118-1)*rand;
        f_num=round(f);
    else
        temp_f_targets=[temp_f_targets;f_num];
    end
end % if stop==0
end % while stop==0
temp_f_targets_L=length(temp_f_targets);
for i=1: temp_f_targets_L
    f_index=temp_f_targets(i);
    f_targets=[f_targets;FAdatabase(f_index,1:4)];
end

f_targets_L=length(f_targets);

%Do the following loop for all directories that contain images
for dr=1:1
    % Get filenames of images
    % d=dir(ImageDirs(dr,:));
    % [NumberOfFiles,Dummy]=size(d);
    % NumberOfFiles

    %imgorder(2)=405;%DELETE this line after inspaction
    %imgorder(1)=405;%DELETE this line after inspaction

    for i=1:imgorder_L
        A2=[];

        imagenumber=imgorder(i);
        mdn=(find(melondatabase(:,4)==imagenumber)); % the lines in the melon DB of the current image
        fdn=(find(f_targets(:,4)==imagenumber)); % the lines in the melon DB of the current image
        true_no=length(mdn); %number of true targets
        Img_R_hit=rand(1,true_no); % the robot hit rate for each melon in the image
        imgnumbstr=num2str(imagenumber);
        fn=['melon day ',imgnumbstr,'.jpg'];

        t2=[t2;cputime,toc,0,0,imagenumber,0,2];
        % A=original image
        A=imread(fn,'jpg');
        r=double(A(:,1))/255;
        g=double(A(:,2))/255;
        b=double(A(:,3))/255;
        imagesize=size(r);
        imgsize=[0 0 imagesize];
        rnew=r;
        gnew=g;
        bnew=b;

        t2=[t2;cputime,toc,0,0,imagenumber,0,3];

        robot_target_n=[];
    end
end

```

```

robot_f_target_n=[];
if true_no>0
    robot_target_n=find(Img_R_hit<robothit); % The melons in the image whom succeed the robot hit rate
    robot_all_tar=[robot_all_tar;melondatabase(mdn(robot_target_n,:))];
    for j=1:length(robot_target_n)
        x=melondatabase(mdn(robot_target_n(j)),2);
        y=melondatabase(mdn(robot_target_n(j)),3);

% subroutine which mark the melon detected
        marksign
    end
end

    for w=1:length(fdn)
        x=f_targets(fdn(w),2);
        y=f_targets(fdn(w),3);
% subroutine which mark the false alarms
        marksign
    end

% robot_FA=find(robot_false(:,1)==imgorder(i)); % robot_false - the list of all robot false alarms in all the
images
% if robot_FA>0
%     img_robot_FA=find(rand(1)<1-robothit-0.05); % The false alarms in the image whom succeed the
robot hit rate
%     robot_all_FA=[robot_all_FA;robot_false(robot_FA,:)];
%     for j=1:length(robot_target_n)
%         x=robot_false(robot_FA(j),2);
%         y=robot_false(robot_FA(j),3);
%     end
% subroutine which mark the false alarms detected
%     marksign
%     end
%     end

    t2=[t2;cputime,toc,0,0,imagenumber,0,4];

    A2(:,:,1)=rnew;
    A2(:,:,2)=gnew;
    A2(:,:,3)=bnew;

% figure(2)
    imshow(A2)
    set(1,'Position',[1 1 scrsz(3) scrsz(4)])
% imshow(rnew,gnew,bnew)
    h = uicontrol('Style','pushbutton','String','NEXT','FontWeight','bold','Position',[2,92,90,400]);
%     h2=uicontrol('Style','text',
'String','scorestr','FontWeight','bold','HorizontalAlignment','left','Position',[135,10,90,45]);
%     h3=uicontrol('Style','text','String',ttstr,'FontWeight','bold','Position',[255,10,90,45]);
%     h6=uicontrol('Style','text','String',tfstr,'FontWeight','bold','Position',[380,10,90,45]);
%     h7=uicontrol('Style','text','String',ftstr,'FontWeight','bold','Position',[505,10,90,45]);
%     h8=uicontrol('Style','text','String','Maximum: 1170','FontWeight','bold','Position',[10,10,90,45]);

    t2=[t2;cputime,toc,0,0,imagenumber,0,5];

% Subroutine in which the HO select and deselect the melon marks
    HOdetectandinsert2

% end
end

```

```
end
```

```
t2=[t2;cputime,toc,0,0,0,0,99];
```

```
snstr=num2str(sn);
```

```
eval(['save Mmarkninssubject' snstr ' t2 HOlogger allimagesdb robot_all_tar score f_targets'])
```

```
% call for subroutine expfinal
```

```
expfinal
```

HOdetectandinsert2.m: interface subroutine which display the human actions in the HO-R collaboration level. Called from HOmarkandinsert2.m

```
clear imagedatabase
```

```
clear robotdatabase
```

```
% the format of imagedatabase is: x and y coordination of the mark, the image number,  
% time it was issued (0 for detected by the robot), and the status (0 for detected by the robot,  
% 2 for detected by the HO and 3 for deleted by the HO.
```

```
%imagedatabase=melondatabase(mdn,2:4);
```

```
%imagedatabase(:,4:5)=0;
```

```
imagedatabase=[];
```

```
if ~isempty(robot_target_n)
```

```
    imagedatabase=[imagedatabase;melondatabase(mdn(robot_target_n),2:4)];
```

```
    imagedatabase(:,4:5)=0;
```

```
end
```

```
if ~isempty(fdn) % inserting false alarms the robot detected
```

```
    for w2=1:length(fdn)
```

```
        imagedatabase=[imagedatabase;f_targets(fdn(w2),2:4),0 0];
```

```
    end
```

```
%    paralelimagedb(:,4:5)=0;
```

```
end
```

```
%if ~isempty(img_robot_FA)
```

```
%    imagedatabase=[imagedatabase;robot_false(robot_FA,2:4)];
```

```
%    imagedatabase(:,4:5)=0;
```

```
%end
```

```
%gx=999;
```

```
gy=999;
```

```
while gy>0
```

```
    [gy gx]=ginput(1)
```

```
t2=[t2;cputime,toc,gx,gy,imagenumber,4,1 1];
```

```
% the format of HOlogger is: the image number, x and y coordination of the mark, and
```

```
% the time it was issued
```

```
HOlogger=[HOlogger;imagenumber,gx,gy,toc];
```

```
if gx>=0 & gy>=0 & gx<imagesize(1) & gy<imagesize(2)
```

```
    x=round(gx);
```

```
    y=round(gy);
```

```
    closetarget=[];
```

```
if ~isempty(imagedatabase)
```

```

    dxy=[abs(x-imagedatabase(:,1)),abs(y-imagedatabase(:,2))];
    sumline=sum((dxy<55)');
    closetarget=find(sumline==2);
    imagedbdim=size(imagedatabase);
end

% this part delete the target and line from DB
if sum(closetarget)==0
    imagedatabase=[imagedatabase;x,y,imagenumber,toc,2];
    t2=[t2;cputime,toc,x,y,imagenumber,2,1 1];
% subroutine wich mark the melon detected
    marksign
    A2(:,:,1)=rnew;
    A2(:,:,2)=gnew;
    A2(:,:,3)=bnew;
    imshow(A2)
    set (l,'Position',[1 1 scrsz(3) scrsz(4)])
    h = uicontrol('Style','pushbutton','String','NEXT','FontWeight','bold','Position',[2,92,90,400]);

else
    x=imagedatabase(closetarget(1),1);
    y=imagedatabase(closetarget(1),2);
    if imagedbdim(1)==closetarget(1)
        imagedatabase=imagedatabase(1:closetarget(1)-1,:);
    else
        imagedatabase(closetarget(1):imagedbdim(1)-1,:)=imagedatabase(closetarget(1)+1:imagedbdim(1),:);
        imagedatabase=imagedatabase(1:imagedbdim(1)-1,:);
    end

    t2=[t2;cputime,toc,x,y,imagenumber,3,1 1];
% subroutine wich unmark the melon detected
    unmarksign
    A2(:,:,1)=rnew;
    A2(:,:,2)=gnew;
    A2(:,:,3)=bnew;
    imshow(A2)
    set (l,'Position',[1 1 scrsz(3) scrsz(4)])
    h = uicontrol('Style','pushbutton','String','NEXT','FontWeight','bold','Position',[2,92,90,400]);

end

end

end

t2=[t2;cputime,toc,0,0,imagenumber,3,31];
% call for subroutine which calculate the image score
imagescore

t2=[t2;cputime,toc,0,0,imagenumber,3,32];
% call for display score figure
scorefigure

t2=[t2;cputime,toc,0,0,imagenumber,3,33];

allimagesdb=[allimagesdb;imagedatabase];

t2=[t2;cputime,toc,0,0,imagenumber,3,34];

```

exptutorial.m: Experiment tutorial subroutine. This subroutine explain the subject about the experiment procedures. Called from the main programs

% Subroutine which explain the experiment

ImageDir=['C:\My Documents\Matlab\Experiments2003\Tutorial\']

```
for t1=1:5
    scrsz = get(0,'ScreenSize');
    h=figure('Position',[1 1 scrsz(3) scrsz(4)])
if t1<5
    tstr=num2str(t1);
    tut_img_no=['tutor',tstr,'.jpg'];
    T=imread(tut_img_no,'jpg');
else
    if add==7
        T=imread('max.jpg');
    end
    if add==3
        T=imread('min.jpg');
    end
end
imshow(T)
set(h,'Position',[1 1 scrsz(3) scrsz(4)])
h2= uicontrol('Style','pushbutton','String','ENTER','FontWeight','bold','Position',[2,92,90,400]);
[gy gx]=ginput(1)
        while (gy>-170 | gx<150 | gx>570)
            [gy gx]=ginput(1)
        end
% pause
end

close all
```

exlearningHO.m: Experiment practice for HO collaboration level. called from the main program, HOMarkalone2.m

% Subroutine which explain the experiment for HO level

```
clear
clc
close all
clear Limagedatabase
ImageDir=['C:\My Documents\Matlab\Experiments2003\learning']

Limgorder=[10 669 669 669];
Limagedatabase=[];
corner=55
A2=[];
detect=0;
t1=0;
stop=0;
signed=0;
deleted=0;
err=0;
closetarget=0;
targetd=0;
scrsz = get(0,'ScreenSize');
```

```

%set (h,'Position',[1 1 scrsz(3) scrsz(4)])
for t1=1:4
    h=figure('Position',[1 1 scrsz(3) scrsz(4)])
    if t1<4
        lstr=num2str(t1);
        learn_img_no=['learn',lstr,'.jpg'];
        L=imread(learn_img_no,'jpg');
        imshow(L)
        set (h,'Position',[1 1 scrsz(3) scrsz(4)])
        pause
    end
    if targetd==1 & t1==2
        A=imread('melon day 10.jpg');
        imshow(A)
    else
        if targetd==1 & t1==4
            if err==0
                A=imread('melon day 10.jpg');
                imshow(A)
            else
                A=imread('melon day 666.jpg');
                imshow(A)
            end
        else
            if closetarget==1 & t1==4 & err==1
                A=imread('melon day 664.jpg');
                imshow(A)
            end
            if closetarget==1 & t1==4 & err==0
                A=imread('melon day 333.jpg');
                imshow(A)
            end
        end
    end
end
if t1<4
    showimage
end
gy=999;
gx=999;
detect=0;
go=0;
stop=0;
err=0;
closetarget=0;
targetd=0;
flag==0;
while detect==0
    if gy<0 & flag==1
        detect=1;
    else
        gy=999;
    end
    while gy>0 & go==0
        [gy gx]=ginput(1)
        while (gx<0) & flag==0
            [gy gx]=ginput(1)
        end
        if gx>=0 & gy>=0 & gx<imagesize(1) & gy<imagesize(2) & (stop==0)
            x=round(gx)
            y=round(gy)
% Check if the HO inserted points and if the new mark close to them
            if (t1==2 & detect==0) | (t1==3 & detect==0) | (t1==4 & detect==0)
                dxy=[abs(x-293),abs(y-196)]
            end
        end
    end
end

```

```

        sumline=sum((dxy<55));
        targetd=find(sumline==2);
    end
    if (t1==1 & detect==0) | (t1==3 & detect==0) | (t1==4 & detect==0)
        dxy=[abs(x-133),abs(y-336)]
        sumline=sum((dxy<55));
        closetarget=find(sumline==2);
    end
    % reorganizing the DB of imagedatabase
    if sum(closetarget)>0 & signed==0
        if detect==0
            MARKSIGN
            A2(:,:,1)=rnew;
            A2(:,:,2)=gnew;
            A2(:,:,3)=bnew;
        end
        if t1==1
            imshow(A2)
        end
        if t1==3
            A=imread('melon day 333.jpg');
            imshow(A)
        end
        if t1==4
            A=imread('melon day 444.jpg');
            imshow(A)
        end
        h1= uicontrol('Style','pushbutton','String',
'NEXT','FontWeight','bold','Position',[2,92,90,400]);
        flag=1;
        detect=1;
        if t1==3
            go=1;
            signed=1;
        end
    else % sum(closetarget)>0
        if sum(targetd)>0 & deleted==0
            if (t1<4) | (t1==4 & closetarget==1)
                A=imread('melon day 10.jpg');
                imshow(A)
            else
                A=imread('melon day 444.jpg');
                imshow(A)
            end
            h1= uicontrol('Style','pushbutton','String',
'NEXT','FontWeight','bold','Position',[2,92,90,400]);
            flag=1;
            if (detect==0 & t1==1) | (detect==0 & t1==2)
                [gy gx]=ginput(1)
            end
            h1= uicontrol('Style','pushbutton','String',
'NEXT','FontWeight','bold','Position',[2,92,90,400]);
            detect=1;
            stop=1;
            if t1==3
                go=1;
                deleted=1;
            end
        else
            estr=num2str(t1);
            error_img_no=['error',lstr,'.jpg'];
            R=imread(error_img_no,'jpg');
            err=1;

```

```

        imshow(R)
        pause
        if t1==1 & err==1
            B=imread('melon day 666.jpg');
            imshow(B)
        end
        if t1==2 & err==1
            B=imread('melon day 667.jpg');
            imshow(B)
        end
        if t1==3 & err==1
            B=imread('melon day 665.jpg');
            imshow(B)
        end
        if t1==4 & err==1
            if deleted==0
                B=imread('melon day 664.jpg');
                imshow(B)
            else
                B=imread('melon day 666.jpg');
                imshow(B)
            end
        end
    end
end %closetarget==0) & (dtarget==0)
end

        end %if gx>=0 & gy>=0 & gx<imagesize(1) & gy<imagesize(2)
        flag=0;
    end %while gy>0
    close all

    end %while detect==0
    if t1<4
        close all
    end
end % for t1=1:2
T=imread('finish.jpg');
imshow(T)
pause
close all

```

exlearningHOR.m: Experiment practice for HO-R collaboration level. Called from the main program, HOrmarkandinsert2.m

```

% Subroutine which explain the experiment for HO-R level
clear
clc
close all
clear Limagedatabase
ImageDir=['C:\My Documents\Matlab\Experiments2003\learning']

Limgorder=[10 669 669];
Limagedatabase=[];
corner=55
A2=[];
detect=0;
t1=0;

```

```

stop=0;
signed=0;
deleted=0;
err=0;
closetarget=0;
targetd=0;
scrsz = get(0,'ScreenSize');

for t1=1:3
    h=figure('Position',[1 1 scrsz(3) scrsz(4)])
    lstr=num2str(t1);
    learn_img_no=['HORlearn',lstr,'.jpg'];
    L=imread(learn_img_no,'jpg');
    imshow(L)
    set(h,'Position',[1 1 scrsz(3) scrsz(4)])
    pause
    if targetd==1 & t1==2
        A=imread('melon day 10.jpg');
        imshow(A)
    end
    if t1<3
        showimage
    else
        A=imread('melon day 333.jpg');
        imshow(A)
    end
    gy=999;
    gx=999;
    detect=0;
    go=0;
    stop=0;
    err=0;
    closetarget=0;
    targetd=0;
    flag=0;
    while detect==0
        if gy<0 & flag==1
            detect=1;
        else
            gy=999;
        end
        while gy>0 & go==0
            [gy gx]=ginput(1)
            while (gx<0) & flag==0
                [gy gx]=ginput(1)
            end
            if gx>=0 & gy>=0 & gx<imagesize(1) & gy<imagesize(2) & (stop==0)
                x=round(gx)
                y=round(gy)
                % Check if the HO inserted points and if the new mark close to them
                if (t1==2 & detect==0) | (t1==3 & detect==0)
                    dxy=[abs(x-293),abs(y-196)]
                    sumline=sum((dxy<55));
                    targetd=find(sumline==2);
                end
                if (t1==1 & detect==0) | (t1==3 & detect==0)
                    dxy=[abs(x-133),abs(y-336)]
                    sumline=sum((dxy<55));
                    closetarget=find(sumline==2);
                end
                % reorganizing the DB of imagedatabase
                if sum(closetarget)>0 & signed==0
                    if detect==0

```

```

MARKSIGN
A2(:,1)=rnew;
A2(:,2)=gnew;
A2(:,3)=bnew;
end
if t1==1
    imshow(A2)
    h1= uicontrol('Style','pushbutton','String',
'NEXT','FontWeight','bold','Position',[2,92,90,400]);
    flag=1;
end
if (t1<3)
    detect=1;
    signed=1;
    stop=1;
end
else % sum(closetarget)>0
    if sum(targetd)>0 & deleted==0
        if (t1==2)
            A=imread('melon day 10.jpg');
        end
        if (t1==3)
            A=imread('melon day 444.jpg');
        end
        imshow(A)
        h1= uicontrol('Style','pushbutton','String',
'NEXT','FontWeight','bold','Position',[2,92,90,400]);
        flag=1;
        if (detect==0 & t1==1) | (detect==0 & t1==2)
            [gy gx]=ginput(1)
        end
        h1= uicontrol('Style','pushbutton','String',
'NEXT','FontWeight','bold','Position',[2,92,90,400]);
        flag=1;
        detect=1;
        stop=1;
        if t1==3
            go=1;
            deleted=1;
        end
    else
        err=1;
        if (t1<3)
            estr=num2str(t1);
            error_img_no=['error',lstr,'.jpg'];
            R=imread(error_img_no,'jpg');
            imshow(R)
            pause
        end
        if t1==1
            E=imread('melon day 666.jpg');
            imshow(E)
        end
        if t1==2
            E=imread('melon day 667.jpg');
            imshow(E)
        end
        if t1==3
            if closetarget==1
                E=imread('HORerr.jpg');
                imshow(E)
                pause
                closetarget=0;
            end
        end
    end
end

```

```

        B=imread('melon day 664.jpg');
        imshow(B)
    else
        estr=num2str(t1);
        error_img_no=['error',lstr,'.jpg'];
        R=imread(error_img_no,'.jpg');
        imshow(R)
        pause
        C=imread('melon day 664.jpg');
        imshow(C)
    end
end
end
end % closetarget==0 & (dtarget==0)
end % while gy>0 & go==0
end % if gx>=0 & gy>=0 & gx<imagesize(1) & gy<imagesize(2)
flag=0;
end % while gy>0
close all
end % while detect==0
if t1<4
    close all
end
end % for t1=1:2
T=imread('finish.jpg');
imshow(T)
pause
close all

```

exlearningHORr.m: Experiment practice for HO-Rr collaboration level. Called from the main program, HOrmark2.m

```

% Subroutine which explain the experiment for HO-Rr level
clear
clc
close all
clear Limagedatabase
ImageDir=['C:\My Documents\Matlab\Experiments2003\learning']
Limgorder=[10 10 777];
Limagedatabase=[];
corner=55
A2=[];
detect=0;
t1=0;
stop=0;
signed=0;
deleted=0;
scrsz = get(0,'ScreenSize');

for t1=1:3
    h=figure('Position',[1 1 scrsz(3) scrsz(4)])
    lstr=num2str(t1);
    learn_img_no=['HORrlearn',lstr,'.jpg'];
    L=imread(learn_img_no,'.jpg');
    imshow(L)
    set(h,'Position',[1 1 scrsz(3) scrsz(4)])
    pause
    closetarget=0;

```

```

targetd=0;
err=0;
showimage
if targetd==1
    A=imread('melon day 10.jpg');
    imshow(A)
end
gy=999;
gx=999;
detect=0;
go=0;
stop=0;
flag=0;
while detect==0
    if gy<0 & flag==1
        detect=1;
    else
        gy=999;
    end
    while gy>0 & go==0
        if (t1==2 & detect==0 & err==0)
            A=imread('melon day 669.jpg');
            imshow(A)
        end
        [gy gx]=ginput(1)
        while (gx<0) & flag==0
            [gy gx]=ginput(1)
        end
        if gx>=0 & gy>=0 & gx<imagesize(1) & gy<imagesize(2) & (stop==0)
            x=round(gx)
            y=round(gy)
            if (t1==2 & detect==0) | (t1==3 & detect==0) & (stop==0)
                dxy=[abs(x-293),abs(y-196)]
                sumline=sum((dxy<55));
                targetd=find(sumline==2);
            end
            if (t1==1 & detect==0) | (t1==3 & detect==0) & (stop==0)
                dxy=[abs(x-133),abs(y-336)]
                sumline=sum((dxy<55));
                closetarget=find(sumline==2);
            end
            if sum(closetarget)>0 & signed==0
                if detect==0 & t1==1
                    MARKSIGN
                    A2(:,1)=rnew;
                    A2(:,2)=gnew;
                    A2(:,3)=bnew;
                end
                if detect==0 & t1==3
                    crosssign
                    A2(:,1)=rnew;
                    A2(:,2)=gnew;
                    A2(:,3)=bnew;
                end
                if t1<3
                    imshow(A2)
                else
                    A=imread('melon day 888.jpg');
                    imshow(A)
                end
                h1= uicontrol('Style','pushbutton','String',
'NEXT','FontWeight','bold','Position',[2,92,90,400]);
                flag=1;
            end
        end
    end
end

```

```

detect=1;
if t1==3
    stop=1;
    signed=1;
end
else % sum(closetarget)>0
    if sum(targetd)>0 & deleted==0 & t1==2
        A=imread('melon day 10.jpg');
        imshow(A)
        h1= uicontrol('Style','pushbutton','String',
'NEXT','FontWeight','bold','Position',[2,92,90,400]);
        flag=1;
        detect=1;
        stop=1;
        if t1==3
            deleted=1;
        end
    else
        err=1;
        if t1<3
            estr=num2str(t1);
            error_img_no=['error',lstr,'.jpg'];
            R=imread(error_img_no,'jpg');
            imshow(R)
            pause
        end
        if t1==1
            E=imread('melon day 666.jpg');
            imshow(E)
        end
        if t1==2
            E=imread('melon day 667.jpg');
            imshow(E)
        end
        if t1==3 %& err==1
            if targetd==1
                E=imread('HORrrr.jpg');
                imshow(E)
                pause
                targetd=0;
                B=imread('melon day 668.jpg');
                imshow(B)
            else
                estr=num2str(t1);
                error_img_no=['error',lstr,'.jpg'];
                R=imread(error_img_no,'jpg');
                imshow(R)
                pause
                C=imread('melon day 668.jpg');
                imshow(C)
            end
        end
    end

end

end %closetarget==0) & (dtarget==0)

end %if gx>=0 & gy>=0 & gx<imagesize(1) & gy<imagesize(2)
flag=0;
end %while gy>0

```

```

end %while detect==0
if t1<4
close all
end
end%   for t1=1:2
T=imread('finish.jpg');
imshow(T)
pause
close all

```

Unmarksign.m: subroutine which unmark previous selection of an object by human or robot. Called from the interface subroutine.

```

% unmarksign subroutine

```

```

frameleft=corner;
frameright=corner;
frameup=corner;
framedown=corner;

```

```

if x<=corner
    frameup=x-1;
end
if imagesize(1)-x<=corner
    framedown=imagesize(1)-x-1;
end
if y<=corner
    frameleft=y-1;
end
if imagesize(2)-y<=corner
    frameright=imagesize(2)-y-1;
end

```

```

rnew(x-frameup:x+framedown,y-frameleft:y+frameright)=r(x-frameup:x+framedown,y-frameleft:y+frameright);
gnew(x-frameup:x+framedown,y-frameleft:y+frameright)=g(x-frameup:x+framedown,y-frameleft:y+frameright);
bnew(x-frameup:x+framedown,y-frameleft:y+frameright)=b(x-frameup:x+framedown,y-frameleft:y+frameright);

```

marksign.m: subroutine which mark an object. Called from the main program or interface subroutine.

```

% marksign subroutine compound from the cross sign and the frame sign

```

```

% the crosssign subroutine call
crosssign

```

```

% the framesign subroutine call
framesign

```

crosssign.m: subroutine which draw a black cross on the marked object. Called from marksign.m subroutine.

% The crosssign subroutine

```
if x>=11 & y>=11 & imagesize(1)-x>=11 & imagesize(2)-y>=11
    rnew(x-10:x+10,y-1:y+1)=0;
    gnew(x-10:x+10,y-1:y+1)=0;
    bnew(x-10:x+10,y-1:y+1)=0;
    rnew(x-1:x+1,y-10:y+10)=0;
    gnew(x-1:x+1,y-10:y+10)=0;
    bnew(x-1:x+1,y-10:y+10)=0;
else
    crosscoor=[10-x,10-y,x+10,y+10]
    limits=imagesize-crosscoor
    overlimit=find(limits<=0)
    crosscoor=[x-10,y-10,x+10,y+10];
    crosscoor(overlimit)=imagesize(overlimit)
    deltacross=abs(crosscoor-[x y x y])-[1 1 1 1]
    coornewcroos=abs([11 11 -11 -11]-deltacross)
    newcross=tcross(coornewcroos(1):coornewcroos(3),coornewcroos(2):coornewcroos(4));
    [tcx tcy]=find(newcross==1);
    cx=tcx+x-deltacross(1)-1;
    cy=tcy+y-deltacross(2)-1;
    for c1=1:length(cx)
        rnew(cx(c1),cy(c1))=0;
        gnew(cx(c1),cy(c1))=0;
        bnew(cx(c1),cy(c1))=0;
    end
end
```

framesign.m: subroutine which draws a red frame around the marked object. Called from marksign.m subroutine.

% the framesign subroutine

```
frameleft=corner;
frameright=corner;
frameup=corner;
framedown=corner;

if x<=corner
    frameup=x-1;
end
if imagesize(1)-x<=corner
    framedown=imagesize(1)-x-1;
end
if y<=corner
    frameleft=y-1;
end
if imagesize(2)-y<=corner
    frameright=imagesize(2)-y-1;
end

rnew(x-frameup:x-frameup+20,y-frameleft:y-frameleft+2)=1;
rnew(x-frameup:x-frameup+20,y+frameright-2:y+frameright)=1;
```

```

rnew(x+framedown-20:x+framedown,y-frameleft:y-frameleft+2)=1;
rnew(x+framedown-20:x+framedown,y+frameright-2:y+frameright)=1;
rnew(x-frameup:x-frameup+2,y-frameleft:y-frameleft+20)=1;
rnew(x-frameup:x-frameup+2,y+frameright-20:y+frameright)=1;
rnew(x+framedown-2:x+framedown,y-frameleft:y-frameleft+20)=1;
rnew(x+framedown-2:x+framedown,y+frameright-20:y+frameright)=1;

```

```

gnew(x-frameup:x-frameup+20,y-frameleft:y-frameleft+2)=0;
gnew(x-frameup:x-frameup+20,y+frameright-2:y+frameright)=0;
gnew(x+framedown-20:x+framedown,y-frameleft:y-frameleft+2)=0;
gnew(x+framedown-20:x+framedown,y+frameright-2:y+frameright)=0;
gnew(x-frameup:x-frameup+2,y-frameleft:y-frameleft+20)=0;
gnew(x-frameup:x-frameup+2,y+frameright-20:y+frameright)=0;
gnew(x+framedown-2:x+framedown,y-frameleft:y-frameleft+20)=0;
gnew(x+framedown-2:x+framedown,y+frameright-20:y+frameright)=0;

```

```

bnew(x-frameup:x-frameup+20,y-frameleft:y-frameleft+2)=0;
bnew(x-frameup:x-frameup+20,y+frameright-2:y+frameright)=0;
bnew(x+framedown-20:x+framedown,y-frameleft:y-frameleft+2)=0;
bnew(x+framedown-20:x+framedown,y+frameright-2:y+frameright)=0;
bnew(x-frameup:x-frameup+2,y-frameleft:y-frameleft+20)=0;
bnew(x-frameup:x-frameup+2,y+frameright-20:y+frameright)=0;
bnew(x+framedown-2:x+framedown,y-frameleft:y-frameleft+20)=0;
bnew(x+framedown-2:x+framedown,y+frameright-20:y+frameright)=0;

```

imgscore.m: subroutine which calculate the score of each image. Called from the interface subroutines.

% Subroutine which calculate the image score

```

img_tt=0;
img_tf=0;
clear delta
sys_target=[];

true_target=melondatabase(mdn,2:3);
if ~isempty(imagedatabase)
    sys_detect=imagedatabase(:,1:2);
    n_sys_detect=length(sys_detect(:,1));
    if true_no==0
        img_tt=0;
        img_tf=n_sys_detect;
        img_ft=0;
    else
        for t=1:n_sys_detect
            for r1=1:true_no
                sys_target(r1,:)=sys_detect(t,:);
            end
            delta=abs(true_target-sys_target)
            radius=((delta(:,1).^2+delta(:,2).^2).^0.5)
            current_tt=find(radius<=50);
            n_ctt=length(current_tt);
            if n_ctt>=1
                img_tt=img_tt+1;
            else
                img_tf=img_tf+1;
            end
        end
    end
end

```

```

        img_ft=true_no-img_tt;
    end
else
    n_sys_detect=0;
    img_tt=0;
    img_tf=0;
    img_ft=true_no;
end

score=score+img_tt*add-img_tf*sub;
scorestr=['SCORE: ',num2str(score)];
ttstr=['Detection: ',num2str(img_tt)];
tfstr=['False: ',num2str(img_tf)];
ftstr=['Missed: ',num2str(img_ft)];

```

scorefigure.m: subroutine which display the score after each image. Called from the interface subroutines.

% Subroutine which shows the scores on a different figure

```

%close figure no 2
fig2pos=get(1,'position');
fignum=figure('position',fig2pos);
h2=uicontrol('Style','text','String','SCORE:
','FontWeight','bold','fontsize',24,'fontname','arial','backgroundcolor',[0.8 0.8
0.8],'HorizontalAlignment','left','Position',[300,450,200,50]);
h21=uicontrol('Style','text','String',score,'FontWeight','bold','fontsize',24,'fontname','arial','foregroundcolor',[1 0
0],'HorizontalAlignment','left','Position',[440,450,100,50]);

h3=uicontrol('Style','text',
'String','Detections','FontWeight','bold','fontsize',16,'fontname','arial','backgroundcolor',[0.8 0.8
0.8],'HorizontalAlignment','center','Position',[125,300,200,30]);
h31=uicontrol('Style','text','String',img_tt,'FontWeight','bold','fontsize',16,'fontname','arial','foregroundcolor',[1
0 0],'HorizontalAlignment','center','Position',[175,270,100,30]);

h6=uicontrol('Style','text','String','False','FontWeight','bold','fontsize',16,'fontname','arial','backgroundcolor',[0.8
0.8 0.8],'HorizontalAlignment','center','Position',[300,300,200,30]);
h61=uicontrol('Style','text','String',img_tf,'FontWeight','bold','fontsize',16,'fontname','arial','foregroundcolor',[1
0 0],'HorizontalAlignment','center','Position',[350,270,100,30]);

h7=uicontrol('Style','text',
'String','Misses','FontWeight','bold','fontsize',16,'fontname','arial','backgroundcolor',[0.8 0.8
0.8],'HorizontalAlignment','center','Position',[475,300,200,30]);
h71=uicontrol('Style','text','String',img_ft,'FontWeight','bold','fontsize',16,'fontname','arial','foregroundcolor',[1
0 0],'HorizontalAlignment','center','Position',[525,270,100,30]);

%h3=uicontrol('Style','text','String',ttstr,'FontWeight','bold','Position',[255,10,90,45]);
%h6=uicontrol('Style','text','String',tfstr,'FontWeight','bold','Position',[380,10,90,45]);
%h7=uicontrol('Style','text','String',ftstr,'FontWeight','bold','Position',[505,10,90,45]);

pause(2)
close(fignum)

```

exp_input.m: Assigning subject number and determination of robot quality

```
sn=input('subject s/n= ');
add=input('add= ');
sub=input('sub= ');
robothit=input('robot hit= ');
robotfalse=0;
if robothit==0.9
    robotfalse=12;
end
if robothit==0.5
    robotfalse=106;
end
```

Expfinal.m: subroutine which end the experiment. Called from all main programs

```
% This subroutine end the experiment
```

```
fig2pos=get(1,'position');
fignum=figure('position',fig2pos);
```

```
h9=uicontrol('Style','text','String','Thank you for your cooperation',
'FontWeight','bold','fontsize',24,'fontname','arial','backgroundcolor',[0.8 0.8 0.8],
'HorizontalAlignment','left','Position',[100,450,550,50]);
```

```
h9l=uicontrol('Style','text','String','Your final score:
','FontWeight','bold','fontsize',24,'fontname','arial','backgroundcolor',[0.8 0.8 0.8],
'HorizontalAlignment','left','Position',[300,350,280,50]);
```

```
h92=uicontrol('Style','text','String',score,'FontWeight','bold','fontsize',24,'fontname','arial','foregroundcolor',[1 0 0],
'HorizontalAlignment','left','Position',[570,350,100,50]);
```

```
% pause(10)
% close (fignum)
```

Appendix VIII: Example for subjects' raw data

HOlogger.mat: this database contains the image coordinates, the image number and the time of the human marks.

Image no.	mark coordinates		Time	74	301	-99	253.48
	x	y		96	295	-101	261.04
35	269	364	2.86	58	274	340	267.75
35	269	362	4.06	58	285	396	271.26
35	279	-80	8.44	58	291	-93	273.50
408	37	496	16.39	12	305	-80	279.64
408	36	495	21.00	222	297	-99	285.59
408	318	-63	23.08	51	300	-115	291.39
105	288	-87	35.08	62	33	367	298.20
49	284	-107	42.84	62	263	-88	300.28
59	223	264	48.70	57	229	205	307.76
59	274	-96	53.37	57	263	-83	309.54
231	221	278	60.90	411	304	-85	315.92
231	277	-60	65.14	323	303	-92	321.09
37	320	377	70.79	68	302	-94	325.79
37	293	-84	76.82	327	283	172	332.49
102	204	256	82.35	327	284	-85	335.73
102	294	-89	87.28	204	270	-71	341.07
319	323	389	94.85	315	163	379	346.57
319	195	186	100.32	315	249	-90	348.65
319	276	-92	102.18	214	271	-57	358.51
329	262	-73	113.01	16	285	-85	365.01
97	284	-87	120.73	29	289	-96	369.74
308	306	-78	128.18	52	328	352	375.01
92	307	-109	134.41	52	301	-96	377.44
216	92	368	139.80	46	299	-92	381.68
216	242	283	142.21	110	297	-99	388.33
216	264	-90	144.52	209	292	-62	395.71
321	31	272	151.37	88	295	-96	401.93
321	251	-102	154.83	309	298	-57	407.38
228	263	-67	160.91	301	289	-79	415.91
98	282	-75	168.00	27	293	-106	421.75
75	231	170	173.77	306	216	-84	430.53
75	287	-84	177.80	82	267	-80	435.50
22	281	-77	186.46	227	257	-68	440.24
401	290	-90	192.97	85	417	298	445.97
202	83	314	198.24	85	310	-73	447.66
202	251	-56	202.00	63	306	-89	452.17
111	200	171	206.88	71	296	-112	458.51
111	34	180	208.97	210	293	-73	463.72
111	250	-95	211.75	2	103	437	468.59
225	287	-77	217.55	2	241	-50	471.06
107	265	-84	222.97	54	238	-93	474.98
313	222	363	230.08	86	202	364	479.86
313	273	-69	231.58	86	268	-100	481.69
405	243	-57	241.22	320	272	-93	486.15
402	268	-70	248.23	112	191	139	490.26
				112	147	362	492.26

112	257	-83	494.22	13	164	606	735.67
317	286	419	501.75	13	240	322	737.82
317	290	-84	503.51	13	275	-64	739.53
17	159	28	509.12	42	262	-95	744.46
17	273	-77	511.32	5	161	540	750.15
206	250	-49	516.31	5	274	-80	752.31
9	285	609	522.54	3	377	209	756.77
9	296	-60	525.01	3	295	-50	758.82
21	305	-68	530.57	47	291	-91	762.99
64	299	-91	535.02	61	290	-88	767.82
229	408	238	540.79	220	291	-68	772.55
229	311	-52	543.68	311	289	-63	778.35
1	301	-66	549.49	212	337	251	783.26
53	259	389	556.32	212	299	-70	786.70
53	310	-85	558.45	303	301	-92	791.85
7	275	-57	566.23	77	80	534	796.46
230	263	-74	570.52	77	278	-101	798.59
217	314	202	577.69	232	190	489	803.41
217	279	-58	579.27	232	259	-63	805.13
6	283	-52	584.62	24	256	-91	809.52
34	263	186	589.26	15	280	-82	814.01
34	280	-93	591.30	41	275	-118	818.18
223	258	205	598.99	106	219	-87	823.04
223	242	202	600.57	403	188	296	827.74
223	297	-57	602.76	403	188	297	832.60
10	288	473	609.63	403	290	-61	834.27
10	416	350	611.91	412	259	-68	838.94
10	411	350	614.74	18	260	-51	843.33
10	294	-58	617.50	109	265	-106	848.22
326	296	-82	623.21	31	264	-95	852.42
69	297	-79	628.28	203	269	-96	858.30
4	298	-57	633.66	36	268	-120	863.21
76	335	176	638.46	19	312	-81	868.27
76	342	-89	640.27	66	230	473	875.64
302	349	299	648.14	66	290	-90	878.47
302	322	-57	650.44	104	309	-89	883.22
72	316	-77	654.88	310	49	99	890.58
38	313	-84	660.31	310	264	-51	892.31
324	310	-89	665.13	70	280	-101	897.22
65	310	-100	670.42	78	280	-97	901.95
205	70	307	675.30	25	281	-87	906.86
205	232	-46	677.61	40	280	-94	911.64
218	200	235	681.83	55	280	-95	916.47
218	276	-80	683.65	404	437	486	921.62
103	274	-81	689.28	404	288	-60	923.98
94	273	-97	693.98	14	310	-66	928.29
314	272	-97	699.40	208	319	-60	932.56
409	460	349	705.61	33	325	-104	936.58
409	460	350	708.97	219	326	-85	941.37
409	470	349	710.92	30	325	-110	946.01
409	292	-55	714.34	224	239	340	951.82
89	257	-115	718.61	224	294	-66	953.67
406	295	-55	722.68	410	255	-67	958.89
307	294	-76	727.47	44	261	-118	963.03
13	315	42	732.53	87	260	-116	968.21

20	256	-46	974.34	23	286	-95	1078.90
325	264	-91	979.27	305	146	525	1083.80
322	268	-98	983.85	305	286	-62	1085.30
90	100	325	988.88	316	265	-86	1092.30
90	270	-83	990.20	221	267	-56	1096.90
28	285	-83	994.91	318	269	-88	1101.30
39	285	-85	999.09	407	274	-53	1105.70
80	290	-99	1003.10	73	299	-96	1110.80
101	274	134	1007.80	45	298	-88	1117.30
101	299	-83	1009.80	56	285	-105	1121.30
211	315	-75	1014.30	328	285	-101	1126.00
67	314	-101	1018.40	84	283	-92	1130.00
32	174	264	1025.70	108	285	-112	1135.70
32	292	-140	1027.00	60	283	-102	1141.60
201	300	-54	1032.50	50	281	-107	1145.60
11	301	-73	1037.10	91	287	-110	1150.90
100	299	-98	1042.30	95	280	-111	1155.90
213	296	-67	1049.50	83	222	304	1160.10
48	306	-99	1055.10	83	247	-84	1161.40
304	299	-76	1059.50	43	119	285	1165.70
312	298	-53	1064.40	43	262	-91	1167.70
226	228	400	1068.40	26	279	-90	1171.70
226	271	-66	1070.10	207	283	-49	1176.20
215	284	-60	1074.50				

Allimgdb.mat: list of all melons/targets inserted by the human.

The status number indicates: 0 - detected by the robot, 1 - detected by the robot and inserted to the database by the human, 2 - detected by the human and 3 - deleted by the human.

image coordinates		Image no.	time	status	384	146	22	0.00	0
x	y				369	297	22	0.00	0
269	362	35	4.06	2	307	141	401	0.00	0
136	435	105	0.00	0	83	314	202	198.24	2
290	168	49	0.00	0	200	171	111	206.88	2
204	303	49	0.00	0	34	180	111	208.97	2
83	333	59	0.00	0	78	387	402	0.00	0
223	264	59	48.70	2	356	140	74	0.00	0
190	338	37	0.00	0	204	370	74	0.00	0
320	377	37	70.79	2	161	216	96	0.00	0
165	332	329	0.00	0	285	396	58	271.26	2
125	65	97	0.00	0	161	22	12	0.00	0
412	313	308	0.00	0	313	246	12	0.00	0
207	178	92	0.00	0	225	542	12	0.00	0
92	368	216	139.80	2	304	304	222	0.00	0
242	283	216	142.21	2	124	483	222	0.00	0
250	417	321	0.00	0	340	358	51	0.00	0
138	180	98	0.00	0	77	244	51	0.00	0
323	301	98	0.00	0	196	322	62	0.00	0
441	317	75	0.00	0	85	300	57	0.00	0
231	170	75	173.77	2	229	205	57	307.76	2
87	264	22	0.00	0	357	158	411	0.00	0

278	315	323	0.00	0	130	346	10	0.00	0
112	140	323	0.00	0	266	607	10	0.00	0
303	218	68	0.00	0	411	350	10	614.74	2
312	372	327	0.00	0	164	374	326	0.00	0
77	384	204	0.00	0	417	503	326	0.00	0
289	336	315	0.00	0	199	260	69	0.00	0
163	379	315	346.57	2	332	96	4	0.00	0
52	291	214	0.00	0	387	463	4	0.00	0
354	387	214	0.00	0	98	574	4	0.00	0
233	218	16	0.00	0	335	176	76	638.46	2
263	136	29	0.00	0	210	36	302	0.00	0
148	198	29	0.00	0	68	296	302	0.00	0
41	267	52	0.00	0	349	299	302	648.14	2
328	352	52	375.01	2	345	351	72	0.00	0
281	297	46	0.00	0	257	183	324	0.00	0
131	365	209	0.00	0	182	218	65	0.00	0
211	440	88	0.00	0	70	307	205	675.30	2
217	203	309	0.00	0	200	235	218	681.83	2
201	410	27	0.00	0	418	85	94	0.00	0
203	412	306	0.00	0	165	220	94	0.00	0
170	444	82	0.00	0	264	124	409	0.00	0
232	481	227	0.00	0	470	349	409	710.92	2
173	227	85	0.00	0	200	238	406	0.00	0
417	298	85	445.97	2	239	430	307	0.00	0
181	488	63	0.00	0	315	42	13	732.53	2
192	351	71	0.00	0	240	322	13	737.82	2
68	302	71	0.00	0	295	165	42	0.00	0
412	419	210	0.00	0	386	72	5	0.00	0
399	327	2	0.00	0	96	180	5	0.00	0
103	437	2	468.59	2	161	540	5	750.15	2
255	313	54	0.00	0	84	313	3	0.00	0
202	364	86	479.86	2	377	209	3	756.77	2
295	371	320	0.00	0	239	226	47	0.00	0
191	139	112	490.26	2	287	183	61	0.00	0
147	362	112	492.26	2	373	391	220	0.00	0
206	288	317	0.00	0	305	521	212	0.00	0
319	271	17	0.00	0	337	251	212	783.26	2
159	28	17	509.12	2	203	334	303	0.00	0
212	420	206	0.00	0	80	534	77	796.46	2
402	367	9	0.00	0	190	489	232	803.41	2
129	336	9	0.00	0	246	216	15	0.00	0
378	153	21	0.00	0	255	158	41	0.00	0
371	304	21	0.00	0	362	401	403	0.00	0
81	265	21	0.00	0	86	327	412	0.00	0
161	410	64	0.00	0	377	438	412	0.00	0
25	288	229	0.00	0	139	273	18	0.00	0
262	368	229	0.00	0	294	529	18	0.00	0
85	314	1	0.00	0	196	191	109	0.00	0
377	206	1	0.00	0	406	592	203	0.00	0
42	382	53	0.00	0	71	583	203	0.00	0
166	332	7	0.00	0	297	232	36	0.00	0
229	192	230	0.00	0	149	275	36	0.00	0
172	330	6	0.00	0	169	262	19	0.00	0
263	186	34	589.26	2	223	295	66	0.00	0
242	202	223	600.57	2	25	318	66	0.00	0

199	162	104	0.00	0	37	504	201	0.00	0
242	444	310	0.00	0	147	126	11	0.00	0
187	146	70	0.00	0	302	373	11	0.00	0
282	274	78	0.00	0	432	145	11	0.00	0
113	443	78	0.00	0	176	141	100	0.00	0
42	135	25	0.00	0	115	345	100	0.00	0
66	299	25	0.00	0	338	341	100	0.00	0
235	202	40	0.00	0	221	134	48	0.00	0
107	169	40	0.00	0	348	153	304	0.00	0
86	347	40	0.00	0	289	163	312	0.00	0
265	183	55	0.00	0	228	400	226	1068.40	2
61	218	55	0.00	0	127	224	215	0.00	0
437	486	404	921.62	2	411	170	215	0.00	0
232	214	14	0.00	0	43	130	23	0.00	0
263	271	208	0.00	0	68	298	23	0.00	0
158	244	33	0.00	0	298	269	305	0.00	0
202	161	219	0.00	0	146	525	305	1083.80	2
194	219	30	0.00	0	454	450	316	0.00	0
35	180	30	0.00	0	368	297	316	0.00	0
239	340	224	951.82	2	198	322	316	0.00	0
121	147	410	0.00	0	360	203	221	0.00	0
87	447	410	0.00	0	78	159	73	0.00	0
362	455	410	0.00	0	262	397	73	0.00	0
275	273	44	0.00	0	188	157	45	0.00	0
127	223	44	0.00	0	53	166	45	0.00	0
199	132	87	0.00	0	118	207	56	0.00	0
381	169	20	0.00	0	375	152	56	0.00	0
77	286	20	0.00	0	346	412	328	0.00	0
154	629	20	0.00	0	155	288	328	0.00	0
267	150	325	0.00	0	148	184	60	0.00	0
337	408	322	0.00	0	291	272	60	0.00	0
139	234	322	0.00	0	248	239	50	0.00	0
292	275	90	0.00	0	170	389	50	0.00	0
100	325	90	988.88	2	242	336	91	0.00	0
231	188	80	0.00	0	23	263	91	0.00	0
220	375	101	0.00	0	144	298	95	0.00	0
32	346	101	0.00	0	347	367	95	0.00	0
274	134	101	1007.80	2	222	304	83	1160.10	2
320	441	211	0.00	0	285	268	43	0.00	0
102	287	67	0.00	0	22	140	43	0.00	0
81	372	32	0.00	0	119	285	43	1165.70	2
171	399	32	0.00	0	142	179	26	0.00	0
299	365	32	0.00	0	387	102	26	0.00	0
174	264	32	1025.70	2	214	461	207	0.00	0

f_targets.mat: list of non-target objects marked.

sequential no.	mark coordinates		image no.
	x	y	
1	387	102	26
1	347	367	95
1	406	238	229
1	139	234	322
1	229	470	66
1	33	366	62
1	322	388	319
1	274	340	58
1	51	99	310
1	284	171	327
1	83	333	59
1	287	472	10

f_targets.mat: list of non-target objects marked.

sequential no.	mark coordinates		Image no.				
	x	y					
1	268	364	35	2	124	483	222
1	136	435	105	1	340	358	51
1	290	168	49	2	77	244	51
2	204	303	49	1	196	322	62
1	220	277	231	1	85	300	57
1	190	338	37	1	357	158	411
1	205	255	102	1	278	315	323
1	195	187	319	2	112	140	323
1	165	332	329	1	303	218	68
1	125	65	97	1	312	372	327
1	412	313	308	1	77	384	204
1	207	178	92	1	289	336	315
1	250	417	321	1	52	291	214
2	30	272	321	2	354	387	214
1	138	180	98	1	233	218	16
2	323	301	98	1	263	136	29
2	441	317	75	2	148	198	29
1	87	264	22	2	41	267	52
2	384	146	22	1	281	297	46
3	369	297	22	1	131	365	209
1	307	141	401	1	211	440	88
1	221	363	313	1	217	203	309
1	78	387	402	1	201	410	27
1	356	140	74	1	203	412	306
2	204	370	74	1	170	444	82
1	161	216	96	1	232	481	227
1	161	22	12	1	173	227	85
2	313	246	12	1	181	488	63
3	225	542	12	1	192	351	71
1	304	304	222	2	68	302	71
				1	412	419	210
				1	399	327	2
				1	255	313	54

1	295	371	320	1	86	327	412
1	206	288	317	2	377	438	412
2	285	419	317	1	139	273	18
2	319	271	17	2	294	529	18
1	212	420	206	1	196	191	109
1	402	367	9	1	406	592	203
2	129	336	9	2	71	583	203
3	285	608	9	1	297	232	36
1	378	153	21	2	149	275	36
2	371	304	21	1	169	262	19
3	81	265	21	1	223	295	66
1	161	410	64	2	25	318	66
1	25	288	229	1	199	162	104
2	262	368	229	1	242	444	310
1	85	314	1	1	187	146	70
2	377	206	1	1	282	274	78
1	42	382	53	2	113	443	78
2	259	387	53	1	42	135	25
1	166	332	7	2	66	299	25
1	229	192	230	1	235	202	40
1	314	203	217	2	107	169	40
1	172	330	6	3	86	347	40
1	259	205	223	1	265	183	55
1	130	346	10	2	61	218	55
2	266	607	10	1	232	214	14
3	415	349	10	1	263	271	208
1	164	374	326	1	158	244	33
2	417	503	326	1	202	161	219
1	199	260	69	1	194	219	30
1	332	96	4	2	35	180	30
2	387	463	4	1	121	147	410
3	98	574	4	2	87	447	410
2	210	36	302	3	362	455	410
3	68	296	302	1	275	273	44
1	345	351	72	2	127	223	44
1	257	183	324	1	199	132	87
1	182	218	65	1	381	169	20
1	418	85	94	2	77	286	20
2	165	220	94	3	154	629	20
1	264	124	409	1	267	150	325
1	200	238	406	1	337	408	322
1	239	430	307	1	292	275	90
1	164	605	13	1	231	188	80
1	295	165	42	1	220	375	101
1	386	72	5	2	32	346	101
2	96	180	5	1	320	441	211
2	84	313	3	1	102	287	67
1	239	226	47	2	81	372	32
1	287	183	61	3	171	399	32
1	373	391	220	4	299	365	32
1	305	521	212	1	37	504	201
1	203	334	303	1	147	126	11
1	246	216	15	2	302	373	11
1	255	158	41	3	432	145	11
1	362	401	403	1	176	141	100

2	115	345	100
3	338	341	100
1	221	134	48
1	348	153	304
1	289	163	312
1	127	224	215
2	411	170	215
1	43	130	23
2	68	298	23
1	298	269	305
1	454	450	316
2	368	297	316
3	198	322	316
1	360	203	221
1	78	159	73
2	262	397	73
1	188	157	45
2	53	166	45
1	118	207	56
2	375	152	56
1	346	412	328
2	155	288	328
1	148	184	60
2	291	272	60
1	248	239	50
2	170	389	50
1	242	336	91
2	23	263	91
1	144	298	95
1	285	268	43
3	22	140	43
1	142	179	26
1	214	461	207

t2.mat: database of all simulation records.

The command type indicates: 0 - no command, 1 – inserting into database already marked object, 2 - marking and inserting object into database, 3 - deleting detected object, 4 - unknown yet.

The program stage indicates the location of the simulation along the codes.

cpu time	time	mark coordinates		image no,	command type	program stage
		x	y			
1883.7	0	0	0	0	0	0
1883.8	0.063	0	0	0	0	1
1883.8	0.078	0	0	35	0	2
1883.9	0.203	0	0	35	0	3
1883.9	0.219	0	0	35	0	4
1884.2	0.469	0	0	35	0	5
1886.6	2.859	269.28	364.19	35	4	11
1886.6	2.859	268	364	35	3	11
1887.8	4.062	269.28	362.49	35	4	11
1887.8	4.062	269	362	35	2	11
1892.1	8.437	278.6	-80.257	35	4	11
1892.1	8.437	0	0	35	3	31
1892.2	8.468	0	0	35	3	32
1894.4	10.656	0	0	35	3	33
1894.4	10.656	0	0	35	3	34
1894.4	10.656	0	0	408	0	2
1894.5	10.812	0	0	408	0	3
1894.5	10.812	0	0	408	0	4
1894.8	11.062	0	0	408	0	5
1900.1	16.39	37.325	496.16	408	4	11
1900.1	16.39	37	496	408	2	11
1904.7	20.999	36.479	495.31	408	4	11
1904.7	20.999	37	496	408	3	11
1906.8	23.077	318.38	-62.569	408	4	11
1906.8	23.077	0	0	408	3	31
1906.8	23.077	0	0	408	3	32
1908.9	25.217	0	0	408	3	33
1908.9	25.217	0	0	408	3	34
1908.9	25.217	0	0	105	0	2
1909	25.327	0	0	105	0	3
1909.1	25.342	0	0	105	0	4
1909.3	25.608	0	0	105	0	5
1918.8	35.076	287.91	-87.029	105	4	11
1918.8	35.076	0	0	105	3	31
1918.8	35.076	0	0	105	3	32
1921	37.263	0	0	105	3	33
1921	37.263	0	0	105	3	34
1921	37.263	0	0	49	0	2
1921.1	37.357	0	0	49	0	3
1921.1	37.373	0	0	49	0	4
1921.3	37.623	0	0	49	0	5
1926.5	42.841	283.67	-107.35	49	4	11
1926.5	42.841	0	0	49	3	31
1926.5	42.841	0	0	49	3	32
1928.8	45.044	0	0	49	3	33
1928.8	45.044	0	0	49	3	34
1928.8	45.044	0	0	59	0	2
1928.8	45.138	0	0	59	0	3
1928.9	45.169	0	0	59	0	4

1929.1	45.419	0	0	59	0	5
1932.4	48.7	222.72	264.29	59	4	11
1932.4	48.7	223	264	59	2	11
1937.1	53.371	274.36	-96.341	59	4	11
1937.1	53.371	0	0	59	3	31
1937.1	53.371	0	0	59	3	32
1939.3	55.559	0	0	59	3	33
1939.3	55.559	0	0	59	3	34
1939.3	55.559	0	0	231	0	2
1939.4	55.684	0	0	231	0	3
1939.4	55.699	0	0	231	0	4
1939.7	55.981	0	0	231	0	5
1944.6	60.902	221.03	277.75	231	4	11
1944.6	60.902	220	277	231	3	11
1948.8	65.136	276.9	-60.029	231	4	11
1948.8	65.136	0	0	231	3	31
1948.8	65.136	0	0	231	3	32
1951	67.339	0	0	231	3	33
1951	67.339	0	0	231	3	34
1951	67.339	0	0	37	0	2
1951.1	67.433	0	0	37	0	3
1951.2	67.449	0	0	37	0	4
1951.4	67.714	0	0	37	0	5
1954.5	70.792	320.08	376.89	37	4	11
1954.5	70.792	320	377	37	2	11
1960.5	76.823	292.99	-84.489	37	4	11
1960.5	76.823	0	0	37	3	31
1960.5	76.823	0	0	37	3	32
1962.7	79.01	0	0	37	3	33
1962.7	79.01	0	0	37	3	34
1962.7	79.01	0	0	102	0	2
1962.8	79.104	0	0	102	0	3
1962.8	79.12	0	0	102	0	4
1963.1	79.37	0	0	102	0	5
1966.1	82.354	204.1	255.83	102	4	11
1966.1	82.354	205	255	102	3	11
1971	87.275	293.83	-88.722	102	4	11
1971	87.275	0	0	102	3	31
1971	87.275	0	0	102	3	32
1973.2	89.463	0	0	102	3	33
1973.2	89.463	0	0	102	3	34
1973.2	89.463	0	0	319	0	2
1973.3	89.572	0	0	319	0	3
1973.3	89.588	0	0	319	0	4
1973.5	89.838	0	0	319	0	5
1978.6	94.853	323.46	388.74	319	4	11
1978.6	94.853	322	388	319	3	11
1984	100.32	194.79	186.41	319	4	11
1984	100.32	195	187	319	3	11
1985.9	102.18	276.06	-92.108	319	4	11
1985.9	102.18	0	0	319	3	31
1985.9	102.18	0	0	319	3	32
1988	104.31	0	0	319	3	33
1988	104.31	0	0	319	3	34
1988	104.31	0	0	329	0	2
1988.1	104.43	0	0	329	0	3
1988.2	104.45	0	0	329	0	4
1988.4	104.73	0	0	329	0	5

1996.7	113.01	261.66	-72.728	329	4	11
1996.7	113.01	0	0	329	3	31
1996.7	113.01	0	0	329	3	32
1999	115.26	0	0	329	3	33
1999	115.26	0	0	329	3	34
1999	115.26	0	0	97	0	2
1999.1	115.37	0	0	97	0	3
1999.1	115.38	0	0	97	0	4
1999.3	115.62	0	0	97	0	5
2004.4	120.73	283.67	-87.029	97	4	11
2004.4	120.73	0	0	97	3	31
2004.4	120.73	0	0	97	3	32
2006.6	122.85	0	0	97	3	33
2006.6	122.85	0	0	97	3	34
2006.6	122.85	0	0	308	0	2
2006.7	122.96	0	0	308	0	3
2006.7	122.99	0	0	308	0	4
2007	123.26	0	0	308	0	5
2011.9	128.18	305.69	-77.807	308	4	11
2011.9	128.18	0	0	308	3	31
2011.9	128.19	0	0	308	3	32
2014	130.32	0	0	308	3	33
2014	130.32	0	0	308	3	34
2014	130.32	0	0	92	0	2
2014.1	130.41	0	0	92	0	3
2014.2	130.44	0	0	92	0	4
2014.4	130.68	0	0	92	0	5
2018.1	134.41	307.38	-109.04	92	4	11
2018.1	134.41	0	0	92	3	31
2018.1	134.41	0	0	92	3	32
2020.3	136.6	0	0	92	3	33
2020.3	136.6	0	0	92	3	34
2020.3	136.6	0	0	216	0	2
2020.4	136.71	0	0	216	0	3
2020.4	136.71	0	0	216	0	4
2020.7	136.96	0	0	216	0	5
2023.5	139.8	91.505	368.33	216	4	11
2023.5	139.8	92	368	216	2	11
2025.9	142.21	242.19	282.83	216	4	11
2025.9	142.21	242	283	216	2	11
2028.2	144.52	264.2	-89.659	216	4	11
2028.2	144.52	0	0	216	3	31
2028.2	144.52	0	0	216	3	32
2030.4	146.66	0	0	216	3	33
2030.4	146.66	0	0	216	3	34
2030.4	146.66	0	0	321	0	2
2030.5	146.76	0	0	321	0	3
2030.5	146.79	0	0	321	0	4
2030.7	147.01	0	0	321	0	5
2035.1	151.37	30.553	271.91	321	4	11
2035.1	151.37	30	272	321	3	11
2038.5	154.83	250.66	-102.27	321	4	11
2038.5	154.83	0	0	321	3	31
2038.5	154.83	0	0	321	3	32
2040.7	156.94	0	0	321	3	33
2040.7	156.94	0	0	321	3	34
2040.7	156.94	0	0	228	0	2
2040.7	157.04	0	0	228	0	3

2040.7	157.04	0	0	228	0	4
2041	157.29	0	0	228	0	5
2044.6	160.91	263.36	-66.802	228	4	11
2044.6	160.91	0	0	228	3	31
2044.6	160.91	0	0	228	3	32
2046.8	163.11	0	0	228	3	33
2046.8	163.11	0	0	228	3	34
2046.8	163.11	0	0	98	0	2
2046.9	163.21	0	0	98	0	3
2046.9	163.22	0	0	98	0	4
2047.2	163.46	0	0	98	0	5
2051.7	168	281.98	-75.177	98	4	11
2051.7	168	0	0	98	3	31
2051.7	168	0	0	98	3	32
2053.9	170.15	0	0	98	3	33
2053.9	170.15	0	0	98	3	34
2053.9	170.15	0	0	75	0	2
2053.9	170.24	0	0	75	0	3
2054	170.27	0	0	75	0	4
2054.2	170.5	0	0	75	0	5
2057.5	173.77	231.19	170.33	75	4	11
2057.5	173.77	231	170	75	2	11
2061.5	177.8	287.06	-84.489	75	4	11
2061.5	177.8	0	0	75	3	31
2061.5	177.8	0	0	75	3	32
2063.6	179.94	0	0	75	3	33
2063.6	179.94	0	0	75	3	34
2063.6	179.94	0	0	22	0	2
2063.8	180.07	0	0	22	0	3
2063.8	180.1	0	0	22	0	4
2064.1	180.36	0	0	22	0	5
2070.2	186.46	281.13	-76.96	22	4	11
2070.2	186.46	0	0	22	3	31
2070.2	186.46	0	0	22	3	32
2072.3	188.58	0	0	22	3	33
2072.3	188.58	0	0	22	3	34
2072.3	188.58	0	0	401	0	2
2072.4	188.67	0	0	401	0	3
2072.4	188.69	0	0	401	0	4
2072.6	188.92	0	0	401	0	5
2076.7	192.97	289.6	-89.569	401	4	11
2076.7	192.97	0	0	401	3	31
2076.7	192.97	0	0	401	3	32
2078.8	195.1	0	0	401	3	33
2078.8	195.1	0	0	401	3	34
2078.8	195.1	0	0	202	0	2
2078.9	195.24	0	0	202	0	3
2078.9	195.24	0	0	202	0	4
2079.2	195.49	0	0	202	0	5
2081.9	198.24	83.04	314.15	202	4	11
2081.9	198.24	83	314	202	2	11
2085.7	202	250.66	-55.796	202	4	11
2085.7	202	0	0	202	3	31
2085.7	202	0	0	202	3	32
2087.8	204.11	0	0	202	3	33
2087.8	204.11	0	0	202	3	34
2087.8	204.11	0	0	111	0	2
2087.9	204.2	0	0	111	0	3

2087.9	204.2	0	0	111	0	4
2088.1	204.44	0	0	111	0	5
2090.6	206.88	199.87	171.17	111	4	11
2090.6	206.88	200	171	111	2	11
2092.7	208.97	33.939	179.64	111	4	11
2092.7	208.97	34	180	111	2	11
2095.5	211.75	249.81	-95.495	111	4	11
2095.5	211.75	0	0	111	3	31
2095.5	211.75	0	0	111	3	32
2097.6	213.86	0	0	111	3	33
2097.6	213.86	0	0	111	3	34
2097.6	213.86	0	0	225	0	2
2097.7	213.97	0	0	225	0	3
2097.7	213.97	0	0	225	0	4
2097.9	214.22	0	0	225	0	5
2101.3	217.55	287.06	-76.96	225	4	11
2101.3	217.55	0	0	225	3	31
2101.3	217.55	0	0	225	3	32
2103.4	219.67	0	0	225	3	33
2103.4	219.67	0	0	225	3	34
2103.4	219.67	0	0	107	0	2
2103.5	219.75	0	0	107	0	3
2103.5	219.75	0	0	107	0	4
2103.7	219.97	0	0	107	0	5
2106.7	222.97	265.05	-83.643	107	4	11
2106.7	222.97	0	0	107	3	31
2106.7	222.97	0	0	107	3	32
2108.8	225.09	0	0	107	3	33
2108.8	225.09	0	0	107	3	34
2108.8	225.09	0	0	313	0	2
2108.9	225.19	0	0	313	0	3
2108.9	225.22	0	0	313	0	4
2109.2	225.48	0	0	313	0	5
2113.8	230.08	221.88	363.25	313	4	11
2113.8	230.08	221	363	313	3	11
2115.3	231.58	272.67	-69.341	313	4	11
2115.3	231.58	0	0	313	3	31
2115.3	231.58	0	0	313	3	32
2117.4	233.7	0	0	313	3	33
2117.4	233.7	0	0	313	3	34
2117.4	233.7	0	0	405	0	2
2117.6	233.84	0	0	405	0	3
2117.6	233.84	0	0	405	0	4
2117.8	234.08	0	0	405	0	5
2124.9	241.22	243.04	-57.489	405	4	11
2124.9	241.22	0	0	405	3	31
2124.9	241.22	0	0	405	3	32
2127.1	243.36	0	0	405	3	33
2127.1	243.36	0	0	405	3	34
2127.1	243.36	0	0	402	0	2
2127.2	243.5	0	0	402	0	3
2127.2	243.51	0	0	402	0	4
2127.5	243.78	0	0	402	0	5
2131.9	248.23	268.44	-70.188	402	4	11
2131.9	248.23	0	0	402	3	31
2131.9	248.23	0	0	402	3	32
2134.1	250.36	0	0	402	3	33
2134.1	250.36	0	0	402	3	34

2134.1	250.36	0	0	74	0	2
2134.2	250.45	0	0	74	0	3
2134.2	250.48	0	0	74	0	4
2134.4	250.69	0	0	74	0	5
2137.2	253.48	301.45	-98.881	74	4	11
2137.2	253.48	0	0	74	3	31
2137.2	253.5	0	0	74	3	32
2139.3	255.62	0	0	74	3	33
2139.3	255.62	0	0	74	3	34
2139.3	255.62	0	0	96	0	2
2139.4	255.73	0	0	96	0	3
2139.5	255.75	0	0	96	0	4
2139.7	255.97	0	0	96	0	5
2144.8	261.04	294.68	-100.57	96	4	11
2144.8	261.04	0	0	96	3	31
2144.8	261.04	0	0	96	3	32
2146.9	263.2	0	0	96	3	33
2146.9	263.2	0	0	96	3	34
2146.9	263.2	0	0	58	0	2
2147	263.29	0	0	58	0	3
2147	263.31	0	0	58	0	4
2147.2	263.53	0	0	58	0	5
2151.5	267.75	274.36	340.48	58	4	11
2151.5	267.75	274	340	58	3	11
2155	271.26	284.52	396.36	58	4	11
2155	271.26	285	396	58	2	11
2157.2	273.5	291.29	-92.955	58	4	11
2157.2	273.5	0	0	58	3	31
2157.2	273.51	0	0	58	3	32
2159.4	275.73	0	0	58	3	33
2159.4	275.73	0	0	58	3	34
2159.4	275.73	0	0	12	0	2
2159.6	275.87	0	0	12	0	3
2159.6	275.9	0	0	12	0	4
2160	276.29	0	0	12	0	5
2163.3	279.64	304.84	-79.5	12	4	11
2163.3	279.64	0	0	12	3	31
2163.3	279.64	0	0	12	3	32
2165.5	281.82	0	0	12	3	33
2165.5	281.82	0	0	12	3	34
2165.5	281.82	0	0	222	0	2
2165.6	281.93	0	0	222	0	3
2165.7	281.97	0	0	222	0	4
2165.9	282.18	0	0	222	0	5
2169.3	285.57	297.22	-98.971	222	4	11
2169.3	285.59	0	0	222	3	31
2169.3	285.59	0	0	222	3	32
2171.4	287.73	0	0	222	3	33
2171.4	287.73	0	0	222	3	34
2171.4	287.73	0	0	51	0	2
2171.5	287.82	0	0	51	0	3
2171.5	287.84	0	0	51	0	4
2171.8	288.06	0	0	51	0	5
2175.1	291.39	299.76	-114.97	51	4	11
2175.1	291.39	0	0	51	3	31
2175.1	291.39	0	0	51	3	32
2177.2	293.51	0	0	51	3	33
2177.2	293.51	0	0	51	3	34

2177.2	293.51	0	0	62	0	2
2177.3	293.61	0	0	62	0	3
2177.3	293.64	0	0	62	0	4
2177.5	293.84	0	0	62	0	5
2181.9	298.2	33.093	366.73	62	4	11
2181.9	298.2	33	366	62	3	11
2184	300.28	262.51	-87.876	62	4	11
2184	300.28	0	0	62	3	31
2184	300.28	0	0	62	3	32
2186.1	302.42	0	0	62	3	33
2186.1	302.42	0	0	62	3	34
2186.1	302.42	0	0	57	0	2
2186.2	302.5	0	0	57	0	3
2186.2	302.53	0	0	57	0	4
2186.4	302.73	0	0	57	0	5
2191.5	307.76	229.49	205.03	57	4	11
2191.5	307.76	229	205	57	2	11
2193.2	309.52	262.51	-82.796	57	4	11
2193.2	309.54	0	0	57	3	31
2193.2	309.54	0	0	57	3	32
2195.4	311.67	0	0	57	3	33
2195.4	311.67	0	0	57	3	34
2195.4	311.67	0	0	411	0	2
2195.5	311.79	0	0	411	0	3
2195.5	311.82	0	0	411	0	4
2195.8	312.07	0	0	411	0	5
2199.6	315.92	303.99	-85.426	411	4	11
2199.6	315.92	0	0	411	3	31
2199.6	315.92	0	0	411	3	32
2201.8	318.12	0	0	411	3	33
2201.8	318.12	0	0	411	3	34
2201.8	318.12	0	0	323	0	2
2201.9	318.21	0	0	323	0	3
2201.9	318.23	0	0	323	0	4
2202.2	318.45	0	0	323	0	5
2204.8	321.09	303.15	-92.108	323	4	11
2204.8	321.09	0	0	323	3	31
2204.8	321.09	0	0	323	3	32
2207	323.27	0	0	323	3	33
2207	323.27	0	0	323	3	34
2207	323.27	0	0	68	0	2
2207.1	323.37	0	0	68	0	3
2207.1	323.4	0	0	68	0	4
2207.3	323.6	0	0	68	0	5
2209.5	325.79	302.3	-93.802	68	4	11
2209.5	325.79	0	0	68	3	31
2209.5	325.79	0	0	68	3	32
2211.7	327.98	0	0	68	3	33
2211.7	327.98	0	0	68	3	34
2211.7	327.98	0	0	327	0	2
2211.8	328.07	0	0	327	0	3
2211.8	328.1	0	0	327	0	4
2212	328.31	0	0	327	0	5
2216.2	332.49	282.83	172.02	327	4	11
2216.2	332.49	284	171	327	3	11
2219.4	335.73	283.67	-85.336	327	4	11
2219.4	335.73	0	0	327	3	31
2219.4	335.73	0	0	327	3	32

2221.6	337.87	0	0	327	3	33
2221.6	337.87	0	0	327	3	34
2221.6	337.87	0	0	204	0	2
2221.7	338.02	0	0	204	0	3
2221.7	338.04	0	0	204	0	4
2222	338.29	0	0	204	0	5
2224.8	341.07	270.13	-71.034	204	4	11
2224.8	341.07	0	0	204	3	31
2224.8	341.07	0	0	204	3	32
2226.9	343.18	0	0	204	3	33
2226.9	343.18	0	0	204	3	34
2226.9	343.18	0	0	315	0	2
2227	343.27	0	0	315	0	3
2227	343.29	0	0	315	0	4
2227.2	343.49	0	0	315	0	5
2230.3	346.57	163.46	378.58	315	4	11
2230.3	346.57	163	379	315	2	11
2232.4	348.65	248.97	-89.569	315	4	11
2232.4	348.65	0	0	315	3	31
2232.4	348.66	0	0	315	3	32
2234.5	350.77	0	0	315	3	33
2234.5	350.77	0	0	315	3	34
2234.5	350.77	0	0	214	0	2
2234.6	350.88	0	0	214	0	3
2234.6	350.91	0	0	214	0	4
2234.9	351.15	0	0	214	0	5
2242.2	358.51	270.98	-57.489	214	4	11
2242.2	358.51	0	0	214	3	31
2242.2	358.51	0	0	214	3	32
2244.4	360.66	0	0	214	3	33
2244.4	360.66	0	0	214	3	34
2244.4	360.66	0	0	16	0	2
2244.5	360.8	0	0	16	0	3
2244.5	360.83	0	0	16	0	4
2244.8	361.08	0	0	16	0	5
2248.7	365.01	284.52	-84.579	16	4	11
2248.7	365.01	0	0	16	3	31
2248.7	365.01	0	0	16	3	32
2250.8	367.12	0	0	16	3	33
2250.8	367.12	0	0	16	3	34
2250.8	367.12	0	0	29	0	2
2250.9	367.21	0	0	29	0	3
2250.9	367.24	0	0	29	0	4
2251.2	367.44	0	0	29	0	5
2253.4	369.74	288.75	-96.341	29	4	11
2253.4	369.74	0	0	29	3	31
2253.4	369.74	0	0	29	3	32
2255.6	371.87	0	0	29	3	33
2255.6	371.87	0	0	29	3	34
2255.6	371.87	0	0	52	0	2
2255.7	371.96	0	0	52	0	3
2255.7	371.97	0	0	52	0	4
2255.9	372.19	0	0	52	0	5
2258.7	375.01	327.7	352.34	52	4	11
2258.7	375.01	328	352	52	2	11
2261.2	377.44	301.45	-96.341	52	4	11
2261.2	377.44	0	0	52	3	31
2261.2	377.44	0	0	52	3	32

2263.4	379.64	0	0	52	3	33
2263.4	379.64	0	0	52	3	34
2263.4	379.64	0	0	46	0	2
2263.4	379.74	0	0	46	0	3
2263.5	379.77	0	0	46	0	4
2263.7	379.99	0	0	46	0	5
2265.4	381.68	298.91	-92.108	46	4	11
2265.4	381.68	0	0	46	3	31
2265.4	381.68	0	0	46	3	32
2267.5	383.79	0	0	46	3	33
2267.5	383.79	0	0	46	3	34
2267.5	383.79	0	0	110	0	2
2267.6	383.88	0	0	110	0	3
2267.6	383.88	0	0	110	0	4
2267.8	384.08	0	0	110	0	5
2272	388.33	297.22	-98.881	110	4	11
2272	388.33	0	0	110	3	31
2272	388.33	0	0	110	3	32
2274.2	390.46	0	0	110	3	33
2274.2	390.46	0	0	110	3	34
2274.2	390.46	0	0	209	0	2
2274.3	390.6	0	0	209	0	3
2274.3	390.61	0	0	209	0	4
2274.6	390.86	0	0	209	0	5
2279.4	395.71	292.14	-61.722	209	4	11
2279.4	395.71	0	0	209	3	31
2279.4	395.71	0	0	209	3	32
2281.6	397.89	0	0	209	3	33
2281.6	397.89	0	0	209	3	34
2281.6	397.89	0	0	88	0	2
2281.7	397.99	0	0	88	0	3
2281.7	398.02	0	0	88	0	4
2281.9	398.22	0	0	88	0	5
2285.6	401.93	294.68	-96.341	88	4	11
2285.6	401.93	0	0	88	3	31
2285.6	401.93	0	0	88	3	32
2287.8	404.07	0	0	88	3	33
2287.8	404.07	0	0	88	3	34
2287.8	404.07	0	0	309	0	2
2287.9	404.18	0	0	309	0	3
2287.9	404.19	0	0	309	0	4
2288.1	404.44	0	0	309	0	5
2291.1	407.38	298.07	-56.643	309	4	11
2291.1	407.38	0	0	309	3	31
2291.1	407.38	0	0	309	3	32
2293.2	409.53	0	0	309	3	33
2293.2	409.53	0	0	309	3	34
2293.2	409.53	0	0	301	0	2
2293.4	409.64	0	0	301	0	3
2293.4	409.64	0	0	301	0	4
2293.6	409.86	0	0	301	0	5
2299.6	415.91	288.75	-78.563	301	4	11
2299.6	415.91	0	0	301	3	31
2299.6	415.91	0	0	301	3	32
2301.8	418.1	0	0	301	3	33
2301.8	418.1	0	0	301	3	34
2301.8	418.1	0	0	27	0	2
2301.9	418.19	0	0	27	0	3

2301.9	418.2	0	0	27	0	4
2302.1	418.42	0	0	27	0	5
2305.5	421.75	292.99	-105.65	27	4	11
2305.5	421.75	0	0	27	3	31
2305.5	421.75	0	0	27	3	32
2307.6	423.88	0	0	27	3	33
2307.6	423.88	0	0	27	3	34
2307.6	423.88	0	0	306	0	2
2307.7	423.97	0	0	306	0	3
2307.7	423.99	0	0	306	0	4
2307.9	424.2	0	0	306	0	5
2314.2	430.53	215.95	-84.489	306	4	11
2314.2	430.53	0	0	306	3	31
2314.2	430.53	0	0	306	3	32
2316.4	432.66	0	0	306	3	33
2316.4	432.66	0	0	306	3	34
2316.4	432.66	0	0	82	0	2
2316.5	432.77	0	0	82	0	3
2316.5	432.78	0	0	82	0	4
2316.7	433	0	0	82	0	5
2319.2	435.5	266.74	-80.257	82	4	11
2319.2	435.5	0	0	82	3	31
2319.2	435.5	0	0	82	3	32
2321.3	437.63	0	0	82	3	33
2321.3	437.63	0	0	82	3	34
2321.3	437.63	0	0	227	0	2
2321.4	437.74	0	0	227	0	3
2321.5	437.75	0	0	227	0	4
2321.7	438.02	0	0	227	0	5
2323.9	440.24	257.43	-67.648	227	4	11
2323.9	440.24	0	0	227	3	31
2323.9	440.24	0	0	227	3	32
2326.1	442.38	0	0	227	3	33
2326.1	442.38	0	0	227	3	34
2326.1	442.38	0	0	85	0	2
2326.2	442.47	0	0	85	0	3
2326.2	442.5	0	0	85	0	4
2326.4	442.7	0	0	85	0	5
2329.7	445.97	416.58	298.16	85	4	11
2329.7	445.97	417	298	85	2	11
2331.4	447.66	309.92	-73.484	85	4	11
2331.4	447.66	0	0	85	3	31
2331.4	447.66	0	0	85	3	32
2333.5	449.78	0	0	85	3	33
2333.5	449.78	0	0	85	3	34
2333.5	449.78	0	0	63	0	2
2333.6	449.88	0	0	63	0	3
2333.6	449.91	0	0	63	0	4
2333.8	450.11	0	0	63	0	5
2335.9	452.17	305.69	-88.722	63	4	11
2335.9	452.17	0	0	63	3	31
2335.9	452.17	0	0	63	3	32
2338	454.31	0	0	63	3	33
2338	454.31	0	0	63	3	34
2338	454.31	0	0	71	0	2
2338.1	454.41	0	0	71	0	3
2338.1	454.42	0	0	71	0	4
2338.3	454.64	0	0	71	0	5

2342.2	458.51	296.37	-112.43	71	4	11
2342.2	458.51	0	0	71	3	31
2342.2	458.51	0	0	71	3	32
2344.4	460.65	0	0	71	3	33
2344.4	460.65	0	0	71	3	34
2344.4	460.65	0	0	210	0	2
2344.5	460.8	0	0	210	0	3
2344.5	460.83	0	0	210	0	4
2344.8	461.08	0	0	210	0	5
2347.4	463.72	292.99	-72.728	210	4	11
2347.4	463.72	0	0	210	3	31
2347.4	463.73	0	0	210	3	32
2349.6	465.84	0	0	210	3	33
2349.6	465.84	0	0	210	3	34
2349.6	465.84	0	0	2	0	2
2349.7	465.95	0	0	2	0	3
2349.7	465.98	0	0	2	0	4
2349.9	466.23	0	0	2	0	5
2352.3	468.59	102.51	436.9	2	4	11
2352.3	468.59	103	437	2	2	11
2354.8	471.06	241.35	-49.87	2	4	11
2354.8	471.06	0	0	2	3	31
2354.8	471.06	0	0	2	3	32
2356.9	473.2	0	0	2	3	33
2356.9	473.2	0	0	2	3	34
2356.9	473.2	0	0	54	0	2
2357	473.3	0	0	54	0	3
2357	473.33	0	0	54	0	4
2357.2	473.53	0	0	54	0	5
2358.7	474.98	237.96	-92.955	54	4	11
2358.7	474.98	0	0	54	3	31
2358.7	474.98	0	0	54	3	32
2360.8	477.12	0	0	54	3	33
2360.8	477.12	0	0	54	3	34
2360.8	477.12	0	0	86	0	2
2360.9	477.22	0	0	86	0	3
2360.9	477.22	0	0	86	0	4
2361.1	477.42	0	0	86	0	5
2363.6	479.86	202.4	364.19	86	4	11
2363.6	479.86	202	364	86	2	11
2365.4	481.69	268.44	-99.728	86	4	11
2365.4	481.69	0	0	86	3	31
2365.4	481.69	0	0	86	3	32
2367.6	483.86	0	0	86	3	33
2367.6	483.86	0	0	86	3	34
2367.6	483.86	0	0	320	0	2
2367.6	483.94	0	0	320	0	3
2367.7	483.97	0	0	320	0	4
2367.9	484.19	0	0	320	0	5
2369.9	486.15	271.82	-92.955	320	4	11
2369.9	486.15	0	0	320	3	31
2369.9	486.15	0	0	320	3	32
2372	488.28	0	0	320	3	33
2372	488.28	0	0	320	3	34
2372	488.28	0	0	112	0	2
2372.1	488.37	0	0	112	0	3
2372.1	488.37	0	0	112	0	4
2372.3	488.57	0	0	112	0	5

2374	490.26	190.55	139	112	4	11
2374	490.26	191	139	112	2	11
2376	492.26	147.38	361.65	112	4	11
2376	492.26	147	362	112	2	11
2377.9	494.22	256.58	-82.796	112	4	11
2377.9	494.22	0	0	112	3	31
2377.9	494.22	0	0	112	3	32
2380.1	496.4	0	0	112	3	33
2380.1	496.4	0	0	112	3	34
2380.1	496.4	0	0	317	0	2
2380.2	496.53	0	0	317	0	3
2380.3	496.54	0	0	317	0	4
2380.5	496.75	0	0	317	0	5
2385.5	501.75	286.21	419.21	317	4	11
2385.5	501.75	285	419	317	3	11
2387.2	503.51	289.6	-83.643	317	4	11
2387.2	503.51	0	0	317	3	31
2387.2	503.51	0	0	317	3	32
2389.4	505.68	0	0	317	3	33
2389.4	505.68	0	0	317	3	34
2389.4	505.68	0	0	17	0	2
2389.5	505.81	0	0	17	0	3
2389.5	505.84	0	0	17	0	4
2389.8	506.09	0	0	17	0	5
2392.8	509.12	159.23	28.013	17	4	11
2392.8	509.12	159	28	17	2	11
2395	511.32	272.67	-76.96	17	4	11
2395	511.32	0	0	17	3	31
2395	511.32	0	0	17	3	32
2397.2	513.45	0	0	17	3	33
2397.2	513.45	0	0	17	3	34
2397.2	513.45	0	0	206	0	2
2397.3	513.57	0	0	206	0	3
2397.3	513.61	0	0	206	0	4
2397.6	513.86	0	0	206	0	5
2400	516.31	249.81	-49.024	206	4	11
2400	516.31	0	0	206	3	31
2400	516.32	0	0	206	3	32
2402.2	518.45	0	0	206	3	33
2402.2	518.45	0	0	206	3	34
2402.2	518.45	0	0	9	0	2
2402.3	518.57	0	0	9	0	3
2402.3	518.6	0	0	9	0	4
2402.5	518.84	0	0	9	0	5
2406.2	522.54	284.52	608.75	9	4	11
2406.2	522.54	285	608	9	3	11
2408.7	525.01	295.53	-60.029	9	4	11
2408.7	525.01	0	0	9	3	31
2408.7	525.01	0	0	9	3	32
2410.8	527.13	0	0	9	3	33
2410.8	527.13	0	0	9	3	34
2410.8	527.13	0	0	21	0	2
2411	527.28	0	0	21	0	3
2411	527.29	0	0	21	0	4
2411.2	527.54	0	0	21	0	5
2414.3	530.57	304.84	-68.495	21	4	11
2414.3	530.57	0	0	21	3	31
2414.3	530.57	0	0	21	3	32

2416.5	532.77	0	0	21	3	33
2416.5	532.77	0	0	21	3	34
2416.5	532.77	0	0	64	0	2
2416.6	532.87	0	0	64	0	3
2416.6	532.88	0	0	64	0	4
2416.8	533.1	0	0	64	0	5
2418.7	535.02	298.91	-91.262	64	4	11
2418.7	535.02	0	0	64	3	31
2418.7	535.02	0	0	64	3	32
2420.9	537.15	0	0	64	3	33
2420.9	537.15	0	0	64	3	34
2420.9	537.15	0	0	229	0	2
2421	537.26	0	0	229	0	3
2421	537.29	0	0	229	0	4
2421.2	537.52	0	0	229	0	5
2424.5	540.79	408.12	237.96	229	4	11
2424.5	540.79	406	238	229	3	11
2427.4	543.68	310.76	-52.41	229	4	11
2427.4	543.68	0	0	229	3	31
2427.4	543.68	0	0	229	3	32
2429.5	545.82	0	0	229	3	33
2429.5	545.82	0	0	229	3	34
2429.5	545.82	0	0	1	0	2
2429.7	545.95	0	0	1	0	3
2429.7	545.98	0	0	1	0	4
2430	546.24	0	0	1	0	5
2433.2	549.49	301.45	-65.955	1	4	11
2433.2	549.49	0	0	1	3	31
2433.2	549.49	0	0	1	3	32
2435.4	551.66	0	0	1	3	33
2435.4	551.66	0	0	1	3	34
2435.4	551.66	0	0	53	0	2
2435.5	551.76	0	0	53	0	3
2435.5	551.79	0	0	53	0	4
2435.7	551.99	0	0	53	0	5
2440	556.32	259.12	388.74	53	4	11
2440	556.32	259	387	53	3	11
2442.2	558.45	309.92	-85.336	53	4	11
2442.2	558.45	0	0	53	3	31
2442.2	558.45	0	0	53	3	32
2444.4	560.66	0	0	53	3	33
2444.4	560.66	0	0	53	3	34
2444.4	560.66	0	0	7	0	2
2444.5	560.81	0	0	7	0	3
2444.5	560.84	0	0	7	0	4
2444.8	561.09	0	0	7	0	5
2449.9	566.23	275.21	-57.489	7	4	11
2449.9	566.23	0	0	7	3	31
2449.9	566.24	0	0	7	3	32
2452.1	568.41	0	0	7	3	33
2452.1	568.41	0	0	7	3	34
2452.1	568.41	0	0	230	0	2
2452.2	568.51	0	0	230	0	3
2452.2	568.54	0	0	230	0	4
2452.5	568.77	0	0	230	0	5
2454.2	570.52	262.51	-74.421	230	4	11
2454.2	570.52	0	0	230	3	31
2454.2	570.52	0	0	230	3	32

2456.4	572.66	0	0	230	3	33
2456.4	572.66	0	0	230	3	34
2456.4	572.66	0	0	217	0	2
2456.5	572.79	0	0	217	0	3
2456.5	572.8	0	0	217	0	4
2456.8	573.07	0	0	217	0	5
2461.4	577.69	314.15	202.4	217	4	11
2461.4	577.69	314	203	217	3	11
2463	579.27	278.6	-58.336	217	4	11
2463	579.27	0	0	217	3	31
2463	579.27	0	0	217	3	32
2465.1	581.43	0	0	217	3	33
2465.1	581.43	0	0	217	3	34
2465.1	581.43	0	0	6	0	2
2465.3	581.57	0	0	6	0	3
2465.3	581.6	0	0	6	0	4
2465.6	581.85	0	0	6	0	5
2468.3	584.62	282.83	-51.563	6	4	11
2468.3	584.62	0	0	6	3	31
2468.3	584.62	0	0	6	3	32
2470.5	586.76	0	0	6	3	33
2470.5	586.76	0	0	6	3	34
2470.5	586.76	0	0	34	0	2
2470.6	586.87	0	0	34	0	3
2470.6	586.87	0	0	34	0	4
2470.8	587.07	0	0	34	0	5
2473	589.26	262.51	186.41	34	4	11
2473	589.26	263	186	34	2	11
2475	591.3	280.29	-92.955	34	4	11
2475	591.3	0	0	34	3	31
2475	591.3	0	0	34	3	32
2477.2	593.44	0	0	34	3	33
2477.2	593.44	0	0	34	3	34
2477.2	593.44	0	0	223	0	2
2477.3	593.55	0	0	223	0	3
2477.3	593.58	0	0	223	0	4
2477.5	593.82	0	0	223	0	5
2482.7	598.99	258.28	204.94	223	4	11
2482.7	598.99	259	205	223	3	11
2484.3	600.57	242.19	201.56	223	4	11
2484.3	600.57	242	202	223	2	11
2486.5	602.76	297.22	-57.489	223	4	11
2486.5	602.76	0	0	223	3	31
2486.5	602.76	0	0	223	3	32
2488.6	604.88	0	0	223	3	33
2488.6	604.88	0	0	223	3	34
2488.6	604.88	0	0	10	0	2
2488.7	604.99	0	0	10	0	3
2488.7	605.02	0	0	10	0	4
2489	605.27	0	0	10	0	5
2493.3	609.63	287.91	473.3	10	4	11
2493.3	609.63	287	472	10	3	11
2495.6	611.91	415.74	349.71	10	4	11
2495.6	611.91	415	349	10	3	11
2498.4	614.74	410.66	349.71	10	4	11
2498.4	614.74	411	350	10	2	11
2501.2	617.5	293.83	-58.336	10	4	11
2501.2	617.5	0	0	10	3	31

2501.2	617.5	0	0	10	3	32
2503.4	619.64	0	0	10	3	33
2503.4	619.64	0	0	10	3	34
2503.4	619.64	0	0	326	0	2
2503.4	619.74	0	0	326	0	3
2503.5	619.77	0	0	326	0	4
2503.7	619.99	0	0	326	0	5
2506.9	623.21	296.37	-81.95	326	4	11
2506.9	623.21	0	0	326	3	31
2506.9	623.21	0	0	326	3	32
2509.1	625.35	0	0	326	3	33
2509.1	625.35	0	0	326	3	34
2509.1	625.35	0	0	69	0	2
2509.1	625.44	0	0	69	0	3
2509.2	625.47	0	0	69	0	4
2509.4	625.67	0	0	69	0	5
2512	628.28	297.22	-79.41	69	4	11
2512	628.28	0	0	69	3	31
2512	628.28	0	0	69	3	32
2514.1	630.42	0	0	69	3	33
2514.1	630.42	0	0	69	3	34
2514.1	630.42	0	0	4	0	2
2514.3	630.57	0	0	4	0	3
2514.3	630.58	0	0	4	0	4
2514.5	630.83	0	0	4	0	5
2517.4	633.66	298.07	-57.489	4	4	11
2517.4	633.66	0	0	4	3	31
2517.4	633.66	0	0	4	3	32
2519.6	635.86	0	0	4	3	33
2519.6	635.86	0	0	4	3	34
2519.6	635.86	0	0	76	0	2
2519.7	635.96	0	0	76	0	3
2519.7	635.96	0	0	76	0	4
2519.9	636.17	0	0	76	0	5
2522.2	638.46	335.31	176.25	76	4	11
2522.2	638.46	335	176	76	2	11
2524	640.27	342.09	-88.722	76	4	11
2524	640.27	0	0	76	3	31
2524	640.27	0	0	76	3	32
2526.1	642.41	0	0	76	3	33
2526.1	642.41	0	0	76	3	34
2526.1	642.41	0	0	302	0	2
2526.2	642.5	0	0	302	0	3
2526.2	642.53	0	0	302	0	4
2526.5	642.78	0	0	302	0	5
2531.8	648.13	348.86	298.91	302	4	11
2531.8	648.14	349	299	302	2	11
2534.1	650.44	321.77	-56.643	302	4	11
2534.1	650.44	0	0	302	3	31
2534.1	650.44	0	0	302	3	32
2536.3	652.58	0	0	302	3	33
2536.3	652.58	0	0	302	3	34
2536.3	652.58	0	0	72	0	2
2536.4	652.67	0	0	72	0	3
2536.4	652.69	0	0	72	0	4
2536.6	652.92	0	0	72	0	5
2538.6	654.86	315.84	-76.87	72	4	11
2538.6	654.88	0	0	72	3	31

2538.6	654.88	0	0	72	3	32
2540.7	657	0	0	72	3	33
2540.7	657	0	0	72	3	34
2540.7	657	0	0	38	0	2
2540.8	657.1	0	0	38	0	3
2540.8	657.1	0	0	38	0	4
2541	657.31	0	0	38	0	5
2544	660.31	313.3	-84.489	38	4	11
2544	660.31	0	0	38	3	31
2544	660.31	0	0	38	3	32
2546.1	662.44	0	0	38	3	33
2546.1	662.44	0	0	38	3	34
2546.1	662.44	0	0	324	0	2
2546.2	662.52	0	0	324	0	3
2546.3	662.55	0	0	324	0	4
2546.5	662.75	0	0	324	0	5
2548.8	665.13	309.92	-88.722	324	4	11
2548.8	665.13	0	0	324	3	31
2548.8	665.13	0	0	324	3	32
2551	667.25	0	0	324	3	33
2551	667.25	0	0	324	3	34
2551	667.25	0	0	65	0	2
2551.1	667.34	0	0	65	0	3
2551.1	667.38	0	0	65	0	4
2551.3	667.59	0	0	65	0	5
2554.1	670.41	309.92	-99.728	65	4	11
2554.1	670.42	0	0	65	3	31
2554.1	670.42	0	0	65	3	32
2556.3	672.61	0	0	65	3	33
2556.3	672.61	0	0	65	3	34
2556.3	672.61	0	0	205	0	2
2556.5	672.75	0	0	205	0	3
2556.5	672.75	0	0	205	0	4
2556.7	672.97	0	0	205	0	5
2559	675.3	70.341	307.38	205	4	11
2559	675.3	70	307	205	2	11
2561.3	677.61	232.03	-46.484	205	4	11
2561.3	677.61	0	0	205	3	31
2561.3	677.61	0	0	205	3	32
2563.5	679.78	0	0	205	3	33
2563.5	679.78	0	0	205	3	34
2563.5	679.78	0	0	218	0	2
2563.6	679.9	0	0	218	0	3
2563.6	679.9	0	0	218	0	4
2563.8	680.14	0	0	218	0	5
2565.5	681.83	199.87	234.57	218	4	11
2565.5	681.83	200	235	218	2	11
2567.4	683.65	276.06	-79.5	218	4	11
2567.4	683.65	0	0	218	3	31
2567.4	683.65	0	0	218	3	32
2569.5	685.78	0	0	218	3	33
2569.5	685.78	0	0	218	3	34
2569.5	685.78	0	0	103	0	2
2569.6	685.87	0	0	103	0	3
2569.6	685.87	0	0	103	0	4
2569.8	686.08	0	0	103	0	5
2573	689.28	273.52	-81.103	103	4	11
2573	689.28	0	0	103	3	31

2573	689.28	0	0	103	3	32
2575.1	691.42	0	0	103	3	33
2575.1	691.42	0	0	103	3	34
2575.1	691.42	0	0	94	0	2
2575.2	691.5	0	0	94	0	3
2575.2	691.53	0	0	94	0	4
2575.5	691.75	0	0	94	0	5
2577.7	693.98	272.67	-97.188	94	4	11
2577.7	693.98	0	0	94	3	31
2577.7	693.98	0	0	94	3	32
2579.8	696.09	0	0	94	3	33
2579.8	696.09	0	0	94	3	34
2579.8	696.09	0	0	314	0	2
2579.9	696.19	0	0	314	0	3
2579.9	696.19	0	0	314	0	4
2580.1	696.4	0	0	314	0	5
2583.1	699.4	271.82	-97.188	314	4	11
2583.1	699.4	0	0	314	3	31
2583.1	699.4	0	0	314	3	32
2585.3	701.56	0	0	314	3	33
2585.3	701.56	0	0	314	3	34
2585.3	701.56	0	0	409	0	2
2585.4	701.72	0	0	409	0	3
2585.4	701.73	0	0	409	0	4
2585.7	701.98	0	0	409	0	5
2589.3	705.61	459.76	348.86	409	4	11
2589.3	705.61	460	349	409	2	11
2592.7	708.97	459.76	349.71	409	4	11
2592.7	708.97	460	349	409	3	11
2594.6	710.92	469.92	348.86	409	4	11
2594.6	710.92	470	349	409	2	11
2598	714.34	292.14	-54.95	409	4	11
2598	714.34	0	0	409	3	31
2598.1	714.36	0	0	409	3	32
2600.2	716.48	0	0	409	3	33
2600.2	716.48	0	0	409	3	34
2600.2	716.48	0	0	89	0	2
2600.3	716.61	0	0	89	0	3
2600.3	716.61	0	0	89	0	4
2600.5	716.83	0	0	89	0	5
2602.3	718.61	257.43	-114.97	89	4	11
2602.3	718.61	0	0	89	3	31
2602.3	718.61	0	0	89	3	32
2604.5	720.75	0	0	89	3	33
2604.5	720.75	0	0	89	3	34
2604.5	720.75	0	0	406	0	2
2604.5	720.84	0	0	406	0	3
2604.6	720.87	0	0	406	0	4
2604.8	721.12	0	0	406	0	5
2606.4	722.68	294.68	-54.95	406	4	11
2606.4	722.68	0	0	406	3	31
2606.4	722.68	0	0	406	3	32
2608.5	724.84	0	0	406	3	33
2608.5	724.84	0	0	406	3	34
2608.5	724.84	0	0	307	0	2
2608.7	724.95	0	0	307	0	3
2608.7	724.97	0	0	307	0	4
2608.9	725.22	0	0	307	0	5

2611.2	727.47	293.83	-76.114	307	4	11
2611.2	727.47	0	0	307	3	31
2611.2	727.47	0	0	307	3	32
2613.3	729.59	0	0	307	3	33
2613.3	729.59	0	0	307	3	34
2613.3	729.59	0	0	13	0	2
2613.4	729.73	0	0	13	0	3
2613.5	729.75	0	0	13	0	4
2613.7	730.01	0	0	13	0	5
2616.2	732.53	315	42.405	13	4	11
2616.2	732.53	315	42	13	2	11
2619.4	735.67	164.31	606.21	13	4	11
2619.4	735.67	164	605	13	3	11
2621.5	737.82	239.65	321.77	13	4	11
2621.5	737.82	240	322	13	2	11
2623.2	739.51	275.21	-64.262	13	4	11
2623.2	739.53	0	0	13	3	31
2623.2	739.53	0	0	13	3	32
2625.3	741.64	0	0	13	3	33
2625.3	741.64	0	0	13	3	34
2625.3	741.64	0	0	42	0	2
2625.4	741.73	0	0	42	0	3
2625.5	741.75	0	0	42	0	4
2625.7	741.96	0	0	42	0	5
2628.2	744.46	261.66	-94.648	42	4	11
2628.2	744.46	0	0	42	3	31
2628.2	744.46	0	0	42	3	32
2630.3	746.59	0	0	42	3	33
2630.3	746.59	0	0	42	3	34
2630.3	746.59	0	0	5	0	2
2630.4	746.71	0	0	5	0	3
2630.5	746.75	0	0	5	0	4
2630.7	746.98	0	0	5	0	5
2633.9	750.15	160.92	540.18	5	4	11
2633.9	750.15	161	540	5	2	11
2636	752.31	273.52	-80.347	5	4	11
2636	752.31	0	0	5	3	31
2636	752.32	0	0	5	3	32
2638.2	754.52	0	0	5	3	33
2638.2	754.52	0	0	5	3	34
2638.2	754.52	0	0	3	0	2
2638.3	754.62	0	0	3	0	3
2638.4	754.65	0	0	3	0	4
2638.6	754.9	0	0	3	0	5
2640.5	756.77	376.8	209.18	3	4	11
2640.5	756.77	377	209	3	2	11
2642.5	758.82	294.68	-49.87	3	4	11
2642.5	758.82	0	0	3	3	31
2642.5	758.82	0	0	3	3	32
2644.6	760.93	0	0	3	3	33
2644.6	760.93	0	0	3	3	34
2644.6	760.93	0	0	47	0	2
2644.7	761.01	0	0	47	0	3
2644.7	761.04	0	0	47	0	4
2645	761.24	0	0	47	0	5
2646.7	762.99	291.29	-91.262	47	4	11
2646.7	762.99	0	0	47	3	31
2646.7	762.99	0	0	47	3	32

2648.9	765.15	0	0	47	3	33
2648.9	765.15	0	0	47	3	34
2648.9	765.15	0	0	61	0	2
2648.9	765.23	0	0	61	0	3
2649	765.26	0	0	61	0	4
2649.2	765.48	0	0	61	0	5
2651.5	767.82	290.45	-87.876	61	4	11
2651.5	767.82	0	0	61	3	31
2651.5	767.82	0	0	61	3	32
2653.7	769.96	0	0	61	3	33
2653.7	769.96	0	0	61	3	34
2653.7	769.96	0	0	220	0	2
2653.8	770.07	0	0	220	0	3
2653.8	770.1	0	0	220	0	4
2654.1	770.35	0	0	220	0	5
2656.3	772.55	291.29	-68.495	220	4	11
2656.3	772.55	0	0	220	3	31
2656.3	772.55	0	0	220	3	32
2658.4	774.68	0	0	220	3	33
2658.4	774.68	0	0	220	3	34
2658.4	774.68	0	0	311	0	2
2658.5	774.79	0	0	311	0	3
2658.5	774.79	0	0	311	0	4
2658.7	775.02	0	0	311	0	5
2662.1	778.35	288.75	-62.569	311	4	11
2662.1	778.35	0	0	311	3	31
2662.1	778.35	0	0	311	3	32
2664.2	780.48	0	0	311	3	33
2664.2	780.48	0	0	311	3	34
2664.2	780.48	0	0	212	0	2
2664.3	780.6	0	0	212	0	3
2664.3	780.63	0	0	212	0	4
2664.6	780.9	0	0	212	0	5
2667	783.26	337.01	250.66	212	4	11
2667	783.26	337	251	212	2	11
2670.4	786.7	298.91	-70.188	212	4	11
2670.4	786.7	0	0	212	3	31
2670.4	786.71	0	0	212	3	32
2672.6	788.91	0	0	212	3	33
2672.6	788.91	0	0	212	3	34
2672.6	788.91	0	0	303	0	2
2672.7	789.01	0	0	303	0	3
2672.7	789.04	0	0	303	0	4
2673	789.26	0	0	303	0	5
2675.6	791.85	301.45	-92.108	303	4	11
2675.6	791.85	0	0	303	3	31
2675.6	791.85	0	0	303	3	32
2677.7	794.01	0	0	303	3	33
2677.7	794.01	0	0	303	3	34
2677.7	794.01	0	0	77	0	2
2677.8	794.1	0	0	77	0	3
2677.8	794.1	0	0	77	0	4
2678	794.3	0	0	77	0	5
2680.2	796.46	79.653	534.35	77	4	11
2680.2	796.46	80	534	77	2	11
2682.3	798.59	277.75	-101.42	77	4	11
2682.3	798.59	0	0	77	3	31
2682.3	798.59	0	0	77	3	32

2684.5	800.77	0	0	77	3	33
2684.5	800.77	0	0	77	3	34
2684.5	800.77	0	0	232	0	2
2684.6	800.87	0	0	232	0	3
2684.6	800.87	0	0	232	0	4
2684.8	801.12	0	0	232	0	5
2687.1	803.41	189.71	489.39	232	4	11
2687.1	803.41	190	489	232	2	11
2688.8	805.13	259.12	-62.569	232	4	11
2688.8	805.13	0	0	232	3	31
2688.8	805.13	0	0	232	3	32
2691	807.27	0	0	232	3	33
2691	807.27	0	0	232	3	34
2691	807.27	0	0	24	0	2
2691.1	807.38	0	0	24	0	3
2691.1	807.38	0	0	24	0	4
2691.3	807.58	0	0	24	0	5
2693.2	809.52	255.74	-91.262	24	4	11
2693.2	809.52	0	0	24	3	31
2693.2	809.52	0	0	24	3	32
2695.4	811.65	0	0	24	3	33
2695.4	811.65	0	0	24	3	34
2695.4	811.65	0	0	15	0	2
2695.5	811.77	0	0	15	0	3
2695.5	811.8	0	0	15	0	4
2695.8	812.05	0	0	15	0	5
2697.7	814.01	280.29	-82.04	15	4	11
2697.7	814.01	0	0	15	3	31
2697.7	814.01	0	0	15	3	32
2699.9	816.15	0	0	15	3	33
2699.9	816.15	0	0	15	3	34
2699.9	816.15	0	0	41	0	2
2699.9	816.24	0	0	41	0	3
2700	816.26	0	0	41	0	4
2700.2	816.47	0	0	41	0	5
2701.9	818.18	275.21	-118.35	41	4	11
2701.9	818.18	0	0	41	3	31
2701.9	818.18	0	0	41	3	32
2704	820.29	0	0	41	3	33
2704	820.29	0	0	41	3	34
2704	820.29	0	0	106	0	2
2704.1	820.38	0	0	106	0	3
2704.1	820.38	0	0	106	0	4
2704.3	820.6	0	0	106	0	5
2706.7	823.04	219.34	-87.029	106	4	11
2706.7	823.04	0	0	106	3	31
2706.7	823.04	0	0	106	3	32
2708.9	825.18	0	0	106	3	33
2708.9	825.18	0	0	106	3	34
2708.9	825.18	0	0	403	0	2
2709	825.33	0	0	403	0	3
2709.1	825.35	0	0	403	0	4
2709.3	825.6	0	0	403	0	5
2711.4	827.74	188.01	295.53	403	4	11
2711.4	827.74	188	296	403	2	11
2716.3	832.6	188.01	297.22	403	4	11
2716.3	832.6	188	296	403	3	11
2718	834.27	289.6	-60.876	403	4	11

2718	834.27	0	0	403	3	31
2718	834.27	0	0	403	3	32
2720.1	836.41	0	0	403	3	33
2720.1	836.41	0	0	403	3	34
2720.1	836.41	0	0	412	0	2
2720.2	836.5	0	0	412	0	3
2720.2	836.53	0	0	412	0	4
2720.5	836.78	0	0	412	0	5
2722.6	838.94	259.12	-68.495	412	4	11
2722.6	838.94	0	0	412	3	31
2722.6	838.94	0	0	412	3	32
2724.9	841.14	0	0	412	3	33
2724.9	841.14	0	0	412	3	34
2724.9	841.14	0	0	18	0	2
2725	841.28	0	0	18	0	3
2725	841.3	0	0	18	0	4
2725.3	841.55	0	0	18	0	5
2727	843.33	259.97	-50.717	18	4	11
2727	843.33	0	0	18	3	31
2727.1	843.35	0	0	18	3	32
2729.2	845.46	0	0	18	3	33
2729.2	845.46	0	0	18	3	34
2729.2	845.46	0	0	109	0	2
2729.3	845.55	0	0	109	0	3
2729.3	845.57	0	0	109	0	4
2729.5	845.78	0	0	109	0	5
2731.9	848.22	265.05	-105.65	109	4	11
2731.9	848.22	0	0	109	3	31
2731.9	848.22	0	0	109	3	32
2734.1	850.35	0	0	109	3	33
2734.1	850.35	0	0	109	3	34
2734.1	850.35	0	0	31	0	2
2734.1	850.44	0	0	31	0	3
2734.1	850.44	0	0	31	0	4
2734.4	850.66	0	0	31	0	5
2736.1	852.42	264.2	-94.648	31	4	11
2736.1	852.42	0	0	31	3	31
2736.1	852.42	0	0	31	3	32
2738.3	854.57	0	0	31	3	33
2738.3	854.57	0	0	31	3	34
2738.3	854.57	0	0	203	0	2
2738.4	854.69	0	0	203	0	3
2738.4	854.72	0	0	203	0	4
2738.7	854.97	0	0	203	0	5
2742	858.3	269.28	-95.585	203	4	11
2742	858.3	0	0	203	3	31
2742	858.3	0	0	203	3	32
2744.1	860.42	0	0	203	3	33
2744.1	860.42	0	0	203	3	34
2744.1	860.42	0	0	36	0	2
2744.2	860.52	0	0	36	0	3
2744.3	860.55	0	0	36	0	4
2744.5	860.75	0	0	36	0	5
2746.9	863.21	267.59	-120.04	36	4	11
2746.9	863.21	0	0	36	3	31
2746.9	863.21	0	0	36	3	32
2749	865.33	0	0	36	3	33
2749	865.33	0	0	36	3	34

2749	865.33	0	0	19	0	2
2749.2	865.47	0	0	19	0	3
2749.2	865.49	0	0	19	0	4
2749.5	865.75	0	0	19	0	5
2752	868.27	312.46	-81.193	19	4	11
2752	868.27	0	0	19	3	31
2752	868.27	0	0	19	3	32
2754.1	870.41	0	0	19	3	33
2754.1	870.41	0	0	19	3	34
2754.1	870.41	0	0	66	0	2
2754.2	870.5	0	0	66	0	3
2754.2	870.53	0	0	66	0	4
2754.4	870.74	0	0	66	0	5
2759.3	875.64	230.34	473.39	66	4	11
2759.3	875.64	229	470	66	3	11
2762.2	878.47	289.6	-90.415	66	4	11
2762.2	878.47	0	0	66	3	31
2762.2	878.49	0	0	66	3	32
2764.4	880.74	0	0	66	3	33
2764.4	880.74	0	0	66	3	34
2764.4	880.74	0	0	104	0	2
2764.6	880.84	0	0	104	0	3
2764.6	880.86	0	0	104	0	4
2764.8	881.09	0	0	104	0	5
2766.9	883.22	309.07	-88.722	104	4	11
2766.9	883.22	0	0	104	3	31
2766.9	883.22	0	0	104	3	32
2769.1	885.34	0	0	104	3	33
2769.1	885.34	0	0	104	3	34
2769.1	885.34	0	0	310	0	2
2769.2	885.45	0	0	310	0	3
2769.2	885.49	0	0	310	0	4
2769.4	885.74	0	0	310	0	5
2774.3	890.58	49.177	99.124	310	4	11
2774.3	890.58	51	99	310	3	11
2776	892.31	264.2	-50.717	310	4	11
2776	892.31	0	0	310	3	31
2776	892.31	0	0	310	3	32
2778.2	894.5	0	0	310	3	33
2778.2	894.5	0	0	310	3	34
2778.2	894.5	0	0	70	0	2
2778.3	894.61	0	0	70	0	3
2778.3	894.63	0	0	70	0	4
2778.6	894.84	0	0	70	0	5
2780.9	897.22	280.29	-100.57	70	4	11
2780.9	897.22	0	0	70	3	31
2780.9	897.22	0	0	70	3	32
2783.1	899.37	0	0	70	3	33
2783.1	899.37	0	0	70	3	34
2783.1	899.37	0	0	78	0	2
2783.2	899.48	0	0	78	0	3
2783.2	899.5	0	0	78	0	4
2783.4	899.7	0	0	78	0	5
2785.7	901.95	280.29	-97.188	78	4	11
2785.7	901.95	0	0	78	3	31
2785.7	901.97	0	0	78	3	32
2787.8	904.12	0	0	78	3	33
2787.8	904.12	0	0	78	3	34

2787.8	904.12	0	0	25	0	2
2787.9	904.2	0	0	25	0	3
2787.9	904.23	0	0	25	0	4
2788.2	904.45	0	0	25	0	5
2790.6	906.86	281.13	-87.029	25	4	11
2790.6	906.86	0	0	25	3	31
2790.6	906.87	0	0	25	3	32
2792.7	909	0	0	25	3	33
2792.7	909	0	0	25	3	34
2792.7	909	0	0	40	0	2
2792.8	909.09	0	0	40	0	3
2792.8	909.12	0	0	40	0	4
2793.1	909.34	0	0	40	0	5
2795.3	911.64	280.29	-93.802	40	4	11
2795.3	911.64	0	0	40	3	31
2795.3	911.64	0	0	40	3	32
2797.5	913.75	0	0	40	3	33
2797.5	913.75	0	0	40	3	34
2797.5	913.75	0	0	55	0	2
2797.6	913.84	0	0	55	0	3
2797.6	913.86	0	0	55	0	4
2797.8	914.09	0	0	55	0	5
2800.2	916.47	280.29	-95.495	55	4	11
2800.2	916.47	0	0	55	3	31
2800.2	916.47	0	0	55	3	32
2802.4	918.65	0	0	55	3	33
2802.4	918.65	0	0	55	3	34
2802.4	918.65	0	0	404	0	2
2802.5	918.79	0	0	404	0	3
2802.5	918.79	0	0	404	0	4
2802.7	919.01	0	0	404	0	5
2805.3	921.62	436.9	486	404	4	11
2805.3	921.62	437	486	404	2	11
2807.7	923.98	287.91	-60.029	404	4	11
2807.7	923.98	0	0	404	3	31
2807.7	923.98	0	0	404	3	32
2809.8	926.11	0	0	404	3	33
2809.8	926.11	0	0	404	3	34
2809.8	926.11	0	0	14	0	2
2810	926.25	0	0	14	0	3
2810	926.26	0	0	14	0	4
2810.2	926.53	0	0	14	0	5
2812	928.29	309.92	-65.955	14	4	11
2812	928.29	0	0	14	3	31
2812	928.31	0	0	14	3	32
2814.2	930.47	0	0	14	3	33
2814.2	930.47	0	0	14	3	34
2814.2	930.47	0	0	208	0	2
2814.3	930.61	0	0	208	0	3
2814.3	930.62	0	0	208	0	4
2814.6	930.86	0	0	208	0	5
2816.3	932.56	319.23	-60.029	208	4	11
2816.3	932.56	0	0	208	3	31
2816.3	932.56	0	0	208	3	32
2818.4	934.7	0	0	208	3	33
2818.4	934.7	0	0	208	3	34
2818.4	934.7	0	0	33	0	2
2818.5	934.81	0	0	33	0	3

2818.5	934.84	0	0	33	0	4
2818.8	935.04	0	0	33	0	5
2820.3	936.58	325.16	-103.96	33	4	11
2820.3	936.58	0	0	33	3	31
2820.3	936.58	0	0	33	3	32
2822.5	938.76	0	0	33	3	33
2822.5	938.76	0	0	33	3	34
2822.5	938.76	0	0	219	0	2
2822.6	938.87	0	0	219	0	3
2822.6	938.9	0	0	219	0	4
2822.8	939.14	0	0	219	0	5
2825.1	941.37	326	-85.426	219	4	11
2825.1	941.37	0	0	219	3	31
2825.1	941.37	0	0	219	3	32
2827.2	943.5	0	0	219	3	33
2827.2	943.5	0	0	219	3	34
2827.2	943.5	0	0	30	0	2
2827.3	943.59	0	0	30	0	3
2827.3	943.62	0	0	30	0	4
2827.5	943.82	0	0	30	0	5
2829.7	946.01	325.16	-109.89	30	4	11
2829.7	946.01	0	0	30	3	31
2829.7	946.01	0	0	30	3	32
2831.9	948.18	0	0	30	3	33
2831.9	948.18	0	0	30	3	34
2831.9	948.18	0	0	224	0	2
2832	948.29	0	0	224	0	3
2832	948.29	0	0	224	0	4
2832.2	948.51	0	0	224	0	5
2835.5	951.82	238.81	340.39	224	4	11
2835.5	951.82	239	340	224	2	11
2837.4	953.67	293.83	-65.955	224	4	11
2837.4	953.67	0	0	224	3	31
2837.4	953.67	0	0	224	3	32
2839.6	955.86	0	0	224	3	33
2839.6	955.86	0	0	224	3	34
2839.6	955.86	0	0	410	0	2
2839.7	956	0	0	410	0	3
2839.7	956.01	0	0	410	0	4
2840	956.28	0	0	410	0	5
2842.6	958.89	254.89	-66.802	410	4	11
2842.6	958.89	0	0	410	3	31
2842.6	958.89	0	0	410	3	32
2844.7	961.03	0	0	410	3	33
2844.7	961.03	0	0	410	3	34
2844.7	961.03	0	0	44	0	2
2844.8	961.12	0	0	44	0	3
2844.8	961.14	0	0	44	0	4
2845.1	961.35	0	0	44	0	5
2846.7	963.03	260.82	-117.51	44	4	11
2846.7	963.03	0	0	44	3	31
2846.8	963.06	0	0	44	3	32
2848.9	965.17	0	0	44	3	33
2848.9	965.17	0	0	44	3	34
2848.9	965.17	0	0	87	0	2
2849	965.26	0	0	87	0	3
2849	965.29	0	0	87	0	4
2849.2	965.5	0	0	87	0	5

2851.9	968.21	259.97	-115.81	87	4	11
2851.9	968.21	0	0	87	3	31
2851.9	968.21	0	0	87	3	32
2854.1	970.35	0	0	87	3	33
2854.1	970.35	0	0	87	3	34
2854.1	970.35	0	0	20	0	2
2854.2	970.48	0	0	20	0	3
2854.2	970.51	0	0	20	0	4
2854.5	970.76	0	0	20	0	5
2858	974.34	255.74	-46.484	20	4	11
2858	974.34	0	0	20	3	31
2858	974.34	0	0	20	3	32
2860.2	976.46	0	0	20	3	33
2860.2	976.46	0	0	20	3	34
2860.2	976.46	0	0	325	0	2
2860.3	976.62	0	0	325	0	3
2860.3	976.63	0	0	325	0	4
2860.6	976.85	0	0	325	0	5
2863	979.27	264.2	-91.262	325	4	11
2863	979.27	0	0	325	3	31
2863	979.27	0	0	325	3	32
2865.1	981.43	0	0	325	3	33
2865.1	981.43	0	0	325	3	34
2865.1	981.43	0	0	322	0	2
2865.2	981.51	0	0	322	0	3
2865.2	981.54	0	0	322	0	4
2865.5	981.74	0	0	322	0	5
2867.6	983.85	268.44	-98.034	322	4	11
2867.6	983.85	0	0	322	3	31
2867.6	983.85	0	0	322	3	32
2869.7	985.99	0	0	322	3	33
2869.7	985.99	0	0	322	3	34
2869.7	985.99	0	0	90	0	2
2869.8	986.09	0	0	90	0	3
2869.8	986.1	0	0	90	0	4
2870	986.32	0	0	90	0	5
2872.6	988.88	99.971	325.25	90	4	11
2872.6	988.88	100	325	90	2	11
2873.9	990.2	270.13	-82.796	90	4	11
2873.9	990.2	0	0	90	3	31
2873.9	990.2	0	0	90	3	32
2876	992.34	0	0	90	3	33
2876	992.34	0	0	90	3	34
2876	992.34	0	0	28	0	2
2876.1	992.43	0	0	28	0	3
2876.1	992.43	0	0	28	0	4
2876.4	992.65	0	0	28	0	5
2878.6	994.91	284.52	-82.796	28	4	11
2878.6	994.91	0	0	28	3	31
2878.6	994.91	0	0	28	3	32
2880.8	997.07	0	0	28	3	33
2880.8	997.07	0	0	28	3	34
2880.8	997.07	0	0	39	0	2
2880.9	997.16	0	0	39	0	3
2880.9	997.16	0	0	39	0	4
2881.1	997.38	0	0	39	0	5
2882.8	999.09	285.37	-85.336	39	4	11
2882.8	999.09	0	0	39	3	31

2882.8	999.1	0	0	39	3	32
2884.9	1001.2	0	0	39	3	33
2884.9	1001.2	0	0	39	3	34
2884.9	1001.2	0	0	80	0	2
2885	1001.3	0	0	80	0	3
2885	1001.3	0	0	80	0	4
2885.3	1001.6	0	0	80	0	5
2886.8	1003.1	289.6	-98.881	80	4	11
2886.8	1003.1	0	0	80	3	31
2886.8	1003.1	0	0	80	3	32
2889	1005.3	0	0	80	3	33
2889	1005.3	0	0	80	3	34
2889	1005.3	0	0	101	0	2
2889.1	1005.4	0	0	101	0	3
2889.1	1005.4	0	0	101	0	4
2889.3	1005.6	0	0	101	0	5
2891.5	1007.8	274.36	133.92	101	4	11
2891.5	1007.8	274	134	101	2	11
2893.5	1009.8	298.91	-82.796	101	4	11
2893.5	1009.8	0	0	101	3	31
2893.5	1009.8	0	0	101	3	32
2895.6	1011.9	0	0	101	3	33
2895.6	1011.9	0	0	101	3	34
2895.6	1011.9	0	0	211	0	2
2895.7	1012	0	0	211	0	3
2895.8	1012.1	0	0	211	0	4
2896	1012.3	0	0	211	0	5
2898	1014.3	315	-75.267	211	4	11
2898	1014.3	0	0	211	3	31
2898	1014.3	0	0	211	3	32
2900.1	1016.4	0	0	211	3	33
2900.1	1016.4	0	0	211	3	34
2900.1	1016.4	0	0	67	0	2
2900.2	1016.5	0	0	67	0	3
2900.2	1016.5	0	0	67	0	4
2900.4	1016.7	0	0	67	0	5
2902.1	1018.4	314.15	-101.42	67	4	11
2902.1	1018.4	0	0	67	3	31
2902.1	1018.4	0	0	67	3	32
2904.3	1020.6	0	0	67	3	33
2904.3	1020.6	0	0	67	3	34
2904.3	1020.6	0	0	32	0	2
2904.4	1020.6	0	0	32	0	3
2904.4	1020.7	0	0	32	0	4
2904.6	1020.9	0	0	32	0	5
2909.4	1025.7	174.47	264.29	32	4	11
2909.4	1025.7	174	264	32	2	11
2910.7	1027	292.14	-139.52	32	4	11
2910.7	1027	0	0	32	3	31
2910.7	1027	0	0	32	3	32
2912.8	1029.1	0	0	32	3	33
2912.8	1029.1	0	0	32	3	34
2912.8	1029.1	0	0	201	0	2
2913	1029.3	0	0	201	0	3
2913	1029.3	0	0	201	0	4
2913.2	1029.5	0	0	201	0	5
2916.2	1032.5	299.76	-54.103	201	4	11
2916.2	1032.5	0	0	201	3	31

2916.2	1032.5	0	0	201	3	32
2918.3	1034.6	0	0	201	3	33
2918.3	1034.6	0	0	201	3	34
2918.3	1034.6	0	0	11	0	2
2918.4	1034.7	0	0	11	0	3
2918.5	1034.8	0	0	11	0	4
2918.7	1035	0	0	11	0	5
2920.8	1037.1	301.45	-72.728	11	4	11
2920.8	1037.1	0	0	11	3	31
2920.8	1037.1	0	0	11	3	32
2923	1039.3	0	0	11	3	33
2923	1039.3	0	0	11	3	34
2923	1039.3	0	0	100	0	2
2923.1	1039.3	0	0	100	0	3
2923.1	1039.4	0	0	100	0	4
2923.3	1039.6	0	0	100	0	5
2926.1	1042.3	298.91	-98.034	100	4	11
2926.1	1042.3	0	0	100	3	31
2926.1	1042.3	0	0	100	3	32
2928.2	1044.5	0	0	100	3	33
2928.2	1044.5	0	0	100	3	34
2928.2	1044.5	0	0	213	0	2
2928.3	1044.6	0	0	213	0	3
2928.3	1044.6	0	0	213	0	4
2928.5	1044.8	0	0	213	0	5
2933.2	1049.5	296.37	-66.802	213	4	11
2933.2	1049.5	0	0	213	3	31
2933.2	1049.5	0	0	213	3	32
2935.4	1051.6	0	0	213	3	33
2935.4	1051.6	0	0	213	3	34
2935.4	1051.6	0	0	48	0	2
2935.4	1051.7	0	0	48	0	3
2935.5	1051.8	0	0	48	0	4
2935.7	1052	0	0	48	0	5
2938.8	1055.1	305.69	-98.881	48	4	11
2938.8	1055.1	0	0	48	3	31
2938.8	1055.1	0	0	48	3	32
2941	1057.3	0	0	48	3	33
2941	1057.3	0	0	48	3	34
2941	1057.3	0	0	304	0	2
2941.1	1057.3	0	0	304	0	3
2941.1	1057.4	0	0	304	0	4
2941.3	1057.6	0	0	304	0	5
2943.2	1059.5	298.91	-76.024	304	4	11
2943.2	1059.5	0	0	304	3	31
2943.2	1059.5	0	0	304	3	32
2945.3	1061.6	0	0	304	3	33
2945.3	1061.6	0	0	304	3	34
2945.3	1061.6	0	0	312	0	2
2945.4	1061.7	0	0	312	0	3
2945.4	1061.7	0	0	312	0	4
2945.7	1062	0	0	312	0	5
2948.1	1064.4	298.07	-53.257	312	4	11
2948.1	1064.4	0	0	312	3	31
2948.1	1064.4	0	0	312	3	32
2950.3	1066.6	0	0	312	3	33
2950.3	1066.6	0	0	312	3	34
2950.3	1066.6	0	0	226	0	2

2950.4	1066.7	0	0	226	0	3
2950.4	1066.7	0	0	226	0	4
2950.6	1066.9	0	0	226	0	5
2952.1	1068.4	227.8	399.65	226	4	11
2952.1	1068.4	228	400	226	2	11
2953.8	1070.1	270.98	-65.955	226	4	11
2953.8	1070.1	0	0	226	3	31
2953.8	1070.1	0	0	226	3	32
2955.9	1072.2	0	0	226	3	33
2955.9	1072.2	0	0	226	3	34
2955.9	1072.2	0	0	215	0	2
2956.1	1072.3	0	0	215	0	3
2956.1	1072.4	0	0	215	0	4
2956.3	1072.6	0	0	215	0	5
2958.2	1074.5	283.67	-60.029	215	4	11
2958.2	1074.5	0	0	215	3	31
2958.2	1074.5	0	0	215	3	32
2960.3	1076.6	0	0	215	3	33
2960.3	1076.6	0	0	215	3	34
2960.3	1076.6	0	0	23	0	2
2960.4	1076.7	0	0	23	0	3
2960.4	1076.7	0	0	23	0	4
2960.6	1076.9	0	0	23	0	5
2962.6	1078.9	286.21	-95.495	23	4	11
2962.6	1078.9	0	0	23	3	31
2962.6	1078.9	0	0	23	3	32
2964.7	1081	0	0	23	3	33
2964.7	1081	0	0	23	3	34
2964.7	1081	0	0	305	0	2
2964.8	1081.1	0	0	305	0	3
2964.8	1081.1	0	0	305	0	4
2965.1	1081.4	0	0	305	0	5
2967.5	1083.8	145.69	524.94	305	4	11
2967.5	1083.8	146	525	305	2	11
2969	1085.3	286.21	-61.722	305	4	11
2969	1085.3	0	0	305	3	31
2969	1085.3	0	0	305	3	32
2971.1	1087.4	0	0	305	3	33
2971.1	1087.4	0	0	305	3	34
2971.1	1087.4	0	0	316	0	2
2971.2	1087.5	0	0	316	0	3
2971.2	1087.5	0	0	316	0	4
2971.5	1087.8	0	0	316	0	5
2976.1	1092.3	265.05	-86.183	316	4	11
2976.1	1092.3	0	0	316	3	31
2976.1	1092.3	0	0	316	3	32
2978.2	1094.5	0	0	316	3	33
2978.2	1094.5	0	0	316	3	34
2978.2	1094.5	0	0	221	0	2
2978.3	1094.6	0	0	221	0	3
2978.3	1094.6	0	0	221	0	4
2978.6	1094.9	0	0	221	0	5
2980.6	1096.9	266.74	-55.796	221	4	11
2980.6	1096.9	0	0	221	3	31
2980.6	1096.9	0	0	221	3	32
2982.8	1099.1	0	0	221	3	33
2982.8	1099.1	0	0	221	3	34
2982.8	1099.1	0	0	318	0	2

2983	1099.3	0	0	318	0	3
2983	1099.3	0	0	318	0	4
2983.2	1099.5	0	0	318	0	5
2985.1	1101.3	269.28	-87.876	318	4	11
2985.1	1101.3	0	0	318	3	31
2985.1	1101.3	0	0	318	3	32
2987.2	1103.5	0	0	318	3	33
2987.2	1103.5	0	0	318	3	34
2987.2	1103.5	0	0	407	0	2
2987.3	1103.6	0	0	407	0	3
2987.3	1103.6	0	0	407	0	4
2987.6	1103.9	0	0	407	0	5
2989.4	1105.7	274.36	-53.257	407	4	11
2989.4	1105.7	0	0	407	3	31
2989.4	1105.7	0	0	407	3	32
2991.6	1107.8	0	0	407	3	33
2991.6	1107.8	0	0	407	3	34
2991.6	1107.8	0	0	73	0	2
2991.6	1107.9	0	0	73	0	3
2991.7	1108	0	0	73	0	4
2991.9	1108.2	0	0	73	0	5
2994.5	1110.8	298.91	-96.341	73	4	11
2994.5	1110.8	0	0	73	3	31
2994.6	1110.8	0	0	73	3	32
2996.7	1113	0	0	73	3	33
2996.7	1113	0	0	73	3	34
2996.7	1113	0	0	45	0	2
2996.8	1113	0	0	45	0	3
2996.8	1113.1	0	0	45	0	4
2997	1113.3	0	0	45	0	5
3001	1117.3	298.07	-87.876	45	4	11
3001	1117.3	0	0	45	3	31
3001	1117.3	0	0	45	3	32
3003.1	1119.4	0	0	45	3	33
3003.1	1119.4	0	0	45	3	34
3003.1	1119.4	0	0	56	0	2
3003.2	1119.5	0	0	56	0	3
3003.2	1119.5	0	0	56	0	4
3003.4	1119.7	0	0	56	0	5
3005	1121.3	284.52	-104.81	56	4	11
3005	1121.3	0	0	56	3	31
3005	1121.3	0	0	56	3	32
3007.2	1123.5	0	0	56	3	33
3007.2	1123.5	0	0	56	3	34
3007.2	1123.5	0	0	328	0	2
3007.3	1123.6	0	0	328	0	3
3007.3	1123.6	0	0	328	0	4
3007.5	1123.8	0	0	328	0	5
3009.7	1126	284.52	-101.42	328	4	11
3009.7	1126	0	0	328	3	31
3009.7	1126	0	0	328	3	32
3011.9	1128.2	0	0	328	3	33
3011.9	1128.2	0	0	328	3	34
3011.9	1128.2	0	0	84	0	2
3012	1128.3	0	0	84	0	3
3012	1128.3	0	0	84	0	4
3012.2	1128.5	0	0	84	0	5
3013.7	1130	282.83	-92.108	84	4	11

3013.7	1130	0	0	84	3	31
3013.7	1130	0	0	84	3	32
3015.8	1132.1	0	0	84	3	33
3015.8	1132.1	0	0	84	3	34
3015.8	1132.1	0	0	108	0	2
3015.9	1132.2	0	0	108	0	3
3015.9	1132.2	0	0	108	0	4
3016.1	1132.4	0	0	108	0	5
3019.4	1135.7	285.37	-111.58	108	4	11
3019.4	1135.7	0	0	108	3	31
3019.4	1135.7	0	0	108	3	32
3021.5	1137.8	0	0	108	3	33
3021.5	1137.8	0	0	108	3	34
3021.5	1137.8	0	0	60	0	2
3021.6	1137.9	0	0	60	0	3
3021.6	1137.9	0	0	60	0	4
3021.9	1138.2	0	0	60	0	5
3025.3	1141.6	282.83	-102.27	60	4	11
3025.3	1141.6	0	0	60	3	31
3025.3	1141.6	0	0	60	3	32
3027.5	1143.8	0	0	60	3	33
3027.5	1143.8	0	0	60	3	34
3027.5	1143.8	0	0	50	0	2
3027.6	1143.9	0	0	50	0	3
3027.6	1143.9	0	0	50	0	4
3027.8	1144.1	0	0	50	0	5
3029.3	1145.6	281.13	-106.5	50	4	11
3029.3	1145.6	0	0	50	3	31
3029.3	1145.6	0	0	50	3	32
3031.4	1147.7	0	0	50	3	33
3031.4	1147.7	0	0	50	3	34
3031.4	1147.7	0	0	91	0	2
3031.5	1147.8	0	0	91	0	3
3031.5	1147.8	0	0	91	0	4
3031.8	1148.1	0	0	91	0	5
3034.6	1150.9	287.06	-109.89	91	4	11
3034.6	1150.9	0	0	91	3	31
3034.6	1150.9	0	0	91	3	32
3036.8	1153.1	0	0	91	3	33
3036.8	1153.1	0	0	91	3	34
3036.8	1153.1	0	0	95	0	2
3036.9	1153.2	0	0	95	0	3
3036.9	1153.2	0	0	95	0	4
3037.1	1153.4	0	0	95	0	5
3039.6	1155.9	280.29	-110.73	95	4	11
3039.6	1155.9	0	0	95	3	31
3039.6	1155.9	0	0	95	3	32
3041.7	1158	0	0	95	3	33
3041.7	1158	0	0	95	3	34
3041.7	1158	0	0	83	0	2
3041.8	1158.1	0	0	83	0	3
3041.8	1158.1	0	0	83	0	4
3042	1158.3	0	0	83	0	5
3043.8	1160.1	221.88	304.08	83	4	11
3043.8	1160.1	222	304	83	2	11
3045.1	1161.4	247.27	-83.643	83	4	11
3045.1	1161.4	0	0	83	3	31
3045.1	1161.4	0	0	83	3	32

3047.3	1163.6	0	0	83	3	33
3047.3	1163.6	0	0	83	3	34
3047.3	1163.6	0	0	43	0	2
3047.4	1163.7	0	0	43	0	3
3047.4	1163.7	0	0	43	0	4
3047.6	1163.9	0	0	43	0	5
3049.4	1165.7	118.6	284.61	43	4	11
3049.4	1165.7	119	285	43	2	11
3051.4	1167.7	261.66	-91.262	43	4	11
3051.4	1167.7	0	0	43	3	31
3051.4	1167.7	0	0	43	3	32
3053.5	1169.8	0	0	43	3	33
3053.5	1169.8	0	0	43	3	34
3053.5	1169.8	0	0	26	0	2
3053.6	1169.9	0	0	26	0	3
3053.6	1169.9	0	0	26	0	4
3053.9	1170.2	0	0	26	0	5
3055.4	1171.7	279.44	-89.569	26	4	11
3055.4	1171.7	0	0	26	3	31
3055.4	1171.7	0	0	26	3	32
3057.5	1173.8	0	0	26	3	33
3057.5	1173.8	0	0	26	3	34
3057.5	1173.8	0	0	207	0	2
3057.7	1173.9	0	0	207	0	3
3057.7	1174	0	0	207	0	4
3057.9	1174.2	0	0	207	0	5
3059.9	1176.2	282.83	-49.024	207	4	11
3059.9	1176.2	0	0	207	3	31
3059.9	1176.2	0	0	207	3	32
3062	1178.3	0	0	207	3	33
3062	1178.3	0	0	207	3	34
3062	1178.3	0	0	0	0	99

Appendix IX: Algorithm for extracting the subjects' performance measures from the raw data recorded in the experiment.

```
% calculating the subject performances
clear
clc

tic
for d=1:3
    for set=1:3
        tmpname=['dssum',num2str(d),num2str(set)];
        eval([tmpname,'=[]']);
    end
end

load melondatabase % matrix of all the melons in all images: melon's number, x, y, image number
load image_levels % includes 3 vectors that includes all the image's numbers by complexity: easy, medium,
difficult
load GROUPS % the matrix of students according to groups, each line is a group

ImageDirs=['C:\Documents and Settings\user\My Documents\phd\exp2003\']

%Do the following loop for all directories that contain images
dr=1
% Get filenames of images
dname=dir(ImageDirs(dr,:));
[NumberOfFiles,Dummy]=size(dname);
NumberOfFiles

for i=1:NumberOfFiles
    if ~dname(i).isdir
        fn=[dname(i).name];
        lfn=length(fn);
        if lfn>7 & fn(1:7)=='student'
            robot_all_tar=[];
            robohit=[];
            robotFA=[];
            sdnstr=fn(8:lfn-4);
            sdnum=str2num(sdnstr);
            t1=[];
            t2=[];
            t3=[];
            eval(['load ' fn(1:lfn-4)])
            [stgroup locy]=find(GROUPS==sdnum);

%load student100

% finding the image order of the experiment
imgord=Hologger(1,1);
for j=2:length(Hologger(:,1))
    if Hologger(j,1)~=imgord(length(imgord))
        imgord=[imgord,Hologger(j,1)];
    end
end

%finding the start point and end point of each image
if ~isempty(t1)
```

```

imgstartmark=find(t1(:,7)==5);
imgendmark=find(t1(:,7)==31);
imgstart=t1(imgstartmark,2);
imgend=t1(imgendmark,2);
end
if ~isempty(t2)
    imgstartmark=find(t2(:,7)==5);
    imgendmark=find(t2(:,7)==31);
    imgstart=t2(imgstartmark,2);
    imgend=t2(imgendmark,2);
end
if ~isempty(t3)
    imgstartmark=find(t3(:,7)==5);
    imgendmark=find(t3(:,7)==31);
    imgstart=t3(imgstartmark,2);
    imgend=t3(imgendmark,2);
end
deltaimgtime=imgend-imgstart;

block=[imgord(1:60);imgord(61:120);imgord(121:180)]; % setting the images into 3 sets
deltaimgtimeblock=[deltaimgtime(1:60);deltaimgtime(61:120);deltaimgtime(121:180)]; % setting the image
time into 3 sets
blocktime=sum(deltaimgtimeblock');
compblock=zeros(3,60);

% finding the image complexities of each experiment in 3 sets block
for b=1:3
    for k=1:60
        tmpeasy=find(easy==block(b,k));
        tmpmed=find(medium==block(b,k));
        tmpdiff=find(difficult==block(b,k));
        if ~isempty(tmpeasy)
            compblock(b,k)=1;
        elseif ~isempty(tmpmed)
            compblock(b,k)=2;
        elseif ~isempty(tmpdiff)
            compblock(b,k)=3;
        end
    end
end
%toc

imgdata=[];

for d=1:3
    for set=1:3
        comploc=find(compblock(set,:)==d); % location of each d complexity images in the block
        tmpcomp=block(set,comploc); % the images no. in that block and complexity

        tmpdeltatime=deltaimgtimeblock(set,comploc); % the images time in that block and complexity
        grossdtaverage(d,set)=mean(tmpdeltatime); % average time of all images in that block and complexity
        grossdtstd(d,set)=std(tmpdeltatime); % std time of all images in that block and complexity
        grossdsettime(d,set)=sum(tmpdeltatime);
        netdimage=find(tmpcomp~=13 & tmpcomp~=112 & tmpcomp~=212);
        tmpnetdeltatime=tmpdeltatime(netdimage); % list of images times w/o the time of the problematic images
        netdtaverage(d,set)=mean(tmpnetdeltatime); % average time of all GOOD images in that block and
complexity
        netdtstd(d,set)=std(tmpnetdeltatime); % std time of all GOOD images in that block and complexity
        netdsettime(d,set)=sum(tmpnetdeltatime);

        trueobjno=0;
        numberofimages=length(tmpcomp);

```

```

problemgroup=find(tmpcomp==13);
if ~isempty(problemgroup)
    numberofimages=numberofimages-1;
end
problemgroup=find(tmpcomp==112);
if ~isempty(problemgroup)
    numberofimages=numberofimages-1;
end
problemgroup=find(tmpcomp==212);
if ~isempty(problemgroup)
    numberofimages=numberofimages-1;
end

numofimg(d,set)=numberofimages;

for imgno=1:length(tmpcomp)

    if tmpcomp(imgno)~=13 & tmpcomp(imgno)~=112 & tmpcomp(imgno)~=212 % removing the
problematic images from the statistics *****
        trueobjline=find(melondatabase(:,4)==tmpcomp(imgno)); % the number of true targets in each image
        trueobjno=trueobjno+length(trueobjline); % the number of true targets in each set and complexity
        sysmarkline=find(allimagesdb(:,3)==tmpcomp(imgno)); % the number of marked targets by the
system in each image
        if ~isempty(robot_all_tar)
            robothit=find(robot_all_tar(:,4)==tmpcomp(imgno)); % the number of robot hits in each image
            robotFA=find(f_targets(:,4)==tmpcomp(imgno)); % the number of robot false alarms in each image
        end
        imghit=0;
        imgfalse=0;
        RHhit=0;
        RFA=0;

        if ~isempty(sysmarkline)
            imgfalse=length(sysmarkline); % the number of false alarm by the system for each image
            if ~isempty(robot_all_tar)
                for v=1:length(sysmarkline)
                    dxyRFA=[abs(allimagesdb(sysmarkline(v),1)-
f_targets(robotFA,2)),abs(allimagesdb(sysmarkline(v),2)-f_targets(robotFA,3))]; % distance between robot hit
and HO mark
                    sumlineRFA=sum((dxyRFA'<55));
                    closenumRFA=find(sumlineRFA==2);
                    if ~isempty(closenumRFA)
                        RFA=RFA+1; % HO mark of Robot false alarm for each image
                    end
                end
            end
            if ~isempty(trueobjline)
                imgfalse=0;
                RFA=0;
                for v=1:length(sysmarkline)
                    dxy=[abs(allimagesdb(sysmarkline(v),1)-
melondatabase(trueobjline,2)),abs(allimagesdb(sysmarkline(v),2)-melondatabase(trueobjline,3))]; % distance
between true target and marked one
                    sumline=sum((dxy'<55));
                    closenum=find(sumline==2);
                    if ~isempty(closenum)
                        imghit=imghit+1; % system hit for each image
                        if ~isempty(robot_all_tar)
                            dxyRH=[abs(allimagesdb(sysmarkline(v),1)-
robot_all_tar(robothit,2)),abs(allimagesdb(sysmarkline(v),2)-robot_all_tar(robothit,3))]; % distance between
robot hit and HO mark
                            sumlineRH=sum((dxyRH'<55));

```



```

toc
blockscore1=dssum11(:,31)+dssum21(:,31)+dssum31(:,31);
blockscore2=dssum12(:,31)+dssum22(:,31)+dssum32(:,31);
blockscore3=dssum13(:,31)+dssum23(:,31)+dssum33(:,31);
blockscore=[dssum11(:,1:2),blockscore1,blockscore2,blockscore3];
save blockscore blockscore
save blockscore.csv blockscore -ascii -tabs

save dssumALL dssum11 dssum12 dssum13 dssum21 dssum22 dssum23 dssum31 dssum32 dssum33
save dssumtitle dssumtitle
save dssumtitle.csv dssumtitle -ascii -tabs

for d=1:3
    for set=1:3
        tmpname=['dssum',num2str(d),num2str(set)];
        eval(['save ',tmpname,'.csv ',tmpname,' -ascii -tabs']);
    end
end

save numofimg numofimg
resperset1=dssum11+dssum21+dssum31;
resperset2=dssum12+dssum22+dssum32;
resperset3=dssum13+dssum23+dssum33;
setimgno=sum(numofimg);
allimgno=sum(sum(numofimg));

exptime=dssum11(:,28).*numofimg(1,1)+dssum21(:,28).*numofimg(2,1)+dssum31(:,28).*numofimg(3,1)+dssu
m12(:,28).*numofimg(1,2)+dssum22(:,28).*numofimg(2,2)+dssum32(:,28).*numofimg(3,2)+dssum13(:,28).*nu
mofimg(1,3)+dssum23(:,28).*numofimg(2,3)+dssum33(:,28).*numofimg(3,3);
expaveragetime=exptime./allimgno;
resallsets=resperset1+resperset2+resperset3;
set1=[dssum11(:,1),dssum11(:,2),dssum11(:,4),resperset1(:,7)./resperset1(:,5),resperset1(:,8)./setimgno(1),resper
set1(:,9)./(resperset1(:,5)-
resperset1(:,11)),resperset1(:,10)./setimgno(1),resperset1(:,13)./resperset1(:,11),resperset1(:,14)./resperset1(:,12)]
;
set2=[dssum22(:,1),dssum22(:,2),dssum22(:,4),resperset2(:,7)./resperset2(:,5),resperset2(:,8)./setimgno(2),resper
set2(:,9)./(resperset2(:,5)-
resperset2(:,11)),resperset2(:,10)./setimgno(2),resperset2(:,13)./resperset2(:,11),resperset2(:,14)./resperset2(:,12)]
;
set3=[dssum33(:,1),dssum33(:,2),dssum33(:,4),resperset3(:,7)./resperset3(:,5),resperset3(:,8)./setimgno(3),resper
set3(:,9)./(resperset3(:,5)-
resperset3(:,11)),resperset3(:,10)./setimgno(3),resperset3(:,13)./resperset3(:,11),resperset3(:,14)./resperset3(:,12)]
;
allsets=[dssum11(:,1),dssum11(:,2),dssum11(:,4),resallsets(:,7)./resallsets(:,5),resallsets(:,8)./allimgno,resallsets(
(:,9)./(resallsets(:,5)-
resallsets(:,11)),resallsets(:,10)./allimgno,resallsets(:,13)./resallsets(:,11),resallsets(:,14)./resallsets(:,12),expavera
getime];

save allsets set1 set2 set3 allsets
save allsets.csv allsets -ascii -tabs
save set1.csv set1 -ascii -tabs
save set2.csv set2 -ascii -tabs
save set3.csv set3 -ascii -tabs
save allsetstimes exptime expaveragetime
allsetstimes=[dssum11(:,1),dssum11(:,2),dssum11(:,4),exptime expaveragetime];
save allsetstimes.csv allsetstimes -ascii -tabs

% calling for subroutine subper2 for preperation of a mat file for the
% anovan function
%subper2c

```

Appendix X: Statistica data sheets

Collaboration	Rewards	RobPerf	Group	NewGroup	No	S1C1SyH	S1C1SyF	S1C1HoH	S1C1HoF	S1C1pHh	S1C1pHfa
1	1	0	1	1	10	1	1	1.00	1		
1	1	0	1	1	1001	1	0	1.00	0		
1	1	0	1	1	1002	1	1	1.00	1		
1	1	0	1	1	11	1	1	1.00	1		
1	1	0	1	1	12	1	1	1.00	1		
1	1	0	1	1	13	0.92	1	0.92	1		
1	1	0	1	1	14	1	2	1.00	2		
1	1	0	1	1	15	0.92	2	0.92	2		
1	1	0	1	1	16	0.92	3	0.92	3		
1	1	0	1	1	17	0.88	1	0.88	1		
1	1	0	1	1	18	1	2	1.00	2		
1	1	0	1	1	19	1	2	1.00	2		
1	2	0	2	1	20	1	4	1.00	4		
1	2	0	2	1	2001	1	2	1.00	2		
1	2	0	2	1	2002	1	2	1.00	2		
1	2	0	2	1	21	0.88	0	0.88	0		
1	2	0	2	1	22	1	4	1.00	4		
1	2	0	2	1	23	1	4	1.00	4		
1	2	0	2	1	24	0.96	2	0.96	2		
1	2	0	2	1	25	1	2	1.00	2		
1	2	0	2	1	26	1	1	1.00	1		
1	2	0	2	1	27	1	1	1.00	1		
1	2	0	2	1	28	0.92	2	0.92	2		
1	2	0	2	1	29	0.92	0	0.92	0		
2	1	1	3	2	30	1	2		2	1.000	0.00
2	1	1	3	2	3001	0.84	1	1.00	1	0.818	
2	1	1	3	2	3002	0.52	1	1.00	1	0.455	
2	1	1	3	2	31	1	1	1.00	1	1.000	
2	1	1	3	2	32	1	5	1.00	5	1.000	
2	1	1	3	2	33	1	0	1.00	0	1.000	
2	1	1	3	2	34	1	1	1.00	1	1.000	
2	1	1	3	2	35	1	2	1.00	2	1.000	
2	1	1	3	2	36	1	0	1.00	0	1.000	
2	1	1	3	2	37	0.96	2	0.50	2	1.000	0.00
2	1	1	3	2	38	0.92	0	1.00	0	0.909	
2	1	1	3	2	39	1	2	1.00	2	1.000	0.00
2	1	2	4	4	40	1	2	1.00	0	1.000	0.29
2	1	2	4	4	4001	1	0	1.00	0	1.000	0.00
2	1	2	4	4	4002	0.92	2	0.86	0	0.944	0.25
2	1	2	4	4	41	0.96	2	1.00	1	0.933	0.14
2	1	2	4	4	42	1	3	1.00	1	1.000	0.29
2	1	2	4	4	43	0.92	2	1.00	0	0.867	0.29
2	1	2	4	4	44	1	3	1.00	1	1.000	0.29
2	1	2	4	4	45	1	2	1.00	0	1.000	0.29
2	1	2	4	4	46	0.84	1	0.90	0	0.800	0.14
2	1	2	4	4	47	1	4	1.00	2	1.000	0.29
2	1	2	4	4	48	1	2	1.00	0	1.000	0.29
2	1	2	4	4	49	1	1	1.00	0	1.000	0.14
2	2	1	5	2	50	0.96	0	1.00	0	0.955	
2	2	1	5	2	5001	1	3	1.00	3	1.000	

2	2	1	5	2	5002	1	2	1.00	2	1.000	0.00
2	2	1	5	2	51	1	2	1.00	2	1.000	
2	2	1	5	2	52	1	0	1.00	0	1.000	
2	2	1	5	2	53	1	0	1.00	0	1.000	
2	2	1	5	2	54	1	2	1.00	2	1.000	
2	2	1	5	2	55	1	6	1.00	6	1.000	
2	2	1	5	2	56	1	0	1.00	0	1.000	
2	2	1	5	2	57	0.92	0	1.00	0	0.905	0.00
2	2	1	5	2	58	0.96	0	1.00	0	0.957	0.00
2	2	1	5	2	59	1	0	1.00	0	1.000	
2	2	2	6	4	60	0.96	2	1.00	1	0.933	0.14
2	2	2	6	4	6001	1	2	1.00	1	1.000	0.14
2	2	2	6	4	6002	1	5	1.00	2	1.000	0.43
2	2	2	6	4	61	0.92	1	1.00	1	0.867	0.00
2	2	2	6	4	62	1	0	1.00	0	1.000	0.00
2	2	2	6	4	63	1	4	1.00	2	1.000	0.29
2	2	2	6	4	64	1	6	1.00	2	1.000	0.57
2	2	2	6	4	65	0.92	1	0.90	0	0.933	0.14
2	2	2	6	4	66	1	2	1.00	0	1.000	0.29
2	2	2	6	4	67	1	1	1.00	0	1.000	0.14
2	2	2	6	4	68	1	3	1.00	1	1.000	0.29
2	2	2	6	4	69	1	0	1.00	0	1.000	0.00
3	1	1	7	3	70	1	0	1.00	0	1.000	0.00
3	1	1	7	3	7001	1	2	1.00	2	1.000	
3	1	1	7	3	7002	1	0	1.00	0	1.000	0.00
3	1	1	7	3	71	1	0	1.00	0	1.000	
3	1	1	7	3	72	0.88	2	1.00	2	0.864	
3	1	1	7	3	73	0.96	0	1.00	0	0.955	
3	1	1	7	3	74	1	2	1.00	2	1.000	
3	1	1	7	3	75	1	1	1.00	1	1.000	
3	1	1	7	3	76	0.96	1	1.00	1	0.955	
3	1	1	7	3	77	1	0	1.00	0	1.000	0.00
3	1	1	7	3	78	0.96	0	1.00	0	0.955	
3	1	1	7	3	79	1	2	1.00	2	1.000	
3	1	2	8	5	80	0.84	3	0.50	2	0.905	0.14
3	1	2	8	5	8001	0.96	7	1.00	4	0.944	0.43
3	1	2	8	5	8002	1	4	1.00	1	1.000	0.43
3	1	2	8	5	81	1	2	1.00	1	1.000	0.14
3	1	2	8	5	82	1	0	1.00	0	1.000	0.00
3	1	2	8	5	83	0.88	0	1.00	0	0.800	0.00
3	1	2	8	5	84	1	1	1.00	0	1.000	0.14
3	1	2	8	5	85	0.68	1	0.80	1	0.600	0.00
3	1	2	8	5	86	0.96	1	1.00	1	0.933	0.00
3	1	2	8	5	87	1	0	1.00	0	1.000	0.00
3	1	2	8	5	882	1	1	1.00	0	1.000	0.14
3	1	2	8	5	89	1	2	1.00	0	1.000	0.29
3	2	1	9	3	90	0.92	1	0.67	1	0.955	
3	2	1	9	3	9001	1	15	1.00	15	1.000	
3	2	1	9	3	9002	1	2	1.00	2	1.000	
3	2	1	9	3	91	1	2	1.00	2	1.000	
3	2	1	9	3	92	1	0	1.00	0	1.000	
3	2	1	9	3	93	1	1	1.00	1	1.000	
3	2	1	9	3	94	1	1	1.00	1	1.000	
3	2	1	9	3	95	0.92	1	1.00	1	0.917	0.00
3	2	1	9	3	96	1	0	1.00	0	1.000	

3	2	1	9	3	97	1	2	1.00	2	1.000	0.00
3	2	1	9	3	98	1	3	1.00	3	1.000	0.00
3	2	1	9	3	99	1	0	1.00	0	1.000	
3	2	2	10	5	100	0.96	3	0.75	1	1.000	0.29
3	2	2	10	5	101	1	0	1.00	0	1.000	0.00
3	2	2	10	5	102	1	1	1.00	1	1.000	0.00
3	2	2	10	5	103	1	0	1.00	0	1.000	0.00
3	2	2	10	5	104	1	1	1.00	0	1.000	0.14
3	2	2	10	5	105	1	3	1.00	2	1.000	0.14
3	2	2	10	5	106	1	1	1.00	0	1.000	0.13
3	2	2	10	5	107	0.96	1	1.00	0	0.933	0.14
3	2	2	10	5	108	0.88	3	1.00	1	0.833	0.29
3	2	2	10	5	109	1	3	1.00	1	1.000	0.29
3	2	2	10	5	110	1	1	1.00	0	1.000	0.14
3	2	2	10	5	111	0.92	4	0.86	0	0.944	0.57

Appendix XI: Numerical analysis programs

operationalcost5c.m

```
% This program calculates the hit and false alarm probabilities and the
% value of the operational cost according to betas and dtags
% all betas are given and the optimal betas for each case are checked.
% In this case all decision time parameters are CONSTANTS!!!!!!!!!!
% This version will show the objective fbcion values for all collaboration
% levels and for all betas combinations.
% with more resolution of d'r, d'h and Ps

clear
clc
close all

tic
N=1000; % # of objects
Nstr=num2str(N);

%VFA2H=[0.1 0.333 1 3 10]; % [0.05:0.05:1,1:0.1:10,10:1:100]; % VFA/VH aspect ratio range
VFA2H=10; % [0.05:0.05:1,1:0.1:10,10:1:100]; % VFA/VH aspect ratio range
for VAR=1:length(VFA2H)
    VARstr=num2str(VFA2H(VAR)*10);
    if VFA2H(VAR)==0.333
        VARstr=num2str(3);
    end

    %Psvector=[0.2 0.5 0.8]; %probability for object to be target
    Psvector=[0.1,0.2,0.5,0.8,0.9]; %probability for object to be target

    for Pscount=1:length(Psvector)
        Ps=Psvector(Pscount);
        Psstr=num2str(Ps*100);

        dhvector=[-0.5:-0.25:-3];
        drvector=[-0.5:-0.25:-3];

        for dh=1:11
            dtag=dhvector(dh) % [-0.1:-0.1:-4]; % the range of d' for human (second detector)
            Dh=num2str(-dtag*100);

            for dr=1:11
                dtagR=drvector(dr) % [-0.1:-0.1:-4]%-2
                Dr=num2str(-dtagR*100);
                %Inbetar=1 % [-3:0.1:3]

                VH=50;
                VM=0;
                VCR=0;
                VHstr=num2str(VH);
                VFA=-VH.*VFA2H(VAR);
                Vc=-2;
                VCstr=num2str(-Vc);
                Vt=-2000/3600;
                Vtstr=num2str(-Vt*3600);

                tr=10;

                c3=0;
```

```

for Inbetar=-4:0.2:4
    c3=c3+1;
    c2=0;
    for Inbetah=-4:0.2:4
        c2=c2+1;
        c1=0;
        for Inbetarh=-4:0.2:4
            c1=c1+1;

% the probabilities of the robot
Zsr(c1,c2,c3)=(-2.*Inbetar+dtagR.^2)./(2.*dtagR);
Znr(c1,c2,c3)=(-2.*Inbetar-dtagR.^2)./(2.*dtagR);
phr(c1,c2,c3)=1-normcdf(Zsr(c1,c2,c3));
pfar(c1,c2,c3)=1-normcdf(Znr(c1,c2,c3));
ratio1=pfar(c1,c2,c3)./phr(c1,c2,c3);
ratio2=(1-pfar(c1,c2,c3))./(1-phr(c1,c2,c3));

if Inbetar==0 & Inbetah==0 & Inbetarh==0
    Zsrtest=(-2.*Inbetar+dtagR.^2)./(2.*dtagR);
    Znrtest=(-2.*Inbetar-dtagR.^2)./(2.*dtagR);
    phrtest=1-normcdf(Zsr(c1,c2,c3));
    pfartest=1-normcdf(Znr(c1,c2,c3));
    ratio1=pfar(c1,c2,c3)./phr(c1,c2,c3);
    ratio2=(1-pfar(c1,c2,c3))./(1-phr(c1,c2,c3));

end

%the optimal parameters of the robot if he was a single detector
betastar(c1,c2,c3)=((1-Ps)./Ps).*VFA2H(VAR); % calculating Beta*
ZsRstar(c1,c2,c3)=(-2.*log(betastar(c1,c2,c3))+dtagR.^2)./(2.*dtagR);
ZnRstar(c1,c2,c3)=(-2.*log(betastar(c1,c2,c3))-dtagR.^2)./(2.*dtagR);
phrstar(c1,c2,c3)=1-normcdf(ZsRstar(c1,c2,c3));
pfarstar(c1,c2,c3)=1-normcdf(ZnRstar(c1,c2,c3));

%the probabilities of the HO (second detector) for object that the
%robot didn't detect
ZsH(c1,c2,c3)=(-2.*Inbetah+dtag.^2)./(2.*dtag);
ZnH(c1,c2,c3)=(-2.*Inbetah-dtag.^2)./(2.*dtag);
phh(c1,c2,c3)=1-normcdf(ZsH(c1,c2,c3));
pfah(c1,c2,c3)=1-normcdf(ZnH(c1,c2,c3));

% the probabilities of the HO (second detector) for object that the robot
%already detected
ZsRH(c1,c2,c3)=(-2.*Inbetarh+dtag.^2)./(2.*dtag);
ZnRH(c1,c2,c3)=(-2.*Inbetarh-dtag.^2)./(2.*dtag);
phrh(c1,c2,c3)=1-normcdf(ZsRH(c1,c2,c3));
pfarh(c1,c2,c3)=1-normcdf(ZnRH(c1,c2,c3));

% the time parameters

tHh(c1,c2,c3)=5;
tFAh(c1,c2,c3)=5;
tHrh(c1,c2,c3)=5;
tFARh(c1,c2,c3)=5;

tMh(c1,c2,c3)=5;
tCRh(c1,c2,c3)=5;
tMrh(c1,c2,c3)=5;
tCRrh(c1,c2,c3)=5;
tmotor=2;

```

$PHs(c1,c2,c3)=phr(c1,c2,c3).*phrh(c1,c2,c3)+(1-phr(c1,c2,c3)).*phh(c1,c2,c3);$
 $VHs(c1,c2,c3)=N.*Ps.*PHs(c1,c2,c3).*VH;$
 $PMs(c1,c2,c3)=phr(c1,c2,c3).*(1-phrh(c1,c2,c3))+(1-phr(c1,c2,c3)).*(1-phh(c1,c2,c3));$
 $VMs(c1,c2,c3)=N.*Ps.*PMs(c1,c2,c3).*VM;$
 $FFAs(c1,c2,c3)=N.*(1-Ps).*pfar(c1,c2,c3).*pfarh(c1,c2,c3)+N.*(1-Ps).(1-pfar(c1,c2,c3)).*pfah(c1,c2,c3);$
 $VFAs(c1,c2,c3)=FFAs(c1,c2,c3).*VFA;$
 $FCRs(c1,c2,c3)=N.*(1-Ps).*pfar(c1,c2,c3).*(1-pfarh(c1,c2,c3))+N.*(1-Ps).(1-pfar(c1,c2,c3)).*(1-pfah(c1,c2,c3));$
 $VCRs(c1,c2,c3)=FCRs(c1,c2,c3).*VCR;$

$ts(c1,c2,c3)=N.*Ps.*phr(c1,c2,c3).*phrh(c1,c2,c3).*tHrh(c1,c2,c3)+N.*Ps.*(1-phr(c1,c2,c3)).*phh(c1,c2,c3).*tHh(c1,c2,c3)+N.*(1-Ps).*pfar(c1,c2,c3).*pfarh(c1,c2,c3).*tFArh(c1,c2,c3)+N.*(1-Ps).(1-pfar(c1,c2,c3)).*pfah(c1,c2,c3).*tFAh(c1,c2,c3)...$
 $+N.*Ps.*phr(c1,c2,c3).*(1-phrh(c1,c2,c3)).*tMrh(c1,c2,c3)+N.*Ps.*(1-phr(c1,c2,c3)).*(1-phh(c1,c2,c3)).*tMh(c1,c2,c3)+N.*(1-Ps).*pfar(c1,c2,c3).*(1-pfarh(c1,c2,c3)).*tCRrh(c1,c2,c3)+N.*(1-Ps).(1-pfar(c1,c2,c3)).*(1-pfah(c1,c2,c3)).*tCRh(c1,c2,c3)+tr;$

$tsHORr(c1,c2,c3)=N.*Ps.*phr(c1,c2,c3).*phrh(c1,c2,c3).*(tHrh(c1,c2,c3)+tmotor)+N.*Ps.*(1-phr(c1,c2,c3)).*phh(c1,c2,c3).*(tHh(c1,c2,c3)+tmotor)+N.*(1-Ps).*pfar(c1,c2,c3).*pfarh(c1,c2,c3).*(tFArh(c1,c2,c3)+tmotor)+N.*(1-Ps).(1-pfar(c1,c2,c3)).*pfah(c1,c2,c3).*(tFAh(c1,c2,c3)+tmotor)...$
 $+N.*Ps.*phr(c1,c2,c3).*(1-phrh(c1,c2,c3)).*tMrh(c1,c2,c3)+N.*Ps.*(1-phr(c1,c2,c3)).*(1-phh(c1,c2,c3)).*tMh(c1,c2,c3)+N.*(1-Ps).*pfar(c1,c2,c3).*(1-pfarh(c1,c2,c3)).*tCRrh(c1,c2,c3)+N.*(1-Ps).(1-pfar(c1,c2,c3)).*(1-pfah(c1,c2,c3)).*tCRh(c1,c2,c3)+tr;$

$tsHOR(c1,c2,c3)=N.*Ps.*phr(c1,c2,c3).*phrh(c1,c2,c3).*tHrh(c1,c2,c3)+N.*Ps.*(1-phr(c1,c2,c3)).*phh(c1,c2,c3).*(tHh(c1,c2,c3)+tmotor)+N.*(1-Ps).*pfar(c1,c2,c3).*pfarh(c1,c2,c3).*tFArh(c1,c2,c3)+N.*(1-Ps).(1-pfar(c1,c2,c3)).*pfah(c1,c2,c3).*(tFAh(c1,c2,c3)+tmotor)...$
 $+N.*Ps.*phr(c1,c2,c3).*(1-phrh(c1,c2,c3)).*(tMrh(c1,c2,c3)+tmotor)+N.*Ps.*(1-phr(c1,c2,c3)).*(1-phh(c1,c2,c3)).*tMh(c1,c2,c3)+N.*(1-Ps).*pfar(c1,c2,c3).*(1-pfarh(c1,c2,c3)).*(tCRrh(c1,c2,c3)+tmotor)+N.*(1-Ps).(1-pfar(c1,c2,c3)).*(1-pfah(c1,c2,c3)).*tCRh(c1,c2,c3)+tr;$

$Ndetect(c1,c2,c3)=(N.*Ps.*phr(c1,c2,c3).*phrh(c1,c2,c3)+N.*Ps.*(1-phr(c1,c2,c3)).*phh(c1,c2,c3)+N.*(1-Ps).*pfar(c1,c2,c3).*pfarh(c1,c2,c3)+N.*(1-Ps).(1-pfar(c1,c2,c3)).*pfah(c1,c2,c3));$
 $VTs(c1,c2,c3)=ts(c1,c2,c3).*Vt+(N.*Ps.*phr(c1,c2,c3).*phrh(c1,c2,c3)+N.*Ps.*(1-phr(c1,c2,c3)).*phh(c1,c2,c3)+N.*(1-Ps).*pfar(c1,c2,c3).*pfarh(c1,c2,c3)+N.*(1-Ps).(1-pfar(c1,c2,c3)).*pfah(c1,c2,c3)).*Vc;$
 $VTsHORr(c1,c2,c3)=tsHORr(c1,c2,c3).*Vt+(N.*Ps.*phr(c1,c2,c3).*phrh(c1,c2,c3)+N.*Ps.*(1-phr(c1,c2,c3)).*phh(c1,c2,c3)+N.*(1-Ps).*pfar(c1,c2,c3).*pfarh(c1,c2,c3)+N.*(1-Ps).(1-pfar(c1,c2,c3)).*pfah(c1,c2,c3)).*Vc;$
 $VTsHOR(c1,c2,c3)=tsHOR(c1,c2,c3).*Vt+(N.*Ps.*phr(c1,c2,c3).*phrh(c1,c2,c3)+N.*Ps.*(1-phr(c1,c2,c3)).*phh(c1,c2,c3)+N.*(1-Ps).*pfar(c1,c2,c3).*pfarh(c1,c2,c3)+N.*(1-Ps).(1-pfar(c1,c2,c3)).*pfah(c1,c2,c3)).*Vc;$
 $VIs(c1,c2,c3)=VHs(c1,c2,c3)+VMs(c1,c2,c3)+VFAs(c1,c2,c3)+VCRs(c1,c2,c3)+VTs(c1,c2,c3);$
 $VIsHORr(c1,c2,c3)=VHs(c1,c2,c3)+VMs(c1,c2,c3)+VFAs(c1,c2,c3)+VCRs(c1,c2,c3)+VTsHORr(c1,c2,c3);$
 $VIsHOR(c1,c2,c3)=VHs(c1,c2,c3)+VMs(c1,c2,c3)+VFAs(c1,c2,c3)+VCRs(c1,c2,c3)+VTsHOR(c1,c2,c3);$

$PHsR(c1,c2,c3)=phr(c1,c2,c3);$
 $VHsR(c1,c2,c3)=N.*Ps.*PHsR(c1,c2,c3).*VH;$
 $FFAsR(c1,c2,c3)=N.*(1-Ps).*pfar(c1,c2,c3);$
 $VFAsR(c1,c2,c3)=FFAsR(c1,c2,c3).*VFA;$
 $tsR(c1,c2,c3)=tr;$
 $VTsR(c1,c2,c3)=tsR(c1,c2,c3).*Vt+(N.*Ps.*phr(c1,c2,c3)+N.*(1-Ps).*pfar(c1,c2,c3)).*Vc;$
 $VIsR(c1,c2,c3)=VHsR(c1,c2,c3)+VFAsR(c1,c2,c3)+VTsR(c1,c2,c3);$

% the probabilities of teh HO collaboration level were take from the
 % robot probabilities and the different between the HO and the R
 % collaboration levels is just on the times parameters.
 $PHsHO(c1,c2,c3)=phr(c1,c2,c3);$

```

VHsHO(c1,c2,c3)=N.*Ps.*PHsHO(c1,c2,c3).*VH;
FFAsHO(c1,c2,c3)=N.*(1-Ps).*pfar(c1,c2,c3);
VFAsHO(c1,c2,c3)=FFAsHO(c1,c2,c3).*VFA;

tsHO(c1,c2,c3)=N.*Ps.*PHsHO(c1,c2,c3).*(tHh(c1,c2,c3)+tmotor)+FFAsHO(c1,c2,c3).*(tFAh(c1,c2,c3)+tmotor)
or)...
+N.*Ps.*(1-PHsHO(c1,c2,c3)).*tMh(c1,c2,c3)+N.*(1-Ps).*(1-pfar(c1,c2,c3)).*tCRh(c1,c2,c3);
VTsHO(c1,c2,c3)=tsHO(c1,c2,c3).*Vt+(N.*Ps.*phr(c1,c2,c3)+N.*(1-Ps).*pfar(c1,c2,c3)).*Vc;
VIsHO(c1,c2,c3)=VHsHO(c1,c2,c3)+VFAsHO(c1,c2,c3)+VTsHO(c1,c2,c3);

Nsyshit(c1,c2,c3)=VHs(c1,c2,c3)./VH; % number of system hits
NsysFA(c1,c2,c3)=VFAs(c1,c2,c3)./VFA; % number of system FA
phs(c1,c2,c3)=Nsyshit(c1,c2,c3)./(N.*Ps); % same as PHs
pfas(c1,c2,c3)=NsysFA(c1,c2,c3)./(N.*(1-Ps)); % probability of system FA
Zss(c1,c2,c3)=norminv(phs(c1,c2,c3));
Zns(c1,c2,c3)=norminv(pfas(c1,c2,c3));
dtagSYS(c1,c2,c3)=Zns(c1,c2,c3)-Zss(c1,c2,c3); % dtag of the overall system
lnbetasys(c1,c2,c3)=-0.5.*(Zss(c1,c2,c3).^2-Zns(c1,c2,c3).^2);
betasys(c1,c2,c3)=exp(lnbetasys(c1,c2,c3)); % the system beta
    end % c1
end % c2
c3
VAR
[dhvector(dh),drvector(dr)]
end % c3

toc
lnbetar_graph=-3:0.2:3;

lnbetar=-4:0.2:4;
lnbetah=-4:0.2:4;
lnbetarh=-4:0.2:4;

fn=['OF1dh',Dh,'dr',Dr,'_',VARstr,'_',VHstr,'_',VCstr,'_',Vtstr,'_Ps',Psstr]
allvariables=[' N VFA2H VAR Ps dtag dtagR lnbetar lnbetah lnbetarh VH VFA Vc Vt Zsr Znr ZsH ZnH ZsRH
ZnrH Zsrstar ZnRstar betastar phr pfar phh pfah phrh pfarh phrstar pfarstar tmotor tHh tHrh tFAh tFArh tMh
tMrh tCRh tCRrh tr PHs VHs PMs VMs FCRs VCRs FFAs VFAs ts tsHORr tsHOR Ndetect VTs VTsHORr
VTsHOR VIs VIsHORr VIsHOR Nsyshit NsysFA phs pfas Zss Zns dtagSYS lnbetasys betasys PHsR VHsR
FFAsR VFAsR tsR VTsR VIsR PHsHO VHsHO FFAsHO VFAsHO tsHO VTsHO VIsHO']

eval(['save ',fn allvariables])
%save OC1dh3dr3_3_3_1_1000 N VFA2H VAR Ps dtag dtagR lnbetar lnbetah lnbetarh VH VFA Vc Vt ...
% Zsr Znr ZsH ZnH ZsRH ZnRH Zsrstar ZnRstar betastar phr pfar phh pfah phrh pfarh phrstar pfarstar ...
% myuHh myuFAh myuHrh myuFArh tHh tHrh tFAh tFArh tr PHs VHs FFAs VFAs ts Ndetect VTs VIs
Nsyshit NsysFA phs pfas ...
% Zss Zns dtagSYS lnbetasys betasys

end % dr
end % dh
end % PScout
end % VAR

toc

```

OFoptPS1.m:

% This program compare the different files prodced with operationalcost5c
% and calculate the parameters maps for all collaboration levels.

```
clear  
clc  
close all  
pause(1)
```

```
tic
```

```
allvariables=[' N VFA2H VAR Ps dtag dtagR Inbetar Inbetah Inbetarh VH VFA Vc Vt Zsr Znr ZsH ZnH ZsRH  
ZnRH ZsRstar ZnRstar betastar phr pfar phh pfah phrh pfarh phrstar pfarstar tmotor tHh tHrh tFAh tFArh tMh  
tMrh tCRh tCRrh tr PHs VHs PMs VMs FCRs VCRs FFAs VFAs ts tsHORr tsHOR Ndetect VTs VTsHORr  
VTsHOR VIs VIsHORr VIsHOR Nsyshit NsysFA phs pfas Zss Zns dtagsys Inbetasys betasys PHsR VHsR  
FFAsR VFAsR tsR VTsR VIsR PHsHO VHsHO FFAsHO VFAsHO tsHO VTsHO VIsHO'];
```

```
dhvector=[-0.5:-0.25:-3];  
drvector=[-0.5:-0.25:-3];
```

```
VFA2H=10; % VFA2H=[0.1 1 10]; % [0.05:0.05:1,1:0.1:10,10:1:100]; % VFA/VH aspect ratio range  
for VARcall=1:length(VFA2H)  
    VARstr=num2str(VFA2H(VARcall)*10);  
    if VFA2H(VARcall)==0.333  
        VARstr=num2str(3);  
    end
```

```
%Ps=0.1; %probability for object to be target  
%Psstr=num2str(Ps*100);  
VH=50;  
VM=0;  
VCR=0;  
VHstr=num2str(VH);  
VFA=-VH.*VFA2H(VARcall);  
Vc=-2;  
VCstr=num2str(-Vc);  
Vt=-2000/3600;  
Vtstr=num2str(-Vt*3600);  
tr=10;  
bestbetarh=zeros(11,11);  
bestbetah=zeros(11,11);  
bestbetar=zeros(11,11);
```

```
Ps=[0.1,0.2,0.5,0.8,0.9] %probability for object to be target  
for P=1:length(Ps)  
    Ps=[0.1,0.2,0.5,0.8,0.9] %probability for object to be target  
    Psstr=num2str(Ps(P)*100)
```

```
for dh=1:11  
    dtag=dhvector(dh) % [-0.1:-0.1:-4]; % the range of d' for human (second detector)  
    Dh=num2str(-dtag*100);  
  
    for dr=1:11  
        dtagR=drvector(dr) % [-0.1:-0.1:-4]% -2  
        Dr=num2str(-dtagR*100);
```

```
fn=['OF1dh',Dh,'dr',Dr,'_',VARstr,'_',VHstr,'_',VCstr,'_',Vtstr,'_Ps',Psstr]  
eval(['load ',fn allvariables])
```

HOVIs(dh,dr,P)=max(max(max(VIsHO))); % the dh, dr coordinates are oposit since it is that way in the databases

```
[x y]=find(VIsHO==HOVIs(dh,dr,P));  
brhs_VIsHO(dh,dr,P)=x(1);  
bhs_VIsHO(dh,dr,P)=ceil(y(1)/41);  
brs_VIsHO(dh,dr,P)=y(1)-41*(bhs_VIsHO(dh,dr,P)-1);
```

```
HOPHs(dh,dr,P)=PHsHO(brhs_VIsHO(dh,dr,P),brs_VIsHO(dh,dr,P),bhs_VIsHO(dh,dr,P));  
HOts(dh,dr,P)=tsHO(brhs_VIsHO(dh,dr,P),brs_VIsHO(dh,dr,P),bhs_VIsHO(dh,dr,P));  
HOVTs(dh,dr,P)=VTsHO(brhs_VIsHO(dh,dr,P),brs_VIsHO(dh,dr,P),bhs_VIsHO(dh,dr,P));  
HOPfa(dh,dr,P)=pfar(brhs_VIsHO(dh,dr,P),brs_VIsHO(dh,dr,P),bhs_VIsHO(dh,dr,P));
```

```
RVIs(dr,dh,P)=max(max(max(VIsR)));  
[x y]=find(VIsR==RVIs(dr,dh,P));  
brhs_VIsR(dr,dh,P)=x(1);  
brs_VIsR(dr,dh,P)=ceil(y(1)/41);  
bhs_VIsR(dr,dh,P)=y(1)-41*(brs_VIsR(dr,dh,P)-1);
```

```
RPHs(dr,dh,P)=PHsR(brhs_VIsR(dr,dh,P),bhs_VIsR(dr,dh,P),brs_VIsR(dr,dh,P));  
Rts(dr,dh,P)=tsR(brhs_VIsR(dr,dh,P),bhs_VIsR(dr,dh,P),brs_VIsR(dr,dh,P));  
RVTs(dr,dh,P)=VTsR(brhs_VIsR(dr,dh,P),bhs_VIsR(dr,dh,P),brs_VIsR(dr,dh,P));  
RPfa(dr,dh,P)=pfar(brhs_VIsR(dr,dh,P),brs_VIsR(dr,dh,P),bhs_VIsR(dr,dh,P));
```

```
HORVIs(dr,dh,P)=max(max(max(VIsHOR)));  
[x y]=find(VIsHOR==HORVIs(dr,dh,P));  
brhs_VIsHOR(dr,dh,P)=x(1);  
bhs_VIsHOR(dr,dh,P)=ceil(y(1)/41);  
brs_VIsHOR(dr,dh,P)=y(1)-41*(bhs_VIsHOR(dr,dh,P)-1);
```

```
HORPHs(dr,dh,P)=PHs(brhs_VIsHOR(dr,dh,P),bhs_VIsHOR(dr,dh,P),brs_VIsHOR(dr,dh,P));  
HOrts(dr,dh,P)=tsHOR(brhs_VIsHOR(dr,dh,P),bhs_VIsHOR(dr,dh,P),brs_VIsHOR(dr,dh,P));  
HORVTs(dr,dh,P)=VTsHOR(brhs_VIsHOR(dr,dh,P),bhs_VIsHOR(dr,dh,P),brs_VIsHOR(dr,dh,P));  
HORPfa(dr,dh,P)=pfas(brhs_VIsHOR(dr,dh,P),brs_VIsHOR(dr,dh,P),bhs_VIsHOR(dr,dh,P));
```

```
HORrVIs(dr,dh,P)=max(max(max(VIsHORr)));  
[x y]=find(VIsHORr==HORrVIs(dr,dh,P));  
brhs_VIsHORr(dr,dh,P)=x(1);  
bhs_VIsHORr(dr,dh,P)=ceil(y(1)/41);  
brs_VIsHORr(dr,dh,P)=y(1)-41*(bhs_VIsHORr(dr,dh,P)-1);
```

```
HORrPHs(dr,dh,P)=PHs(brhs_VIsHORr(dr,dh,P),bhs_VIsHORr(dr,dh,P),brs_VIsHORr(dr,dh,P));  
HORrts(dr,dh,P)=tsHORr(brhs_VIsHORr(dr,dh,P),bhs_VIsHORr(dr,dh,P),brs_VIsHORr(dr,dh,P));
```

```
HORrVTs(dr,dh,P)=VTsHORr(brhs_VIsHORr(dr,dh,P),bhs_VIsHORr(dr,dh,P),brs_VIsHORr(dr,dh,P));  
HORrPfa(dr,dh,P)=pfas(brhs_VIsHORr(dr,dh,P),brs_VIsHORr(dr,dh,P),bhs_VIsHORr(dr,dh,P));
```

```
Vi_Temp=[HOVIs(dr,dh,P),HORrVIs(dr,dh,P),HORVIs(dr,dh,P),RVIs(dr,dh,P)];  
Vi_max(dr,dh,P)=max(Vi_Temp);  
Temp_CL=find(Vi_Temp==Vi_max(dr,dh,P));  
BestCL(dr,dh,P)=Temp_CL(1);
```

```
PH_Temp=[HOPHs(dh,dr,P),HORrPHs(dr,dh,P),HORPHs(dr,dh,P),RPHs(dr,dh,P)];  
PFA_Temp=[HOPfa(dh,dr,P),HORrPfa(dr,dh,P),HORPfa(dr,dh,P),RPfa(dr,dh,P)];
```

```
BestZss(dr,dh,P)=norminv(PH_Temp(Temp_CL(1)));  
BestZns(dr,dh,P)=norminv(PFA_Temp(Temp_CL(1)));
```

```

Bestdtagsys(dr,dh,P)=BestZns(dr,dh,P)-BestZss(dr,dh,P); % drtag of the overall system
Bestlnbetasys(dr,dh,P)=-0.5.*(BestZss(dr,dh,P).^2-BestZns(dr,dh,P).^2);
if Temp_CL(1)==4
    Bestdtagsys(dr,dh,P)=drvector(dr);
    Bestlnbetasys(dr,dh,P)=-4+(brs_VIsR(dr,dh,P)-1).*0.2;
end

end % dr
end % dh
toc
beep
end % P

HOVIs2ts=HOVIs./HOts;
HOVIs2VTs=HOVIs./HOVTs;
RVIs2ts=RVIs./Rts;
RVIs2VTs=RVIs./RVTs;
HORVIs2ts=HORVIs./HORts;
HORVIs2VTs=HORVIs./HORVTs;
HORrVIs2ts=HORrVIs./HORrts;
HORrVIs2VTs=HORrVIs./HORrVTs;

toc

beta_rhHO=-4+(brhs_VIsHO-1).*0.2;
beta_rhR=-4+(brhs_VIsR-1).*0.2;
beta_rhHORr=-4+(brhs_VIsHORr-1).*0.2;
beta_rhHOR=-4+(brhs_VIsHOR-1).*0.2;

beta_hHO=-4+(bhs_VIsHO-1).*0.2;
beta_hR=-4+(bhs_VIsR-1).*0.2;
beta_hHORr=-4+(bhs_VIsHORr-1).*0.2;
beta_hHOR=-4+(bhs_VIsHOR-1).*0.2;

beta_rHO=-4+(brs_VIsHO-1).*0.2;
beta_rR=-4+(brs_VIsR-1).*0.2;
beta_rHORr=-4+(brs_VIsHORr-1).*0.2;
beta_rHOR=-4+(brs_VIsHOR-1).*0.2;

save OFoptPs_data1

Allbeta_rh(:,:,1)=beta_rhHO;
Allbeta_rh(:,:,2)=beta_rhHORr;
Allbeta_rh(:,:,3)=beta_rhHOR;
Allbeta_rh(:,:,4)=beta_rhR;

Allbeta_h(:,:,1)=beta_hHO;
Allbeta_h(:,:,2)=beta_hHORr;
Allbeta_h(:,:,3)=beta_hHOR;
Allbeta_h(:,:,4)=beta_hR;

Allbeta_r(:,:,1)=beta_rHO;
Allbeta_r(:,:,2)=beta_rHORr;
Allbeta_r(:,:,3)=beta_rHOR;
Allbeta_r(:,:,4)=beta_rR;

save OFoptPs_data2
pause

end % VAR

```

Appendix XII: Sensitivity analysis programs

sensPs1a.m:

% sensitivity analysis of beta

```
clear
clc
close all
pause(1)
```

```
tic
```

```
allvariables=[' N VFA2H VAR Ps dtag dtagR Inbetar Inbetah Inbetarh VH VFA Vc Vt Zsr Znr ZsH ZnH ZsRH
ZnRH ZsRstar ZnRstar betastar phr pfar phh pfah phrh pfarh phrstar pfarstar tmotor tHh tHrh tFAh tFArh tMh
tMrh tCRh tCRrh tr PHs VHs PMs VMs FCRs VCRs FFAs VFAs ts tsHORr tsHOR Ndetect VTs VTsHORr
VTsHOR VIs VIsHORr VIsHOR Nsyshit NsysFA phs pfas Zss Zns dtagsys Inbetasys betasys PHsR VHsR
FFAsR VFAsR tsR VTsR VIsR PHsHO VHsHO FFAsHO VFAsHO tsHO VTsHO VIsHO'];
```

```
dhvector=[-1:-1:-3];
drvector=[-1:-1:-3];
```

```
VFA2H=1; % VFA2H=[0.1 1 10]; % [0.05:0.05:1,1:0.1:10,10:1:100]; % VFA/VH aspect ratio range
```

```
for VARcall=1:length(VFA2H)
    VARstr=num2str(VFA2H(VARcall)*10);
    if VFA2H(VARcall)==0.333
        VARstr=num2str(3);
    end
```

```
%Ps=0.1; %probability for object to be target
%Psstr=num2str(Ps*100);
VH=50;
VM=0;
VCR=0;
VHstr=num2str(VH);
VFA=-VH.*VFA2H(VARcall);
Vc=-2;
VCstr=num2str(-Vc);
Vt=-2000/3600;
Vtstr=num2str(-Vt*3600);
tr=10;
```

```
Ps=[0.1:0.1:0.9] %probability for object to be target
for P=1:length(Ps)
    Ps=[0.1:0.1:0.9] %probability for object to be target
    Psstr=num2str(Ps(P)*100)
```

```
for dh=1:3
    dtag=dhvector(dh) % [-0.1:-0.1:-4]; % the range of d' for human (second detector)
    Dh=num2str(-dtag*100);
```

```
for dr=1:3
    dtagR=drvector(dr) % [-0.1:-0.1:-4]*-2
    Dr=num2str(-dtagR*100);
```

```
fn=['OF1dh',Dh,'dr',Dr,'_',VARstr,'_',VHstr,'_',VCstr,'_',Vtstr,'_Ps',Psstr]
eval(['load ',fn allvariables])
```

```

RVIs(dr,dh,P)=max(max(max(VIsR)));
RVIsmin(dr,dh,P)=min(min(min(VIsR)));
[x y]=find(VIsR==RVIs(dr,dh,P));
brhs_VIsR(dr,dh,P)=x(1);
brs_VIsR(dr,dh,P)=ceil(y(1)./41);
bhs_VIsR(dr,dh,P)=y(1)-41*(brs_VIsR(dr,dh,P)-1);

HORVIs(dr,dh,P)=max(max(max(VIsHOR)));
HORVIsmin(dr,dh,P)=min(min(min(VIsHOR)));
[x y]=find(VIsHOR==HORVIs(dr,dh,P));
brhs_VIsHOR(dr,dh,P)=x(1);
brs_VIsHOR(dr,dh,P)=ceil(y(1)./41);
bhs_VIsHOR(dr,dh,P)=y(1)-41*(brs_VIsHOR(dr,dh,P)-1);

HORrVIs(dr,dh,P)=max(max(max(VIsHORr)));
HORrVIsmin(dr,dh,P)=min(min(min(VIsHORr)));
[x y]=find(VIsHORr==HORrVIs(dr,dh,P));
brhs_VIsHORr(dr,dh,P)=x(1);
brs_VIsHORr(dr,dh,P)=ceil(y(1)./41);
bhs_VIsHORr(dr,dh,P)=y(1)-41*(brs_VIsHORr(dr,dh,P)-1);

fn=['OF1dh',Dr,'dr',Dh,'_',VARstr,'_',VHstr,'_',VCstr,'_',Vtstr,'_Ps',Psstr]
eval(['load ',fn allvariables])

HOVIs(dh,dr,P)=max(max(max(VIsHO))); % the dh, dr coordinates are oposit since it is that way in
the databases
HOVIsmin(dh,dr,P)=min(min(min(VIsHO))); % the dh, dr coordinates are oposit since it is that way in
the databases
[x y]=find(VIsHO==HOVIs(dh,dr,P));
brhs_VIsHO(dh,dr,P)=x(1);
brs_VIsHO(dh,dr,P)=ceil(y(1)./41);
bhs_VIsHO(dh,dr,P)=y(1)-41*(bhs_VIsHO(dh,dr,P)-1);

end % dr
end % dh
end % P

Ps=[0.1:0.1:0.9] %probability for object to be target
for P=1:length(Ps)
Ps=[0.1:0.1:0.9] %probability for object to be target
Psstr=num2str(Ps(P)*100)

for dh=1:3
dtag=dhvector(dh) %[-0.1:-0.1:-4]; % the range of d' for human (second detector)
Dh=num2str(-dtag*100);

for dr=1:3
dtagR=drvvector(dr) %[-0.1:-0.1:-4]% -2
Dr=num2str(-dtagR*100);

Vi_Temp=[HOVIs(dr,dh,P),HORrVIs(dr,dh,P),HORVIs(dr,dh,P),RVIs(dr,dh,P)];

Vimin_Temp=[HOVIsmin(dr,dh,P),HORrVIsmin(dr,dh,P),HORVIsmin(dr,dh,P),RVIsmin(dr,dh,P)];
Vi_max(dr,dh,P)=max(Vi_Temp);
Temp_CL=find(Vi_Temp==Vi_max(dr,dh,P));
BestCL(dr,dh,P)=Temp_CL(1);
Vimin(dr,dh,P)=Vimin_Temp(Temp_CL);
deltaVi(dr,dh,P)=Vi_max(dr,dh,P)-Vimin(dr,dh,P);

```

```

    end    % dr
end    % dh
end    % P

toc

beta_rhHO=-4+(brhs_VIsHO-1).*0.2;
beta_rhR=-4+(brhs_VIsR-1).*0.2;
beta_rhHORr=-4+(brhs_VIsHORr-1).*0.2;
beta_rhHOR=-4+(brhs_VIsHOR-1).*0.2;

beta_hHO=-4+(bhs_VIsHO-1).*0.2;
beta_hR=-4+(bhs_VIsR-1).*0.2;
beta_hHORr=-4+(bhs_VIsHORr-1).*0.2;
beta_hHOR=-4+(bhs_VIsHOR-1).*0.2;

beta_rHO=-4+(brs_VIsHO-1).*0.2;
beta_rR=-4+(brs_VIsR-1).*0.2;
beta_rHORr=-4+(brs_VIsHORr-1).*0.2;
beta_rHOR=-4+(brs_VIsHOR-1).*0.2;

save sensiPs1

Allbeta_rh(:,:,:,1)=beta_rhHO;
Allbeta_rh(:,:,:,2)=beta_rhHORr;
Allbeta_rh(:,:,:,3)=beta_rhHOR;
Allbeta_rh(:,:,:,4)=beta_rhR;

Allbeta_h(:,:,:,1)=beta_hHO;
Allbeta_h(:,:,:,2)=beta_hHORr;
Allbeta_h(:,:,:,3)=beta_hHOR;
Allbeta_h(:,:,:,4)=beta_hR;

Allbeta_r(:,:,:,1)=beta_rHO;
Allbeta_r(:,:,:,2)=beta_rHORr;
Allbeta_r(:,:,:,3)=beta_rHOR;
Allbeta_r(:,:,:,4)=beta_rR;

save sensiPs2

end    % VAR

```

sensPs2a.m:

% plotting the objective function for different betas sensitivity analysis

```

clear
clc
close all
pause(1)

tic
load sensibeta2

```

```
allvariables=[' N VFA2H VAR Ps dtag dtagR Inbetar Inbetah Inbetarh VH VFA Vc Vt Zsr Znr ZsH ZnH ZsRH
ZnRH ZsRstar ZnRstar betastar phr pfar phh pfah phrh pfarh phrstar pfarstar tmotor tHh tHrh tFAh tFArh tMh
tMrh tCRh tCRrh tr PHs VHs PMs VMs FCRs VCRs FFAs VFAs ts tsHORr tsHOR Ndetect VTs VTsHORr
VTsHOR VIs VIsHORr VIsHOR Nsyshit NsysFA phs pfas Zss Zns dtagsys Inbetasys betasys PHsR VHsR
FFAsR VFAsR tsR VTsR VIsR PHsHO VHsHO FFAsHO VFAsHO tsHO VTsHO VIsHO'];
```

```
dhvector=[-1:-1:-3];
drvector=[-1:-1:-3];
```

```
VFA2H=1; % VFA2H=[0.1 1 10]; % [0.05:0.05:1,1:0.1:10,10:1:100]; % VFA/VH aspect ratio range
```

```
for VARcall=1:length(VFA2H)
    VARstr=num2str(VFA2H(VARcall)*10);
    if VFA2H(VARcall)==0.333
        VARstr=num2str(3);
    end
```

```
%Ps=0.1; %probability for object to be target
```

```
%Psstr=num2str(Ps*100);
```

```
VH=50;
```

```
VM=0;
```

```
VCR=0;
```

```
VHstr=num2str(VH);
```

```
VFA=-VH.*VFA2H(VARcall);
```

```
Vc=-2;
```

```
VCstr=num2str(-Vc);
```

```
Vt=-2000/3600;
```

```
Vtstr=num2str(-Vt*3600);
```

```
tr=10;
```

```
Ps=[0.1:0.1:0.9] %probability for object to be target
```

```
for P=1:length(Ps)
```

```
Ps=[0.1:0.1:0.9] %probability for object to be target
```

```
Psstr=num2str(Ps(P)*100)
```

```
for dh=1:3
```

```
    dtag=dhvector(dh) % [-0.1:-0.1:-4]; % the range of d' for human (second detector)
```

```
    Dh=num2str(-dtag*100);
```

```
for dr=1:3
```

```
    dtagR=drvector(dr) % [-0.1:-0.1:-4]%-2
```

```
    Dr=num2str(-dtagR*100);
```

```
    fn=['OF1dh',Dh,'dr',Dr,'_',VARstr,'_',VHstr,'_',VCstr,'_',Vtstr,'_Ps',Psstr]
```

```
    eval(['load ',fn allvariables])
```

```
    ViAll(:, :, 2)=VIsHORr;
```

```
    ViAll(:, :, 3)=VIsHOR;
```

```
    ViAll(:, :, 4)=VIsR;
```

```
    fn=['OF1dh',Dr,'dr',Dh,'_',VARstr,'_',VHstr,'_',VCstr,'_',Vtstr,'_Ps',Psstr]
```

```
    eval(['load ',fn allvariables])
```

```
    ViAll(:, :, 1)=VIsHO;
```

```
    fn=['OF1dh',Dh,'dr',Dr,'_',VARstr,'_',VHstr,'_',VCstr,'_',Vtstr,'_Ps',Psstr]
```

```
    eval(['load ',fn allvariables])
```

```
    curr_CL=BestCL(dr,dh,P)
```

```
    curr_maxVi= Vi_max(dr,dh,P)
```

```

Brh=Allbeta_rh(dr,dh,P,curr_CL)
Bh=Allbeta_h(dr,dh,P,curr_CL)
Br=Allbeta_r(dr,dh,P,curr_CL)

Brh_pos=round(((Brh+4)./0.2)+1)
Bh_pos=round(((Bh+4)./0.2)+1)
Br_pos=round(((Br+4)./0.2)+1)

brh_HORr=Brh_pos;
brh_HOR=Brh_pos;
brh_HO=Brh_pos;

bh_HORr=Bh_pos;
bh_HOR=Bh_pos;
bh_HO=Bh_pos;

br_HORr=Br_pos;
br_HOR=Br_pos;
br_HO=Br_pos;

if curr_CL==4
    maxHORr=max(max(VIsHORr(:,Br_pos)));
    [x y]=find(VIsHORr(:,Br_pos)==maxHORr);
    brh_HORr=x(1);
    bh_HORr=y(1);

    maxHOR=max(max(VIsHOR(:,Br_pos)));
    [x y]=find(VIsHOR(:,Br_pos)==maxHOR);
    brh_HOR=x(1);
    bh_HOR=y(1);

    fn=['OF1dh',Dr,'dr',Dh,'_',VARstr,'_',VHstr,'_',VCstr,'_',Vtstr,'_Ps',Psstr]
    eval(['load ',fn allvariables])

    for m=1:41
        tmp_VIsHO(m)=VIsHO(1,1,m);
    end

    maxHO=max(tmp_VIsHO);
    y=find(tmp_VIsHO==maxHO);
    brh_HO=1;
    bh_HO=y(1);
end

for Psens=1:9
    Psens_str=num2str(Psens*10);
    fn=['OF1dh',Dh,'dr',Dr,'_',VARstr,'_',VHstr,'_',VCstr,'_',Vtstr,'_Ps',Psens_str]
    eval(['load ',fn allvariables])

    AllCL(2,Psens)=VIsHORr(brh_HORr,bh_HORr,Br_pos);
    AllCL(3,Psens)=VIsHOR(brh_HOR,bh_HOR,Br_pos);
    AllCL(4,Psens)=VIsR(Brh_pos,Bh_pos,Br_pos);

    fn=['OF1dh',Dr,'dr',Dh,'_',VARstr,'_',VHstr,'_',VCstr,'_',Vtstr,'_Ps',Psens_str]
    eval(['load ',fn allvariables])
    AllCL(1,Psens)=VIsHO(brh_HO,Br_pos,bh_HO);
end

```

Ps=[0.1:0.1:0.9]; %probability for object to be target

```

figure(P)
subplot(3,3,dr+(dh-
1).*3);plot(Ps,AllCL(1,:), 'b',Ps,AllCL(2,:), 'c',Ps,AllCL(3,:), 'g',Ps,AllCL(4,:), 'r',Ps(P),curr_maxVi, 'ok')
titleline=['V_I_s  P_s= ',num2str(Ps(P)), ' d_r=',Dr, ' d_h=',Dh];
title(titleline)
grid on

pause(1)

end % dr
end % dh
toc
end % P

end % VAR

save sensiPs3

```

Appendix XIII: Analysis of β_{rh}

Analysis of β_{rh} for objects that were marked by the robot. Here we can compute p_{Hit} and p_{FA} for the human, and accordingly compute β_{rh} . The independent variables will be level of cooperation (all, except HO), robot performance, and rewards (combined over all levels of complexity and blocks).

The likelihood ratio parameter β_{rh} is a function of the hit and false alarm probabilities (chapter 4). The probabilities are transferred into distribution standard deviation values (Z). When the FA probability is zero, its theoretical Z value is $-\infty$. In the experiment, only a few participants avoided marking any robot false alarms, resulting in a FA probability of 0. Since these results were achieved due to the finite number of robot FA and it is impossible to statistically analyze results with infinite values, for those few cases we determine the Z value to be -4 (in standard deviation units). The calculated FA probability for that value is 0.0000317, which can be regarded as zero for our purposes.

When $\ln(\beta) = 0$ (or $\beta = 1$) the participant consider to be an ideal observer (Cheng et al., 2001), for positive $\ln(\beta)$ the participant consider to be conservative and for negative $\ln(\beta)$ the participant consider to be liberal.

Table A-26 shows the statistical output of the univariate tests of significance performed on the experiment results.

Table A-26: The univariate tests of significance results.

	DoF	MS	F	p
Collaboration	1, 88	40.104	9.235	0.003
Rewards	1, 88	21.615	4.978	0.028
Robot quality	1, 88	13.895	3.200	N.S.
Collaboration*Rewards	1, 88	4.608	1.061	N.S.
Collaboration*Robot quality	1, 88	11.793	2.716	N.S.
Rewards*Robot quality	1, 88	37.417	8.617	0.004
Collaboration*Rewards*Robot quality	1, 88	2.290	0.527	N.S.

The logarithm of the likelihood ratio, β_{rh} , decreased with the increase in the automation level (Figure A-100). Both the probability of a human hit and false alarm of objects marked by the robot decreased with the increase in the automation level, but the probability of false alarm decreased more drastically. It seems that the human operators reduced their intervention when the system automation level was high (HO-R), and that their behavior was liberal. For low automation level the human operators performance is consider to be conservative.

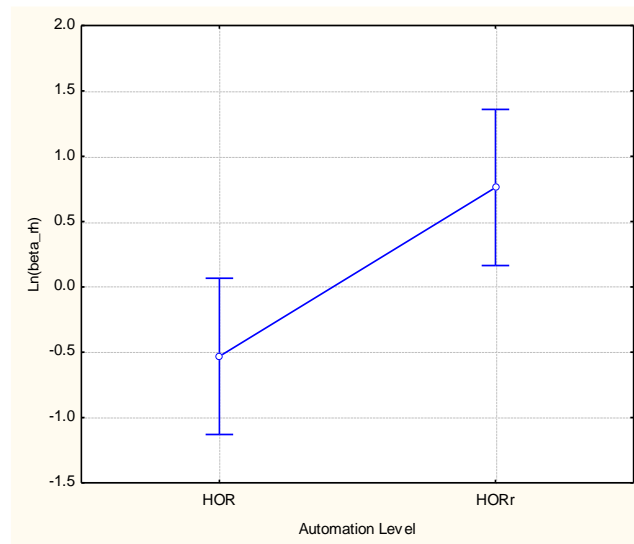


Figure A-100: The human likelihood ratio for objects marked by the robot as a function of the automation level.

The reward system had a significant effect on participant decision, $\text{Ln}(\beta_{rh})$. The values of the logarithm of the likelihood ratio were higher in the maximized hit reward system than in the minimized FA reward system (Figure A-101). It could be that the participants were simply better able to confirm the robot hits as opposed to eliminate its false alarms. In a similar fashion, an increase in participant sensitivity was noticed when aiming for target detection than for false alarm elimination. The participants behavior were liberal for the minimized FA reward system and conservative for the maximized hit reward system.

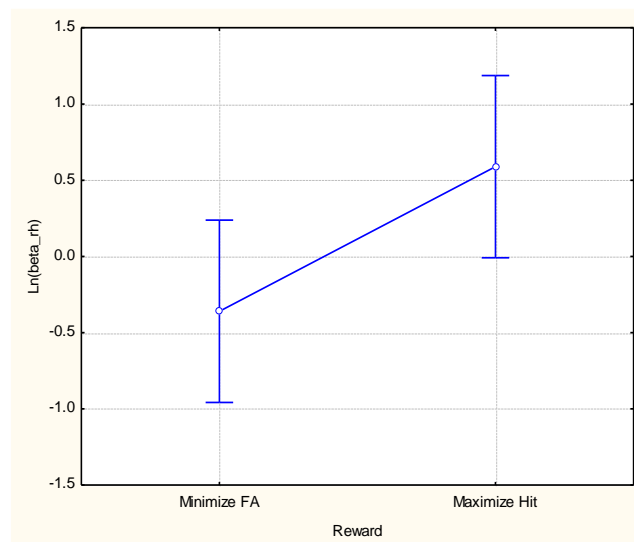


Figure A-101: The human likelihood ratio for objects marked by the robot as a function of the reward system.

Figure A-102 shows the influence of robot quality on human likelihood ratio. The human likelihood ratio for objects marked by the robot increases with the increase in robot quality. Although it was found to be marginally significant ($p < .1$), it seems that the participant's awareness of the robot quality influence the likelihood ratio value due to their reliance on the

robotic system. The participants behavior were conservative for low robot quality and liberal for nigh robot quality.

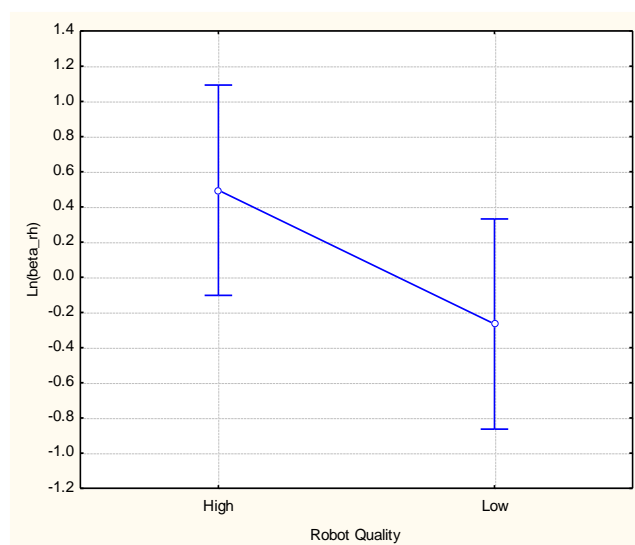


Figure A-102: The human likelihood ratio for objects marked by the robot as a function of robot quality.

The effect of robot quality-reward system interaction (Figure A-103) was significant. In the maximum hit reward system human likelihood ratio increased with the increase in robot quality. In the minimum FA reward system, robot quality had a little effect on human likelihood ratio.

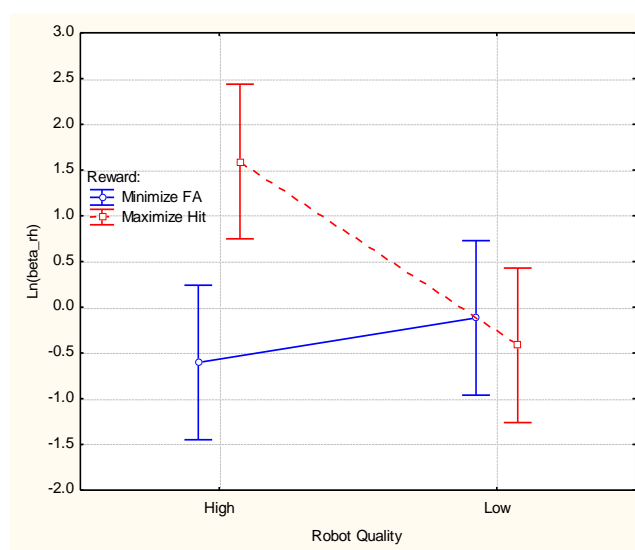


Figure A-103: The human likelihood ratio for objects marked by the robot as a function of the reward system and robot quality.

תקציר

רובוטים אוטונומיים הינם מערכות המבצעות משימות, מקבלות החלטות ופועלות ללא התערבות אדם. הן יעילות ביותר ביישומים הדורשים דיוק לאורך זמן ותפוקה גבוהה בתנאים סטטיים ומוגדרים היטב. אך מערכות אלו חסרות יכולת לפעול בסביבות בלתי מובנות. סביבות לא מובנות מאופיינות באירועים שאינם מוגדרים כהלכה, אינם ידועים, דינאמיים ובלתי צפויים. במצב הנוכחי המערכות האוטונומיות עדיין לא נותנות פתרון מעשי לרוב היישומים ב"עולם האמיתי". בנוסף לכך, הבעיות הינן קשות יותר ביישומים הכוללים אובייקטים טבעיים בשל השונות הרבה בין האובייקטים ומאחר ומיקומם אינו ידוע מראש. כל אלו מכבידים על המערכת הרובוטית והופכים אותה לקשה ויקרה לפיתוח. שילוב מפעיל אנושי במערכת רובוטית יכול להגביר את מהימנותה ושיעור זיהוי המטרות, להפחית את מורכבותה ולאפשר למערכת לטפל באירועים בלתי ידועים ובלתי צפויים שמערכות אוטונומיות אינן כשירות להם.

עבודה זו מתמקדת בהיבטים של רמות שיתוף הפעולה במערכות משולבות אדם-רובוט למשימת זיהוי מטרות בסביבות בלתי מובנות. אנו מציגים שיטה לקביעת רמת שיתוף הפעולה המיטבית על פי משתני המערכת, הסביבה והמשימה ואת חיזוי והערכת ביצועי המערכת.

ארבע רמות שונות לשיתוף פעולה בין אדם לרובוט למשימות זיהוי מטרות הוגדרו, נבדקו והוערכו. הרמות השונות יועדו במיוחד למשימות זיהוי מטרה והותאמו לרמות אוטומציה שונות מידיני לחלוטין ועד אוטונומי. רמות שיתוף הפעולה ניתנות להתאמה לאדם או לרובוט בכדי לשפר את ביצועי המערכת.

פותחה פונקציית מטרה לזיהוי מטרות במערכות אדם-רובוט המאפשרת את חישוב הערך המצופה של ביצועי המערכת בהינתן ערכי האדם, הרובוט, הסביבה והמשימה. פונקציית המטרה כוללת עלויות זמן ותפעול אשר חשובים להערכה ואופטימיזציה של ביצועי המערכת. פונקציית המטרה מכמתת מספר רב של משתנים באמצעות סיכום משוקלל של מדדי הביצוע ומאפשרת לחזות את ביצועי המערכת ורמת שיתוף הפעולה ולעזור בתכנון מערכת אופטימאלית למשימה ייעודית.

פותחה שיטה לקביעת רמת שיתוף הפעולה המיטבית בהתאם למשתני האדם, הרובוט, המשימה והסביבה. יושמה אנליזה נומרית של פונקציית המטרה בשילוב עם תאוריית זיהוי אותות, לרמות שיתוף הפעולה שהוגדרו, ובוצעו ניתוחי רגישות על הערכים האופטימלים של המשתנים החשובים. פיתוחים אלו מספקים את הבסיס להתאמה של מערכת משולבת אדם-רובוט למשימה ולפיתוח יעיל של מערכת דומה.

המחקר הנוכחי מספק כלים לפיתוח של מערכת משולבת אדם-רובוט לזיהוי מטרות בסביבות בילתי מובנות אשר יפשטו את המערכת הרובוטית, יקטינו את העלויות, וישפרו את חוסנה וביצועיה. מפתחי מערכות יכולים לבצע שימוש בפונקציית המטרה בכדי לנבא את ביצועי המערכת שבפיתוח ולקבוע את רמות שיתוף הפעולה המיטביות מלכתחילה. ניתן גם לפתח את המערכת כך שתותאם למשימות או סביבות ייעודיות.

שיטות

נושאי המחקר שפותחו

המחקר מכיל שלושה פיתוחים עצמאיים ובעלי זיקה הדדית הקשורים לשיתוף פעולה בין אדם לרובוט במשימות זיהוי מטרות: רמות שיתוף פעולה בין אדם לרובוט, פונקציית מטרה להערכת ביצועי המערכת ושיטה לקביעת רמת שיתוף הפעולה המיטבית.

הפיתוח הראשון כולל הגדרה של ארבע רמות שיתוף פעולה בין אדם לרובוט המותאמות למשימות זיהוי מטרה. רמות שיתוף הפעולה מבוססות על סולם האוטונומיות של Sheridan ומתאימות לטווח רחב של רמות אוטומציה. הן הוגדרו כ-H, HR, HOR ו-R מידיני ועד אוטונומי לחלוטין בהתאמה. תהליך זיהוי

המטרות מתבצע בשני שלבים: תחילה הרובוט מזהה את המטרות ובהמשך האדם פועל לפי החלטות הזיהוי של הרובוט.

פונקציית המטרה מתוכננת לאפשר קביעה של הערכים המצופים של ביצוע המשימה, בהינתן משתני המערכת, המשימה והסביבה. ניתן לסווג את פרמטרי פונקציית המטרה לארבע קבוצות: אדם, רובוט, סביבה ומשימה. פונקציית המטרה כוללת חמישה חלקים: זיהוי נכון (hit), זיהוי מוטעה (false alarm), כישלון (miss), (false-false) correct rejection ועלויות התפעול. חלק עלויות התפעול כולל עלויות הקשורות לזמן הביצוע ועלויות הקשורות לפעולות הנובעות מעצם הזיהוי.

פותחה שיטה לקביעת רמת שיתוף הפעולה המיטבית למערכת ייעודית, למידול ולסימולציה של ביצועיה. על מנת לתאר את הקשר בין המשתנים השונים בפונקציית המטרה בוצעה התאמה של תאוריית גילוי אותות, אשר הקטינה את מספר המשתנים הבילתי תלויים על ידי שיוך מדדי הביצוע של האדם והרובוט (כגון שיעורי זיהוי) למאפיינים הבסיסיים (כגון רגישות ואיכות קביעת ערך סף).

אנליזה נומרית

האנליזה הנומרית מומשה על מחשב אישי PC באמצעות תוכנת Matlab 7™. האנליזה הנומרית בחנה את השפעת המאפיינים הבסיסיים של האדם והרובוט ורמות שיתוף הפעולה בפונקציית המטרה. היא קבעה את המאפיינים האופטימליים של האדם והרובוט עבור משתני משימה שונים, ואת רמת שיתוף הפעולה המיטבית עבור משתני אדם, רובוט ומשימה שונים. בנוסף בוצעו ניתוחי רגישות על הערכים האופטימליים ונמדדה השפעתם על רמת שיתוף הפעולה המיטבית וביצועי המערכת.

ניסוי

בוצע ניסוי להערכת השפעת רמות שיתוף הפעולה במשימת זיהוי מטרות ייעודית. הניסוי כלל סימולאטור אשר הציג תמונות של מלונים בשדה אשר צולמו במצלמת וידאו המותקנת על רובוט לקטיפ מלונים תוך כדי מעבר בשדה. 120 סטודנטים ללימודי הסמכה השתתפו בניסוי. הסטודנטים הוקצו באופן אקראי ל- 10 קבוצות, בכל קבוצה 12 סטודנטים. בכל קבוצה הוגדרו אחד משני סוגי משקולות פונקציית המטרה, אחת משתי רמות איכות של הרובוט ואחת משלוש רמות שיתוף הפעולה בהן מעורב אדם. התמונות סווגו לשלוש קבוצות מורכבות על ידי פנל מומחים. התמונות חולקו לשלושה בלוקים כאשר בכל בלוק לכל משתתף סדר הופעת התמונות היה אקראי. הסטודנטים נתבקשו לזהות את המלונים שבתמונות. במהלך הניסוי מערכת הסימולאטור רשמה את פעולות האדם, האובייקטים שסומנו, וחתימת הזמן של כל אירוע. מדדי הביצוע חושבו מהנתונים הגולמיים שנרשמו.

ניתוחים סטטיסטיים בחנו את השפעת הבלוק, מורכבות התמונה, רמת שיתוף הפעולה, איכות הרובוט ומשקולות פונקציית המטרה על ביצועי המערכת והאדם. הניתוחים הסטטיסטיים בוצעו בתוכנת Statistica™ 7 וכללו: Fisher LSD post-hoc, repeated measures analysis of variance, comparison ו-general linear model of univariate tests of significance.

תוצאות

אנליזה נומרית

האנליזה הנומרית בוצעה עבור יחסי מטר-אובייקט שונים, רגישויות אדם ורובוט, ויחסי תגמול שונים המתבטאים במשקולות השונים בפונקציית המטרה. ערכי הסף האופטימאליים ($\beta_{rh}, \beta_r, \beta_h$) חושבו. פונקציית המטרה נותחה עבור מקרים הכוללים את חלק עלויות התפעול ועבור מקרים ללא חלק זה. פונקציית המטרה ללא חלק עלויות התפעול מהווה סף עליון של ביצועי המערכת ומייצגת מקרים בהם עלויות התפעול אינן קיימות והשפעתן על רמת שיתוף הפעולה המיטבית.

באנליזה הנומרית כל רמת שיתוף פעולה מיוצגת כמשטח במרחב הפרמטרים, כאשר ציר Z הינו ערכי פונקציית המטרה. חיתוך כל המשטחים יוצר את משטח הערכים המקסימליים של פונקציית המטרה עבור כל שילוב של פרמטרים. רמת שיתוף הפעולה המשיגה את הערך הגבוה ביותר בשילוב מסוים מוגדרת כרמת שיתוף הפעולה המיטבית עבור השילוב המסוים.

ניתוחי הרגישות בוצעו על משתני האדם, הרובוט והסביבה מאחר והם יכולים להשתנות במהלך ביצוע המשימה וערכם המדויק אינו ידוע. השפעת השינוי בערכים האופטימליים של הפרמטרים על ערך פונקציית המטרה ורמת השיתוף המיטבית נותחה על מנת לשקף מקרים בהם ערכי האדם, הרובוט או הסביבה סטו מערכיהם האופטימאליים.

האנליזה הנומרית מראה כי כאשר היחס מטר-אובייקט גדל, המערכת פחות מושפעת מזיהויים מוטעים ולכן שיעורי הזיהוי האמיתי והמוטעה עולים, ערכי הסף יורדים, עלויות התפעול וערך פונקציית המטרה עולים. נמצא כי בכל רמות שיתוף הפעולה ערכי פונקציית המטרה עלו עם עלייה ברגישות האדם והרובוט. השוואה בין רמות השיתוף HOR ו-HR מראות כי ביצועי המערכת עבור ערכי יחס מטר-אובייקט נמוכים ורגישות רובוט נמוכה, טובים יותר עבור HR. רמת שיתוף מסוג H לעולם אינה רמת השיתוף המיטבית במקרים האופטימליים. כתוצאה משיעורי זיהוי נמוכים ועלויות תפעול גבוהות ביחס לרמות שיתוף פעולה אחרות, שיתוף בין אדם לרובוט במשימות זיהוי מטרות ישפר תמיד את ביצועי המערכת בהשוואה לעבודה בצורה ידנית (H) במקרים אופטימליים. הממצאים מראים כי כאשר רגישות הרובוט גבוהה משל האדם רמת השיתוף המיטבית הינה R. כאשר עובדים ברמת שיתוף הפעולה המיטבית, הרגישות וערך הסף של המערכת הכוללת קטנים עם הגדלת יחס מטר-אובייקט. בנוסף, נמצא כי רגישות המערכת הכוללת אינה קטנה מזו של הרובוט.

הסרה של עלויות התפעול מפונקציית המטרה יאחד את HOR ו-HR לרמת שיתוף אחת מאחר וההבדל ביניהן מבוסס במשתני הזמן של פונקציית המטרה אשר נמצאים בחלק עלויות התפעול. בנוסף, ערך פונקציית המטרה יעלה ורמת השיתוף המיטבית תהיה הרמה המשותפת לכל מרחב הרגישויות ויחסי מטר-אובייקט.

בניתוח הרגישויות של ערכי הסף $\beta_{rh}, \beta_r, \beta_h$ - עבור רמת השיתוף המיטבית במקרים האופטימליים נמצא כי כל שינוי בערכי הסף מקטין את ערך פונקציית המטרה. ניתוח רגישויות על יחס מטר-אובייקט ורגישויות האדם והרובוט הראה סטיות חיוביות קטנות מהערכים האופטימליים המגדילים את ערך פונקציית המטרה עבור רמת השיתוף המיטבית.

ניתוחי הרגישויות הראו כי סטיות מהערכים האופטימליים עלולים לשנות את רמת שיתוף הפעולה המיטבית מאחת לאחרת. לכל משתנה שנבדק קיימת חוקיות שונה במעבר מרמה לרמה אך הסטיות בערכי רגישויות האדם והרובוט וערכי הסף לעולם יגרמו לרמת השיתוף המיטבית להיות H.

תוצאות הניסוי מראות כי שיטת התגמול (משקלי פונקציית המטרה) יש השפעה מובהקת על שיעורי הזיהוי האמיתי והזיהוי המוטעה של המערכת הכוללת וערך פונקציית המטרה. שיעור הזיהוי האמיתי למערכת עבור משתתפים אשר תוגמלו על זיהוי נכון היה גבוה בהשוואה למשתתפים שתוגמלו עבור שיעור נמוך של זיהוי מוטעה. באופן דומה שיעור הזיהוי המוטעה למערכת עבור נבחנים שתוגמלו עבור שיעור זיהוי נמוך, היה נמוך משל האחרים. שיטת התגמול לא השפיעה על זמן ביצוע המשימה.

לאיכות ביצועי הרובוט היתה השפעה מובהקת על שיעור הזיהוי האמיתי של המערכת ועל ערך פונקציית המטרה. הגדלת איכות הרובוט הגדילה את ערך פונקציית המטרה והקטינה את שיעור הזיהוי המוטעה של המערכת. אולם, רמת אוטונומיה גבוהה שברמת שיתוף HOR יחד עם איכות רובוט נמוכה הגדילה באופן מובהק את מספר הזיהויים המוטעים בהשוואה לרמה הידנית HO. עבור איכות רובוט נמוכה שינוי רמת שיתוף הפעולה לאוטונומית יותר גרמה להגדלת זמן הזיהוי, תופעה הפוכה התקבלה עבור איכות רובוט גבוהה. עלייה במורכבות התמונה הביאה לירידה בשיעור הזיהוי האמיתי של המערכת ולעליה במספר הזיהויים המוטעים וזמן הזיהוי.

נמדדה גם השפעה של שיטת התגמול על מדדי ביצוע של האדם. רמות הזיהוי האמיתי של האדם עבור אובייקטים שסומנו על ידי הרובוט ואובייקטים שלא סומנו היו גבוהות עבור משתתפים שתוגמלו על זיהוי נכון מאשר לאחרים. מסתמן כי המשתתפים הפנימו את שיטת התגמול והפנו את תשומת ליבם במשימה בהתאם לכך. באופן דומה נמצא כי לאיכות הרובוט יש השפעה ניכרת על רמות הזיהוי האמיתי והמוטעה של האדם והמשתתפים הבחינו באיכות הרובוט במהלך הניסוי והסתמכו על החלטות הרובוט כאשר איכותו היתה גבוהה.

למורכבות התמונה היתה השפעה מובהקת על ביצועי האדם באובייקטים שלא סומנו על ידי הרובוט. עלייה במורכבות התמונה הקטינה את שיעור הזיהוי האמיתי של האדם על אובייקטים שלא סומנו על ידי הרובוט והגדילה את מספר הזיהויים המוטעים.

נמצאה השפעה מובהקת של רמות שיתוף הפעולה הכוללות אדם ורובוט לבין ביצועי האדם על אובייקטים שסומנו על ידי הרובוט. הגדלת רמת האוטומציה (מעבר מ-HR ל-HOR) הגדילה את שיעור הזיהוי האמיתי והמוטעה של האדם על אובייקטים אשר סומנו על ידי הרובוט. נראה כי עבור רמות אוטומציה גבוהות האדם נוטה לקבל את החלטות הרובוט. בנוסף נמצא כי העלייה ברמת האוטומציה עבור משתתפים עם רובוט באיכות גבוהה, הקטינה את רגישות האדם. ממצא זה יכול להצביע על כך שהעלייה ברמת האוטומציה מקטינה את שליטת האדם ורגישותו.

נמצא כי עלייה במספר הבלוקים בניסוי שיפרה באופן מובהק את ביצועי האדם והמערכת הכוללת. מאחר וביצועי הרובוט היו קבועים לאורך כל הניסוי בכל הקבוצות, נראה כי התקיים אפקט למידה במהלך הניסוי.

סיכום

בוצעה עבודה מקיפה לניתוח והערכת ההשפעה של רמות שיתוף פעולה שונות על ביצועיה של מערכת משותפת אדם-רובוט למשימות זיהוי מטרה. העבודה כללה פיתוח של רמות שיתוף ייעודיות, פונקציית מטרה לכימות ביצועי המערכת הכוללת ושיטה לקביעת רמת שיתוף הפעולה המיטבית. פונקציית המטרה נחקרה באמצעות אנליזה נומרית וניסוי.

תוצאות האנליזה הנומרית מצביעות על כך כי רמת שיתוף הפעולה המיטבית, הערכים האופטימליים של מדדי הביצוע וביצועי המערכת המיטביים תלויים במשתני המשימה, האדם, הרובוט והסביבה ובמאפייני

המערכת. מאחר ומספר המשתנים רב, ובנוסף קיימת אינטראקציה בין המשתנים השונים, חיזוי ביצועי המערכת והפיתרון האופטימלי אינו ברור, אך ניתן להעריכו באמצעות חקירת פונקציית המטרה. את ממצאי ניתוחי הרגישות ניתן לנצל לפיתוח והפעלה של מערכות רובוטיות משולבות אדם בתנאים דינאמיים ומציאותיים בהם הערכים של המשתנים אינם ידועים, הדיוק נמוך או במצב שהמשתנים דינאמיים. במהלך הפיתוח הוקדשה חשיבה רבה לכימות המשתנים הבלתי תלויים והתוצאות ולתיקוף הממצאים התיאורטיים באמצעות ניסוי. פונקציית המטרה פותחה כך שתאפשר השוואה של מערכות, סביבות, ומשימות שונות.

יתרונות השיטה היא ביכולת לחקור את השפעת המשתנים השונים על ביצועי המערכת באופן לא מקוון ואפילו בהעדר מערכת ממשית. מפתחי מערכות יכולים לאמץ שיטות אלו לפיתוח והתאמה של מערכות רובוטיות משולבות אדם למשימות זיהוי מטרות בסביבות בילתי מובנות. בנוסף, השיטה יכולה לשמש לניתוח ביצועי המערכת והאדם באופן מקוון.

תרומה מדעית

התרומות העיקריות של מחקר זה הן :

- הגדרה והערכה של רמות שיתוף פעולה בין אדם לרובוט למשימות זיהוי מטרות. רמות השיתוף מבוססות על סולם עשר הדרגות של Sheridan אשר הותאמו במיוחד למשימות זיהוי מטרות. רמת השיתוף ניתנת להתאמה לאדם או לרובוט לשם שיפור ביצועי המערכת הכוללת. רמות שיתוף הפעולה מודלו מתמטית וכומתה השפעתן על פונקציית המטרה.
- פונקציית מטרה למערכת רובוטית משולבת אדם למשימת זיהוי מטרות מאפשרת חישוב ביצועי המערכת בהינתן משתני האדם, הרובוט המשימה והסביבה. ניתן להתאים את פונקציית המטרה למשימות או סביבות שונות ולחזות את ביצועי המערכת ואת רמת שיתוף הפעולה הרצויה. פונקציית המטרה כוללת עלויות זמן ועלויות תפעול אשר חשובים לאופטימיזציה של ביצועי המערכת.
- פותחה שיטה לקביעת רמת השיתוף המיטבית על פי משתני האדם, הרובוט, הסביבה והמשימה. השיטה כוללת אנליזה נומרית של פונקציית המטרה יחד עם תיאורית גילוי אותות. השיטה מאפשרת את שיפור ביצועי המערכת והתאמת רמת שיתוף הפעולה הטובה ביותר לכל מקרה.

העבודה נעשתה בהדרכתם של פרופ' יעל אידן ופרופ' יואכים מאיר

המחלקה להנדסת תעשייה וניהול

הפקולטה למדעי ההנדסה

שיתוף פעולה אדם – רובוט לזיהוי מטרות בסביבות בילתי מובנות

מחקר לשם מילוי חלקי של הדרישות לקבלת
"דוקטורט לפילוסופיה"

מאת

אביטל בכר

הוגש לסינאט אוניברסיטת בן-גוריון בנגב

אישור מנחה פרופ' יעל אידן

אישור מנחה פרופ' יואכים מאיר

אישור דיקן בית הספר ללימודי מחקר מתקדמים

2006

תשס"ו

באר-שבע

שיתוף פעולה אדם – רובוט לזיהוי מטרות בסביבות בילתי מובנות

מחקר לשם מילוי חלקי של הדרישות לקבלת
"דוקטורט לפילוסופיה"

מאת

אביטל בכר

הוגש לסנאט אוניברסיטת בן-גוריון בנגב

2006

תשס"ו

באר-שבע